SESSION V

ADSORBENTS AND ABSORBENTS

Tuesday, August 8, 1978
CHAIRMEN: R. D. Rivers, C. A. Burchsted

CONFIRMATORY RESEARCH PROGRAM - EFFECTS OF ATMOSPHERIC CONTAMINANTS ON COMMERCIAL CHARCOALS *

Ronald R. Bellamy
U.S. Nuclear Regulatory Commission
Washington, D.C. 20555

Victor R. Deitz
Naval Research Laboratory
Washington, D.C. 20315

ABSTRACT

The increased use of activated charcoals in engineered-safety-feature and normal ventilation systems of nuclear power stations to continually remove radioiodine from flowing air prior to release to the environment has added importance to the question of the effect of atmospheric contaminants on the useful life of the charcoal. In January of 1977 the Naval Research Laboratory (NRL) began an investigation** to determine the extent to which atmospheric contaminants in ambient concentrations degrade the efficiency of various commercially-available charcoals for removing methyl iodide. A report summarizing the FY77 effort has been published as NUREG/CR-0025, "Effects of Weathering on Impregnant Charcoal Performance."[1] This paper will briefly summarize that report and present the results available from the FY78 investigations.

The approach employed by NRL is two-fold. First, charcoal samples are exposed to unmodified outdoor air for periods of one to nine months, then examined for methyl iodide retention, increase in weight, and the pH of water extract. The atmospheric contaminants are identified by the NRL Air Quality Monitoring Station, and concentrations of the various contaminants (ozone, SO_2, NO_2, CO_2, methane and total hydrocarbons) are also available. Moisture content data is obtained from a neighboring station (Washington National Airport) of the U.S. Department of Commerce. Second, additional charcoal samples are exposed to the same pollutants under controlled laboratory conditions in various pollutant combinations.

Results from FY77 indicate that the water vapor-charcoal interaction is an important factor in the degradation of the commercial charcoals. Laboratory results indicate the pollutant sulfur dioxide plus water vapor can result in significant charcoal deterioration, as did ozone plus water vapor. Conversely, carbon monoxide did not appear to affect the charcoal. Also, differences were observed for various charcoals. The FY78 laboratory work will expand the pollutants to include a hydrocarbon mixture, use various concentrations of pollutants, verify differences in charcoals, and attempt to determine if the effects are because of the base charcoal, the impregnation, or both.

*Paper to be presented at the 15th DOE Air Cleaning Conference, Boston, Mass, August 7-10, 1978.

**Work performed under contract for the U.S. Nuclear Regulatory Commission under Interagency Agreement No. AT(49-24)-9006.

The outdoor exposures at NRL consider the integrated and accumulative effect of the pollutants. FY77 results indicate more degradation after three months than after one month exposure for the same charcoal; FY78 results will extend the exposure time to nine months for various charcoals. FY77 preliminary results indicate two different charcoals differ in their ability to survive the weathering process over time; FY78 results will include up to twelve different charcoals.

This paper will discuss the progressive effect of the pollutants through the charcoal bed. Both the laboratory and outdoor samples were layered to allow analysis of weight increase, methyl iodide removal, and pH of water extract as a function of bed depth. These results on exposed charcoals are compared to the known semi-logarithmic dependance of decrease in penetration with increased bed depth for unexposed charcoals.

This paper will also present the proposed scope of work for the remainder of FY78 and FY79, including a discussion of plans to examine the weathering effects exhibited by spent charcoals of known history from power reactors.

I. INTRODUCTION

The impregnated activated carbon installed in engineered-safety-feature and normal ventilation systems at nuclear power stations to remove radioiodine prior to release to the environment will not adsorb radioiodine indefinitely. The active sites on the carbon surface have a finite capacity for adsorption, and once that capacity is reached, the carbon is saturated and will no longer remove radioiodine from flowing air. The adsorption sites can be blocked by atmospheric contaminants, quickly destroying the adsorption capacity of the carbon. Commonly termed "weathering", there has not been (as of January 1977) an in-depth engineering analysis of the problem, to determine the extent to which atmospheric contaminants in ambient concentrations degrade the efficiency of various commercially - available charcoals for removing radioiodine. Recognizing this deficiency, the U.S. Nuclear Regulatory Commission contracted with the Naval Research Laboratory to perform such confirmatory research. Results on various carbons are not to be interpreted as a recommendation of any manufacturer's carbon, but are presented to illustrate the effect of the carbon base and impregnant. This paper will discuss the results obtained to date, the work in progress, and the experiments planned for the remainder of the fiscal year, 1978, and 1979.

A two-fold approach has been undertaken to obtain the necessary data. First, charcoal samples are exposed to unmodified outdoor air for various periods of time, and then examined for changes in methyl iodide retention capability, weight and pH of water extract. This approach allows no control over the concentration or type of atmospheric contaminant. Second, additional charcoal samples (of the same charcoal as used for the outdoor exposures) are exposed to the same pollutants under controlled laboratory conditions in various pollutant combinations. This approach allows pollutant types, concentrations, and combinations to be varied and controlled under the discretion of the investigator.

II. Accomplishment in Fiscal Year 1977

There are two elements of the procedure for analysis of weathered samples that can significantly affect the results and conclusions, yet are unrelated to the weathering phenomenon. The first is related to the preparation of weathered samples for subsequent laboratory analysis for methyl iodide retention, the second is related to the laboratory procedures employed for the methyl iodide retention analysis.

There are three methods available for preparation of weathered samples for laboratory methyl iodide analysis:

A. The weathered samples are prepared in four separate layers, each 4 inches in diameter and 0.5 inches high. Each layer may be tested separately and independently by transferring each layer (with mixing) to a test canister 2 inches in diameter and 2 inches high.

B. One-fourth of each layer of the weathered sample can be used to construct a test bed in which the same sequence of entrance to exit is preserved in the bed, again yielding a test canister 2 inches in diameter and 2 inches high.

C. Examine the weathered sample without removal of the charcoal from the exposure configuration. This requires exposure canisters 2 inches in diameter and 2 inches high which are presently being fabricated.

The preferred procedure depends on the information that is desired. Procedure A yields information on the gradient within the bed brought about by weathering, while Procedures B and C yield information on the lifetime of the exposed carbon. Results to date have been determined using Procedure A, in order to elicit as much information as possible from one weathering exposure.

The second element that will effect the results but is not directly associated with the weathering phenomenon is the laboratory procedure employed for the methyl iodide retention analysis. Testing procedures are being established by the American Society for Testing and Materials[2] (ASTM) for both new (unexposed) and weathered carbons. For laboratory determination of methyl iodide penetration for new carbons, the test temperatures, relative humidities and periods of equilibration (with water vapor), feed (with methyl iodide), and purge (with air) are well-defined. However, the proposed procedures for testing of weathered carbons are only preliminary, and are being tried in various laboratories today.

As Table 1 illustrates, for new carbons there is considerably less penetration without prehumidification (the charcoals performed better). This effect is reversed for exposed carbons, as the prehumidification period cleans and regenerates the carbon, leading to better performance with prehumidification. Accordingly, the proposed ASTM procedures recommend static temperature equilibrium with no flow. This results in temperature excursions of 20°C or more when the 95% RH air enters the charcoal bed, due to the heat of adsorption.[3] To obtain consistent results, NRL weathered samples are today being prehumidified for 1 hour or until the temperature rise is less than 1°C.

An alternate procedure under investigation is to statically equilibrate the carbon in an oven containing a water source until the carbon has adsorbed sufficient moisture to eliminate any significant temperature excursion.

A. Exposures To Outdoor Air

In FY77 there were 8 different commercially-available charcoals weathered on the roof of the NRL Chemistry Building. Most of those were only exposed for one month, however, there were two carbons exposed for periods of one, two, and three months to examine accumulative effects. Samples of the same charcoal were exposed for various one-month periods to analyze monthly weathering variations, and different charcoals were exposed for the same one-month period to begin an analysis of the effect of the base material and impregnant complex. FY77 results will be briefly

TABLE 1

METHYL IODIDE PENETRATION FOR NEW COCONUT-BASE COMMERCIAL CHARCOALS AT 21°C

	Nominal Size	Water Extract pH	Penetration, % Prehumidification 16 Hours	Penetration, % Prehumidification None
BC 717	8 X 16	9.5	0.99	0.05
BC 727	8 X 16	9.5	4.8, 4.0	0.014
MSA 463563	8 X 16	8.5	2.5	0.13
NACAR G-615	8 X 16	9.8	0.27, 0.23	0.05
NACAR G-617	8 X 16	9.3	3.8	0.1
NACAR G-617-A	8 X 16	9.3	5.7	0.07

discussed to aid in the explanation of the work in progress and future plans.

The two charcoals for periods one, two and three months were Barnebey-Cheney BC-727 (cocoanut base with KI impregnant) and North American Carbon NACAR G-615 (cocoanut base with KI and TEDA impregnant).

The entrance layer showed the greatest degradation for all tests, both in a higher penetration of methyl iodide and a lower pH of the water extract.(4) The charcoal in the three subsequent layers exhibited less penetration than the first layer, indicating the initial layer acting as a guard bed. However, there is no monotonic decrease in penetration with the bed depth, as experienced for unexposed charcoals. Of these two charcoals, NACAR G-615 performed better than BC-727 for the same exposure period (Table 2). Additional tests are required before the role of the impregnation complex can be identified with confidence. Also, an increase in exposure time resulted in greater penetration for the first bed layer, but not always in subsequent layers. In general the longer exposure time did weather the entire bed to a greater extent. These results are presented in Table 2.

Identical charcoals exposed different months showed that dryer months result in less weathering than wet months. It is not clear if this effect can be attributed to the total water vapor content during the month, or the water vapor content during the last 2-3 days prior to termination of weathering. It is planned to study this effect in the laboratory under controlled conditions.

TABLE 2

GRADIENTS IN THE PENETRATIONS (P) OF METHYL IODIDE
AND THE pH OF WATER EXTRACTS AFTER 1, 2, AND 3 MONTHS EXPOSURE

Exposure	First Layer pH	First Layer P	Second Layer pH	Second Layer P	Third Layer pH	Third Layer P	Fourth Layer pH	Fourth Layer P
NACAR G-615								
5016 1 month	9.3	1.77	9.5	0.64	9.6	0.34	9.7	0.70
5031 2 "	8.2	3.42	9.8	1.32	10.0	0.86	10.0	1.02
5022 3 "	7.5	8.62	9.8	1.38	10.0	1.19	10.0	0.81
BC 727								
5014 1 month	8.8	2.67	9.3	1.20	9.3	0.68	9.3	1.31
5032 2 "	7.3	5.81	9.3	2.58	9.5	3.09	9.5	3.45
5020 3 "	7.0	21.6	9.4	5.4	9.5	5.0	9.5	5.7

Available data for pollutant concentrations at NRL were obtained from the NRL Air Quality Monitoring Station. The pollutants identified and the range of monthly average concentrations inlude ozone (0.007 to 0.04 volume parts per million), sulfur dioxide (0.020 to 0.052 ppm), nitrogen dioxide (0.018 to 0.12 ppm), total hydrocarbons (1.8 to 3.1 ppm), methane (1.5 to 2.5 ppm), and carbon monoxide (0.6 to 1.9 ppm). For one-month continuous exposures these concentrations yield integrated insults on the order of hundredths of grams (see Table 18 in Reference 1).

B. Laboratory Exposures

Concentrations of pollutants for laboratory exposures were chosen in an attempt to represent the magnitudes prevalent in the outdoor exposures. Water vapor was added since in magnitude the water vapor constituent is present in far greater amounts than any other pollutant (kilograms for 100-hour exposures compared to grams for one-month exposures). Of the many possible combinations of pollutants to study, FY77 work was limited to single component (water vapor) weathering or binary mixtures (water-vapor plus contaminant). In addition, only two charcoals (BC-727 and NACAR G-615) have been examined.

Testing with water vapor as the only pollutant was performed at 50, 70 and 90% RH. The carbons increased in weight by approximately 50% after 100 hours exposure. Significant penetrations of methyl iodide were observed, as high as 16% for the entrance layer of BC 727; pH of water extract values did not drop significantly. In the cases evaluated, the NACAR G-615 carbon performed better than the BC-727

carbon (Table 9a in Reference 1), but these are only two of the carbons to be tested, and no conclusion as to a more suitable carbon or impregnant can be made at this time.

A water vapor (70 and 90% RH) plus sulfur dioxide (0.5 ppm SO_2) combination was used to weather the two carbons for 100 hours. In all cases, no sulfur dioxide was evident in the exit gases from the test bed, and the penetrations of methyl iodide (as high as 66% for the first layer) and the pH of water extract values (as low as 2.7 for the first layer) indicate drastic deterioration of the carbon. Total SO_2 insult was determined to be approximately 0.75 gm, which is significantly higher (by approximately a factor of 10) than expected due to ambient concentrations. Future work will attempt to reach the expected ambient concentration in the insult mixture.

Similarly to sulfur dioxide, no ozone was detected in the exit gases when 1-3 ppm were combined with 70 and 90% RH air. High penetrations for methyl iodide were observed (as high as 21.5% for the fourth layer), but pH valves were not significantly affected (Table 9b of Reference 1). Lower inlet concentrations will be achieved in future work.

Converse to sulfur dioxide and ozone, carbon monoxide (2.5 ppm in 90% RH air), passed through the charcoal unadsorbed. No change in carbon monoxide concentration from inlet to outlet of the test bed was observed.

In summary, the laboratory results obtained in FY77 show that the three pollutants water vapor, water vapor plus sulfur dioxide, and water vapor plus ozone degrade the two charcoals significantly in a short time, while carbon monoxide showed no degradation of the carbon.

III. Work in Progress and Results

Present efforts are directed towards weathering various carbons to outdoor exposures and to laboratory pollutant mixtures.

A. Exposures to Outdoor Air

Outdoor exposures are obtained by drawing air through the carbon samples as explained in Reference 1. The number of independent exposure positions has been increased to allow 12 samples to be weathered simultaneously.

Table 3 indicates the entire outdoor weathering program under evaluation. Entries in the table indicate the number of repetitive samples for the same charcoal that will be exposed for each time period listed, and entries in parentheses indicate that the exposures have not been completed.

Partial results are available for those samples that have completed their outdoor exposures in FY78. Values of the pH of water extract have been determined, but penetrations of methyl iodide are not yet available due to the procedural questions of equilibration for laboratory methyl iodide determinations as previously discussed in Section II of this paper. These results covering the NRL progress in FY78, will be published by December 1978.

Table 4 presents the results available on the two carbons BC 727 and NACAR G-615 that have been weathered for 6 months on the roof of the NRL Chemistry Building. The results for 1, 2, and 3 months from Table 2 are included for completeness. Using a lower pH value as indicating additional degradation, the monotonic decrease in expected carbon performance as exposure time increases is illustrated for the

TABLE 3

OUTDOOR WEATHERING PROGRAM

Exposure	EXPOSURE PERIOD, MONTHS 1	2	3	6	9
NACAR G-615	1	1	(4)	1	(1)
BC 727	(10)	2	1	1	(1)
SS 207	(5)	0	1	(1)	(1)
MSA 463563	2	0	1	1	(1)
2701	2	0	1	(1)	(1)
KITEG	1	0	1	(1)	(1)

Entries indicate the number of independent exposure periods.
Parentheses indicate tests not completed.

first bed layer, but it appears that the pollutants are not reaching subsequent layers of the bed to any great extent (pH of water extract values for unweathered carbons are 9.8 for NACAR G-615 and 9.5 for BC 727). These conclusions should be substantiated when 9-month exposure data are available and when the penetrations of methyl iodide for the exposed carbons are available.

Table 4 also includes the available data for the carbon MSA 463563. The indicated degradations for 3 and 6 months are values obtained during FY78; 1 month values are included for completeness from Reference 1. The expected increase of degradation with increased weathering time is observed, and it also appears that the pollutants are reaching the second layer to a significant degree after 6 months exposure (initial pH of water extract for unexposed MSA 463563 is 8.5). Results for 9 month exposures and for all penetrations of methyl iodide will be published by December 1978.

Three month outdoor exposures have also been completed for Sutcliffe Speakman 207B plus 5% TEDA (coal based, with an initial pH of water extract of 8.8), and KITEG (initial pH of 8.2). These results are presented in Table 5, including the 3-month data for NACAR G-615 and BC 727, to illustrate the effect of the carbon base, the impregnant, and the effect of the type of exposure (winter versus summer, wet versus dry period).

The meteorological conditions and pollutants, and the additional penetration of methyl iodide data will be published when available. The results presented for carbons MSA 463563 and 2701 are for the same exposure period, and for carbons Sutcliffe Speakman and KITEG are for the same exposure period.

TABLE 4

GRADIENTS IN THE PENETRATIONS (P) OF METHYL IODIDE AND THE pH OF WATER EXTRACTS AFTER 1, 2, AND 3 MONTHS EXPOSURE

Exposure	First Layer pH	First Layer P	Second Layer pH	Second Layer P	Third Layer pH	Third Layer P	Fourth Layer pH	Fourth Layer P
NACAR G-615								
5016 1 month	9.3	1.77	9.5	0.64	9.6	0.34	9.7	0.70
5031 2 "	8.2	3.42	9.8	1.32	10.0	0.86	10.0	1.02
5022 3 "	7.5	8.62	9.8	1.38	10.0	1.19	10.0	0.81
5056 6 "	3.8		9.4		9.6		9.6	
BC 727								
5014 1 month	8.8	2.67	9.3	1.20	9.3	0.68	9.3	1.31
5032 2 "	7.3	5.81	9.3	2.58	9.5	3.09	9.5	3.45
5020 3 "	7.0	21.6	9.4	5.4	9.5	5.0	9.5	5.7
5056 6 "	3.1		8.9		9.1		9.0	
MSA 463563								
5015 1 month	7.45	4.0	7.65	1.9	7.65	3.6	7.8	2.1
5021 1 "	6.7	15.5	8.2	8.0	8.2	8.8	8.2	8.4
5060 3 "	3.4		7.5		7.7		7.8	
5059 6 "	2.5		6.9		7.8		8.0	

TABLE 5

GRADIENTS IN THE PENETRATION (P) OF METHYL IODIDE AND THE pH OF WATER EXTRACTS AFTER 3 MONTHS EXPOSURE

Exposure	First Layer pH	First Layer P	Second Layer pH	Second Layer P	Third Layer pH	Third Layer P	Fourth Layer pH	Fourth Layer P
5022 NACAR G 615	7.5	8.62	9.8	1.38	10.0	1.14	10.0	0.81
5020 BC 727	7.0	21.6	9.4	5.4	9.5	5.0	9.5	5.7
5060 MSA 463563	3.4		7.5		7.7		7.8	
5063 SS	4.5		8.7		8.9		8.9	
5061 2701	3.6		8.2		8.5		8.6	
5069 KITEG	2.8		7.2		7.3		7.4	

The final results available for FY78 are additional one-month and two-month exposures for BC 727. Table 6 presents the pH of water extract values, and comparative values for FY77 exposures are included. From the two-month exposures, it appears that two winter months degrade the carbon to a greater degree than two summer months. An identical type of profile for the two month (February - March 1978) period is observed as was reported in Reference 1. That is, the first layer appears to act as a guard bed to remove the bulk of the contaminants, then any migration of impregnant complex will lead to a decrease in penetration for the subsequent layer, except for the fourth layer for which the penetration could increase due to the net loss of impregnant in the expelled air.

B. Laboratory Exposures

There are now two independent installations available to conduct the laboratory weathering experiments, allowing a greater accumulation of data in less time. Laboratory exposures that have been completed in FY78 have used water vapor as the single pollutant, and all exposures have been for 100 hours. Charcoals MSA 463563, AAF 2701, KITEG, and Sutcliffe Speakman have been exposed to air with both 50% and 90% RH. Table 7 lists the results available for the 90% RH exposures, including BC 727 and NACAR G-615 results as published in Reference 1, and Table 8 lists identical information for the 50% RH exposures. The penetration of methyl iodide values listed for MSA 463563 and NACAR G-617 carbons were evaluated according to Method B as discussed in Section II of this paper, i.e., use of one-fourth of each layer of the weathered sample to construct a test bed preserving the same entrance-to-exit sequence, and performing one methyl iodide penetration test on the 2-inch deep bed. Future tests for penetrations of methyl iodide to complete Tables

TABLE 6

CHARCOAL BC 727 EXPOSURES

Exposures	First Layer pH	First Layer P	Second Layer pH	Second Layer P	Third Layer pH	Third Layer P	Fourth Layer pH	Fourth Layer P
5014 June 77	8.8	2.67	9.3	1.20	9.3	0.68	9.3	1.31
5070 April 78	8.3		9.2		9.2		9.2	
5032 Aug-Sept 77	7.3	5.81	9.3	2.58	9.5	3.09	9.5	3.45
5065 Feb-Mar 78	7.3	13.4	9.3	5.4	9.2	5.1	9.4	6.0

TABLE 7

LABORATORY EXPOSURES AT 90% RH

Exposures	First Layer pH	First Layer P(%)	Second Layer pH	Second Layer P(%)	Third Layer pH	Third Layer P(%)	Fourth Layer pH	Fourth Layer P(%)
5036 BC 727	8.2	12.7	9.1	5.1	9.1	7.3	9.2	3.4
5037 NACAR G-615	9.5	2.0	9.5		9.4		8.8	2.1
5072 SS	8.6		8.7		8.7		8.7	
5074 NACAR G-617 P*=9.2%	9.6		9.6		9.6		9.6	
5076 KITEG	7.8		7.7		7.7		7.7	
5086 MSA 463563	8.3		8.3		8.3		8.2	

*= Penetration for a two-inch bed.

TABLE 8

LABORATORY EXPOSURES AT 50% RH

Exposures	First Layer pH	Second Layer pH	Third Layer pH	Fourth Layer pH
5053 BC 727	9.5	9.5	9.5	9.6
5054 NACAR G-615	9.9	9.9	9.9	9.9
5071 2701	9.0	9.0	9.1	9.1
5073 MSA 463563 P* = 4.7%	8.2	8.3	8.3	8.3
5075 KITEG	8.4	8.4	8.4	8.4
5085 SS	8.4	8.4	8.4	8.4

*= Penetration for a two-inch bed.

7 and 8 will also be performed according to Method B. From the pH of water extract values listed there does not appear to be sufficient variation to draw any meaningful conclusions.

IV. FUTURE WORK

Plans for future experimentation include outdoor exposures at NRL, laboratory exposures, examination of spent charcoals of known weathering history, and outdoor exposures at locations other than NRL.

A. Exposures to Outdoor Air

Table 3 indicates the charcoal samples that will be weathered in outdoor air at NRL. At the end of the program, all charcoals listed will have been weathered for 1, 3, 6 and 9 month periods. A number of charcoals will have been weathered for the same time periods, and one carbon (BC 727) will be weathered for nine 1-month periods to observe any seasonal variations. Selected exposed samples will be tested for methyl iodide penetration according to Method A (test each layer after mixing to obtain the profile), but most samples will be tested for methyl iodide penetration according to Method B, (use one-fourth of each layer of the weathered sample to construct a test bed preserving the same entrance-to-exit sequence and determine only one methyl iodide penetration). Samples will also be tested for methyl iodide penetration according to Method C (test without disturbing the weathered sample), once fabrication of appropriate canisters is complete.

Two carbons (BC 727 and Sutcliffe Speakman) will also be evaluated to determine any influence of "resting" a sample. For these tests, samples will be exposed for one month, held dormant (no weathering-inactive) for one month, then exposing for one additional month, and then analyzed for pH of water extract and penetration of methyl iodide values.

The sequence expose-inactive-expose-inactive-expose-test (resulting in a total of three months weathering) will also be examined.

B. Laboratory Exposures

Laboratory exposures are to be completed using water vapor as the single pollutant for the carbons MSA 463563, Sutcliffe Speakman, 2701, KITEG and NACAR G-617 at 70% RH, for 2701 at 90% RH, and for NACAR G-617 at 50% RH. This will result in all the carbons under study being evaluated at 50, 70 and 90% RH for 100 hours exposures.

An atmospheric pollutant will be added to the water vapor plus air mixture. First, hexane (2.5 to 5 ppm) will be added to 50, 70 and 90% RH air and used as the insult gas for BC 727 and NACAR G-615 carbons. Hexane will also be added to 70% RH air and used as the insult gas for MSA 463563, Sutcliffe Speakman, 2701, KITEG and NACAR G-617 carbons. Hexane is chosen to represent the total hydrocarbon (including methane) pollutant in the environment. Second, methyl isobutyl ketone will be added to 70% RH air and used as the insult gas for BC 727 and NACAR G-615 carbons. Methyl isobutyl ketone is chosen to represent a paint solvent pollutant. Third, ozone levels of 0.1 ppm will be achieved and added to 90% RH air for use as the insult gas for BC 727 and NACAR G-615 carbon. All of the above exposures will be for 100 hours.

Laboratory work will include cycling water vapor levels. For BC 727 and NACAR G-615 carbons, 50% RH air will be used as the insult gas for 50 hours followed by 90% RH air for 50 hours, and then evaluated (after the total exposure of 100 hours). The reverse order of RH values will then be examined; i.e., 90% RH air for 50 hours followed by 50% RH air for 50 hours.

Finally, selected synergistic combinations of pollutants (water vapor plus sulfur dioxide plus hydrocarbon, water vapor plus ozone plus hydrocarbon) will be used as the insult gas.

For all the above analysis of laboratory-exposed carbons, selected samples will be evaluated for penetrations of methyl iodide according to Method A (evaluate each one-half inch layer independently), but the majority will be evaluated for penetration of methyl iodide using Method B (use one-fourth of each layer of the weathered sample to construct a test bed preserving the same entrance-to-exit sequence and performing one penetration test on the 2-inch deep bed). The pH of water extracts and weight gains will be evaluated for all carbons exposed as a function of bed layer.

C. Outdoor Exposures at Locations Other Than NRL

Due to variation of contaminants in the atmosphere in both time and location, it is desirable to expose the carbons to outdoor air at locations other than NRL. General weather considerations will aid in the selection of suitable sites (the dry southwest, the humid southeast, industrial versus non-industrial areas), and data on the contaminants must also be available. Sites in close proximity to nuclear

power stations will be chosen. The exposed charcoals will be changed periodically and returned to the laboratory for examination of penetrations of methyl iodide, pH of water extract and weight gains. It is also planned to attempt to regenerate the spent carbon to recover methyl iodide trapping efficiency, and to analyze the carbon for the pollutants that have accumulated on the carbon (analysis of volatiles on programmed heating), and to determine the ignition temperature.

D. Examination of Charcoals in Different Stages of Service

Charcoals that have been in service at nuclear installations will be procured and will be analyzed similiarly to those carbons exposed at outdoor locations other than NRL. This information, with an indication of what service the carbon has experienced, will aid in correlating laboratory versus outdoor exposure data in order to predict the useful life of carbons.

V. Conclusions

Recognizing the need to determine the effect of atmospheric contaminants on the useful life of activated charcoal, the U.S. Nuclear Regulatory Commission contracted with the Naval Research Laboratory (Surface Chemistry Branch) to determine the extent to which such contaminants degrade commercially - available charcoals. The work is in the second year; results for FY77 have been published in NUREG/CR-0025, "Effects of Weathering on Impregnated Charcoal Performance", March 1978. This paper has briefly summarized the FY77 results, and also highlighted two problems with the evaluation of exposed carbons; the configuration to be employed for the laboratory determinations of the penetration of methyl iodide, and the equilibrium procedure used for such laboratory analysis. The pollutants water vapor, ozone and sulfur dioxide have been seen to seriously degrade the carbons, whereas carbon monoxide did not. It has also been shown that the longer the exposure, the more the carbon degrades, but this effect has not proved to be monotonic with bed depth. The laboratory and outdoor exposure work in progress has been summarized, which extends the time of exposure and the number and type of carbons to be tested. Future work will include different combinations of three (and more) pollutants as the insult gas, outdoor exposures at various U.S. locations, and examination of spent charcoal from nuclear power installations.

REFERENCES

1. U.S. Nuclear Regulatory Commission NUREG/CR-0025, "Effects of Weathering on Impregnated Charcoal Performance," V. R. Deitz (Naval Research Laboratory), March 1978.

2. American Society for Testing and Materials, "Standard Method for Radioiodine Testing of Nuclear Grade Gas-Phase Adsorbents," Draft Version, October 14, 1977.

3. Letter to H. Brockelsby, Reactor and Technology Support Division, Oak Ridge Operations Office, DOE from V. R. Deitz and J. B. Romans, Naval Research Laboratory, "Activities for March 1978, Project KZ, 03 04 03," 6170-211, May 1, 1978.

4. A. G. Evans, "Effect of Service Aging on Iodine Retention of Activated Charcoals," Proceedings of the Fourteenth ERDA Air Cleaning Conference, Sun Valley, Idaho, 2-4 August, 1976, USDOE Report CONF-760822, pp. 251-263.

DISCUSSION

EVANS: Why does charcoal weather faster in the winter?

BELLAMY: Additional data will be gathered during future work, but it appears that the combination of low temperature and moisture weathers the carbon to a greater degree than high temperature and moisture.

DEMPSEY: It appears that an in situ radioiodine test might be carried out through the charcoal samples now that you have accurate proportional flow data, i.e., a sufficiently small amount of radioiodine might be used to permit licensing. Do you think this would be possible?

BELLAMY: The present state of mind of the public with regard to the release of radioactivity to the atmosphere is such that these tests are impractical unless there is a very strong overriding technical reason for using a radioactive in-place test in preference to the standard in-place leak test with Freon and the corresponding laboratory radiotest for the carbon.

A NON-RADIOACTIVE DETERMINATION OF THE PENETRATION OF METHYL IODIDE THROUGH IMPREGNATED CHARCOALS DURING DOSING AND PURGING

J. B. Romans and Victor R. Deitz
Naval Research Laboratory
Washington, D.C. 20375

Abstract

A laboratory procedure is described using methyl iodide-127 which had the same linear flow of air (12.2 m/min) and contact time (0.25 sec.) as the RDT M16 Test Procedure. Only one-fourth of the charcoal was used (in a bed 2.54 cm diameter and 5.08 cm high) and the required dose of methyl iodide-127 was reduced from 5.25 to 1.31 mg. The inlet concentrations were determined with a gas chromatograph and the effluent concentrations with a modified microcoulombmeter. Two calibration procedures were used: (1) known vapor pressure of iodine crystals, and (2) quantitative pyrolysis of the methyl iodide-127 delivered from certified permeation tubes. Five charcoals and three impregnations were used in this study. Typical behaviors are given in 90% RH air with the charcoals either prehumidified for 16 hours at 90% RH or without the prehumidification. The breakthrough curves, concentration versus time, rose very slowly for the first 120 minutes and then more rapidly for an additional time. It is possible to determine the accumulated breakthrough for 120 minutes; good agreement was then found with the penetration for the same impregnated charcoals evaluated by the RDT M16 procedure with methyl iodide-131. It is concluded that the use of methyl iodide-127 is a feasible procedure to evaluate penetration. The lack of a dependence on the magnitude of the dose is compatible with a catalytic trapping mechanism. In the case of KI_x impregnations, there was excess emission of iodine during purging over that introduced as methyl iodide-127 which must have originated in the reservoir of iodine contained in the impregnation.

I. Introduction

Plant-scale and laboratory processes for the removal of airborne iodine by charcoal are examples of kinetic systems in gas adsorption. The iodine breakthrough behavior over the complete range of penetration is very complex (1,2,3). However, it has been demonstrated (4) that for small penetration (less than 2%), where only the beginning of the general sigmoidal dependence (Figure 1) is pertinent, some simplification is possible. The RDT Standard M16-1T, 1977, Test Procedure (5) is based on the total radioactive count in the sample and back-up beds after both the introduction of the methyl iodide dose and the 2-hour elution or purge period. The fraction of the penetration that occurs in each of these periods is not known and one objective of this paper is to obtain the magnitude for each fraction using several impregnated charcoals. The purge behavior is a most important safety feature of the charcoal trapping process.

The ability to make penetration measurements with non-radioactive iodine has several advantages. The necessary health physics requirements for radioactive materials are eliminated, a continuous monitoring of the methyl iodide concentration is possible, the cost of the radioactive methyl iodide is avoided, and in-place testing to monitor plant-scale charcoals filters is without restrictions. The quantity of methyl iodide-127 in a challenge gas is very large relative to that of methyl iodide-131, being in many cases of the order of magnitude of 10^4. Consequently, the detection of the non-radioactive species is favored and this helps to compensate for the higher sensitivity of radioactive counting.

The test procedure for the penetration of radioactive methyl iodide entails separate physical operations. First, the charcoal sample may be prehumidified for 16 hours before the introduction of methyl iodide or it may have been subjected to some systematic weathering program. Second, a specified does of methyl iodide may have been introduced during a known period either continuously or intermittently. The third operation is an air purge of the charcoal for a specified time. At this point the efficiency of the trapping process is generally determined. These operations have a sequential dependence and, therefore, another objective of this paper is to observe the behavior after each operation. The experimental parameters are: the magnitude of the methyl iodide dose, the relative humidity of the air flow, the duration of the purge period, and variations in the impregnation formulation and the base charcoal. All of these variations are readily followed using the non-radioactive technique and the results will be compared where possible with the trapping determined with methyl iodide-131.

2. Experimental Procedure

2.1 Scaling Factors

A dynamic test procedure was developed to study the penetration of non-radioactive methyl iodide. The scaling factor retained the RDT-M16 specification for linear flow, namely 12.2 m/min. (40 feet/min.) and the residence time of 0.25 seconds. A comparison is given below:

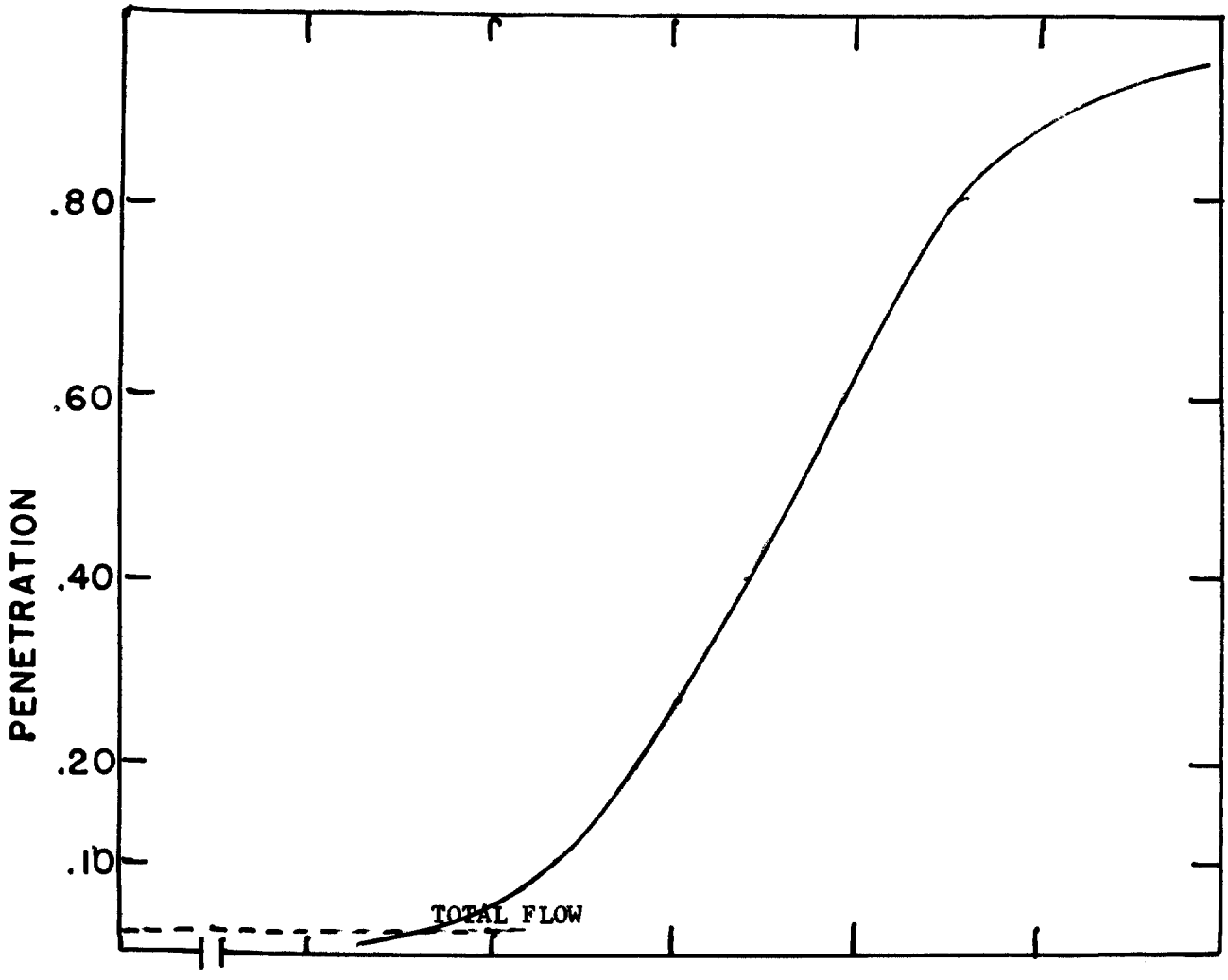

Figure 1: General dependence of fractional penetration over the complete range of breakthrough concentration (dotted line signifies a permissible upper level for satisfactory performance)

	RDT-M16	NRL Laboratory
bed diameter (cm)	5.08	2.54
bed height (cm)	5.08	5.08
linear air velocity (m/min)	12.2	12.2
residence time (sec)	0.25	0.25
volume flow (ℓ/min)	25	6.2
total methyl iodide (mg)	5.25	1.31
total methyl iodide (nm)	36900	9230
temperature ^{o}C	30	30

2.2 Schematic Flow Diagram

The air flow (6.2 ℓ/min) passed in sequence (Figure 2) through: (1) regulator and control valve(s), (2) dry test meter (American DTM 115), (3) particulate and charcoal filter, (4) humidifier, (5) electric hygrometer element, (6) mixing chamber, (7) gas sample opening to chromatograph, (8) thermostated container for the charcoal sample, (9) exit to detection elements, (10) exit to trap and vent. The cylindrical tube (8) was maintained at constant temperature by a surrounding split resistance heater with the controlling thermocouple located beneath the center of the bottom plate holding the charcoal. Additional thermocouples were located at the center of the bottom charcoal support and at the top center of the charcoal. The air flow could be sent either upward or downward through the charcoal; the present results were obtained with upward flow. Two side outlets (2 mm i.d. tubing) were available to sample the gases emerging from the mixing chamber (7) and at the outlet side of the charcoal (9). A mixture of methyl iodide and nitrogen was pressurized in a stainless steel bottle and metered as desired into the mixing chamber through a pressure regulator and a microneedle valve.

2.3 Detector and Calibration

A certified permeation tube containing liquid methyl iodide was used to calibrate a modified Hewlett-Packard gas chromatograph (5710 A series) equipped with a flame-ionization detector. The vapor permeates through the Teflon wall of the tube at a constant rate and the weight loss at constant temperature over a given time period served as the primary standard. The air flow across the tube (maintained at 30.0^{o}C) was varied 100-fold and the corresponding chromatographic peak heights (h) were measured. Typical data and the calculated concentration, $\underline{c}$, at 25^{o}C are given in Table 1. A least squares linear regression analysis gave the following relationship:

$$\underline{c}\ (\text{ppm}) = 0.342\ \underline{h} - 0.139 \quad \ldots\ (1)$$

In order to realize a dose of methyl iodide of 1.31 mg in two hours, an average concentration of 0.30 ppm (V/V) would have to be maintained. At unit attenuation this concentration corresponds to a peak height of 20.5 chart divisions.

The detector for iodine in the charcoal effluent stream was a modified microcoulombmeter (Mast Instrument Co. Model 724-2). Two independent calibrations were made. One was based on the known vapor pressure of iodine crystals and the second on the quantitative pyrolysis of the methyl iodide delivered from the certified permeation tube. Figure 3 is a schematic flow diagram of the calibration source of air + iodine vapor. Air was passed through charcoal and drierite and at position A entered the tube B containing Anhydrone (barium perchlorate). The dried air was then passed over iodine crystals in flask C

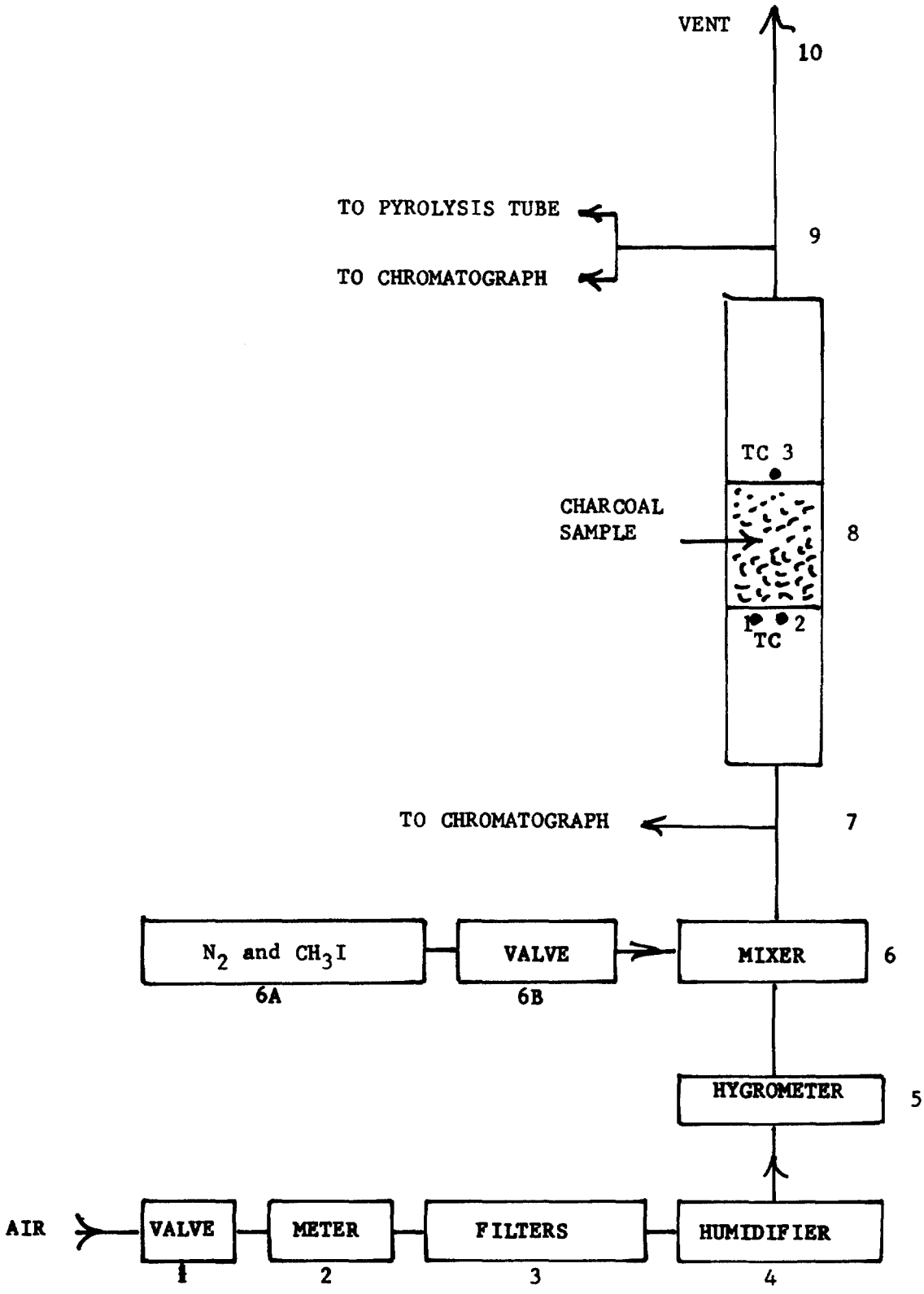

Figure 2: Flow Diagram for Methyl Iodide-127 Experimentation

Table 1: Calibration of gas chromatograph with a Certified Permeation Tube of methyl iodide held at 30.0°C.

Air Flow ml/min	Concn. ppm	Peak Height (attenuation 16) chart-divisions
199	0.23	0.4
203	0.23	0.3
56.7	0.82	1.9
20.9	2.23	6.5
9.80	4.75	14.1
7.01	6.63	19.8
3.64	12.8	36.8
31.7	1.45	5.6
12.3	3.74	13.9
12.7	3.63	13.7
5.2	8.85	28.4
13.4	3.44	10.1
2.6	17.4	51.6
3.6	12.8	34.6
58	0.79	1.4

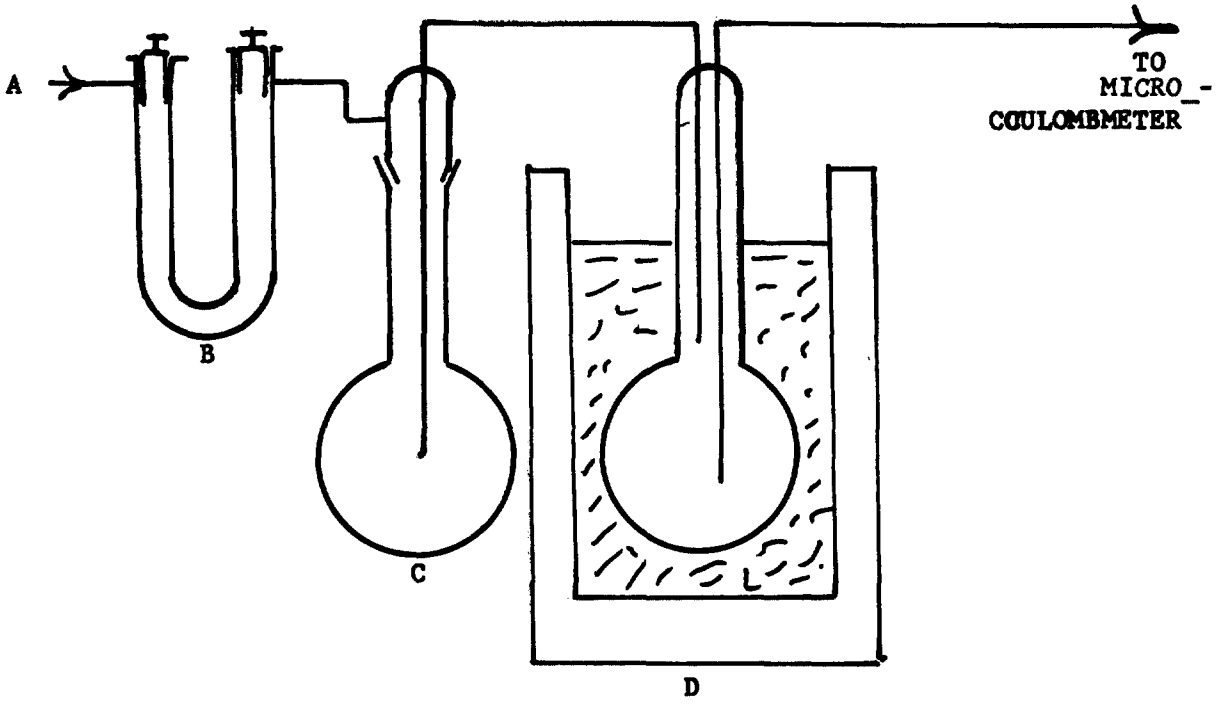

Figure 3: Calibration Source of Air and Iodine Vapor by Passage of Purified Air Over Iodine Crystals Held at Constant Temperature

Table 2: Pyrolysis of Methyl Iodide in Air Flows

Heating Current (amp.)	Temperature (center of tube)	Mast Coulombmeter mv	I_2 (ppm)		% Conversion
			Mast	Permeation Tube (calc.)	
1.4	448	0.08	.0005	.072	0.7
1.6	527	3.69	.056	"	78.
1.8	612	4.24	.067	"	93.
2.0	686	3.99	.062	"	86.
2.2	745	3.58	.054	"	75.

at room temperature and then into a second flask, D, held under the liquid level of a cryostat maintained at the desired temperature. Thus, the approach to the equilibrium vapor pressure of iodine was from a higher vapor pressure, a procedure found necessary to attain steady states.

The published data for the vapor pressure of iodine crystals at and below room temperature were reviewed and a least square linear regression analysis gave equation (2):

$$\ln p_{I_2} \text{ (torr)} = - 8148.4/T^{o}k + 26.361 \quad \ldots (2)$$

The output of the microcoulombmeter was shunted across a resistance of 5250Ω and the voltage drop (mv) was record. A plot of ln mv was made as a function of the reciprocal cryostat temperature (^{o}K) and a least square linear regression analysis gave equation (3):

$$\ln \underline{mv} = 6663/T + 31.736 \quad \ldots (3)$$

Combining equations (2) and (3) the following calibration formula was obtained

$$\ln p_{I_2} = 1.2229 \ln mv - 12.449 \quad \ldots (4)$$

The second calibration was based on the formation of I_2 in the pyrolysis of methyl iodide. It was necessary to regulate the temperature of the quartz tube within a narrow range in order to obtain a quantitative decomposition. The desired mechanism is given by

$$2\ CH_3I + \frac{7}{2}\ O_2 \rightarrow I_2 + 3H_2O + 2CO_2$$

When the temperature of pyrolysis is too high, a second mechanism of decomposition occurs, i.e.

$$2\ CH_3I \rightarrow 2\ HI + C_2H_4$$

The results for one series of pyrolysis experiments are given in Table 2. When the tube furnace around the quartz tube was held at 650 $\pm$ 20^{o}C (inside temperature of the tube), the conversion was practically quantitative (Table 3). The plot of methyl iodide introduced (ppm) as a function of iodine produced (Figure 4) gave a slope of 2 in agreement with theory.

2.4 Impregnated Charcoals

The results given in this report are concerned with five charcoals and three kinds of impregnation, Table 4. Additional studies with other charcoals and impregnations are in progress.

3.0 Results

3.1 Penetration during Introduction of Methyl Iodide

The breakthrough data can be presented as a function of time in terms of concentration (nanomoles/unit flow) or as the accumulated methyl iodide up to a specified time, $\underline{t}$. The latter at $\underline{t}$ = 120 minutes is required to make comparisons with the results obtained using radioactive methyl iodide-131. Typical behaviors are given (Figures 5, 6, 7) for charcoal BC 727 in air of 90% RH, either prehumidified for 16 hours at 90% RH or without prehumidification. The influence of prehumidification is to increase the penetration as previously

Table 3: Pyrolysis of Methyl Iodide-Air Mixtures at Optimum Temperature of 650°C

Mast Microcoulombmeter		Calcd. from Permeation Tube	% Conversion
(mv)	Iodine (I_2) ppm		
3.14	.063	.073	87
3.82	.081	.087	93
4.74	.105	.106	99
4.91	.109	.114	96
4.89	.109	.115	95
4.86	.108	.116	93
9.05	.161	.162	99
9.20	.164	.162	100
9.37	.168	.162	100
9.0	.160	.162	99
9.0	.160	.161	99
3.54	.073	.075	99

Table 4: Summary of charcoals studied in this report

Notation	Base charcoal	Impregnation
BC 727	coconut	$KI + xI_2 = KI_x$
NACAR 615	coconut	KI and TEDA
NRL 4314	coal, ACC	KIO_3 + KI + K_3PO_4 + HMTA
NRL 4315	coal, 207A	ditto
NRL 4316	coal, BPL	ditto

BC 727	8 x 16, Barnebey Cheney
NACAR 615	8 x 16, North American Carbon Inc.
ACC	6 x 14, Columbia Activated Carbon
207A	8 x 16, Sutcliffe, Speakman Co. Ltd.
BPL	8 x 20, Activated Carbon Division, Calgon Corp.
TEDA ≡	triethylenediamine
HMTA ≡	hexamethylenetetramine

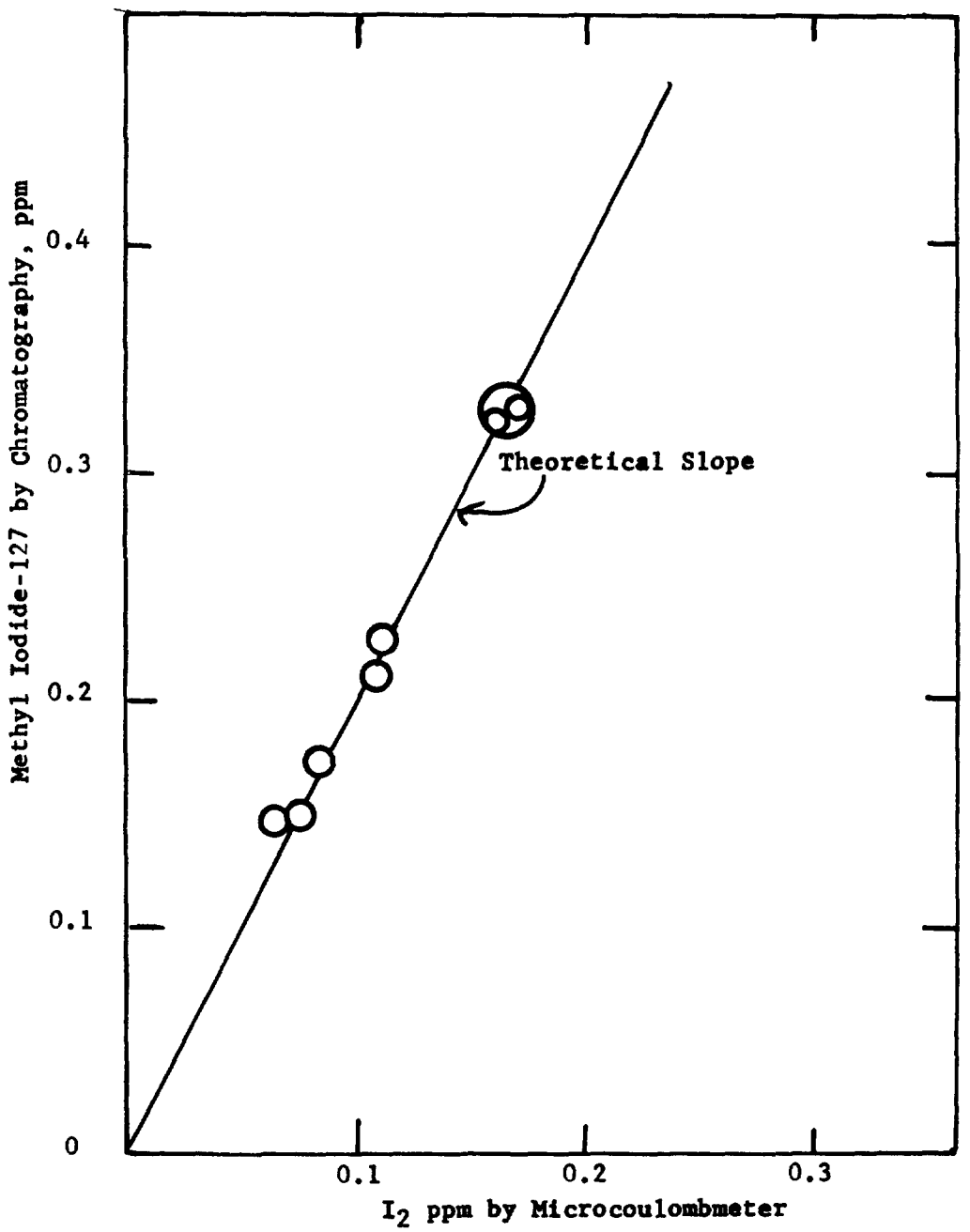

Figure 4: Correlation of CH_3I by Chromatography with I_2 by Microcoulombmeter

reported (6). The effluent concentrations at a specified time (Figure 5) were greater using prehumidification even though the average initial concentration of methyl iodide (21.8 nano m/liter) was less than for the experiment with prehumidification (33.2 nano m/liter). The measurements for the latter case, were also extended beyond 120 minutes.

The same experimental results are also presented in Figure 6 by the ratio of C_o/C as a function of time. The ratio is related to the decontamination factor K and is seen to decrease steadily with the magnitude of the incident dose.

The penetration of methyl iodide (Figure 7) was calculated as follows for a given time t:

$$\text{penetration } (\%) = 100 \frac{\text{Summation of effluent to time t}}{\text{Summation introduced to time t}}$$

When the charcoal sample was prehumidified, the penetration at t = 120 minutes was determined to be 2.1%. At this point the methyl iodide introduced was 16600 nanom. The point R on Figure 7 is the penetration (2.2%) observed with radioactive methyl iodide-131 for a sub-sample of the identical charcoal. This value was determined by the RDT test procedure in which 36,900 nm was introduced in 120 minutes. The corresponding points for the non-prehumidified sample given in Figure 7 are of the correct magnitude.

A comparison of the penetrations at 120 minutes is given for the five charcoals in Table 5. The agreement between the nonradioactive procedure and the RDT M-16 test is rather good. Although procedures use the same residence times and the same linear air velocity, the amount of methyl iodide required for the nonradioactive test is scaled to one fourth, i.e. 9230 nanomoles. It appears, therefore, from these results that the penetration for any given charcoal is independent of the methyl iodide concentration over approximately a 3-fold dose range.

3.2 Elution of Methyl Iodide during Purging

After the introduction of methyl iodide, the iodine in the effluent air stream was further monitored for the period required to reach the base line of the detector. With dry air as a carrier, there was not indication of a detectable penetration during the purge for any of the 5 charcoals. Also, with 90% RH air, there was no appreciable penetration with NACAR 615 charcoal. However, different behaviors were observed for the other charcoals; these are summarized in Table 6.

The effluent iodine from BC 727 (test 3287) continued to increase after the addition of methyl iodide was discontinued. The air flow was maintained at 6.2 L/min and the temperature at 30°C. As shown in Figure 8, it required about 20 hours for the total emission to level off. During the early stages the characteristic chromatographic peak of methyl iodide was observed. A summation of 28000 n moles of iodine were obtained from the time when the CH_3I was discontinued to the time when the detector base line was reached. This magnitude exceeded that introduced and can only have come from the reservoir of iodine in the charcoal impregnant (KI_x). The excess is approximately 1% of that in the charcoal sample.

The effluent iodine from charcoal 4316 (Figure 9) also continued to increase for about 2 hours after the methyl iodide was discontinued. During the early stages the characteristic chromatographic peaks of methyl iodide were observed.

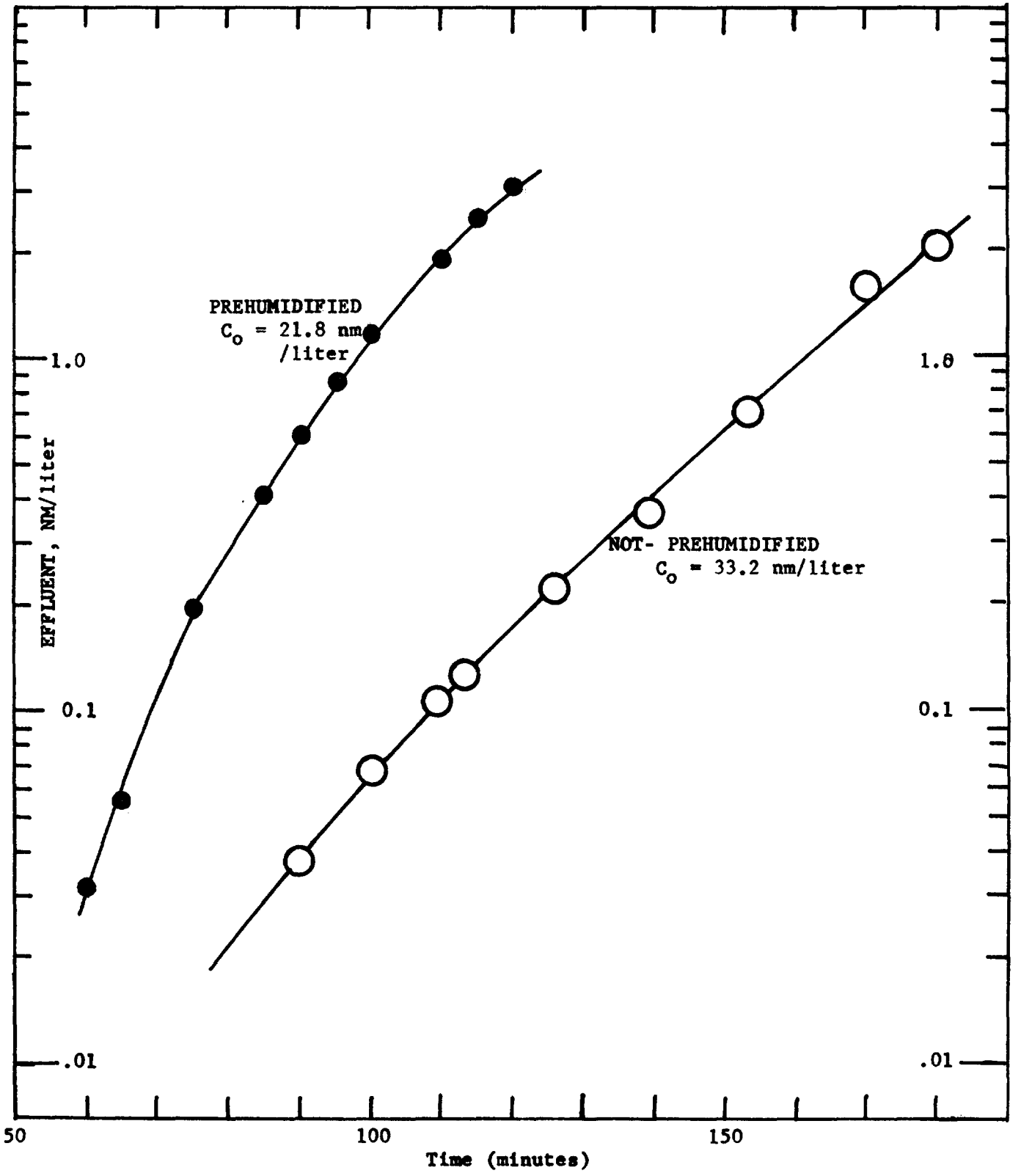

Figure 5: Effluent Concentration of Methyl Iodide-127 as a Function of Time During the Continuous Loading of BC 727 in 90% RH Air with (Test 3287) and without (Test 3283) Prehumidification

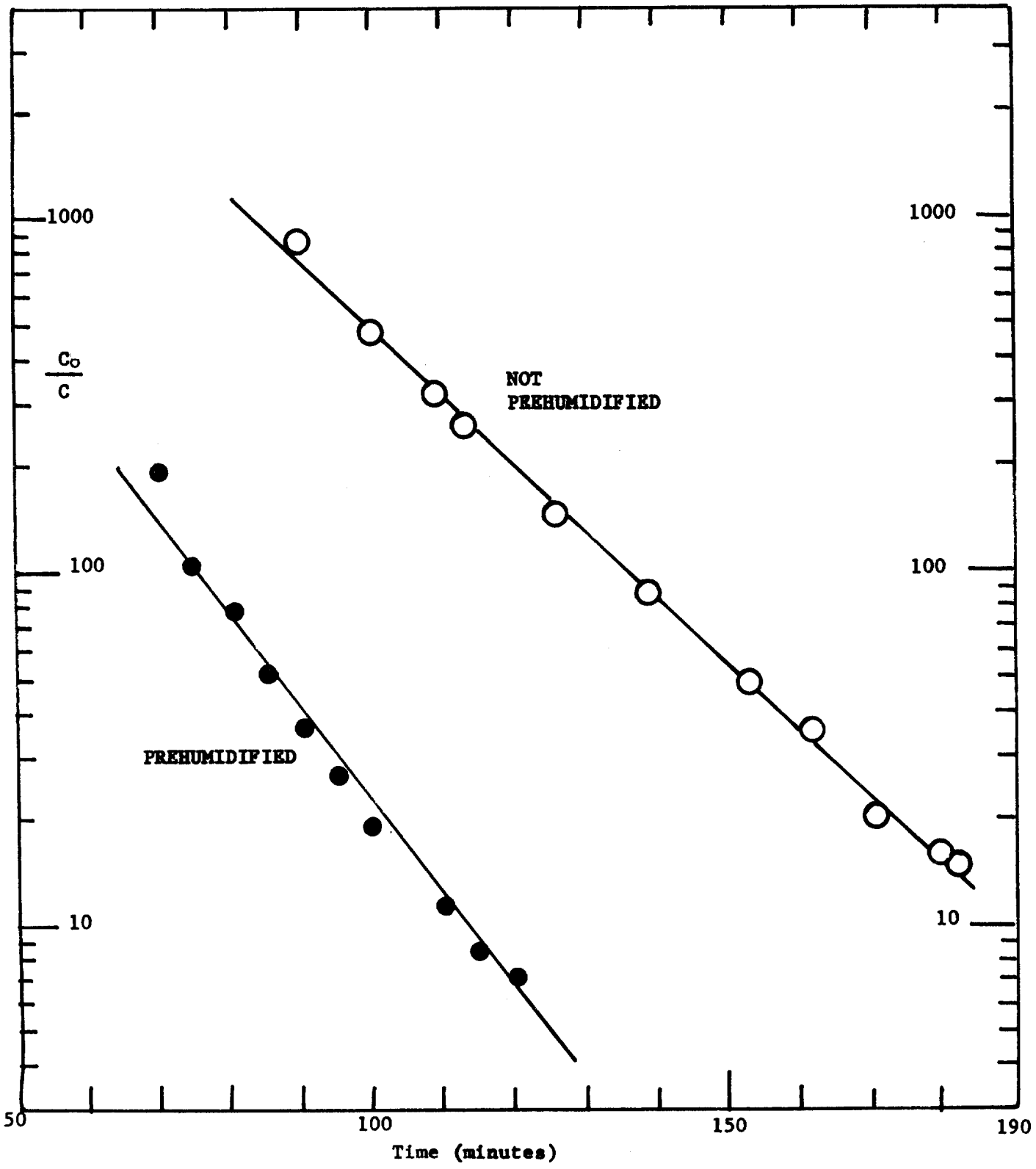

Figure 6: Dependence of C_o/C on Time when Charcoal BC 727 was Challenged Continuously with Methyl Iodide-127 in 90% RH Air with (Test 3287) and without (Test 3283) Prehumidification

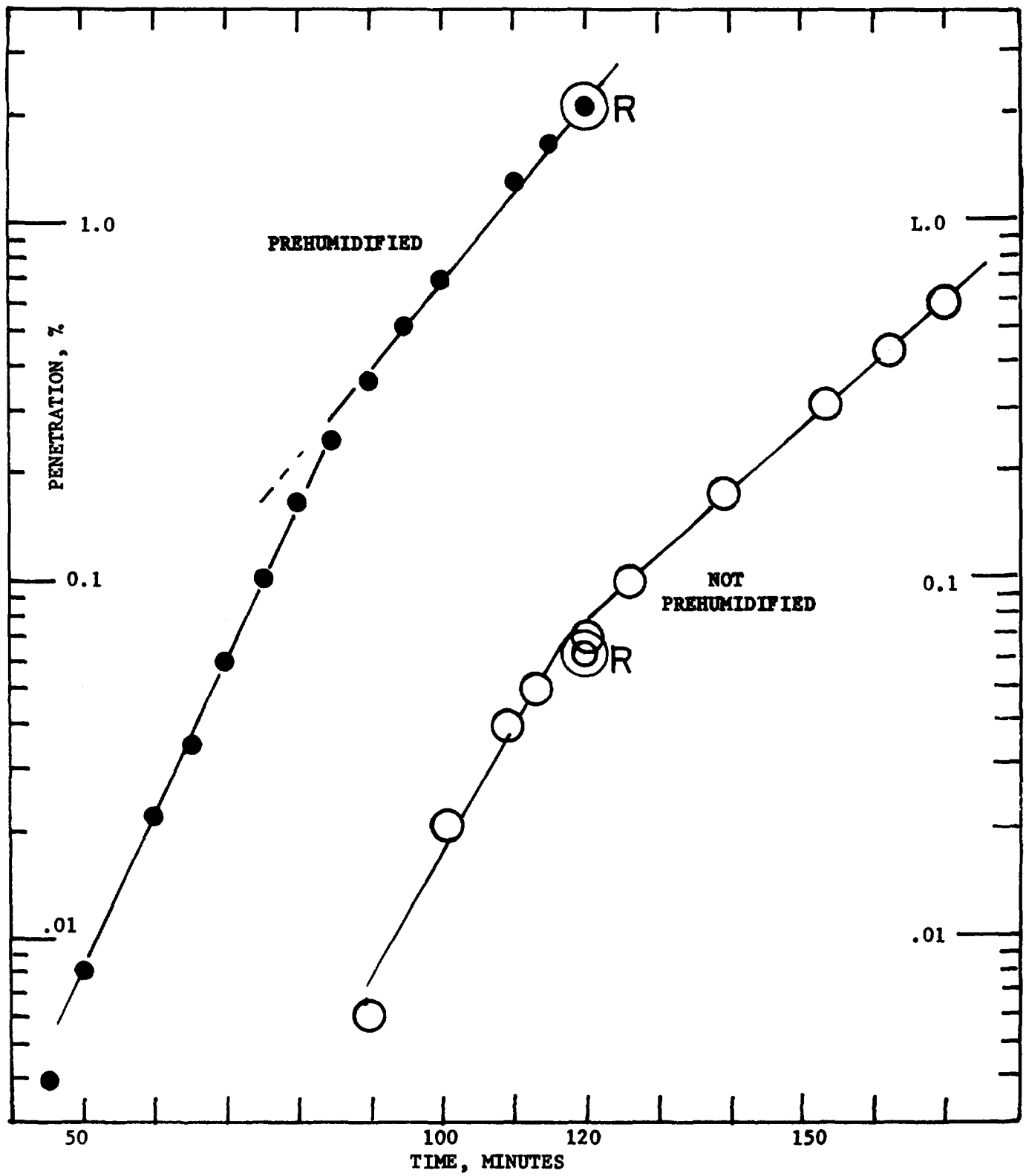

Figure 7: Penetration of Methyl Iodide-127 through BC 727 in 90% RH Air with (Test 3287) and without (Test 3283) Prehumidification. R denotes Independent Results with Methyl Iodide-131.

Table 5: Comparison of Penetrations at 120 minutes for five charcoals in 90% RH air

Charcoal	Procedures	Prehumidification	Test	Introduced n moles	Penetration %
727	CH_3I-131(EET)	yes		36900	2.2
	non-radioactive	yes	3287	16600	2.1
	CH_3I-131(EET)	no		110700	0.056
	non-radioactive	no	3283	26000	0.07
	non-radioactive	no	3276	19300	0.14
4314	CH_3I-131(EET)	yes		36900	1.73
	CH_3I-131(NRL)	yes		36900	1.54
	CH_3I-131(NRL)	yes		36900	1.82
	CH_3I-131(NRL)	no		36900	0.57
	non-radioactive	no	3269	31100	0.38
	CH_3I-131(NRL)	no		36900	0.10
4315	CH_3I-131(EET)	yes		36900	0.14
	CH_3I-131(NES)	yes		36900	0.24
	CH_3I-131(NES)	yes		36900	0.53
	CH_3I-131(NRL)	yes		36900	0.26
	CH_3I-131(NRL)	no		36900	< 0.01
	non-radioactive	no	3285	18400	.008
4316	CH_3I-131(NRL)	yes		36900	0.90
	non-radioactive	no	3286	16600	0.10
	CH_3I-131(NRL)	no		36900	0.051
NACAR 615	CH_3I-131(NRL)	yes		36900	0.27
	CH_3I-131(NRL)	no		36900	0.05
	non-radioactive	no	3277	12900	0.00

EET Environmental Engineering & Testing

NES Nuclear Environmental Services

NRL Naval Research Laboratory

The total of 957 nanomoles realized in the purge corresponds in this case to only 4% of that introduced as methyl iodide to the charcoal.

The five charcoals (Table 6) show quite different behaviors which must be related to both the charcoals and the chemical properties of the impregnant. The moisture concentration in the carrier air is definitely a factor, and for a given charcoal and moisture content of the air, the amount of methyl iodide introduced influences the quantity purged.

The emission of iodine on a programmed heating of impregnated charcoals is another problem and the results of such measurements will be treated in a subsequent report.

4.0 Discussion

In so far as evaluation of the penetration of methyl iodide through impregnated charcoals is concerned, the use of non-radioactive methyl iodide appears to be feasible. The use of a detector of suitable sensitivity will eliminate the need for the preliminary pyrolysis of low-level methyl iodide that was used in the present work. Chromatographic systems using electron capture detectors have been demonstrated to be useful in atmospheric studies and preparations are in progress at NRL to use this system in future iodine penetration studies with impregnated charcoals.

The lack of a strong dependence of penetration on the magnitude of the methyl iodide dose is useful and points to a trapping mechanism which has catalytic attributes. Nevertheless, the adsorption of the reaction products and the unavoidable presence of atmospheric contaminents creates a situation where both adsorptive and catalytic properties are involved.

The excess emission of iodine over that introduced to charcoal as methyl iodide can be explained in part by the reactivity of catalytic surface complexes with the iodine contained in the impregnation formulation. A sequence of reactions results in the gasification of a fraction of the impregnated iodine and the reaction products can readily be detected using the non-radioactive technique. The gasification of impregnated iodine might have an important advantage in expediting an isotope exchange which, in view of the large excess of normal iodine-127 in the impregnation, would contribute significantly to the overall trapping of iodine-131.

Three series of measurements were made with methyl iodide-131 in which the back-up beds were replaced by new material periodically - after the introduction of the dose and after each hour of the purging period. Thus, the total penetrations could be divided into the fraction during the dosing and that during the purge periods. The results (Table 7, using BC-727 prehumidified, BC-727 not prehumidified, and NACAR 615 prehumidified) demonstrate that the major penetration takes place during the introductions of methyl iodide-131 and in relatively much smaller amounts during purging. The sample of BC-727 gave a small steady penetration during purging, much smaller, however, than that observed with CH_3I-127. The sample not prehumidified was challenged with three times the dose (15 mg CH_3I-131) and had considerably more activity (total count 800000 cps). Nevertheless, the purging behavior was almost identical for both prehumidified and not prehumidified samples.

Table 6: Comparison of the Quantities of Methyl Iodide Purged After the Dosing

	Test	Introduced		Purge		
		Total (nano m)	RH %	Time (min)	Total n moles	RH%
BC 727	3283	36900	90	2900	78,800	dry
	3287	16600	90	1210	28,000	90
(prehumidified)						
	3276	29800	90	1125	23,090	90
4314	3268	101700	dry	---	< 1	dry
	3274	13260	dry	1022	< 1	dry
	3273	32960	53	184	945(incompleted)	50
	3272	54560	90	990	7,840	90
4315	3285	26200	90	670	1,400	90
4316	3286	22480	90	1160	957	dry
NACAR 615	3277	19650	90	4020	< 1	90
	3284	24290	90	1120	< 1	90

Table 7: Penetration (%) of Methyl Iodide-131 During the Dosing and the Purging Periods

	Time (hrs)	BC 727 Prehumidified	BC 727 Not Prehumidified	NACAR 615 Prehumidified
Introduction	2	2.178	0.0557	0.382
1st Purge	1	.0333	.0272	.010
2nd Purge	1	.0063	.0086	.000
3rd Purge	1	.0054	.0053	.000
4th Purge	1	nd	.0067	.000
5th Purge	1	nd	.0080	nd

Acknowledgement is made to EET for these measurements; nd ≡ not determined

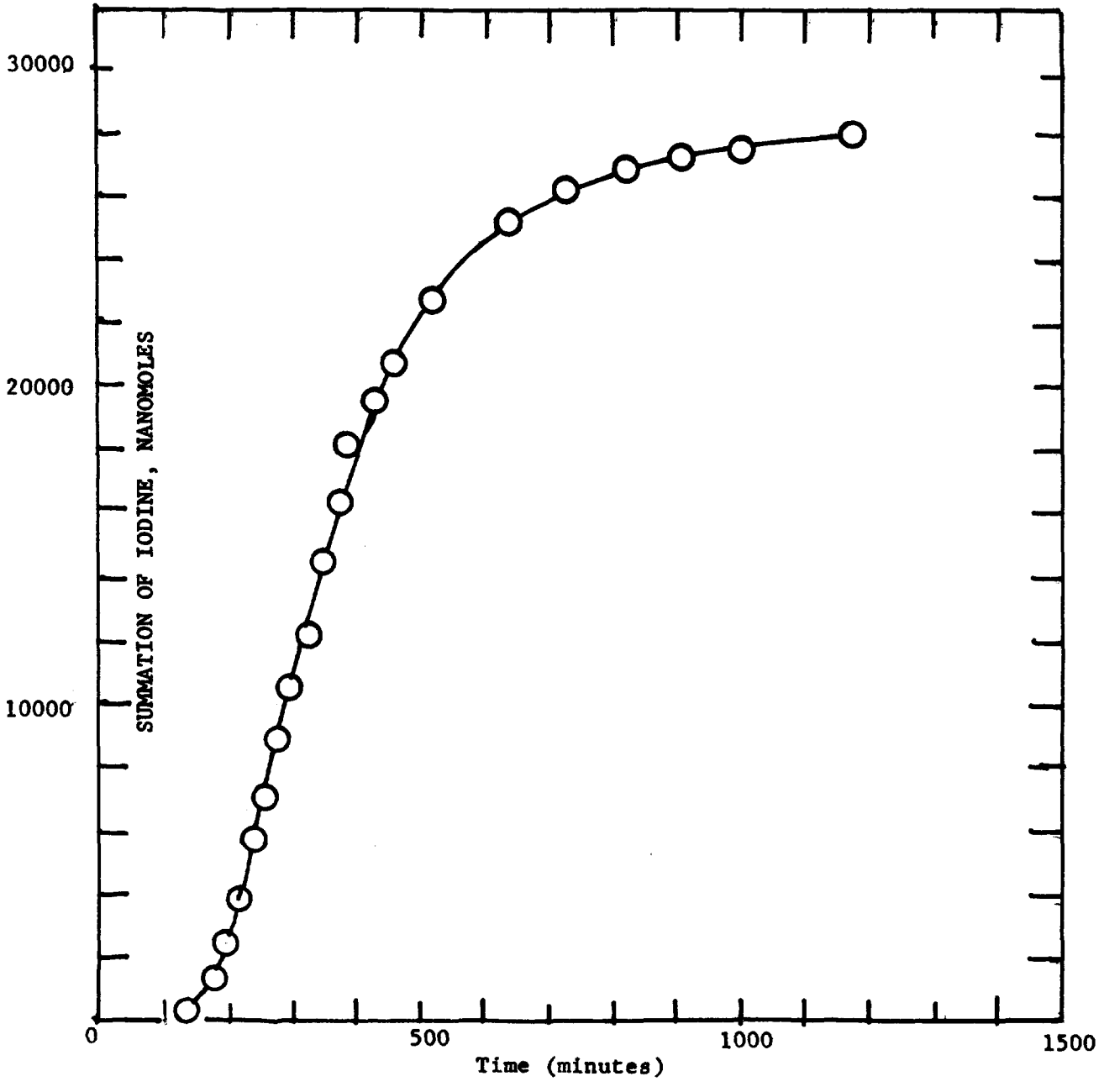

Figure 8: Purging of Charcoal BC 727 (Test 3287) after the Introduction of 16620 nanomoles of CH_3I in 120 minutes

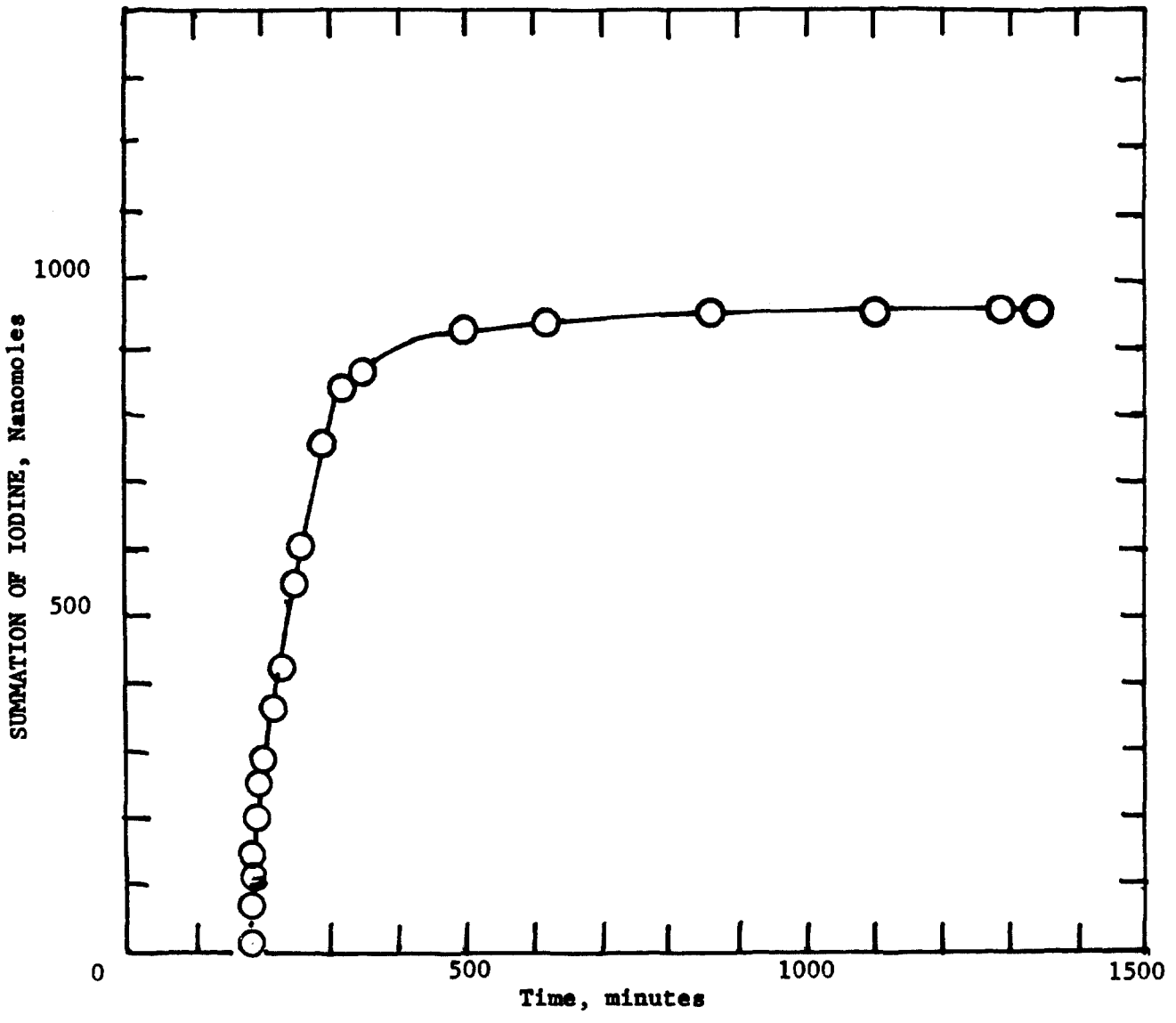

Figure 9: Purging of Charcoal 4316 (Test 3286) after the Introduction of 22480 nanomoles of CH_3I in 180 minutes

Impregnations on charcoals that contain KI_x as part of the formulation could have a special behavior due to the reactions

$$K^+I^-_3 + H_2O \rightleftharpoons K^+I^- + I_2 \cdot H_2O$$

During the purge in the presence of water vapor the small fraction present as molecular iodine will have greater mobility and would in part become airborne. As previously mentioned, in the absence of water vapor there is no release of iodine. Hill and Marsh (7) have shown that the free iodine species and not the total iodine concentration controls the rate of adsorption processes in solutions, but in vapor phase adsorption additional processes may be involved. The iodide species, I^-, on the surface of a charcoal may be slowly oxidized to elementary iodine and the resulting iodine while mostly chemisorbed may also partly gasify. In the absence of water vapor the dominant species at the interface with charcoal is $K^+I^-_3$ and this prevents gasification of both impregnated and adsorbed iodine species. Gasification, of course, is a mechanism that can slowly exhaust the original level of iodine in the impregnation.

Very important questions remain as to the influence of contaminants on both the dosing and purging mechanisms. The kinetics of desorption does not follow a simple exponential decrease and further study is warranted on this important safety feature of the iodine trapping process.

5.0 Conclusions

The use of methyl iodide-127 is a feasible procedure to evaluate penetration. The same results are obtained as with CH_3I-131 which uses a counting technique. One may conclude that the charcoal efficiency in trapping methyl iodide is independent of the iodine isotope species; in fact, the major fraction of the iodine present in a dose of CH_3I-131 is of course CH_3I-127. Moreover, the surface reactions responsible for trapping are independent of the iodine specie. The particular choice of technique may rest on the available instrumentation, i.e. counting equipment or sensitive chromatographic detection. Nevertheless, the charcoal is a sink for all iodine specie and it is important to follow the changes in the major component, i.e. I-127.

The purging of a charcoal with air can be effectively followed using CH_3I-127. The moisture concentration in the carrier is definitely a factor and, for a given charcoal and moisture content of the air, the quantity purged depends on the magnitude of the methyl iodide introduced. The purging of a KI_x impregnated charcoal after dosing with CH_3I-131 (Table 7) shows qualitatively similar behavior to CH_3I-127. The count rate per hour did not appreciably change in the last four hours of purge which is compatible with the purge after the CH_3I-127 challenge. The attainment of an exchange equilibrium between CH_3I-127 and CH_3I-131 when in contact with charcoal is the main problem for the correctness of the results of this analysis.

Acknowledgement

The sponsorship of the Division of Nuclear Fuel Cycles and Production, D.O.E. and the complete cooperation of John C. Dempsey, Contract Manager, are gratefully acknowledged.

References

(1) Klotz, I. M. Chem. Rev. 39, 244 (1946).

(2) Wheeler, A. "Advances in Catalysis" Vol. III, 249-327 Reinhold Publishing Co., New York, N.Y. 1951.

(3) Jonas, L. A. "Gas Adsorption Kinetics," 1970 Thesis to the Graduate Faculty of the University of Maryland in fulfillment for the degree of Doctor of Philosophy.

(4) Deitz, V. R. and Jonas, L. A. Nuclear Technology 37, 59-64 (1978).

(5) RDT Standard, M16-IT, 1977 DOE, Division Nuclear Power Development.

(6) Deitz, V. R. and Blachly, C. H. Proc 14th ERDA AIR CLEANING Confr. 2, 836-843/1976).

(7) Hill, A. and Marsh, H. CARBON 16, 31-39 (1968).

DISCUSSION

KOVACH: What is the difference or improvement in your work using the Mast instrument over the data reported in the 9th Air Cleaning Conference?

DEITZ: The improvements produced by the use of the Mast instrument over that used by Hoffman and Thompson were:

(a) Repeated calibration using (1) the vapor pressure of iodine crystals and (2) the quantitative pyrolysis of methyl iodide from calibrated permeation tubes.
(b) The solutions in the coulomb meter were changed to minimize and to stabilize the base line signal.
(c) Adjusted resistance in the electronics to optimize the response of the recorder used.
(d) Use of glass tubing only, with minimum Teflon tubing for connections.
(e) The Mast instrument avoids exposure to too-high concentrations of iodine and never saturates the electrode.
(f) A one-way clutch drive on the pump for mechanical convenience.

The detection limit of our modified instrument is estimated to be 0.01 mv and the precision about 0.05 mv.

KOVACH: How does your procedure show up $CH_3{}^{131}I$ removal by isotope exchange on KI_x-impregnated carbons?

DEITZ: The use of both $CH_3{}^{127}I$ and $CH_3{}^{131}I$ show the same qualitative behavior with a KI_x-impregnated charcoal. The effluent iodine in the purging periods continued at a constant concentration level. The purging with $CH_3{}^{127}I$ was followed for 20 hours (Figure 8) and that for $CH_3{}^{131}I$ on the same sample for 5 hours (Table 7). The surface reactions involve a heterogenous isotope-exchange

mechanism.

We have not located any published account of an iodine release during the purging of impregnated charcoals with air following a challenge of methyl iodide. It is important to understand that the iodine release occurs only after a challenge of methyl iodide. Before the challenge, no trace of released iodine was observed in the air flow. We postulate that the surface complex, formed in the trapping mechanism of methyl iodide, persists and there is sufficient surface mobility at high relative humidity to gasify the iodine of impregnation.

EFFECT OF PORE STRUCTURE ON THE ACTIVATED CARBON'S CAPABILITY TO SORB AIRBORNE METHYLRADIOIODINE

A. J. Juhola and J. V. Friel
MSA Research Corporation
Evans City, PA 16033

Abstract

A study was conducted to determine the effect pore structure of activated carbons has on their capability to sorb airborne methylradioiodine. Six de-ashed carbons of very diverse pore structure were selected for study. Batches of each were impregnated with (1) 4.3% I_2, (2) 5.6% KI, (3) 2% KI, (4) 3% KI - 2% I_2, (5) 2% I_2, and (6) 3.4% KIO_3. Some carbon was reserved for testing without impregnant. Standard procedures at ambient temperature and pressure were followed in the methyliodide testing, with some changes only made to meet the requirements of the specialized study.

Since water is adsorbed by capillary condensation, the adsorbed water fills the pores to different levels depending on the relative humidity at which the carbon was equilibrated, thus leaving an open-pore volume available for the methyliodide sorptive processes. The surface area of the open-pore volume, for KI impregnated carbons, determined the sorptive efficiency. This relationship is expressed by the equation

$$\ln p = \ln a - ks$$

where p is the fraction of methyliodide penetrating the bed and s the surface area. The quantity (a) is associated with the macropore properties, and determines the capability of the carbon to sorb at very high humidites (>95% RH). Constant k is to a large degree dependent on the mean diameter of the micropores.

Elemental iodine impregnated carbons were considerably less effective than those impregnated with KI, and their sorption of methyliodide did not follow the above equation. Their activity could be increased by a second impregnation with KOH. KI impregnated carbons lost their activity when treated with HCl on converting the KI to I_2. The conversion of KI to I_2 by acid gases in nuclear power plants offers an explanation for the cause of carbon aging.

I. Introduction

It has been amply substantiated that in common usages of activated carbons, such as in solvent recovery, gas masks, sugar refining, waste water treatment, air purification, water purification, and air pollution control, the pore size distribution is the determining factor in the suitability of the carbon for the intended use. The manner in which the pore structure functions in this respect was discussed in a recent lecture by Juhola.[1] Except for the survey conducted by Dietz and Burchsted,[2] no attempts appear to have been made to establish a relationship between pore structure and organic iodide sorption, although, on the basis of observations made in the above mentioned other applications, the pore structure should be a very important factor.

The results presented in this paper are preliminary observations on an in-depth study of the effect of the pore size distributions of several diverse types of activated carbons on their capability to sorb methyliodide. The ultimate objective is that the results of the study will determine the optimum pore structure.

II. Experimental

Methyliodide Test

Standard procedures at ambient temperature and pressure were followed as far as possible, with some changes made only to meet the requirements of the specialized study. A one-inch test bed depth was used, rather than the standard two-inch, to get a larger count in the backup bed, and thereby, improve the accuracy of the test results. Methyliodide injection period was 90 min followed by 90 min pure air flow. Concentration was maintained at a level to deliver 2.0 μl of methyliodide into the carbon beds in the 90 min. For each carbon, tests were conducted at different water contents, from almost dry to saturated state (~99% RH). Sieve size of the carbons was 8 to 16 U.S. standard.

Activated Carbons

Six carbons of very diverse pore structure were selected for study. They were repeatedly leached with HCl, HF, and water to reduce the ash content to low levels to avoid contributions to methyliodide sorption other than that due to pore structure or added impregnants. Table I presents properties, other than pore structure, of the six carbons to indicate the low level of ash attained and diversity of the carbons in other respects.

Table I. Properties of the carbons

Carbon	Base material	Bulk density, g/cc	Ash, %	Total surface area, m^2/g from pore dist.	Total surface area, m^2/g from I_2 No.	Pore vol, cc/g
1	Coal	0.55	0.4	820	730	0.42
2	Coconut	0.49	0.3	1160	1170	0.72
3	Coconut	0.40	0.2	1360	1380	1.10
4	Coal	0.51	0.8	1070	1070	0.69
5	Coal	0.29	0.1	1260	1330	1.60
6	Lignite	0.36	1.4	800	650	1.10

Carbons 2 and 3 are frequently used in nuclear power plants.

Total surface area measurements are included in the table since the area is one of the first properties that many investigators attempt to correlate with whatever sorptive property is being investigated. It is also one of the specifications given for carbons used in the nuclear power plants.

The surface areas from pore size distribution curves were calculated using the equation

$$\text{Surface area, } m^2 = \sum_{\bar{D}=10}^{\bar{D}=100{,}000} 40{,}000\ \Delta V/\bar{D} \qquad (1)$$

where ΔV in cc is a small increment of pore volume having an average diameter $\bar{D}$ in Å.

The surface areas from I_2 No. were calculated using the equation(3)

$$\text{Surface area, } m^2/g = [I_2 \text{ No.}(mg/g) - 17] / 1.07 \qquad (2)$$

The iodine number is determined by liquid phase adsorption from a solution of 0.1 N in I_2 and 0.116 N in KI. It is given in mg/g carbon when final solution concentration is 0.02 N.

The BET surface area was determined only for carbon No. 2 and was 1280 m^2/g. BET surface areas for carbons are generally incorrect on the high side, and the error becomes larger as the area is larger. Areas have been reported of over 3,000 m^2/g although the theoretical maximum is 2,630 m^2/g. BET areas were not used in this study.

Impregnation

Various batches of carbons were impregnated with: (1) 3% KI, 2% I_2, (2) 5.6% KI, (3) 2% KI, (4) 4.3% I_2, (5) 2% I_2, and (6) 4.3% KIO_3. Tests were also made on carbons with no impregnant added. To determine the effect of acidity and basicity, some carbons impregnated with 4.3% I_2 were again impregnated with KOH, and some carbons impregnated with 5.6% KI were treated with HCl acid. Several runs were made on unleached carbon No. 3 impregnated with 3% I_2 to determine the effect of alkaline ash.

The elemental iodine was sublimed into the carbon by placing the weighed mixture into a sealed rotating jar, and rotating it for 3 hr.

The KI, KI-I_2, KOH, KIO_3 were sprayed on from water solutions using the rotating jar to get uniform distribution of solution on the carbon. An attempt was made to use only enough solution to just wet the exterior surface of the granules when all the solution had been sprayed. The pore volumes given in Table I were used as guide in determining the amount of solution needed. However, it was found that the exterior of the granules started to get wet with less solution than that required to fill the pore space. The amount of solution required varied from carbon to carbon, but satisfactory results were obtained when solution volume was 80% of pore volume. The slightly surface-wet carbon was then dried until the granules were surface-dry by blowing an air stream into the rotating jar. Drying was completed in an air convection oven at 110°C.

Analyses were made on several of the carbons impregnated with the 3% KI - 2% I_2 mixture to determine whether any changes in chemical composition occur to the mixture because of contact with the carbon surface or interaction with the remaining ash. The dry, weighed carbon sample was first leached with hot water and then dried and weighed to get weight decrease. The sample was then leached with hot NaOH solution and hot pure water, and then dried and weighed to get second weight decrease. The rationale of the procedure is that pure water only removes KI and iodides formed by reaction of the elemental iodine with the remaining ash, and the NaOH solution removes the elemental iodine. The results of these measurements are given in Table II.

Table II. Measurements to determine chemical changes in 3% KI - 2% I_2 impregnated carbons

	% wt. decrease, based on final wt.				
	Carbon 1	2	3	4	6
Water soluble	2.3	2.5	3.3	2.5	2.3
NaOH sol'n soluble	2.8	2.7	2.3	3.2	3.6
Totals	5.1	5.2	5.6	5.7	5.9

On carbons 1, 2, 4, and 6 there appears to be a conversion of the iodide to the elemental form, while no change occurred in carbon 3. The final leach on de-ashing of carbons 1, 2, 4, and 6 was HF and water until neutral to litmus paper while the final leach on carbon 3 was NaOH and water until neutral. Apparently, enough acidity remained in carbons 1, 2, 4, and 6 to cause conversion of the iodide to iodine.

The weight decrease for each carbon is larger than the 5% impregnant initially added. This may in part be explained by further loss of ash and also by chemical reactions where there is a possible release of H_2O or O_2.

These determinations emphasize the fact that when imprenants are added to even relatively ash-free carbons, the impregnants can undergo chemical changes when subjected to moisture and elevated temperatures during drying. To recognize these possibilities is important to the interpretation of the methyliodide sorption test results.

Pore Size Distribution Curves

Figures 1 and 2 present the pore size distribution curves of the six carbons studied. The pore size distributions were determined from water adsorption data according to the methods developed by Juhola and Wiig,[4,5] with some recent modifications added to the procedures. These are (1) the diameter distribution of the pore cavities are now calculated from the adsorption branch of the water adsorption, and (2) a correction is made for helium adsorption in the helium displacement determinations.[6] The broken line curves represent the distribution of cavity diameters, and the solid line curves the distribution of the constriction diameters. For future reference, micropore volume is defined as volume of pores of diameter less than 30Å on the constriction distribution curve, and of pores that are larger, as macropore volume. The point of division is marked by X on each distribution curve.

The water-adsorption method is effective from about 10Å, at $P/P_o = 0.3$ on the adsorption isotherm, to about 2000Å, at $P/P_o = 0.995$. In pores of less than 10Å, the restrictive size of the pores prevents normal hydrogen bonding between water molecules, hence the vapor pressure of adsorbed molecules in these pores is higher than normal. When the Kelvin equation is used to calculate pore size of carbons with molecular sieve size pores, the pore diameters derived are then erroneously large. However, commercial activated carbons are generally activated to the level where very small volumes of pores less than 10Å are present.

In pores larger than 2,000Å, the mode of water adsorption appears to change from capillary condensation to multilayer, hence, the exterior surface of the carbon granules become visibly wet before enough water has been adsorbed to fill the pore space. This is of academic interest in isotherm determinations, since meas-

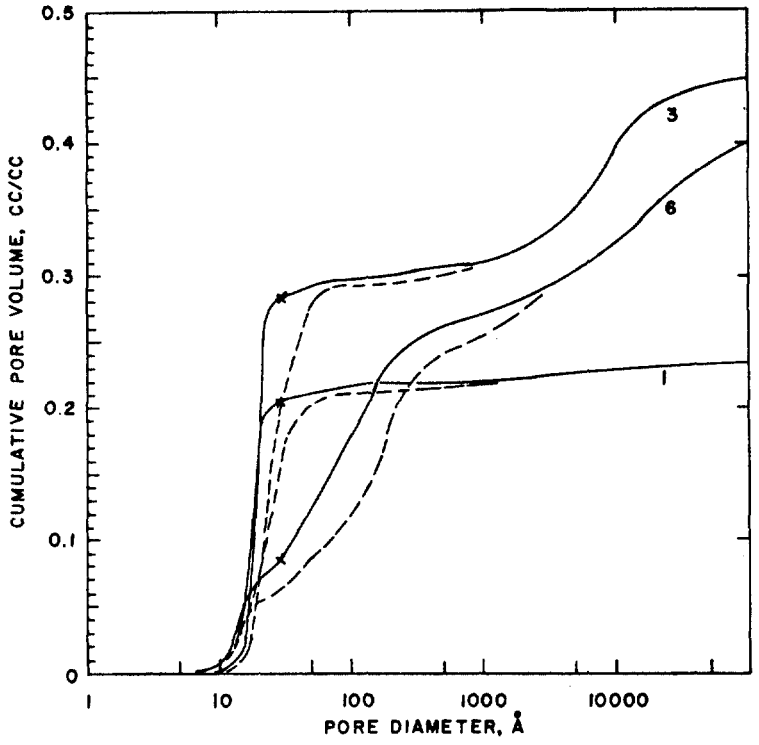

Figure 1 Pore size distribution of activated carbons.

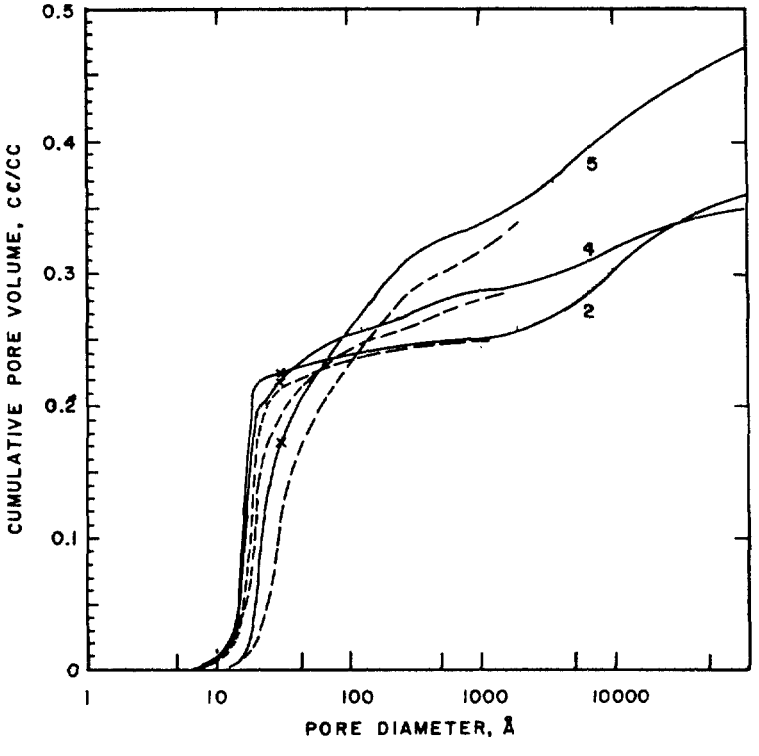

Figure 2 Pore size distribution of activated carbon.

urements at P/P_o over 0.995 are too difficult to attain any degree of accuracy. However, in nuclear power plant applications, humidities above 0.995 P/P_o are attainable, and as will be shown later in this report, this has a large effect on methyliodide sorption.

Available Pore Volume and Surface Area

Since water is adsorbed by capillary condensation, at any water content there is a measurable pore volume and an associated surface area that are available for interreaction with the methyliodide molecules. Figure 3 shows the relationship between these two properties for each carbon. The point of division between micro- and macropores is again marked by X. Macropores are to the left of X on the pore volume scale and micropores to the right. The highest point on each curve represents the total surface area or pore volume of the dry carbon.

In calculating available pore volume, 0.90 g/cc was used for the density of adsorbed water to convert adsorbed weight of water to volume. This volume was then subtracted from total pore volume as determined by helium and mercury displacement measurements.(5) Equation 1 was then used to calculate the surface area associated with the available pore volume.

As is apparent from the location of the X marks on the curves in Figure 3, only a small fraction of the total surface area is in macropores. Table III gives the numerical values of these pore volumes and surface areas.

Table III. Volume and surface area of micro- and macropores of each carbon bed, 51 cc bed volume.

	Pore vol, cc/bed			Surface area, m^2/bed		
Carbon	Micro	Macro	Total	Micro	Macro	Total
1	10.7	1.1	11.8	22,830	170	23,000
2	11.7	6.3	18.0	28.300	700	29,000
3	14.4	8.2	22.6	27,430	720	28,150
4	11.4	6.7	18.1	26,900	1200	28,100
5	8.6	15.1	23.7	15,100	3800	18,900
6	5.0	15.2	20.2	11,700	3200	14,900

The micropores fill with water at 0.80 P/P_o, hence, the micropore volume given in column 2 is also the volume of water in the carbon bed. The macropore volume is the available pore volume for methyliodide sorption at high humidities, and, correspondingly, the macropore surface areas are available for methyliodide sorption. Since acceptance tests are done at P/P_o over 0.80 and the performance, at crucial times, is expected to occur at these high humidities, the macropore volume and area are important properties of the carbons. Carbon 1 has the smallest macropore area, carbons 2 and 3 (which at present are used in nuclear power plants) have intermediate areas, (carbon 4 is not too greatly different from 2 and 3 and may be a candidate for nuclear power plant usage), and carbons 5 and 6 have large macropore areas.

Location of Impregnant in the Pores

Iodine type impregnants are proven necessities for methyliodide sorption,

hence, to be effective they must be located in the pores in such a manner that the methyliodide can react with them, whether directly or in conjunction with the carbon surface.

Elemental iodine sublimed onto ash-free carbon adsorbs by pore filling, starting with the smallest pores, and as more is adsorbed, larger pores fill up.(7) Iodine adsorbed from a KI-I_2 water solution adsorbs by surface coverage. The KI does not appear to be adsorbed but remains dissolved in the solution.(7)

What happens to adsorbed elemental iodine when water is adsorbed by the carbon is not definitely known, but it does not desorb when the carbon is leached with hot water. KI in carbons leaches out readily while elemental iodine adsorbed from aqueous phase does not. Although KI is very soluble in water, it must, at some point, start to crystallize out on the carbon surface when the water is desorbed. Whether it is actually adsorbed or just lays down, presumably in a very fine crystalline aggregate form, is not known.

Another factor that should be considered is the variable amount of impregnant on the different carbons because of difference in density. Table IV presents figures on the amount of impregnant on each carbon impregnated with 3% KI and 2% I_2. Also included are estimates of the fraction of pore volume filled and surface area covered, assuming surface adsorption occurs.

Table IV. Amount of impregnant added to carbon, fraction of pore volume filled and fraction of surface covered, for 3% KI, 2% I_2 impregnant.

Carbon	Impregnant added, g	Fraction pores filled	Fraction surface covered
1	1.40	0.033	0.041
2	1.25	0.019	0.029
3	1.02	0.013	0.024
4	1.30	0.020	0.031
5	0.74	0.009	0.026
6	0.92	0.013	0.041

Carbon 1 has the most impregnant, 5 and 6 the least, and 2, 3, and 4 are in the intermediate range. Approximately 1% to 3% of the pore space is filled with impregnant, or 2.5% to 4.0% of the surface is covered if surface adsorption occurs. There is a preponderance of impregnant; i.e., $\sim$1.0 g impregnant to 0.0046 g methyliodide sorbed, but the impregnant is either widely dispersed or concentrated in the smallest pores. It can easily be submerged under water unless soluble, and become available by migrating through the solution.

Since nothing definite could be determined regarding location of impregnant, attempts to correlate methyliodide sorption with impregnant content by itself or in conjunction with pore structure were abandoned early in the study. Pore volume and surface area were then considered.

III. Experimental Results and Discussion

Correlation of Available Pore Volume with Methyliodide Sorption

Figure 4 shows the relationship between available pore volume and methyliodide penetration. It was apparent from the curves that other properties than pore volume control the methyliodide sorption.

Correlation of Available Surface Area with Methyliodide Sorption

Carbons Impregnated with 3% KI, 2% I_2. Figures 5 and 6 show the relationship between available surface area and methyliodide penetration through the carbon bed. Within experimental error, the straight line correlation shows a close dependence of methyliodide sorption on the available surface area. The relationship obeys the equation

$$\ln p = \ln a - ks \qquad (3)$$

where p is the fraction penetrated, s is the available surface area, a and k are constants for each carbon. The correlation extends from s equal to virtually zero to the total surface area for carbons 1, 3, 5, and 6. For carbon 2, a change in slope occurs at 10,000 m^2, and for carbon 4 at 6,400 m^2. This break in slope occurs at a mean pore diameter of 20Å, indicating that pores of less than 20Å in diameter are less effective for methyliodide sorption than the larger pores for these two carbons, but does not apply to other carbons. Carbons 1, 3, 5, and 6 have considerably less pore volume and/or surface area in pores less than 20Å in diameter, which explains the absence of slope change in their graphs.

The quantity (a) is the fraction of methyliodide penetrating the carbon bed when s is zero. It was possible to check (a) on several runs at $P/P_o = 0.99$, where s is virtually zero; but, when the exterior of the carbon granules became wet on other attempts, the fraction of penetration was much larger than (a). (a) is then the fraction of penetration when the pores are filled with water to the point where the available surface area is virtually zero, but the external surface of the granules is not wet. However, on those runs where high humidities were maintained without causing surface wetness, the amount of water in the carbon was not enough to fill the pore space. Even those carbons that were slightly wet still had available pore space.

Unimpregnated and Carbons Impregnated with KI or I_2. Figures 7, 8, and 9 show the relationship between s and p when the carbon is not impregnated or when impregnated with KI or I_2.

Carbons impregnated with KI give straight line plot close to those observed for carbons impregnated with 3% KI and 2% I_2, Figures 7, 8, and 9.

With no impregnant the plots have considerable curvature; the sorption does not follow equation 3. Methyliodide is adsorbed by physical or van der Waal's forces where the preferred sorption occurs in the smallest pores. Since these pores fill with water first on humidification, the carbon loses much of its adsorptive capacity at low water contents.

The sorption pattern of elemental iodine impregnated carbons in some cases follows one that is between those of the unimpregnated and KI impregnated carbons and in other cases is similar to the unimpregnated. In every case observed, the elemental iodine impregnant is considerably less effective than the KI. Apparently, the small amount of iodine impregnant is adsorbed in the smallest pores, and when

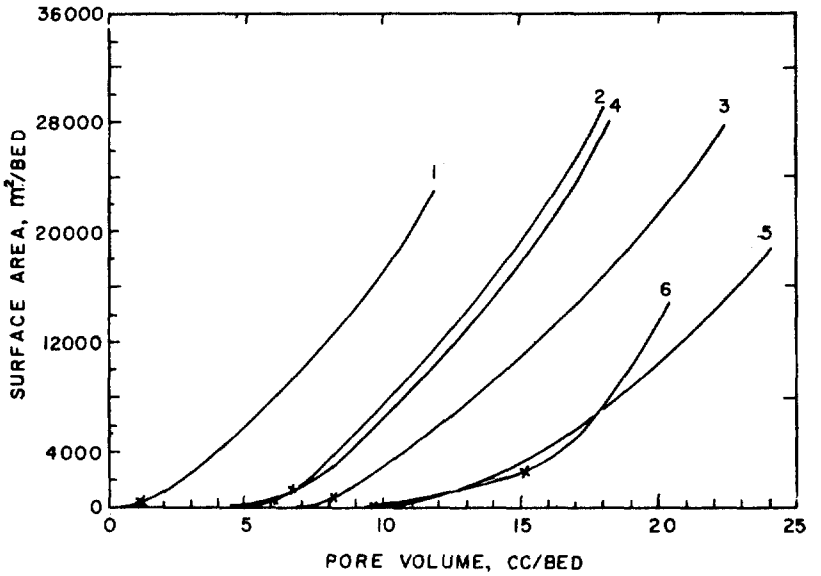

Figure 3 Available surface area as function of available pore volume in carbon bed.

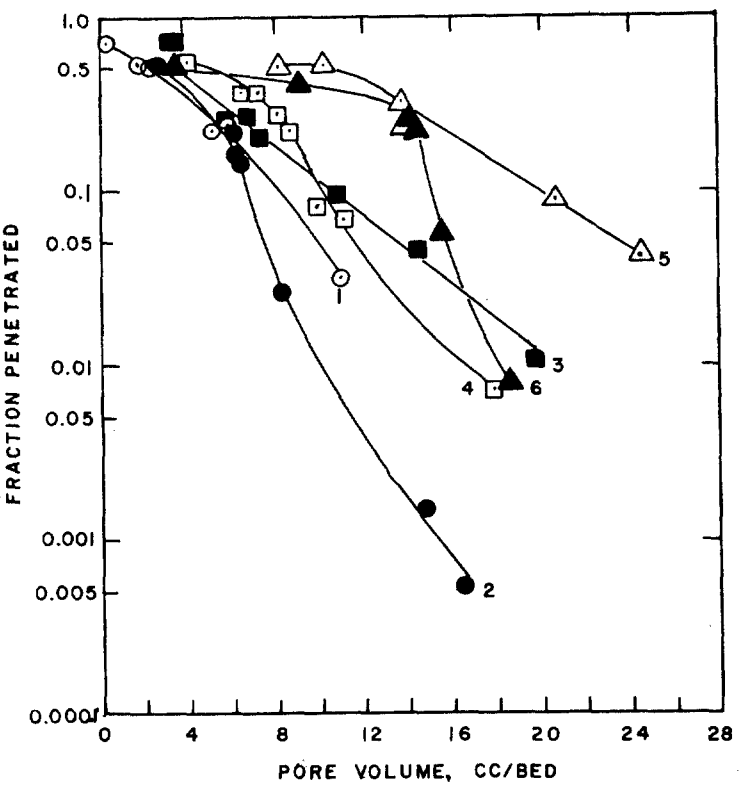

Figure 4 Methyl iodide penetration as function of available pore volume of carbons impregnated with 3% KI, 2% I_2

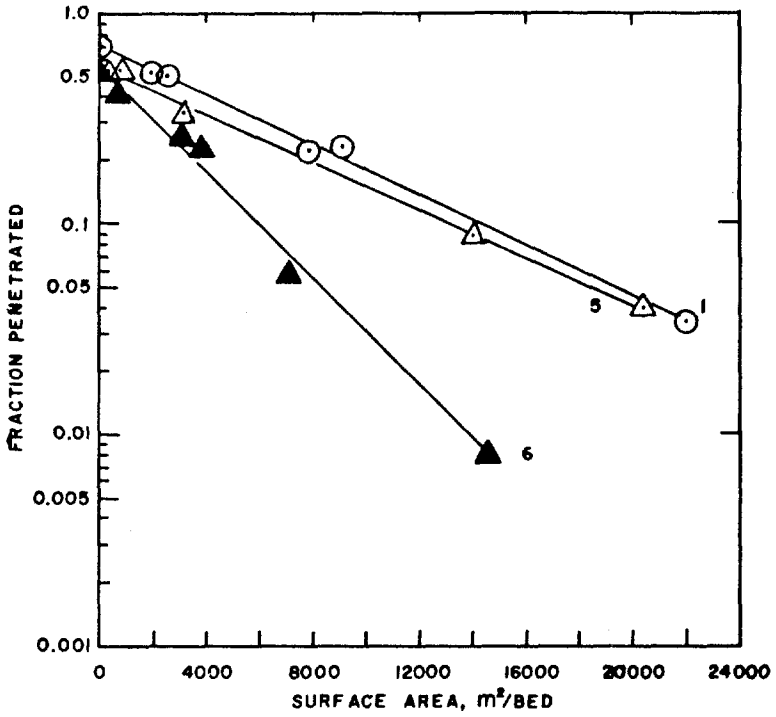

Figure 5 Methyl iodide penetration as function of available surface area of carbons impregnated with 3% KI, 2% I_2

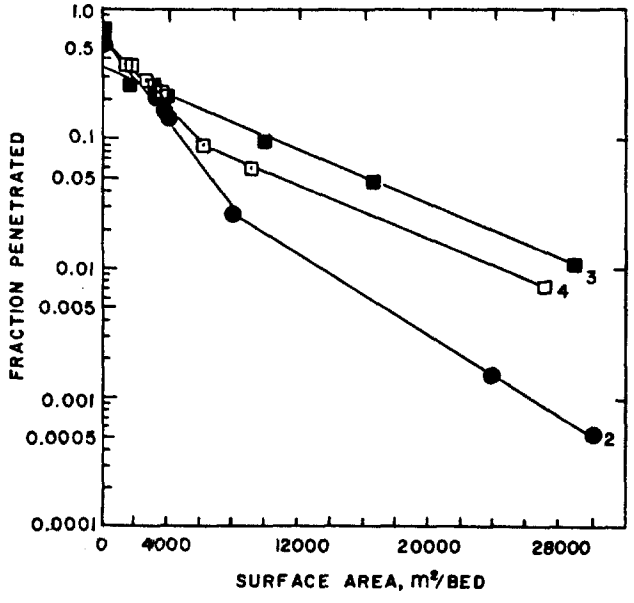

Figure 6 Methyl iodide penetration as function of available surface area of carbons impregnated with 3% KI, 2% I_2

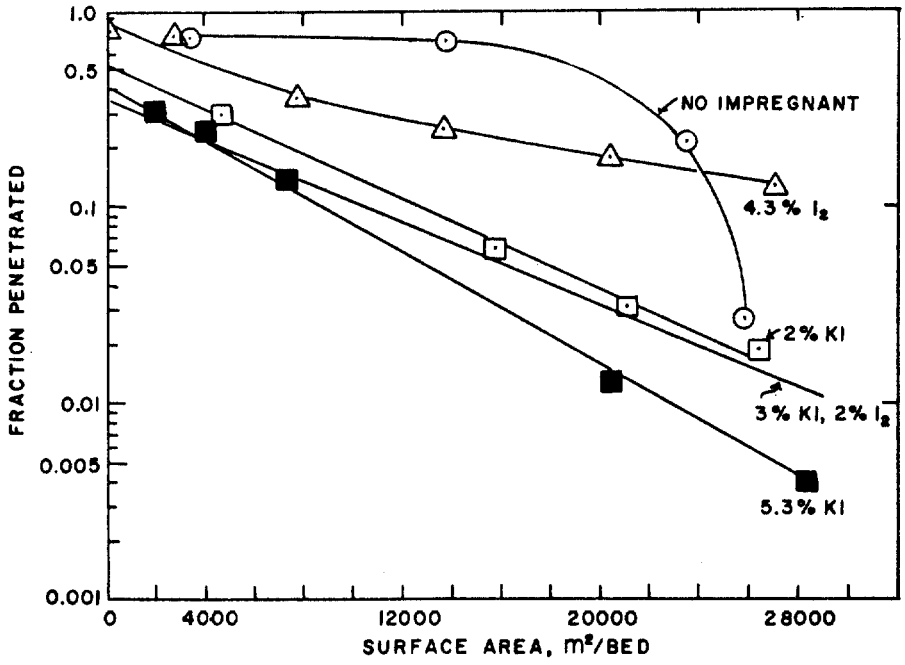

Figure 7 Methyl iodide penetration as function of available surface area of carbon No. 3 with various impregnants.

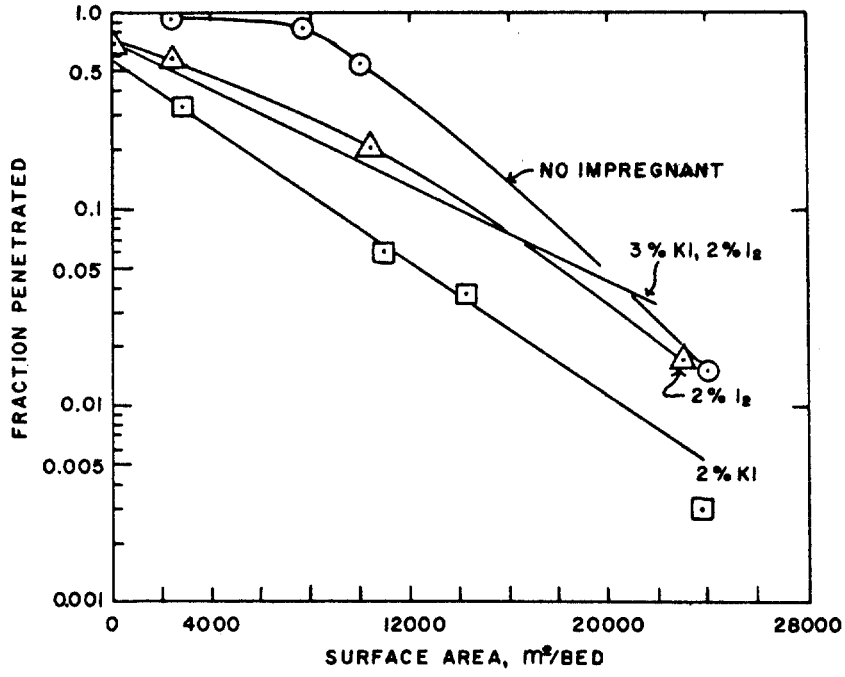

Figure 8 Methyl iodide penetration as function of available surface area of carbon No. 1 with various impregnants.

water is adsorbed, the iodine is submerged or blocked off from external contact. This explanation accounts for the rapid loss of sorptive capacity of carbon 6, Figure 9. Carbons 1 and 3 show some activity.

Effect of Ash, HCl, and KOH

The effect of ash, HCl, and KOH were determined for KI and I_2 impregnated carbon No. 3. The results of these determinations are shown in Figure 10.

The effect of ash was determined by subliming 3% I_2 into the unleached carbon, which has 2.6% ash, mostly alkaline. The lowest curve in Figure 10 has two experimental points, one determined at about 80% RH, at the upper left end, and one at 13% RH, at the lower right end. To determine the lower point, the dry carbon, with the sublimed I_2, was first equilibrated to 90% RH and then dried with a dry air stream. The methyliodide test was then run at 13% RH. When the dry carbon was tested directly, without the 90% pretreatment, the methyliodide penetration was much greater as indicated by the higher experimental point. Moisture is needed to cause the iodine to react with the ash to form KI, NaI, KOI, NaOI and possibly some iodates. Without ash, the curve of the iodine treated carbon would have been near the 4.3% I_2 curve. When the carbon was humidified until the granules were surface-wet, the penetration was higher than would have been predicted by extention of the curve to zero surface area, as indicated by the point at 0.4 penetration.

When a sample of 5.6% KI impregnated carbon was treated with 1.2% HCl, the acid converted the iodide to elemental iodine causing methyliodide penetration to increase from 0.24 to 0.74. This is considerably above the curve for the 4.3% I_2 impregnated carbon.

When a sample of 4.3% I_2 impregnated carbon was treated with 1.9% KOH, the elemental iodine was converted to a mixture of KI, KOI, and KIO_3, causing a decrease of methyliodide penetration from 0.50 to 0.33.

Carbon impregnated with 3.4% KIO_3 gave a penetration of 0.39. The short line beneath the point is for 2% KI impregnated carbon. Although the KIO_3 has the same amount of iodine as 2% KI, the KIO_3 form does not appear to be as effective as KI. KIO_3 is considerably less soluble than KI, hence less mobile in the adsorbed water. This may in part account for its lower activity.

Two observations can be made on the basis of this phase of the study. The presence of acid vapors in the air stream can convert the active KI to inactive I_2, and the carbon bed loses its capacity to sorb methyl iodide. Ash can greatly alter the composition of impregnants added to the carbon, thus introducing an unknown variable. Any research program on the effects of impregnants should take into consideration the effect of the ash on the impregnant.

Effect of Impregnant on pH

Since ash, and addition of HCl or KOH affect the sorptive properties of the carbon by causing changes in impregnant composition, this phase of the overall program was investigated further in regard to pH. It has been observed that loss of sorptive capability is accompanied by decrease of pH of the carbon as measured on the water extract from the carbon.

Table V presents the results of the impregnant versus pH measurements. The tendency is for the pH to increase when the impregnant added to the carbon con-

tains KI. When only I_2 is added, the pH decreases. For initially neutral carbons, such as 3 and 4, the addition of KI produced essentially no change, while the addition of I_2 alone produced a very large decrease in pH.

These results raise an academic question. Is the decreased activity of carbons with low pH due to a high hydrogen ion concentration, or due to the conversion of KI to I_2?

Table V. Effect of impregnant on pH

Carbon	Impregnant	pH
1	none	3.9
1	3% KI, 2% I_2	5.1
1	2% KI	6.2
1	2% I_2	3.3
2	none	4.4
2	3% KI, 2% I_2	6.8
2	2% KI	7.0
2	2% I_2	3.3
3	none	6.9
3	3% KI, 2% I_2	7.1
3	2% KI	6.8
3	5.6% KI	7.0
3	4.3% I_2	3.0
4	none	7.1
4	3% KI, 2% I_2	7.0
5	none	5.0
5	3% KI, 2% I_2	5.7
6	none	2.5
6	2% KI	3.6
6	2% I_2	2.4
6	none	5.0
6	3% KI, 2% I_2	5.8

Constants a and k

The constants a and k of equation 3 were further investigated in their relationship to pore structure. From the study two equations were evolved.

$$a = f/(S_m \times pH^a) \quad (4)$$

$$k = f\ 4/\ \bar{D} \quad (5)$$

where S_m is the area of pores larger than 2000Å diameter and $\bar{D}$ is the mean micropore diameter. Table VI presents the numerical values of (a), k, and $\bar{D}$ for the KI and KI-I_2 impregnated carbons.

Figure 11 summarizes graphically the results which show the dependence of (a) on S_m and pH, equation 4. For carbon 3 which has the largest S_m, the effect of pH is very pronounced. At 6.8 pH (a) was 0.5, but at 9.4 pH (a) had decreased to 0.22, or 0.108 units decrease of (a) per unit of pH increase. For carbon 6, which has a

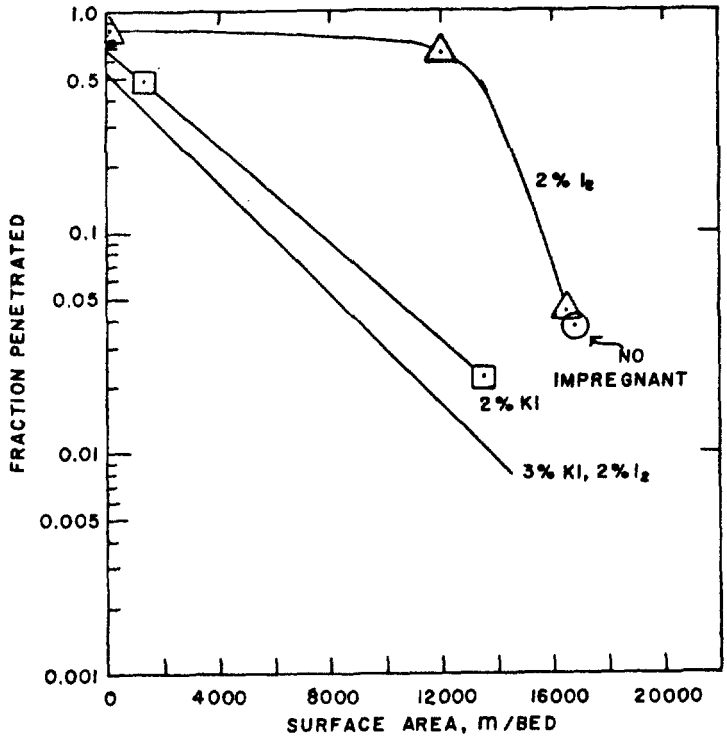

Figure 9 Methyl iodide penetration as function of available surface area of carbon No. 6 with various impregnants.

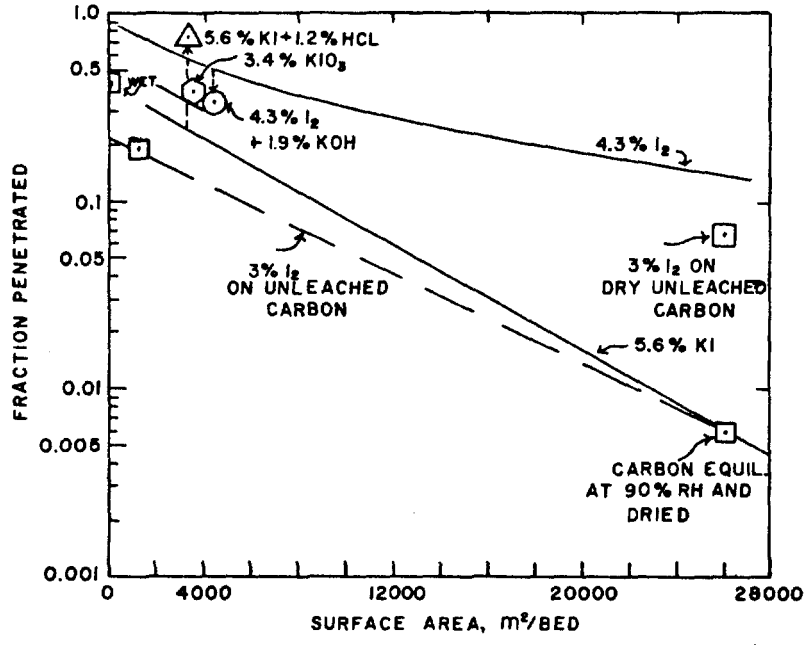

Figure 10 Effect of HCL, KOH, and ash on methyl iodide sorption, carbon No. 3.

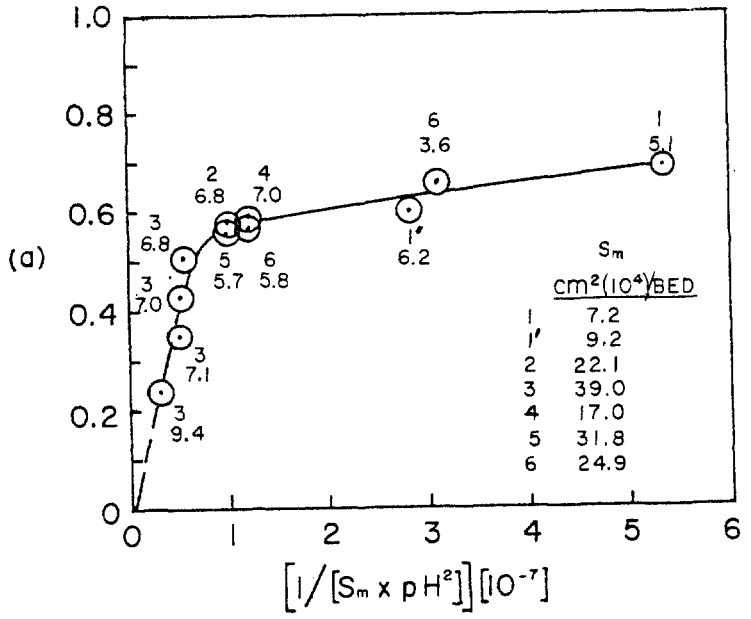

Figure 11 (a) as function of pH^2 and of surface area, S_m, of pores larger than 2000Å diameter

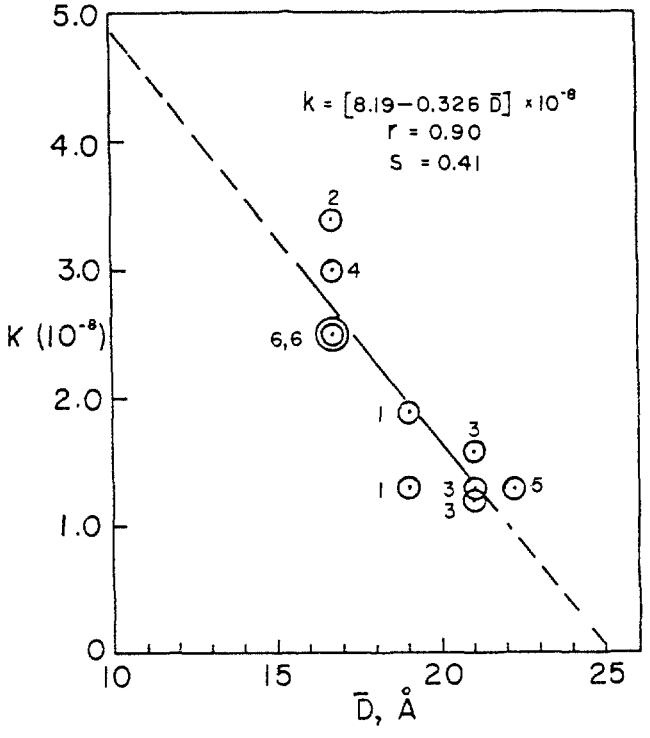

Figure 12 k as function of micropore mean diameter, $\bar{D}$

smaller S_m, the effect of pH is less pronounced. At 3.6 pH (a) was 0.66 and at 5.8 pH (a) decreased to 0.56, or 0.045 units decrease of (a) per unit pH increase. Carbon 1 appears to follow the same pattern. If more data were available for verification, it is probable the carbons of different S_m would have characteristic curvesdependent on pH.

Table VI. Constants a and k of equation 3

Carbon	Impregnant	a	$k(10^{-8})$	$\bar{D}$ Å
1	3% KI, 2% I_2	0.69	1.3	19
2	" "	0.58	3.4	17
3	" "	0.35	1.2	21
4	" "	0.59	3.0	17
5	" "	0.56	1.3	22
6	" "	0.56	2.5	17
1	2% KI	0.55	1.9	19
6	"	0.66	2.5	17
3	"	0.54	1.6	21
3	5.6% KI	0.43	1.3	21

Figure 12 shows the dependence of k on $\bar{D}$, equation 5. The coefficient of correlation, r, is 0.90 and standard error of estimate, s is 0.41.

VII. Conclusions

Pore Structure Effects

The methyliodide penetration, p, through a KI impregnated carbon bed is a function of the available carbon surface area, s, at various levels of moisture content as expressed by the equation

$$\ln p = \ln a - ks$$

(a) is the penetration at high humidities where s is very small. It is inversely proportional to the surface area of pores larger than 2000Å diameter. Constant k is inversely proportional to the mean micropore diameter.

An ideal carbon would have the micropore characteristics of carbon 2, to give a large k, and the macropore characteristics of carbon 3, to give a small (a). Such a carbon would be most effective at all levels of moisture content.

Impregnant Effects

The potential performance of a carbon with the favorable pore structure can be nullified or enhanced by the state of the impregnant and/or pH of the carbon. With decreasing pH, methyliodide penetration increases. Whether this is a direct effect of the hydrogen ion concentration or due to the conversion of alkaline iodide to elemental iodine is not known. It may be due in part to both. By increasing the pH, as by adding caustic, methyliodide penetration is decreased, but there are limits to the amount of caustic that can be added because of its effect on the ignition temperature. In nuclear power plants, acid vapors in the air stream drawn through the carbon bed can in time convert KI to I_2, or decrease pH, and cause in part, the observed loss of sorptive capability.

The amount of KI impregnant in the 2% to 5.6% range did not appear to have any effect on sorptive capability; the critical range must be considerably below 2%.

References

1. Juhola, A. J., "Manufacture, pore structure, and application of activated carbons," Kemia 4, No. 11, pp 543; No. 12, pp 653 (1977).

2. Dietz, V. R. and Burchsted, C. A., "Survey of domestic charcoals for iodine retention," NRL Memorandum Report 2960, Naval Research Laboratory, Washington, D.C. (Jan. 1975).

3. Grant, R. J., "Basic concept of adsorption on activated carbon," an internal report of Pittsburgh Activated Carbon Company (1951).

4. Juhola, A. J. and Wiig, E. O., "Determination of micropore size distribution," J. Am. Chem. Soc., 71, 2069 (1949).

5. Wiig, E. O. and Juhola, A. J., "Determination of macropore size distribution," J. Am. Chem. Soc., 71, 2078 (1949).

6. Juhola, A. J., "Organic vapor adsorption and micropore structure of activated carbons," MSAR Report 78-52 (1977).

7. Juhola, A. J., "Iodine adsorption and structure of activated carbons," Carbon, 13, pp 437 (1975).

METHYL IODIDE RETENTION ON CHARCOAL SORBENTS AT PARTS-PER-MILLION CONCENTRATIONS*

G. O. Wood, G. J. Vogt, and C. A. Kasunic
Los Alamos Scientific Laboratory
University of California
Los Alamos, New Mexico 87545

Abstract

Breakthrough curves for charcoal beds challenged by air containing parts-per-million methyl iodide (I-127) vapor concentrations were obtained and analyzed. A goal of this research is to determine if sorbent tests at relatively high vapor concentrations give data that can be extrapolated many orders of magnitude to the region of interest for radioiodine retention and removal. Another objective is to identify and characterize parameters that are critical to the performance of a charcoal bed in a respirator cartridge application. Towards these ends, a sorbent test system was built that allows experimental variations of the parameters of challenge vapor concentration, volumetric flow rate, bed depth, bed diameter, and relative humidity. Methyl iodide breakthrough was measured at a limit of 0.002 ppm using a gas chromatograph equipped with a linearized electron capture detector.

Several models that have been proposed to describe breakthrough curves were tested against experimental data. Only the equations of a Theory of Statistical Moments, including the first three moments, adequately described the breakthrough curves over the entire three orders of magnitude in breakthrough concentration. These moments, which are easily calculated by data fitting, have physical significance and can be related to measurable parameters. A variety of charcoals used or proposed for use in radioiodine air filtration systems have been tested against 25.7 ppm methyl iodide to obtain these parameters and protection (decontamination) factors.

Effects of challenge concentration, relative humidity, and bed diameter were also investigated. Significant challenge concentration dependence was measured (more efficiency at lower concentration) for two types of charcoals. Increased relative humidity greatly decreased breakthrough times for a given protection factor. Increased bed diameter greatly increased breakthrough times for a given protection factor. Implications of these effects for a test method are discussed.

*Work supported by the Nuclear Regulatory Commission and performed at the Los Alamos Scientific Laboratory operated under the auspices of the U. S. Department of Energy, Contract No. W7405 ENG-36.

I. Introduction

A question that is being raised more frequently is the adequacy of air-purifying respirators for personal protection against airborne radioiodine. The degree of protection that can be expected due to facial fit under a variety of work exercises is becoming better defined by research done at Los Alamos and other places. However, the efficiency of charcoal beds in the form of respirator cartridges remains much in doubt. Therefore, we have undertaken the responsibilities to (1) develop acceptance criteria for an air-purifying respirator to protect against forms of airborne radioiodine and (2) develop test methods for certifying respirator cartridges for such a use.

We have selected for initial investigation the approach of using nonradioactive (I-127) methyl iodide at parts-per-million concentrations for testing the performance of charcoal beds. The big question that appears is how does sorbent efficiency at ppm levels relate to efficiency at much lower ($\sim 10^{-7}$ ppm) levels of concern with radioiodine. In the first phase of our research we have attempted to define performance of sorbents at ppm concentrations of methyl iodide and identify the parameters critical to this performance. In the future we will investigate identical sorbent beds at lower challenge concentrations using radioiodine (I-131) species and counting measurement techniques. Then we should have an answer to the question of validity of extrapolation of charcoal bed efficiencies over orders-of-magnitude differences in challenge vapor concentrations.

Some differences must be recognized between the uses of charcoal beds for radioiodine removal. These mostly involve the ranges of parameters to be considered. For respirator cartridges bed size, weight, and pressure drop are more critical considerations. Also, airflows are cyclical and may range widely depending on the workload of the user. The complete range of relative humidities must be considered in both cases. However, only ambient temperatures must be considered for respirator cartridge beds, since radioiodine loadings must be kept low. Equilibration of a respirator cartridge to ambient humidity and airflows may vary from none to the lifetime of its use, depending on the regulations regarding its preparation, storage, use, and replacement.

The application of a sorbent bed in the form of a respirator cartridge is similar in many ways to the application of a much larger sorbent bed for high volume ambient air cleaning. In fact, the radioiodine air cleaning literature has been most valuable in beginning our investigations. Effects of parameters such as challenge vapor concentration, relative humidity, and airflow velocity on bed performance and testing procedures are similar. Therefore, we are presenting our experimental results and conclusions in this forum with the expectation that they will add to the understanding of charcoal bed performance in both applications.

II. Experimental

Figure 1 is a schematic of the apparatus that was used to measure the performance of charcoal beds for methyl iodide removal. Pressurized air was regulated, filtered, and humidified to obtain

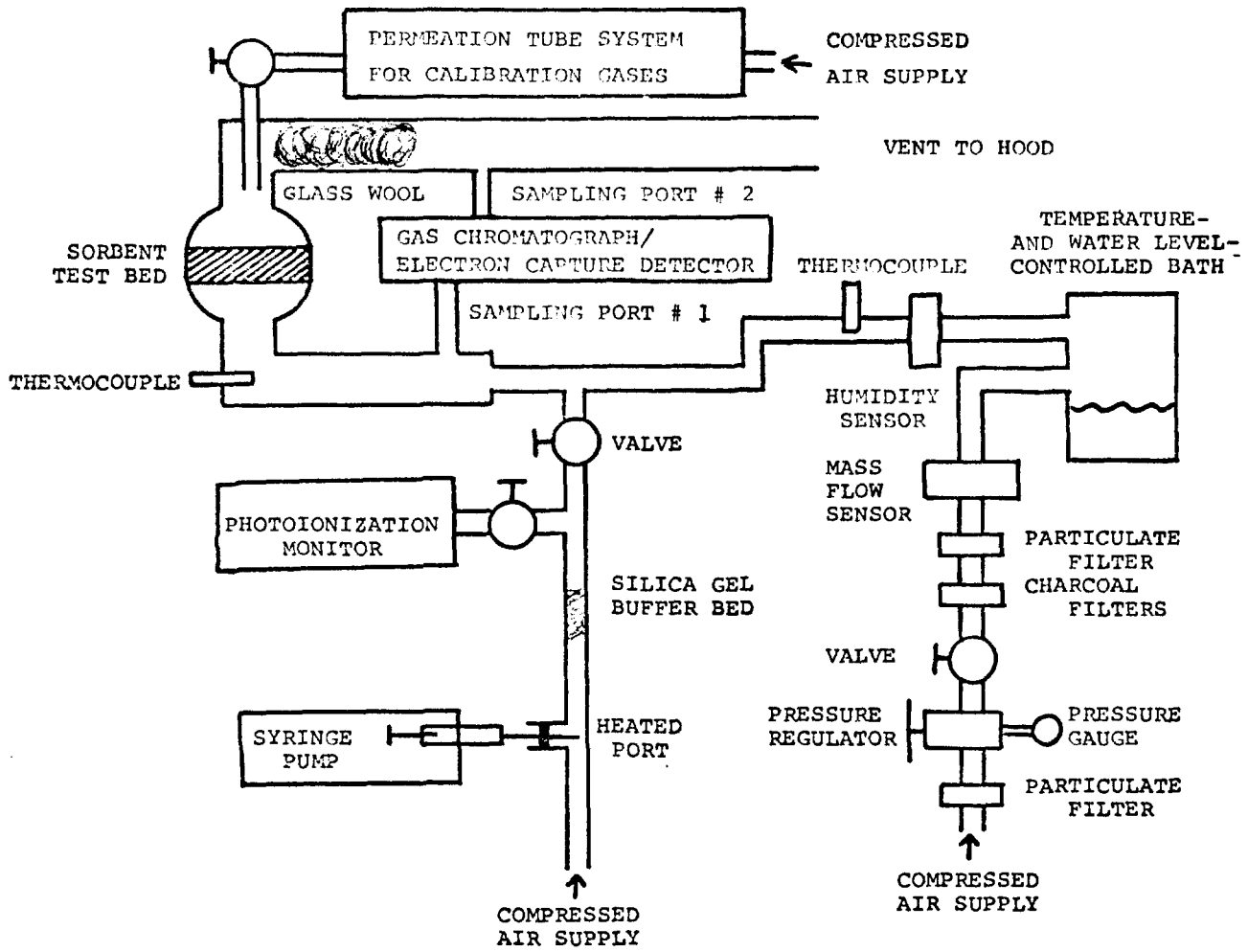

Figure 1 Schematic of the sorbent test flow system.

the conditions desired. A calibrated electronic flow meter and an electronic humidity meter were used to monitor, and in the case of the latter, to control these conditions. Liquid methyl iodide was metered at a calibrated rate by a syringe pump into a heated port where it vaporized and was swept into the main airstream by an auxiliary (0.2 L/min) airstream. From this point in the apparatus to the sorbent bed, all tubing was 2.5-cm glass. An air monitor with a photoionization detector was used to monitor the output of the syringe pump generation system. Air entering the charcoal bed and effluent air were alternately sampled by an automated gas sampling valve with Teflon loops. Such samples were introduced into a gas chromatograph, separated on a silicone OV-7 (15% on 100/120-mesh Chromosorb G) column (4-mm i.d. x 1.8-m long, 100°C, 20 cm^3/min 19:1 Ar/CH_4) and measured for methyl iodide with a Ni-63 linearized electron capture detector. An electronic peak integrator was used to quantitate the methyl iodide peaks and to record elapsed times. Teflon and glass was used throughout the sampling and analysis system except for the sampling valve, which was Hastalloy C, and the detector, which was stainless steel (300°C).

The valve-gas chromatograph-electron capture measuring system was frequently calibrated using Teflon permeation tubes containing liquid methyl iodide. The outputs of these permeation tubes, maintained at constant (±0.3°C) temperatures, were quite constant over periods of many months, as determined by weekly weighings. These known methyl iodide outputs were mixed in known airflows to produce known methyl iodide concentrations (0.03-26 ppm). Calibration indicated that the detector response was indeed linear over at least 3 orders of magnitude and methyl iodide concentration was proportional to measured peak area. The response of the measurement system was affected slightly by relative humidity of the air. The limit of measurement was about 2 parts-per-billion methyl iodide in air.

The experimental procedure was as follows. The airflow (20-40 L/min) was stabilized at a selected relative humidity. The syringe pump was started and its output was diverted to the photoionization monitor. Meanwhile, the output of a calibrated permeation tube was introduced at 1 L/min into the main airstream. The detector system was recalibrated in this way. The flow from the permeation tube to the main airstream was stopped. A charcoal bed was prepared by weight in a cylindrical glass tube of selected diameter. This was placed in the flow system. After 5 min, the syringe pump output was diverted into the main airstream and the experiment was begun. After significant breakthrough (10-20%) of the test bed had occurred, the experiment was terminated.

III. Interpretation of Breakthrough Curves

The raw data obtained from the experiments described above were in the form of peak areas vs elapsed time (t_B). Syringe pump output and volumetric airflow rates were used to calculate challenge concentrations (C_o) in ppm. Detection system calibration factors obtained from permeation tube outputs were used to convert peak areas to breakthrough methyl iodide concentrations (C_B) in ppm. The data were then converted to fractional breakthrough (C_B/C_o) vs elapsed time (t_B) for further analysis.

Several models that have been proposed to describe breakthrough curves were tested against the experimental methyl iodide breakthrough data. The most common descriptions of breakthrough curves are based on the Mecklenburg equation, which has the basic form:

$$t_B = \frac{a_1}{C_o} \quad (b_1 - h) \qquad (1)$$

where h is the "dead layer" depth or the "critical" bed depth, i.e., that value below which breakthrough would be instantaneous. In this equation and those following a_i and b_i refer to combinations of parameters that are constant for a given breakthrough curve. The many variations of the Mecklenburg equation that have been proposed have differed primarily in the expression used to calculate h. For example, the Klotz, Sillen, Van Dongen, Wheeler, and Jonas equations have $h = -a_2 \ln (C_B/C_o)$. The Danby equation has $h = -a_3 \ln [C_B/(C_o - C_B)]$, which is equivalent in form to the others for $C_B/C_o < 0.1$. All these variations of the Mecklenburg equation predict that a plot of t_B vs $\ln (C_B/C_o)$ or vs $\log (C_B/C_o)$ would be linear. Figure 2 shows

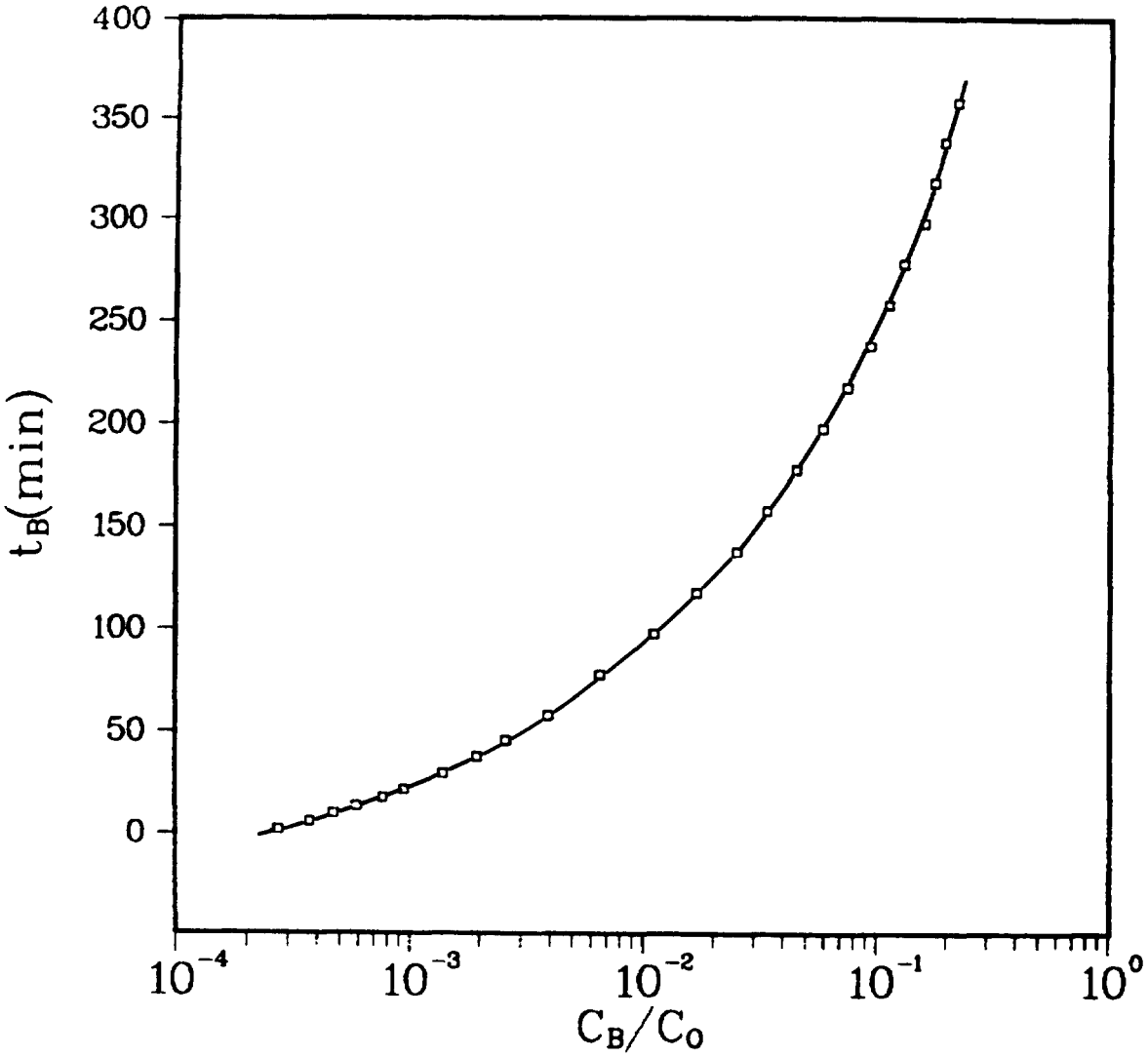

Figure 2 Semilog plot of the breakthrough curve data.

such a plot for data obtained in an experiment with a bed of Barnebey Cheney 487 charcoal (5% TEDA impregnated) at these conditions:

25.7 ppm methyl iodide challenge concentration
20 L/min airflow rate at 21 ± 1°C, 585 torr
50 % relative humidity
4.1-cm-diam x 2.5-cm-deep bed.

Every fifth data point of 90 obtained was plotted in this graph. This plot is clearly nonlinear over the entire range of data. Therefore, the variations of the Mecklenburg equation with $h = -a_2 \ln (C_B/C_o)$ do not adequately describe the breakthrough of methyl iodide in this experiment.

The second description attempted for methyl iodide breakthrough was an empirical relationship,

$$t_B = a_4 \ (C_B/C_o)^{b_4} \qquad (2)$$

This implies that a plot of log t_B vs log (C_B/C_o) is linear. Such a plot (Fig. 3) for the same set of data was linear only in the range C_B/C_o = 0.005 to 0.22 and, therefore Equation 2 is not adequate. Furthermore, the parameters from such a data fit have no known physical significance.

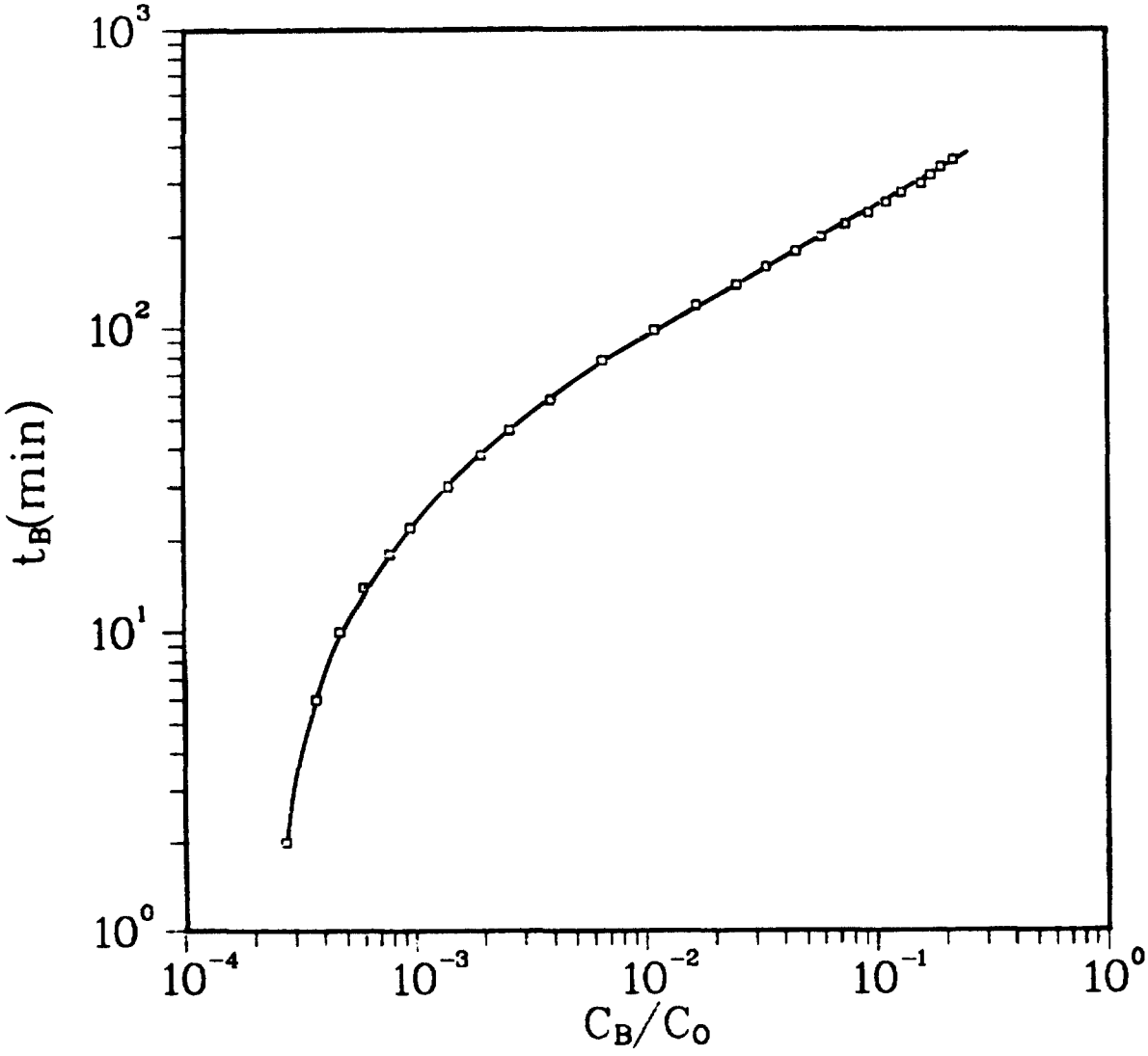

Figure 3 Log-log plot of the breakthrough curve data.

The most successful fit of this set of breakthrough data was obtained using the equations developed for a Theory of Statistical Moments by Otto Grubner and Dwight Underhill.[1-2] By this theory the breakthrough curve can be generated from its moments by a series such as the Gram-Charlier series. Simplifications of the adsorption mechanism are required to obtain analytically useful equations whose parameters are related to parameters of physical significance. The references cited provide further explanation. A basic equation obtained by retaining the first three statistical moments (m_1, m_2, m_3) is

$$t_B = m_1 + \sqrt{m_2}\ (X_B) + \frac{m_3}{6m_2}\ (X_B^2 - 1), \qquad (3)$$

where

$$C_B/C_o = \frac{1}{\sqrt{2\pi}} \int_{-\infty}^{X_B} \exp\left[\frac{-X^2}{2}\right] dx. \qquad (4)$$

Equation 4 is the normal probability integral whose values of X_B for C_B/C_o are readily available in tabulated form or may be calculated on a programmable calculator. Equation 3 predicts a parabolic relationship between t_B and X_B for 3 statistical moments and a linear relationship if 2 statistical moments are sufficient. Figure 4 shows a plot of t_B vs X_B for the same set of data considered previously. This plot is linear only for $-X_B < 1$ or $C_B/C_o > 0.16$. However, a parabolic fit of the data by least-squares regression to $t_B = a_o + a_1 X_B + a_2 X_B^2$ produced a curve such as that drawn through the data points. Such a fit is excellent over the entire range of the data with $m_1 = 578$ min, $\sqrt{m_2} = 274$ min, and $m_3/6m_2 = 34.36$ min.

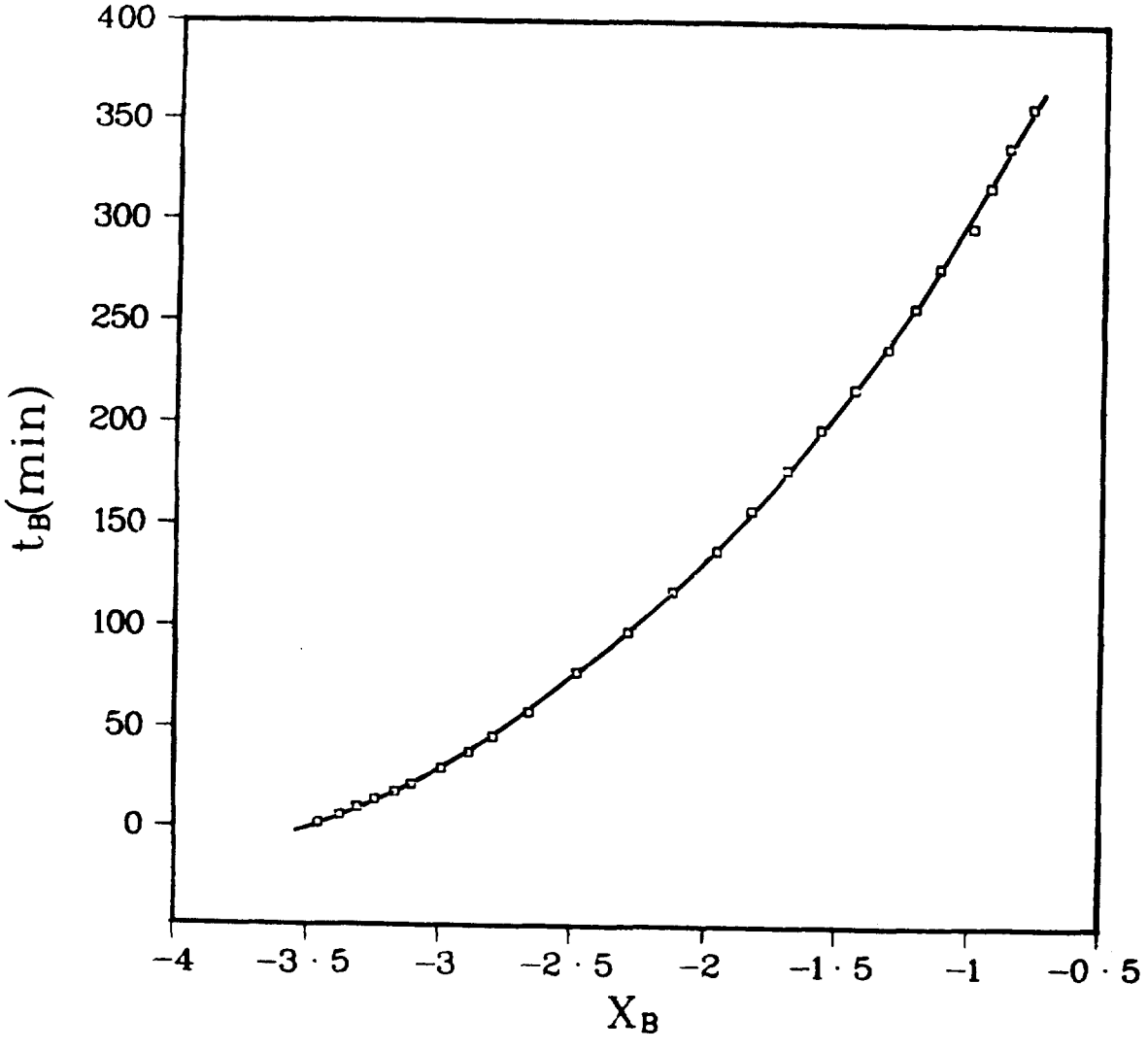

Figure 4 Probability plot of the breakthrough curve data.

Fits of the parabolic form of the Theory of Statistical Moments to breakthrough curves for two other charcoals are shown in Fig. 5. The triangles represent data for a bed of Union Carbide ACC nonimpregnated charcoal and the circles represent data for a bed of North American Carbon G615 KI/TEDA-impregnated charcoal. Experimental conditions were:

25.7 ppm challenge concentration
20 L/min airflow rate
33% relative humidity
6.9-cm-diam x 2.5-cm-deep bed.

The curves drawn through the experimental points are representative of those calculated from parameters m_1, m_2, m_3 obtained by least-squares fitting of the data. Again, the theory described the breakthrough curve very well for these different types of charcoals.

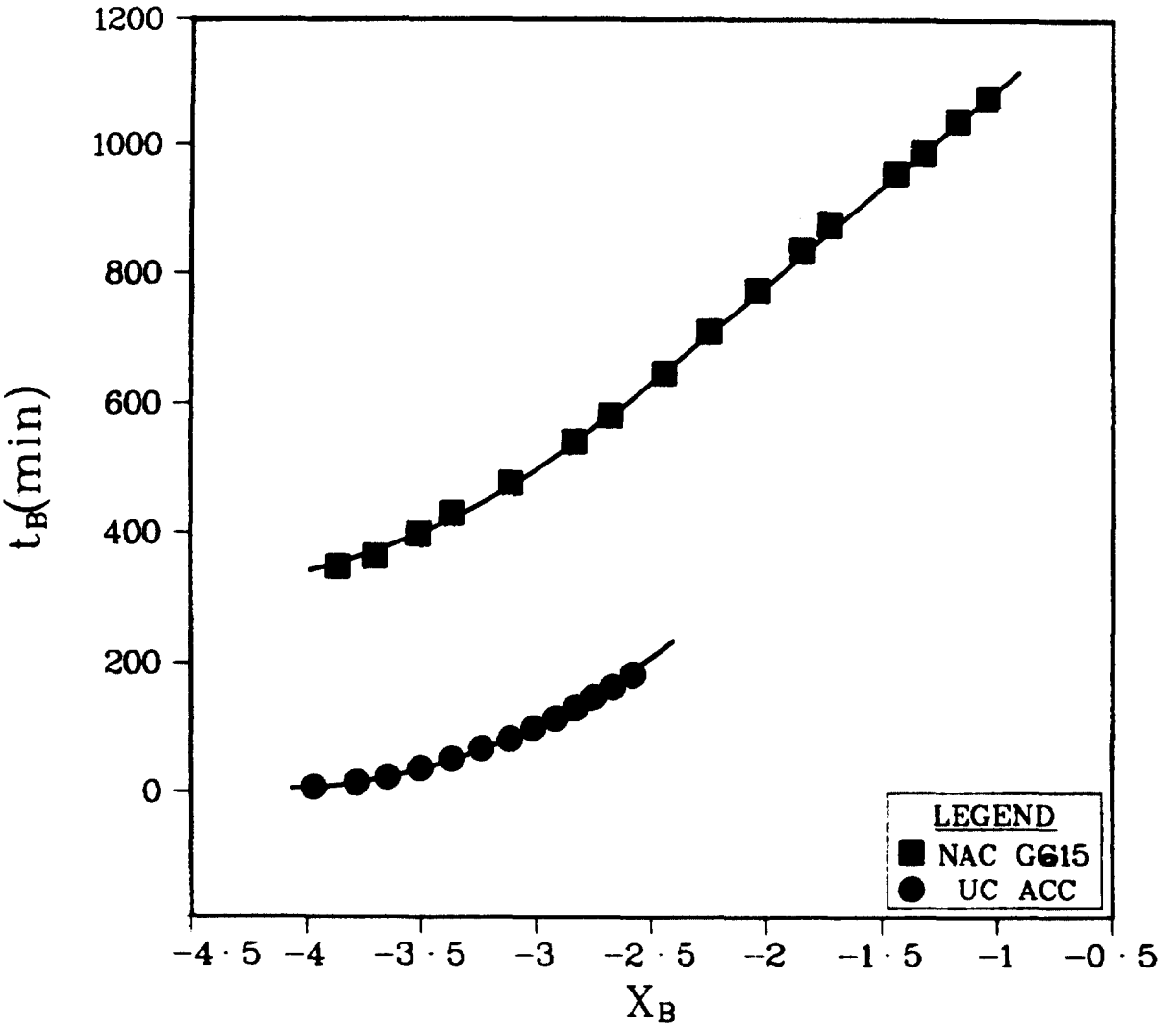

Figure 5 Probability plots of breakthrough curve data for a KI/TEDA-impregnated charcoal (NAC G615) and a non-impregnated charcoal (UC ACC).

One advantage of having such a good description of the breakthrough curve is that it allows interpolation and limited extrapolation of experimental data. Another advantage of the use of the Theory of Statistical Moments is that the parameters obtained in fitting data have physical significance. The first statistical moment, m_1 corresponds approximately to the mean of the breakthrough curve, where $C_B/C_o = 0.5$,

$$t_{0.5} = m_1 - \frac{m_3}{6m_2} . \tag{5}$$

The second statistical moment, m_2, equals the variance (σ^2) which describes the spread of the breakthrough curve. And the third statistical moment, m_3, corresponds to the symmetry of the breakthrough curve. An effective adsorption bed capacity can be calculated as

$$F = 1 + \frac{\sqrt{m_2}}{m_1} (X_B) + \frac{m_3}{6m_1m_2} (X_B^2 - 1). \tag{6}$$

A fractional bed capacity loss due to mass transfer is

$$M = -\frac{\sqrt{m_2}}{m_1} (X_B) - \frac{m_3}{6m_1m_2} (X_B^2 - 1). \tag{7}$$

When appropriate assumptions are made, the parameters obtained by the Theory of Statistical Moments can be further related to measurable factors. For example, the assumption that mass transfer resistance is controlled by internal (pore) diffusion yields

$$\frac{\sqrt{m_2}}{m_1} = \left(\frac{2\ R^2 u}{15\ \varepsilon D_i L} \right)^{1/2} , \tag{8}$$

$$\frac{m_3}{6m_1m_2} = \left(\frac{R^2}{21} \frac{u}{\varepsilon D_i L} \right) , \tag{9}$$

where

R = adsorbent particle radius
u = carrier gas face velocity
L = bed length
D_i = effective pore diffusion coefficient
ε = internal/total porosity ratio.

More details of such relationships are available.[1-2] However, this brief review suggests the possibilities of using this theory, which so well describes the experimental breakthrough curves. Among other things, it can permit the bed designer or tester to predict t_B, F, and M as functions of measurable factors such as those listed above.

IV. Experimental Results

Comparisons of Sorbents

Breakthrough curves were obtained for 6 activated charcoals and 4 impregnated charcoals of the type used in radioiodine air cleaning applications. The conditions were kept constant:

25.7 ppm methyl iodide challenge concentration
20 L/min airflow rate
33% relative humidity at 21 ± 1°C
6.9-cm-diam x 2.5-cm-deep bed

These sets of data were fit to the statistical moments equation (3) to give the parameters listed in Table I. Breakthrough times corresponding to protection factors (decontamination factors) of 10, 100, and 1000 are also listed in Table I.

Table I Parameters and protection factors.

Source	Sorbent Designation	Impregnant	Calculated Parameters (min)			Breakthrough Times (min) For Protection Factors		
			m_1	$\sqrt{m_2}$	$m_{3/6m_2}$	10	100	1000
Union Carbide	ACC	None	1005	417	43.6	499	228	88
			1268	571	67.9	580	241	85
			1179	458	45.2	621	314	149
			1501	675	80.2	688	286	101
Westvaco	WV-H	None	1034	473	58.2	466	192	70
Witco	337	None	1017	416	43.7	512	243	105
Pittsburgh AC	BPL	None	1239	493	49.5	640	312	139
Narbada	NG	None	1619	727	88.1	744	318	125
Fisher	5-685-B	None	1374	585	65.4	667	304	126
North American Carbon	G-618	TEDA	3295	1240	123.4	1786	958	517
	G-615	KI/TEDA	1533	429	32.7	1005	682	488
Barnebey Cheney	487	TEDA	2480	800	62.4	1497	899	543
Sutcliffe-Speakman	208C	TEDA	2923	983	94.2	1725	1055	691

Reproducibility of these early experiments is shown by the four replicate experiments with Union Carbide ACC charcoal. Within this reproducibility, the nonimpregnated adsorbents were similar in performance. The impregnated sorbents were much better for methyl iodide retention. The order of results shown in Table I was not surprising. However, this does demonstrate one use of breakthrough curve fitting by statistical moments.

Challenge Concentration Effects

Breakthrough curves were obtained for two charcoals to study the effects of challenge vapor concentrations on protection factors. The first series used Union Carbide ACC charcoal at the experimental conditions listed immediately above, but with challenge methyl iodide concentrations from 0.90 to 25.7 ppm. Results were plotted as log t_B vs log C_o for protection factors of 10, 100, and 1000 in Fig. 6.

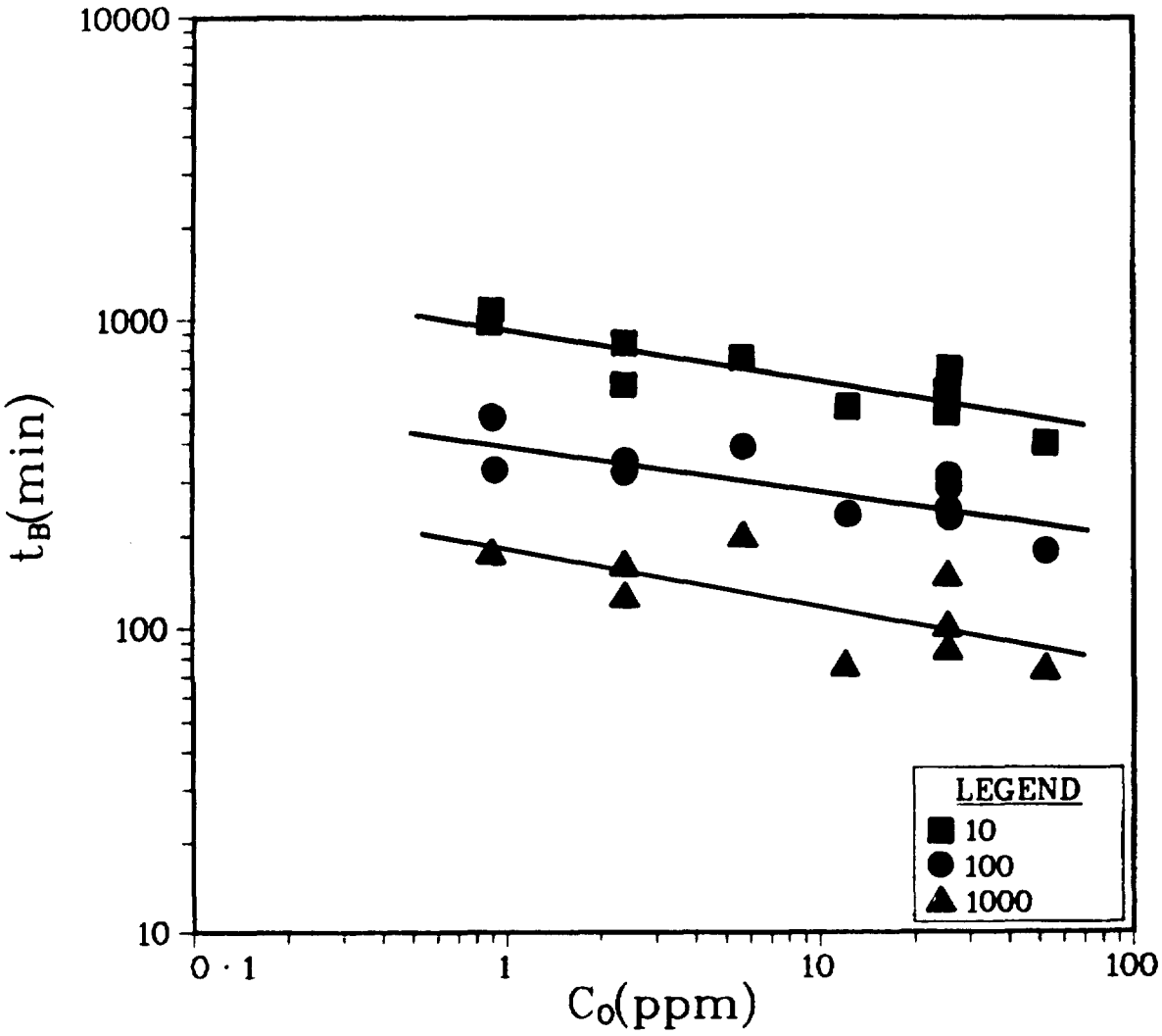

Figure 6 Challenge concentration dependence for protection factors from tests with Union Carbide ACC non-impregnated charcoal.

Since these plots were apparently linear, the following relationships were calculated by linear least-squares fitting:

$$PF = 10, \quad t_B = (940 \pm 81)\ C_o^{-0.17 \pm 0.09}$$

$$PF = 100, \quad t_B = (390 \pm 38)\ C_o^{-0.15 \pm 0.04}$$

$$PF = 1000, \quad t_B = (180 \pm 32)\ C_o^{-0.19 \pm 0.07}$$

The $\pm$ values refer to standard deviations calculated for 11 experimental points. The relative values of the standard deviations confirm that the dependence of protection factors on challenge concentration is real.

A similar series of experiments was done with Barnebey Cheney 487 5% TEDA-impregnated charcoal at challenge methyl iodide concentrations from 0.87 to 29.0 ppm. Other conditions were:

40 L/min airflow rate
50% relative humidity
4.1-cm-diam x 2.5-cm-deep bed

Breakthrough times for protection factors of 10 and 100 were plotted in Fig. 7 as log t_B vs log C_o. Reproducibility was much improved for these experiments as seen by the overlapping of duplicate points at 12.1, 20.6, and 29.0 ppm. Again, these plots were apparently linear with the results:

$$PF = 10, \quad t_B = (2720 \pm 290)\ C_o^{-1.06 \pm 0.04}$$

$$PF = 100, \quad t_B = (290 \pm 44)\ C_o^{-0.80 \pm 0.06}$$

and, again, a significant challenge concentration effect was observed.

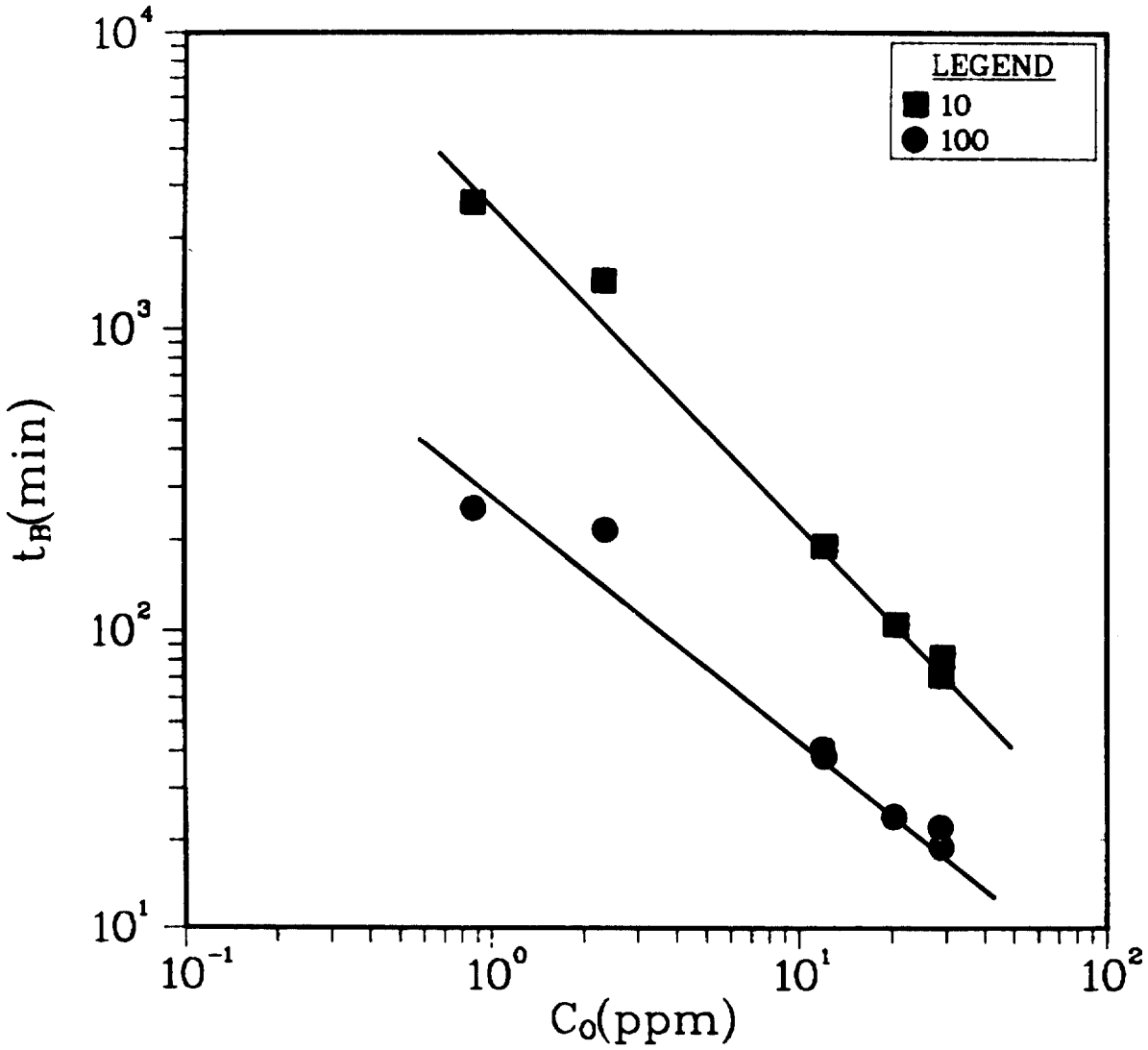

Figure 7 Challenge concentration dependence for protection factors from tests with BC 487 TEDA-impregnated charcoal.

Bed Diameter Effects

Bed diameters were varied for a fixed 2.5-cm depth of Barnebey Cheney 487 charcoal under these constant conditions:

25.7 ppm challenge concentration
20 L/min air flow rate
50 % relative humidity

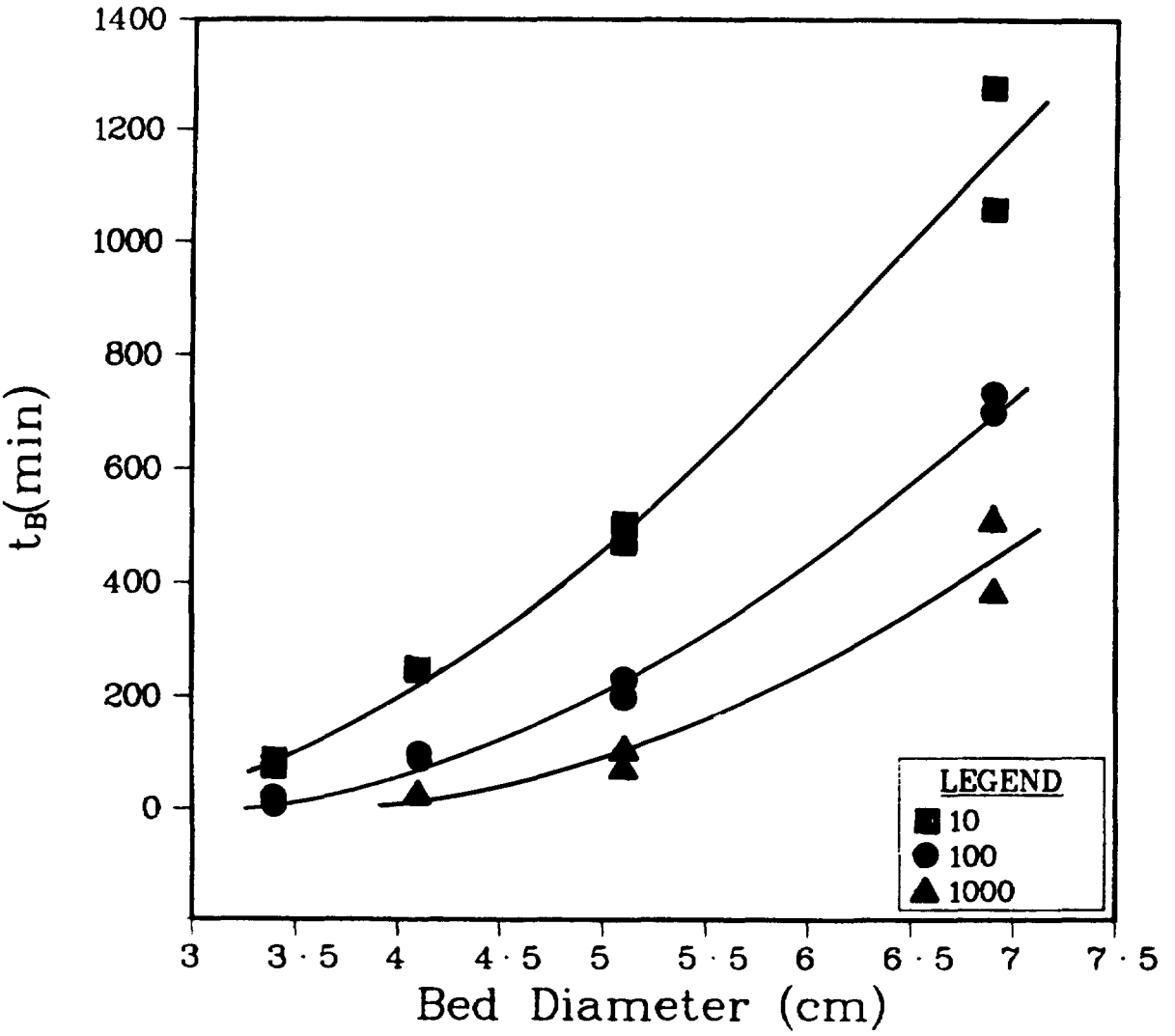

Figure 9 Protection factors as functions of bed diameter for a TEDA-impregnated charcoal (BC 487).

Plots of breakthrough times vs bed diameter for three protection factors are shown in Fig. 9. The effects of increased bed diameter in increasing breakthrough times are large. This is not surprising since increasing bed diameter for a fixed bed depth not only reduces linear flow velocity, but also increases the amount of sorbent in the bed. An interesting observation from Fig. 9 is the apparent convergence of all three protection factor curves to a bed diameter value of 3-3.5 as t_B approaches zero. This suggests that a "critical" bed diameter exists.

Relative Humidity Effects

Variations of protection factors with relative humidity were also investigated for the Barnebey Cheney 487 charcoal under these conditions:

25.7 ppm challenge concentration
20 L/min air flow rate
4.1-cm-diam x 2.5-cm-deep bed

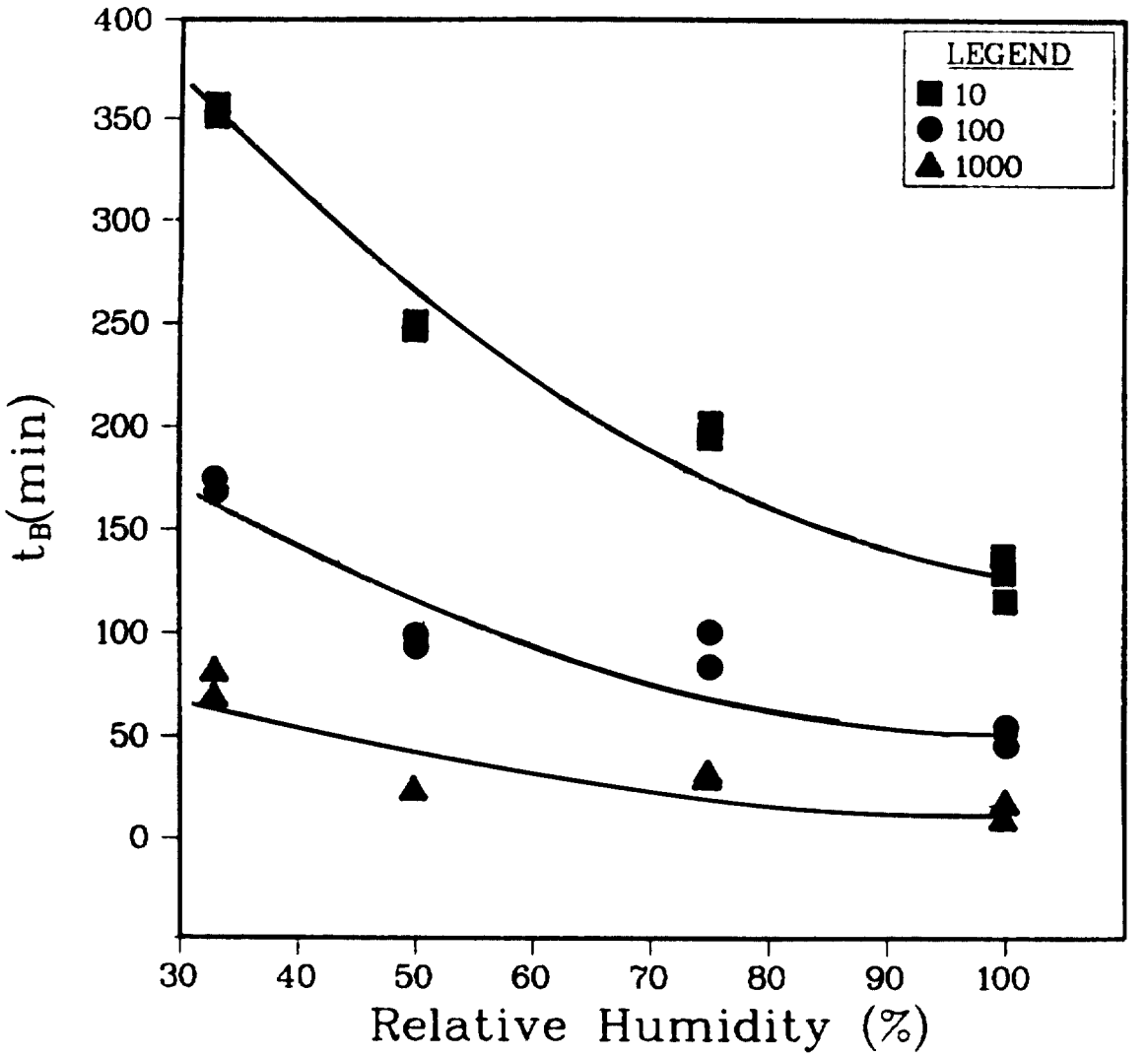

Figure 8 Protection factors as functions of relative humidity for a TEDA-impregnated charcoal (BC 487).

Figure 8 shows plots of breakthrough times vs relative humidities (21 ± 1 °C) for three protection factors. Increased relative humidity greatly decreased the breakthrough times for a given protection factor. Or, stated otherwise, increased relative humidity decreased the protection (or decontamination) afforded after a given time.

V. Conclusions

1. The Theory of Statistical Moments best described breakthrough curves for charcoal beds obtained at ppm methyl iodide challenge concentrations. Parameters obtained from data fitting with this theoretical model have useful, physical significance.

2. Breakthrough curves were useful for comparing the performances of sorbent beds using protection factors.

3. Significant increases in breakthrough times for decreasing challenge concentrations were measured for two charcoal sorbents. If further studies show that this concentration dependence continues to the levels of interest in radioiodine removal, bed testing at ppm methyl iodide concentrations would produce ultraconservative protection factors (bed efficiencies). A challenge concentration effect also has other implications for bed testing procedures. For example, the rate at which a given amount of methyl iodide is released into an air stream will determine its concentration and, thereby, the efficiency measured for a bed downstream.

4. Increased relative humidity resulted in decreased performance of a sorbent bed. This effect is also significant above 50 %. Therefore, a respirator cartridge or other sorbent bed should be tested at 100 % relative humidity or limited in use to the maximum humidity at which it was tested successfully.

5. The effect of increased sorbent bed performance with increased bed diameter was mainly due to decreased air flow velocity. Such a dependence is especially important for a respirator cartridge application, since the air flow in actual use can vary widely, depending on the workload of the user. Therefore, a respirator cartridge or other sorbent bed should be tested at the maximum expected flow velocity or should be limited in its use to certain flow velocities.

VI. References

(1) O. Grubner. "Statistical moments theory of gas chromatography: diffusion controlled kinetics." Advances in Chromatography, Vol. 6. Marcel Dekker, Inc., New York, N.Y.,]968.

(2) O. Grubner and D.W. Underhill. "Calculation of adsorption bed capacity by the theory of statistical moments." Separation Science, 5, pp. 555-582.

DISCUSSION

KOVACH: The velocity used in your experiments is above that used in reactor air cleaning applications. Whereas at gas mask velocities (above ∿ 80 fpm) pore diffusion is the rate controlling step, below that velocity, bulk diffusion is the rate controlling step.

WOOD: The linear velocities we used are of the same order of magnitude as the 12 m/min in the RDT M-16 test procedures. The Equations (8) and (9) were cited only as examples of how statistical moments can be related to physical parameters. Actually, more recent data developed by varying face velocity, show that the velocity dependence of the statistical moment ratios is not that shown in these equations.

TADMOR: Since your paper was not distributed, I did not have the privilege of seeing all your equations. From the equations shown in the slides, I didn't see an explicit expression for the adsorption coefficient. Is it hidden within the effective diffusion coefficient, or is it explicitly expressed?

WOOD: The adsorption coefficient does not appear in Equations (8) and (9), which are for a given sorbent and sorbate. However, the adsorption coefficient and isotherm can be obtained from the breakthrough data using the Theory of Statistical Moments. I refer you to the paper of Grubner and Underhill that we cited.

EVALUATION AND CONTROL OF POISONING OF IMPREGNATED CARBONS USED FOR ORGANIC IODIDE REMOVAL

J. Louis Kovach and L. Rankovic
Nuclear Consulting Services, Inc.
Columbus Ohio

Abstract

By the evaluation of the chemical reactions which have taken place on impregnated activated carbon surfaces exposed to nuclear reactor atmospheric environments, the role of various impregnants has been studied. The evaluation shows several different paths for the aging and poisoning to take place. The four major causes were found to be:

a) Organic solvent contamination.
b) Inorganic acid gas contamination.
c) Formation of organic acids on carbon surface.
d) Formation of SO_2 from carbon sulfur content.

It was found that the prevention of poisoning by path a and b can be accomplished only by procedural changes within the facility. However poisoning paths b, c and d can be controlled to some extent by the selection of carbon pretreatment techniques and the type of impregnant used.

Results were generated by evaluating used carbons from 14 nuclear power plants and by artificial poisoning of laboratory impregnated carbons.

It was found that impregnants which have antioxidant properties, besides reaction with organic iodides, can increase the life of the impregnated activated carbons.

I. Introduction

The two major impregnants used to enhance the organic iodine removal efficiency of activated carbons are iodine and tertiary amine compounds. The initial use of these impregnants was somewhat accidential. The carbons impregnated with these compounds were not initially developed for organic radioiodine removal but for mercury vapor, SO_2, and halide containing war gas removal. It is only recently that conscious effort was being made in the evaluation of existing impregnants or the development of new improved impregnants for organic iodine control. (1)(2)

While most commercial impregnated adsorbents perform well in fresh form, the efficiency of these adsorbents can be reduced in several different manners.

a) Organic solvent contamination.
b) Inorganic acid gas contamination.
c) Formation of organic acids on carbon surface.
d) Formation of SO_2 from carbon sulfur content.

In the following each of these effects are evaluated in relation to their practical occurence and potential preventive methods.

II. Organic Solvent Contamination

Carbon disulfide extraction of impregnated carbons used in various areas of commercial power reactors indicated the presence of the following contaminants.

Paint Solvents: Toluene
Methyl Ethyl Ketone
Methyl Isobutyl Ketone
C_6-C_{10} Straight Chain Hydrocarbons

Degreasing Solvents: Trichloroethylene
Perchloroethylene
Acetone

Welding Fume Decomposition Products:
C_8-C_{15} Aliphatic and Aromatic Hydrocarbons

Organic Acids (probably generated on carbon surface)
Formic
Acetic
Butyric

Additionally, carbon samples from banks of laboratory exhaust hoods showed a very large number of unidentified organic components.

The adsorption of organic solvents on the adsorbent surface results in several paths of decreasing the organic iodide removal efficiency of impregnated carbons and in some cases can actually enhance the formation of organic iodides, while in rare cases the deposition of adsorbed organics can improve the efficiency of these carbons.

As an accelerated laboratory impregnant styrene-butadiene mixtures were tried as simulated poisons, because such mixtures result in plugging of the carbons pore structure. Such poisoning even at severe pore volume and surface area reductions resulted in good methyl iodide removal.

The control of these contaminants is twofold. First it is very important that the administrative control be improved from current practice to lessen exposure of stored or installed adsorbents to paint fumes, degreasing and cleaning solvents and welding fumes. However if exposure of the adsorbent bed to these compounds is unavoidable, such as the case of continuously operated systems,the use of guard beds is highly recommended. Guard beds are unimpregnated beds of carbon (or adsorbents impregnated to control non-radioactive impurities) installed in separate beds. While the use of guard beds will not prevent the transmission of all organic compounds it still gives a very good protection to the main adsorber beds with the exception of possible short durations. The reason for this is that the low molecular weight organics which easily penetrate the guard bed will pass through the main bed relatively fast also. While compounds which are strongly adsorbed and would constitute permanent poisons will be removed at a high efficiency by the guard beds.

III. Inorganic Acid Gas Contamination

The exposure of carbons to SO_2, NO and NO_2 depends primarily in the proximity of the facility to coal fired plants, paper mills, reprocessing facilities, etc. Again, the degree of exposure is more severe in cases of continuously operated systems.

The result of adsorption and/or reaction with acid gases of the impregnant and the carbon can lower organic iodide removal efficiency by several means. As the initial alkalinity of the impregnant (or the adsorbent in case of vegetable base carbons) decreases, iodide compounds are converted to free iodine forms, which are not as strongly retained on the adsorbent particularly at elevated temperatures.

NO_x compounds can react with triamines resulting in either carcinogenic and mutagenic nitrosamines (3), or in the formation of explosives. Such an example is the formation of hexogen or octagen from hexamethylene tetramine in NO_2.

While the NO_x compounds particularly attack the triamine type impregnant the SO_2 reacts with the iodide impregnants.

Additionally NO_2 can also attack the carbon surface itself and result in the oxidation of the carbon surface:

$$NO_2 + C \rightarrow NO + CO$$

While not all of the CO would be released, the oxidation of the carbon surface would eventually also result in surface acidification as discussed later.

This type of contamination is very difficult to control by protective and nearly impossible by administrative measures. However impregnant composition can be varied to greatly lessen the effect of the poisons. Two different additive forms have been successfully evaluated by NUCON to decrease the poisoning effects. These are coimpregnating the carbon - in addition to $CH_3\ ^{131}I$ control impregnants - with a buffer solution which can hold the carbon pH at 10 and the use of small quantities of urea which decomposes both NO and NO_2 to nitrogen, CO_2 and water.

The use of these coimpregnants have increased by more than 50% the life of impregnated carbons exposed to artificially generated NO_x and SO_2 levels under accelerated conditions. The addition of these impregnants have not resulted in the degradation of other properties of the carbon.

Because of the preferential reaction of NO_x with amids compared with amines the urea and other amid compounds results in the lowering of $CH_3\ ^{131}I$ reactant impregnant loss also.

IV. Formation Of Organic Acids On The Carbon Surface

All commercial activated carbons contain carbon-oxygen complexes at the solid-gas interface. These are commonly called surface oxides. The type and quantity of surface oxides depends on the history of the carbon, particularly its exposure to oxygen at various temperatures.

Oxygen present in the form of surface oxides is not physically adsorbed oxygen but chemisorbed. Typical coconutshell carbons used as base for impregnation have approximately 1,000-1300 m^2/g surface area. Chemisorbed oxygen forms can exist in up to 25% of the surface coverage, i.e., 200-300 m^2/g carbon surface filled with various oxygen compounds.

While these surface oxides have very little or no influence on the adsorption of polar compounds they can exert either beneficial or undesirable action on the adsorption of polar compounds, surface acidity and water adsorption. (4) (5) (6) (7)

Formation and/or conversion of these surface oxides is one of the main causes of aging of impregnated carbons. That is,the loss in efficiency during storage of carbons.

As an example the water adsorption isotherm of new and two year aged coconutshell carbon is shown on Figure 1. The shift toward higher water adsorption capacity at all relative humidities is obvious. The effect of humidity on adsorption,isotope exchange and other chemical reactions of $CH_3\ ^{131}I$ is a well known fact and not discussed here in detail.

The presence of the surface oxides does not affect the nitrogen surface area or carbontetrachloride adsorption of activated carbons,thus their presence or form is not directly established by the current test requirements of Regulatory Guide 1.52 or ANSI N509, other than possible different $CH_3\ ^{131}I$ removal efficiency.

In relation to water adsorption at low relative humidities, water adsorption is due to the formation of hydrogen bonds between the water molecules and the most active surface locations. The thus adsorbed water represents secondary adsorption centers which can retain additional water molecules by hydrogen bonds. This leads to the formation of dimeric complexes on the surface. At increasing relative humidity the adsorption will increase based on the number of these secondary adsorption centers. The sharp rise in the water adsorption isotherm at mid range relative humidity is caused by the formation of dimeric groups of water molecules which fuses into the completion of the monomolecular layer. Further increase in RH results in multilayer adsorption thru capillary condensation in the filling of the micropores of the activated carbon.

Surface oxides can be both basic and acidic in character. While carbons exposed to oxygen above 700°C result in an initially basic surface oxide;exposure to oxygen at lower temperature and aging of basic surface oxides results in acidic groups on the surface. In the absence of sufficient alkalinity or buffering on the carbon surface all carbons will show a decreasing pH with aging.(8) (9) (10)

While from a $CH_3\ ^{131}I$ removal standpoint the presence of surface oxides is detrimental,they do have desirable effects also. Similarly to oxide layers on some metal surfaces they do protect the carbon from further oxidation. The carbon is most vulnerable to fast oxidation and subsequent ignition when all surface oxides are removed and the carbon is exposed to oxygen again.

The formation and/or conversion to acidic surface oxides was postulated by several methods.(11) (12) The acidic group formation can proceed from the adsorption of molecular oxygen and its conversion to peroxide group which when hydrated becomes an acid group or through the formation of and oxidation of aldehyde groups on the surface.

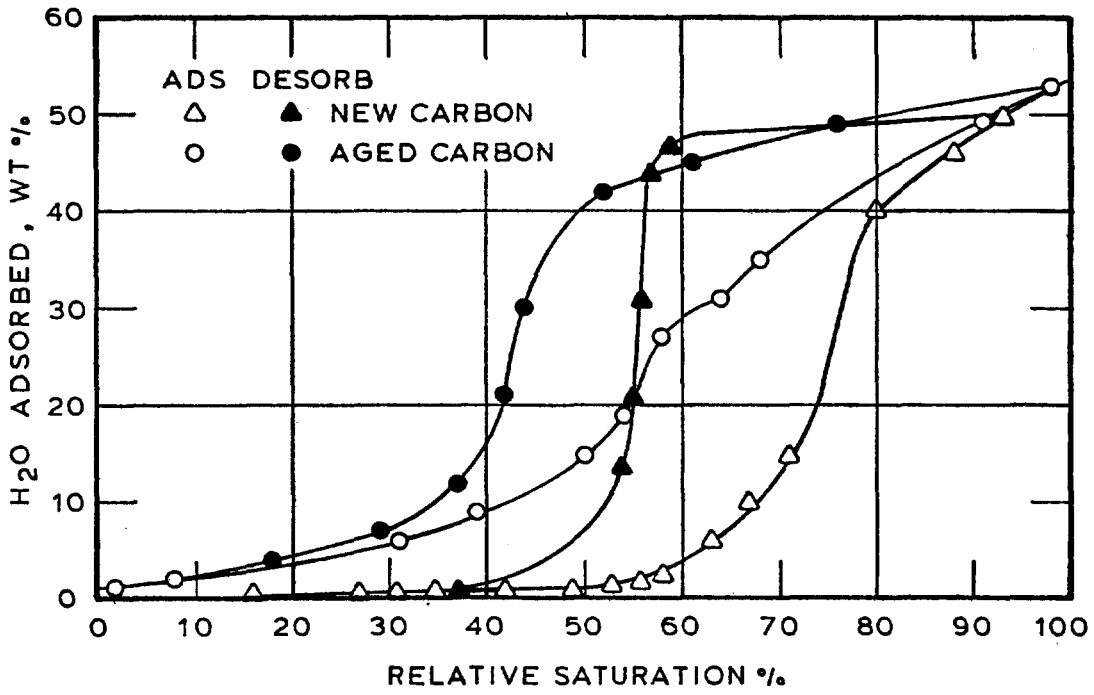

Figure 1 Water adsorption isotherm of new and two year aged unimpregnated coconutshell carbon, 8X16 mesh, 1050 ± 50 m^2/g.

Although impregnated activated carbons can be stored by the manufacturer in oxygen free atomspheres,after they are filled into adsorbers or installed are impossible to protect from oxygen exposure.

However again impregnant selection or addition can decrease the formation of acidic surface by reaction with the surface aldehyde groups or by prevention or decomposition of the peroxide intermediate.

Urea,the impregnant successfully employed to counteract NO_x degradation,also reacts with surface aldehyde groups and can prevent their conversion to surface acid groups. Additional impregnants can also be used to prevent peroxide type oxidation. Some of those tried have detrimental effect on the adsorption or other means of removal of iodine compounds. These are: H_3PO_4, phenol, several organic sulfur compounds. While others have neutral or positive effect in addition to their antioxidant properties. Compounds of the latter group which were evaluated and found acceptable are 4-tert-Butylcatechol, N,N-Diphenyl-p-phenylenediamine, p-Hydroxydiphenylamine, p-Methoxydiphenylamine, benzidine, diphenylamine, phenotiazine, alkylamidinoisurea.(11)

In general the antioxidant selection is based on the following criteria

a) compatibility with other impregnants
b) antioxidant effective
c) neutral or positive effect on organic iodide removal
d) lack of explosive or other adverse chemical formation

The formation of surface oxides does not stop with the generation of chains attached to the bulk carbon, but can result in the formation of detachable, identifiable organic compounds.

Compounds identified as probably originating due to surface oxide formation and decomposition in 0.0001-0.1 μg/g concentrations:

Benzene
Toluene
Furan
Methyl alcohol
Ethyl alcohol
Actone
Methyl isobutyl ketone
Acetaldehyde
Ethyl acetate
1 Butene
C_2 - C_7 Organic acids
CO_2
i Propyl alcohol
i Butyl alcohol

To avoid inclusion of incidental contamination results,the compounds shown are those which occured in all carbon samples tested from various manufacturers' unimpregnated carbons. Compounds which were detected only on one or two carbons were not included in list.

V. Formation Of SO_2 From Carbon Sulfur Content

Numerous activated carbons are prepared from raw materials which contain sulfur (coal, petroleum, coke). It was found that such carbons can slowly release low concentration SO_2 for long times. The reason for the evaluation was the observation of faster aging of a petroleum base carbon identically impregnated to a coconut carbon. Evaluation of the base carbon has shown that the sulfur dioxide is continuously generated. The carbon was evacuated four times at 250°C in less than 10 um Hg vacuum. Even after the fourth evacuation SO_2 was detected in the outgas residue. The residual SO_2 was in the range of 1.0-1.5 μg/g carbon. Similar tests on coconut based carbon resulted only in the decomposed surface oxide residues,no sulfur was detected. Subsequently it was found that a NASA study has resulted in similar findings.(12) That same study identified close to 40 organic compounds in trace quantities removable from the surface of unused carbon. Most of these compounds can be identified as generated by the surface oxidation route and decomposition products surveying the activation process rather than being post production contaminants.

The generation, albeit in trace levels, of SO_2 by activated carbon containing carbon bound sulfur or inorganic sulfides requires the addition of extra alkali or the variation of the buffering composition to assure that the carbon will not reach an undesirably low pH level while in storage or in use. For some of the carbons this would require the addition of so large a quantity of alkali (2-4% by wt) that the ignition temperature of the carbon can not be maintained above the ANSI required level (350°C).

The application of non-vegetable based carbons as base materials for organic radioiodine removal impregnations is dependent on their non-sulfate sulfur content.

VI. Evaluation Of Used Carbons

Often test conditions used in the past have not resulted in pinpointing the degree of poisoning because test pre-equilibration resulted in partial or full regeneration of the carbon. However evaluation of condensate obtained during 130°C tests and CS_2 extraction of carbon samples results in the following observations.

1) The major cause of poisoning is organic solvent contamination, 85% of failed tests showed high organic content. In one case organics in excess of 5.0% by weight were present. Failure rate was approximately 15% of 74 samples tested at 130°C.

2) In 55% of used carbons tested, even though the carbon passed under old test conditions, the condensate collected contained organics corresponding to 14.0-260.0 mg/g carbon.

3) Inorganic acids HNO_3 and H_2SO_4 were identified in all samples from systems operating continousuly when nuclear power station is located within approximately 10 miles of a coal fired station.

4) Organic acids were identified in all samples which were in place for longer than 1 year.

5) Carbons containing tertiary amines showed higher $CH_3\ ^{131}I$ residual efficiency than KI or KI_3 carbons at equal contaminant levels.

Figure 2 shows the aging and poisoning rate of in-place power plant carbons. Figure 3 shows artificial accelerated exposure response of several different impregnation carbons.

The results of in-place carbons can be evaluated only in a trend basis because of great divergence in housekeeping and care exercised for the filter-adsorption systems.

The simulated laboratory exposure consisted of air stream at 85-95% RH, 5-25 ppm organics and 1.0-1.5 ppm NO_x at 40 $\pm$ 2 fpm superficial face velocity on 8X16 mesh carbons.

The carbon types used were:

1) KIG (iodine impregnated coconut)

2) TEG (tertiary amine impregnated coconut)

3) KITEG (iodine and tertiary amine impregnated coconut with buffering)

4) KITEG(CO) (same as No. 3 but coal base)

5) KITEG II (iodine and tertiary amine impregnated with buffering and antioxidant)

VII. Summary And Conclusions

Four major poisoning paths of impregnated carbons used for organic radio-iodine control were evaluated. The most commonly occuring poisoning in continuously operated systems is due to organic solvent contamination which is the most difficult to control by technical means.

The effect of other poisoning paths can be greatly lessened by the selection of $CH_3\ ^{131}I$ reacting impregnants which act as antioxidants and/or by the addition of other impregnants for the control of inorganic acid, carbon surface oxide and sulfur decomposition. The data generated indicates that by selection of impregnants for the specific purpose rather than employing impregnated carbons developed for other application the carbon efficiency and life can be optimized.

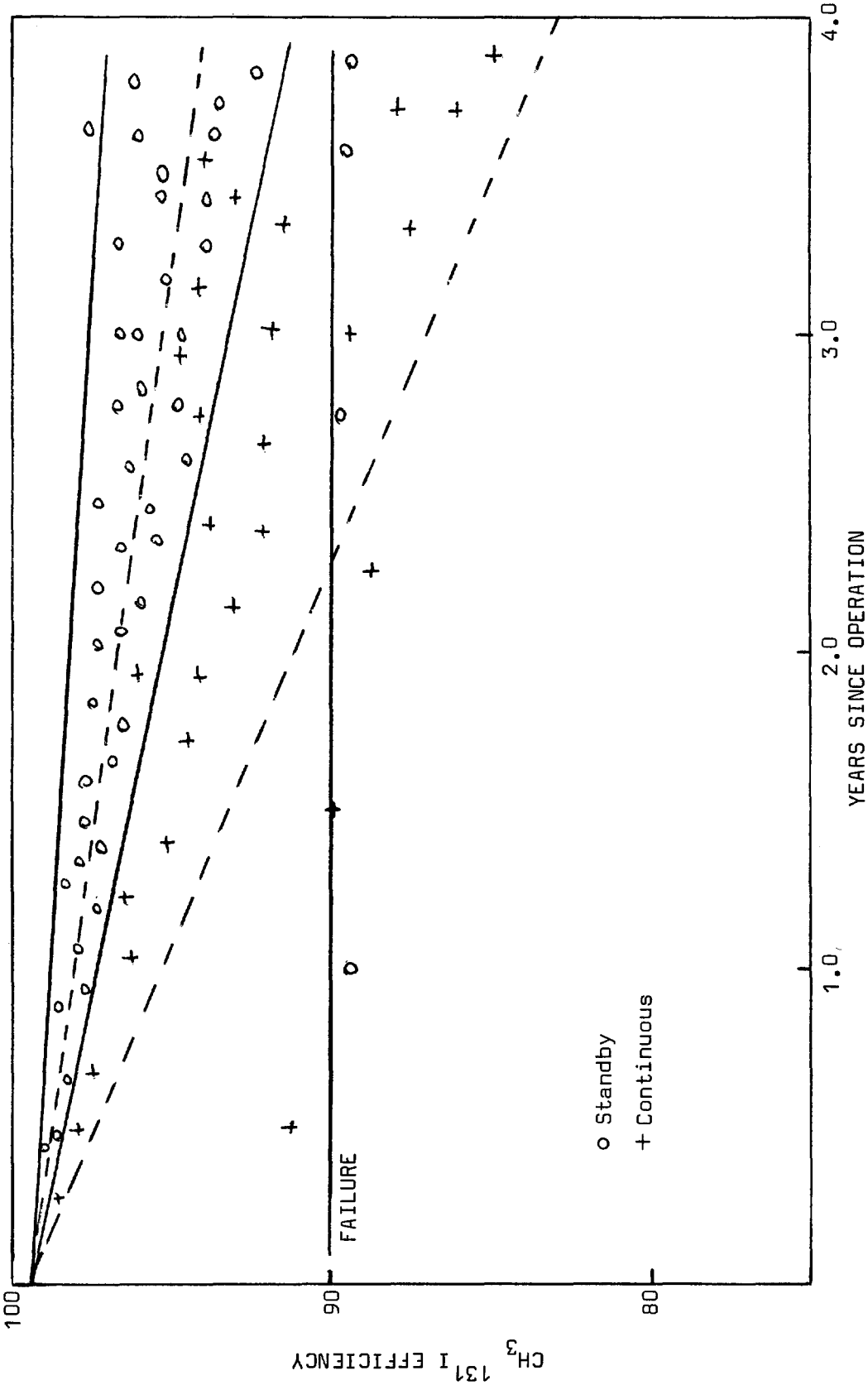

Figure 2 Poisoning rate of plant installed impregnated carbons.

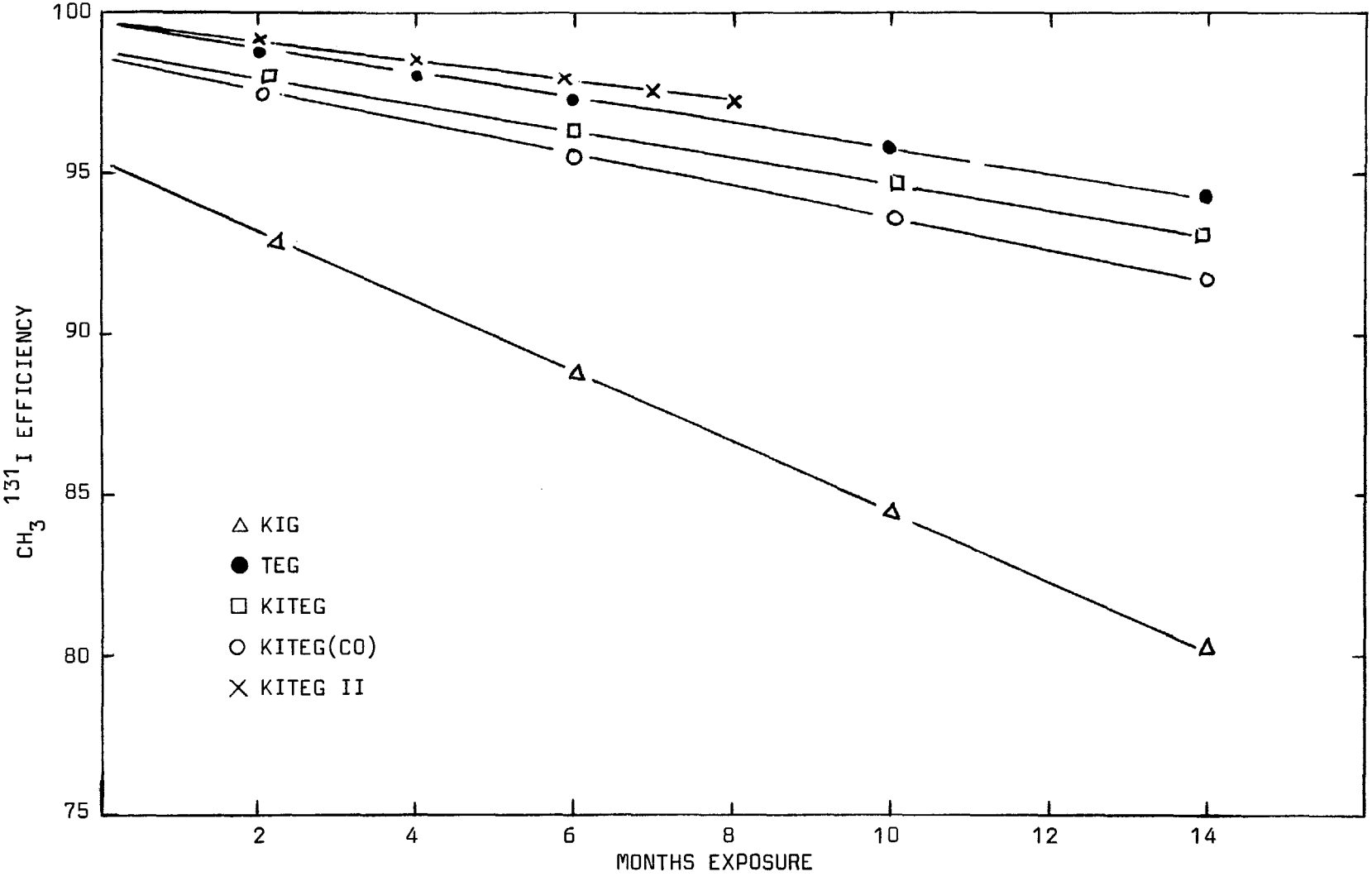

Figure 3 Methyl iodide removal efficiency vs exposure: 25°C, 95% RH, 2.0 inch bed, 40 FPM.

References

1) Deitz, V. R. and Blackley, C. H. ERDA Report CONF-760822 (1977)

2) Evans, A. G. ERDA Reports 1403, 1463 (1975 & 1976)

3) Magee, P. N. and Barnes, J. M. Advances of Cancer Research 10,163 (1967)

4) Sihvonen, V. Trans. Farad. Soc. 34, 1062, (1938)

5) Lendle, A. Zhur. Phys. Chem. A172, 77, (1935)

6) Garten, V. A. and Weiss, D. E. Austral, J. Chem. 8, 68 (1953)

7) Garten, V. A. and Weiss, D. E. Austral, J. Chem. 10, 295 (1957)

8) Puri, B. R. Chemistry & Physics of Carbon Vol 6, M. Dekker (1970)

9) Kruyt, H. R. and deKadt, G. S. Koll. Zblatt. 47, 44 (1929)

10) Strickland-Constable, R. F. Trans. Farad Soc. 34, 1075, (1938)

11) Patent applied for by Nuclear Consulting Services, Inc. (1978)

12) NASA Report CR-115202, Analytical Research Laboratories, Inc. (1971)

DISCUSSION

DEUBER: From the laboratory tests on the retention efficiency of aged carbons, one often gets biased results. With preconditioning, the pollutants are desorbed. Without preconditioning, exact conditions cannot be assured. The best results are to be expected with in-plant tests using radioiodine species samplers and the ^{131}I of the plant.

KOVACH: If the iodine species and concentrations existing in-plant are identical to those expected in accidental releases, then testing with those iodine species will result in a correct approximation of efficiency. However, even without preequilibration, if the test is run long enough to obtain steady state conditions, then laboratory testing is also valid.

PAULING: What, in your opinion, is the advantage and economic value of using a non-impregnated charcoal in a guard bed of a continuously operating system?

KOVACH: The use of a properly designed, testable deep bed system with guard beds has significant advantages. Generally, organic compounds which are only weakly adsorbed on the guard bed will not permanently poison the main bed either, whereas compounds which would permanently poison the main bed would be strongly adsorbed on the guard bed. The economics depend on the particular contamination level in the influent air stream. Adsorbents in unimpregnated form cost approximately 1/3 of the impregnated carbon.

A DETERMINATION OF THE ATTRITION RESISTANCE OF GRANULAR CHARCOALS

Victor R. Deitz
Naval Research Laboratory
Washington, D. C. 20375

Abstract

A laboratory procedure has been developed to evaluate the attrition of granular adsorbent charcoals on passing an air flow through the bed. Two factors observed in plant operations were selected as relevant: (1) the characteristic structural vibrations in plant scale equipment (motors, fans, etc.) that are transmitted to charcoal particles and cause the particles to move and rub each other, and (2) the rapid air flow that results in the movement of the attrited dust. In the test a container for charcoal [50 mm diameter and 50 mm high] was vibrated at a frequency of 60 Hz and at a constant energy input manually controlled using a vibration meter in the acceleration mode. Simultaneously, air was applied and exited through glass fiber filter paper. The quantity of dust trapped on the exit filter was then determined, either optically or gravimetrically. The dust formed per minute (attrition coefficient) was found to approach a constant value. The plateau-values from sequential determinations varied with the source of the charcoal; a 5-fold difference was found among a large variety of commercial products. The first testing of a sample released the excess dust accumulated in previous handling of the charcoal. The plateau values were then attained in the succeeding tests and these were characteristic of the material. The results were compared with those obtained for the same charcoals using older test methods such as the Ball and Pan Hardness Test described in RDTM16-1T (October 1973).

I. Introduction

The evaluation of the mechanical integrity of charcoal granules is admittedly a very difficult problem. Many studies[1,2,3,4] have been based on measurements of particle breakdown and the simultaneous

formation of dust, which in many applications is undesirable. Dust, an imprecise term, refers to particulates capable of temporary suspension in the fluid (air); it may also refer to particles smaller than an arbitrarily selected particle size used for a specified application[5]. Charcoal granules can fragment into smaller pieces and the total material remain in a useful size range, however, some dust is always formed whenever a particle is broken. In addition, neighboring particles have been observed to rub each other more-or-less gently and in the friction process generate small amounts of dust. This paper is concerned with a procedure for quantifying the amount of dust that is formed by the latter process and some results are presented for a number of granular carbon adsorbents.

The published test procedures used to evaluate the attrition of granular charcoals are attempts to simulate the interparticle forces under service conditions. None of these procedures has proven to be generally satisfactory; this fact alone indicates the great complexity of the attrition process in actual applications. The ball and pan hardness test[3,4], developed over 50 years ago, has a considerable backlog of experience which is of value for some producer-user specifications, but the action of steel balls in constant collision with the much smaller charcoal particles is not a good simulation of the mechanical forces at work in an overall adsorbent application.

The proposed procedure is directed to the formation of dust when typical air flows (12 m/min) are passed through beds of granular charcoals. In the selection of relevant factors for modeling, it was observed that plant operations are conducted under engineering conditions that do abrade individual charcoal particles. There are characteristic vibrations in plant scale equipment that are transmitted to the containers that house the charcoal; these vibrations originate in the operating machinery (conveyors, motors, fans, etc.). The charcoal granules subjected to these forces may oscillate and move within the bed as mentioned above. The rapid air flow can then carry the attrited particles from the bed. The present procedure

endeavors to simulate this behavior in a laboratory evaluation of the attrition of charcoals.

II. Experimental

The charcoal container was made of a 50 mm (i.d.) aluminum cylinder with 1/4 inch wall (Figure 1). The bottom was a stainless steel disc (5.6 mm thick) perforated by approximately 225 holes per square inch (0.8 mm diameter). The charcoal sample was placed on a fine mesh wire cloth securely fastened above the retaining disc. The openings of the wire cloth (between 0.17 and 0.21 mm) thus placed a limit on the largest size of particle that could leave the sample. For comparison, the openings of No. 70 and No. 80 U.S. Standard sieves are 0.21 and 0.18 mm, respectively.

The assembly is mounted on a vibration table (Buffalo Dental Mfg. Co., Inc., Brooklyn, New York) which is rated 40 watts at 115 volts, 60 Hz; the different sections were clamped together with 6 mm o.d. tie rods. The vibration table was monitored by controlling the current required to maintain a vibrational intensity at 5g acceleration, the latter being determined by an attached transducer such as the Endevco Accelerometer (Model 2251) with a Signal Conditioner (Model 4416).

The air stream was maintained in a steady downward flow (7ℓ/minute) and upon leaving the charcoal was passed through a Gelman glass fiber filter, Type A/E, 63.5 mm diameter. The filter completely trapped all charcoal dust particles (no darkening of the opposite side occurred) and a weighable deposit of dust was obtained. For smaller deposits of dust, the white filter paper was viewed with a Gardner Colorgrade Portable Reflectometer for measurement of diffuse reflectance (see ASTM Method E 97-55). The illumination was at 45° and viewing at 0° and the spectral response closely approximated the CIE luminosity function Y. The instrument was supplied with a sensor, digital panel meter, and power supply. A ceramic reflectance standard furnished with the instrument was used at frequent intervals to maintain the light intensity at a constant value.

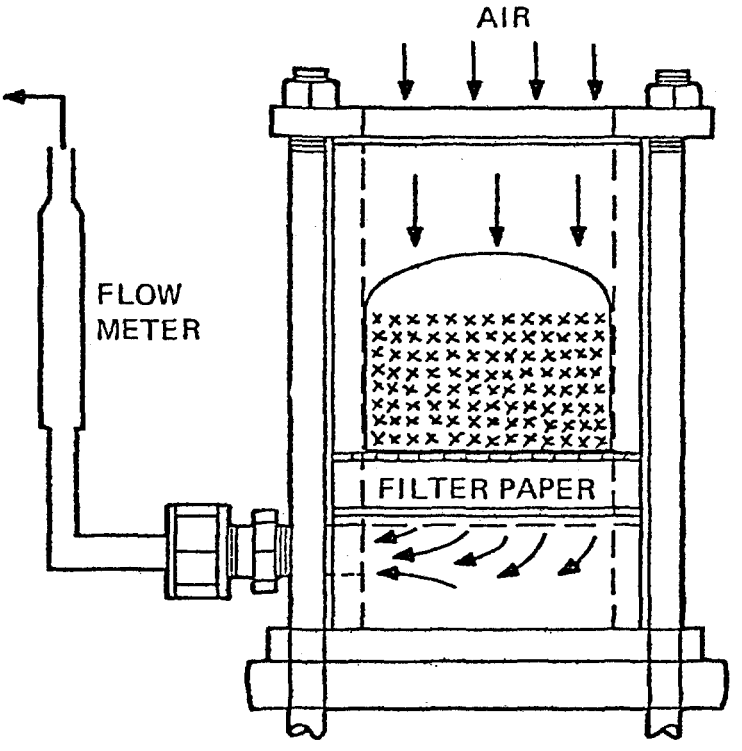

Figure 1: Sketch of a Unit for the Determination of the Attrition of Granular Charcoals

The experimental parameters that may be adjusted are the volume of charcoal, the energy input of the vibrator, the flow of air, the duration of dust collection, and the particle size range accepted as the definition of "dust". The lower limit on particle size is fixed by the Type A/E glass fiber filter rated at 99.9% efficiency (0.3 μm) by the dioctyl phthalate penetration (DOP) test. The upper limit is the opening of the wire cloth described above. A large number of measurements were made with a steady downward air flow of 7 ℓ/min. The vibrator current was maintained at 200 ma and, referring to the calibration curve (Figure 2), this current corresponded to an acceleration value of 5g for the vibrator at 60 Hz. This fixed the energy and the momentum transfer (and therefore the force) between the vibrator and the contacting charcoal particles.

III. Results

Six commercial charcoals were evaluated by the same procedure and the results in Table I align the samples in an increasing

Table I: Dust Formation for Five Granular Charcoals - Repetitive Measurements with Same Sample (Units Based on Relative Reflectance)

	G-210	GX 158	G104	Granular Darco	CAL
1	1.49**	4.61**	3.46**	4.80**	4.78**
2	0.38*	3.56	2.87**	4.48	3.26
3	1.06	3.64	1.69	3.77	3.82
4	1.17	3.73	1.40	4.16	3.38
5	1.07	3.34	1.61	3.98	3.50
6	0.84	3.61	1.57	4.21	3.50
7	0.87	3.17	1.58	4.36	3.25
8				3.80	
9				4.54	
Average	1.00	3.51	1.57	4.16	3.45

* No vibration, air pulse only; ** The first use of the sample releases excess dust accumulated in previous handling; these values were excluded from the average.

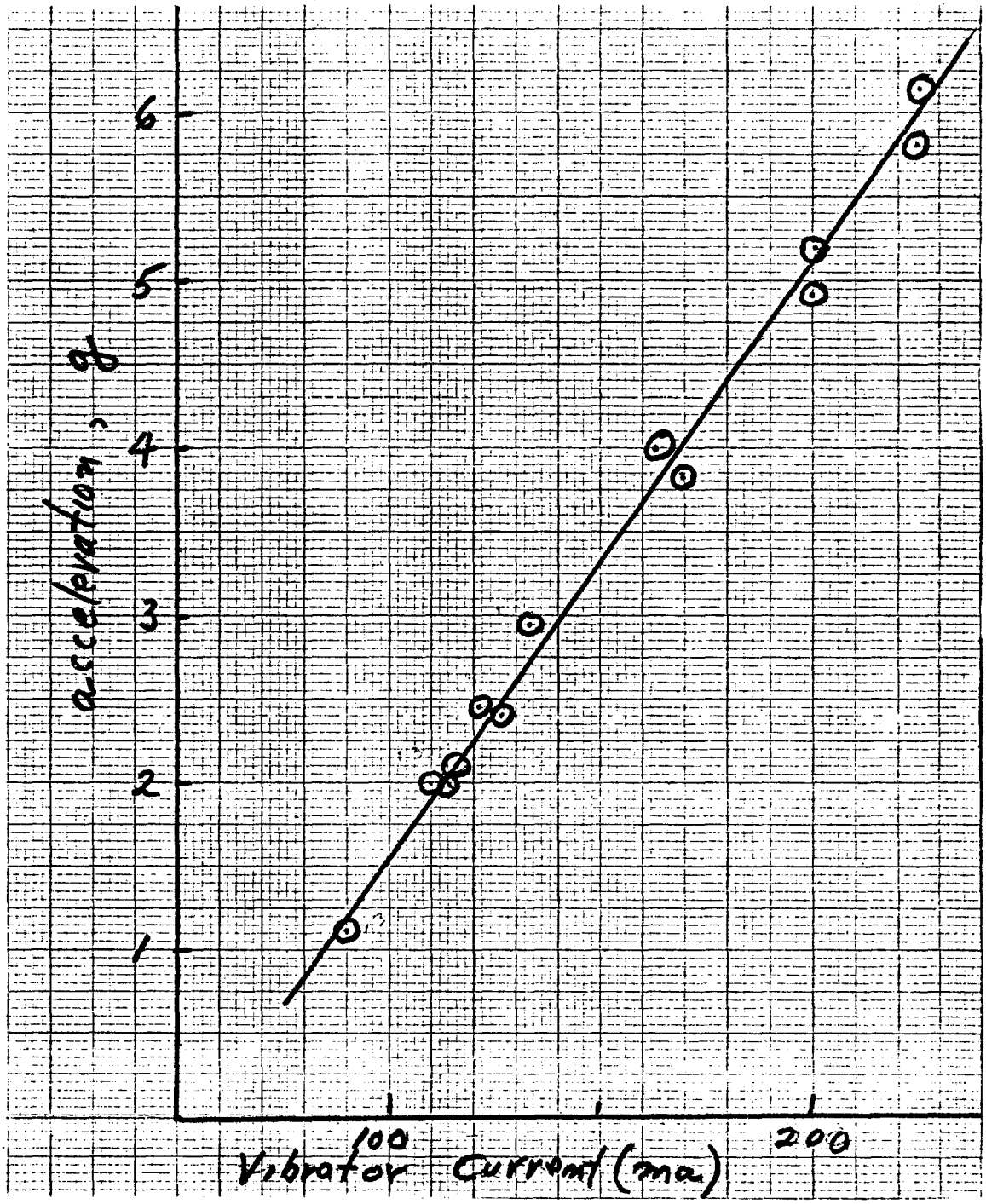

Figure 2: Calibration of the Vibrator Unit Using an Endevco Accelerometer

sequence of dust formation. In these measurements the values are based on the change in reflectance of the initial paper and the same paper plus the dust deposit. The alignment, seen in Figure 3, shows that a coconut shell charcoal, G 210, had the lowest attrition in these tests and one of the coal-base charcoals appears to have a four-fold greater value.

The above preliminary measurements may be considered in terms of known interactions among particles in a vibratory conveying system[6]. The frictional coefficient and the mass of the particles are controlling factors in the motion of particles at constant frequency. The particle translation increases with increase of the frictional coefficient. The observations with charcoal particles in a vibrating bed of constant volume may be summarized as follows:

(1) "Dust" fractions, fragments of the larger particles of charcoal, are generated at a constant rate when an air stream is passed through a vibrating bed.

(2) Very little dust is removed from the charcoal by the air flow when the vibrator is turned off.

(3) The observed dust formation can be used to align samples of different commercial sources in a several-fold variation.

The energy imbalance of the impact and frictional forces result in particle movements which can be viewed when the charcoal is placed in a transparent plastic container. The movement is more rapid with particles of equal size and in those positions in the bed removed from the nodes of the vibrations. When viewed stroboscopically, the frequencies of the particle oscillations cover a continuous range from 60 Hz to rest position.

Additional measurements were made on a number of gas adsorbent charcoals. Series I of Table II was studied with the sample (G 210) loosely packed in a cloth bag; Series II made use of the same sample in loose packing resting on a stretched layer of the same cloth. In the second configuration it is necessary to be alert to possible leakage past the peripheral edge. G-210, a coconut charcoal, has been vibrated about 50 times with little trend in the magnitude of the attrition coefficient. GX-158 is a coal-base charcoal, Granular

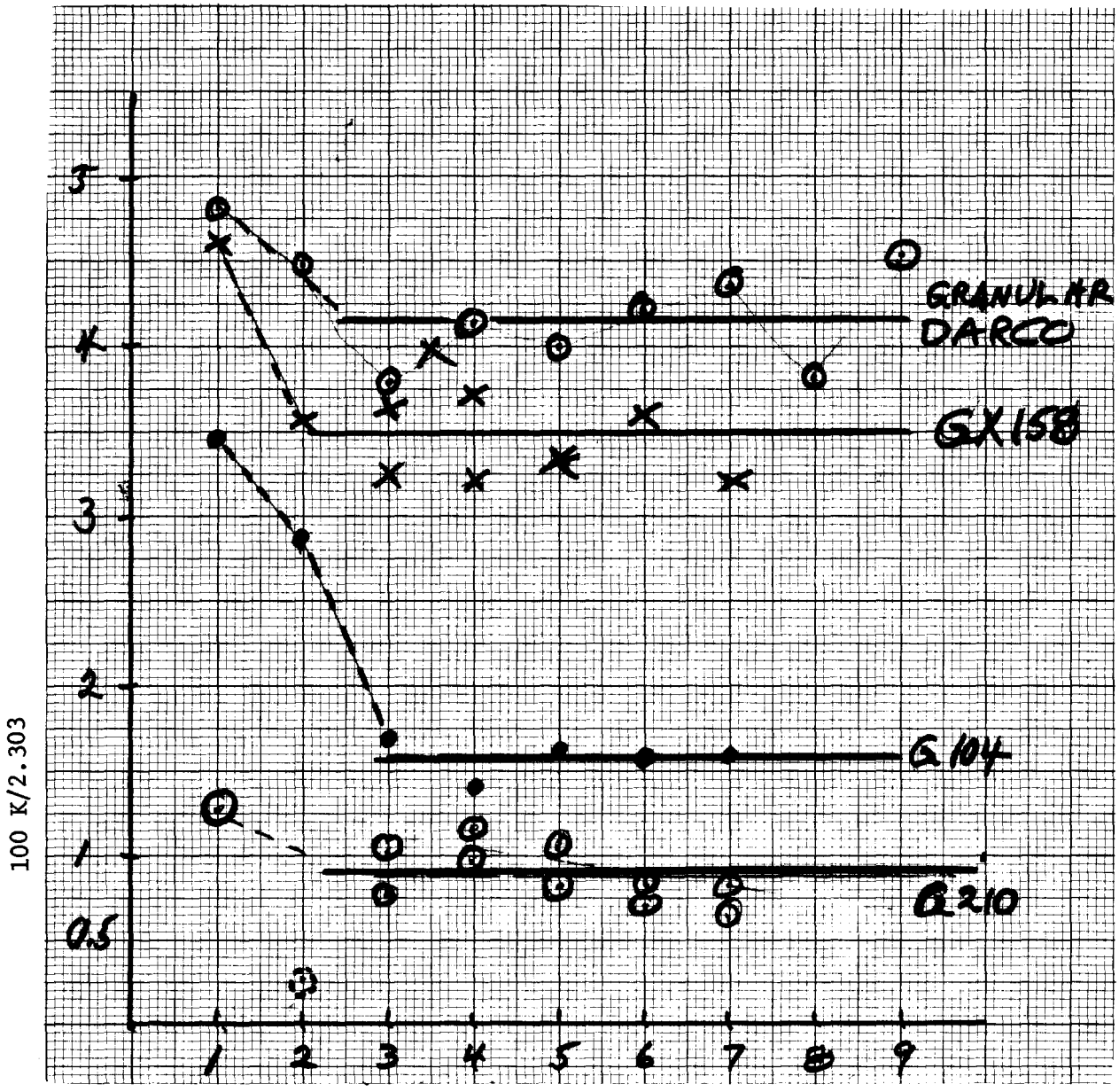

Figure 3: Alignment of Some Granular Charcoals in Formation of Dust

Darco is a lignite-base charcoal and G-104 is a wood-base charcoal. The results in Table II show approximately a 7-fold difference in attrition coefficients (mg/10 minutes).

Table II: Attrition Coefficients (mg per 10 minute vibration) of Some Gas Adsorbent Charcoals (loose packing)

	G-210 Coconut Charcoals (25 g)	GX-158 Coal Base (10.0 g)	Granular Darco wt.		G-104 Wood-Base (15 g)
		4.83	10g	8.45	
I	1.47	5.64	10	7.71	2.05
	1.18	3.78	15	8.91	1.15
	1.30	4.16	15	8.01	1.32
	1.11	3.16	20	9.27	1.10
	1.22	2.40	20	9.02	1.10
		4.0 av.			1.2 av.
II	1.49		25	10.3	
	1.58		25	9.4	
				8.9 av.	
	1.34				
	1.53				
	1.33				
	1.35 av.				

The dependence of the results on the total weight of the sample is not thoroughly understood. The results for a pelleted coal-base charcoal (G-352) are shown in Figure 4. Repetitive use of a 15 g sample lead to an attrition coefficient of about 4 mg/10 minutes. When additional sample, 10 g, was added, the same value was obtained. One explanation is based on the observation that some fraction of the charcoal particles is really at rest in the node positions of 3-dimensional vibrations. As a consequence, charcoal samples must be compared on a constant volume basis, of fixed dimensions.

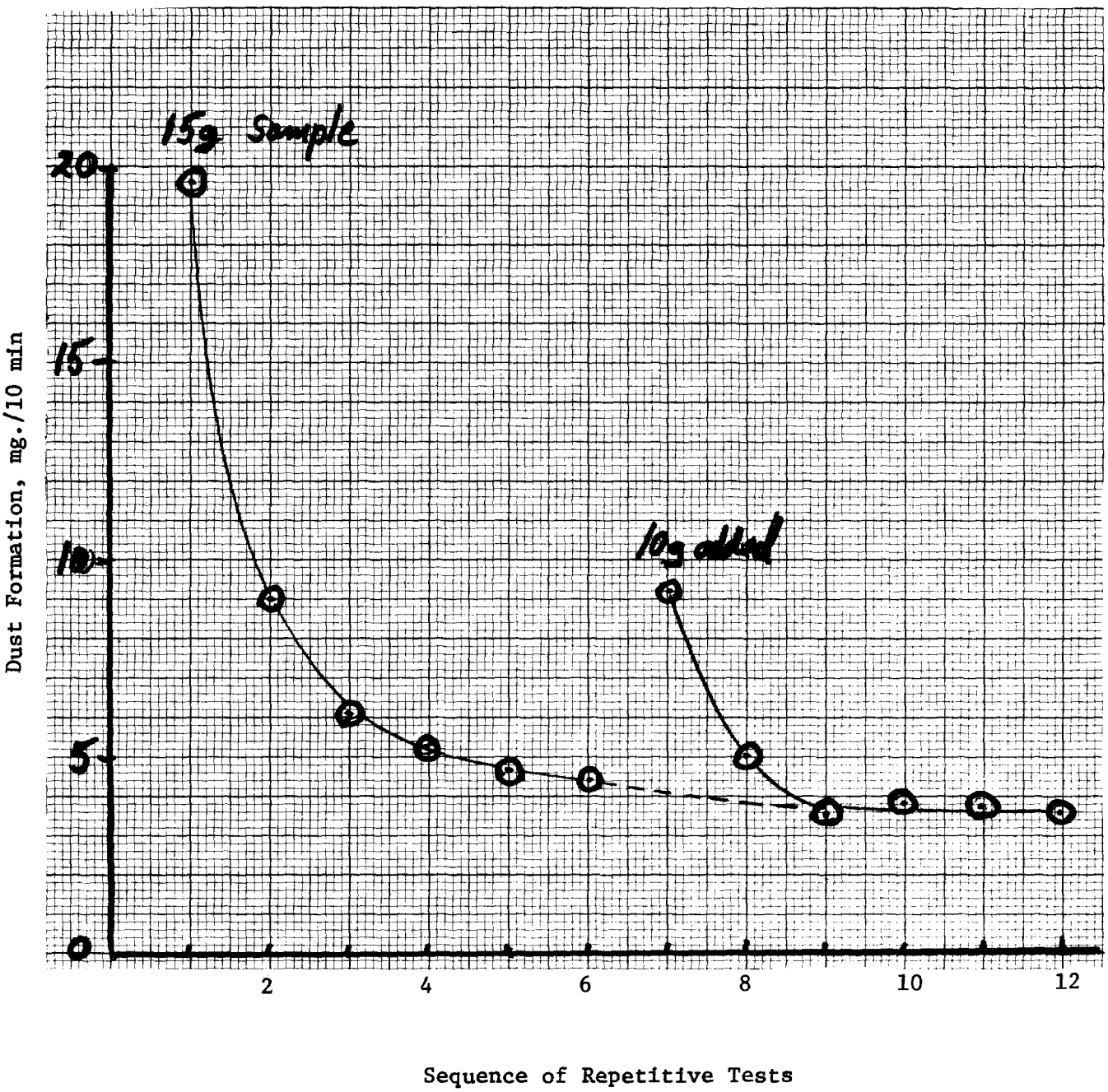

Figure 4: Attrition of a Pelleted Charcoal (G 352, 1/8" cylinders) in Sequential Testing

Some samples were contained in a cloth bag in which the sizes of the rectangular openings varied from 0.1 to 0.25 mm. It may be noted that the opening of a No. 100 U.S. Standard sieve is 0.149 mm and that of a No. 60 sieve is 0.25 mm; thus, no particles greater than that of a No. 60 sieve were counted in the formation of dust. Indeed, in most cases very few individual particles greater than a No. 100 sieve opening were collected on the filters. The same cloth was in other cases stretched across the top of the charcoal-support disc and wedged tightly around the circular edge of the support.

A most interesting behavior was found when a cloth bag containing a charcoal was tightly packed; this configuration markedly reduced the formation of dust. When the closure of the bag was relaxed, the charcoal particles assumed a loose packing and the dust formation then increased to a characteristic value. Typical results are given (Table III) for a Cane CAL sample kindly supplied by the California and Hawaiian Refinery. The marked difference between the tightly-packed and a loosely-packed sample is evident in Table III. The first use of a sample frequently released excess dust that had accumulated in the previous handling of the material in transportation, manufacture, or laboratory operations, but the plateau value formed upon repetitive measurements was characteristic of the charcoal.

Table III: Dusting Coefficient (mg/10 minutes) of Cane CAL: Dependence on Packing during Vibration (Samples Supplied by the C & H Refinery)

	New Cane CAL		Regenerated Cane CAL	
	tightly packed	loosely packed	tightly packed	loosely packed
	8.5*	12.8	2.3	10.1

	3.7	6.1	1.5	9.3
	2.4	10.2	0.2	8.0
	1.7	10.1	0.5	7.2
Av.	2.5	9.5	1.1	8.6

*NOTE: The first use of a sample in the vibrator often releases excess dust accumulated in previous handling.

IV. Discussion

Charcoal particles fracture in a brittle manner, i.e. by a process with little or no plastic deformation. In this respect, the behavior is like most ceramics. Experimentally, the strength of porous ceramics decreases nearly exponentially with increase in the volume fraction of pores[7]. Hence, highly porous charcoal particles can be expected to show a correlation between the friction and attrition mechanism. The factors that increase the friction between charcoal particles should likewise increase the attrition, i.e. the dust formed.

A fundamental treatment of the fracture of charcoal particles is beyond the scope of the present paper. Instead, one application of the findings is to formulate a test procedure whereby different charcoals can be evaluated for use in some individual application. The requirements of a test procedure for technical control purposes are:

1. The experimental details should be relevant to the adsorption application.
2. The results must be adequately precise.
3. The test should be conducted with minimum technician time and maximum simplicity.
4. The maintenance should be practical in time and capital investment.

A test procedure is now being prepared for consideration by the ASTM Committee D-28. The procedure is based on the increase in weight of the glass fiber filter observed during specified parameters.

The present study has been directed to the attrition of charcoal and the generation of dust in adsorbent applications, but the procedure might also be used to estimate the dust already in a sample. The boundary of a charcoal granule is a very rough surface and there are many nooks and crannies to hold small dust particles. It is not known to what degree these are released in the vibrating sample and carrried away by the flow of air. A plausible assumption

is that a steady state is soon attained. It is, of course, necessary to specify the time interval on the vibrating unit that is to be used in the estimate of initial dust in a sample.

There does not appear to be a significant correlation of the attrition coefficient with Ball & Pan Hardness. The latter is concerned with both particle breakdown and attrition and both processes form dust. The new procedure given in this report forms dust alone. There is need to obtain a correlation with some plant experience. Qualitatively, it is possible to align different charcoals by the visual appearance of the cloud of dust obtained by allowing a sample of charcoal to fall about 3 feet. The alignment is subjective, but appears to be in direct proportion to the attrition coefficient. It may be noted that a vibrated sample of charcoal is remarkedly free of dust as judged by appearance in free fall.

There is no satisfactory correlation among samples from different sources with the bulk density or weight per particle. This is understandable since the source of the dust originates from the dynamic process of particles rubbing each other.

Further studies now in progress are concerned with many aspects of the above work: vibrations 20 to 120 Hz, closely sieved fractions of charcoals, methods to maintain tight packings, correlation with published test procedures, and theoretical models for vibrating beds of charcoals with kinetic equations of motion.

V. Acknowledgements

The sponsorship of the Division of Nuclear Fuel Cycle and Production, Department of Energy, and the cooperation of John C. Dempsey are gratefully acknowledged. Many profitable discussions with Frank R. Schwartz, Jr., North American Carbon, Inc. were very helpful.

VI. References

1. Black, R. F., "Hardness Determination by the Shaking Test", 11th Annual Meeting Sugar Industry Technicians, 1951.

2. Carpenter, F. G., "Development of a New Test for the Abrasion Hardness of Bone Char", 1957, Proc. Tech. Sess. Bone Char, 99-135.

3. Military Specification MIL-C-17605B (SHIPS), 21 March 1966, Charcoal, Activated, Technical, Unimpregnated.

4. RDT Standard, Dept. of Energy, Division of Nuclear Power Development RDT M-16-1T, December 1977. Appendix F: "Standard Method of Test for Determining Ball-Pan Hardness of Activated Carbon", 49-53.

5. ANSI/ASTM D2652-76, "Standard Definitions of Terms Relating to Activated Carbon".

6. Hayashi, H., Suzuki, A. and Tanaka, T., Powder Technology 6, 353-362 (1972).

7. Ryshkewitch, E., J. Am. Ceram. Soc. 36, 65-68 (1953).

DISCUSSION

MURROW: Could vibration possibly circulate the carbon from the lower layers toward the top, or inlet?

DEITZ: The vibrated charcoal particles in a 2-inch bed were observed to circulate from the bottom to the top and then follow another path to the bottom. As mentioned in the text, there were regions where the particles did not move and these were identified under stroboscopic illumination to be the nodes of 3-dimensional vibrations of the charcoal bed.

MURROW: Would you anticipate as much circulation in deep bed systems which have a "head" of carbon out of the air stream?

DEITZ: The "head" of carbon could be a factor if some close-packing arrangement of particles were attained. However, the applied forces on the charcoal in a commercial installation originate at the closest metal parts of the filter installation and these will vary with the vibrational modes and the geometry of the structure.

I would like to raise a question for the HEPA filter engineers, and ask how much charcoal dust has been observed to collect on the filtering surfaces when they follow a charcoal installation.

SCHURR: Have you done size and shape studies of attrited charcoal particles to determine if attrition rates are likely to remain constant over a long period?

DEITZ: The dust that was collected on several glass filter papers was observed with an optical microscope (100X) and found to have only normal features. Extruded charcoal gives some curved particles. Cylindrical and spherical particles generated least dust per unit time, as might be expected in a wear-friction process. As mentioned in the text, a particular coconut charcoal was vibrated in 50 separate experiments with only a slight trend towards smaller values of the attrition coef-

ficients. Determinations are planned using closely-sieved fractions from some charcoals. However, the friction of porous and rough charcoal particles rubbing each other in a vibrating bed could be expected to continue to abrade at the relatively small constant rate that is observed.

Our plans are to make ten vibrating devices similar to that described in the paper and these will be made available, at cost, to would-be investigators. Please write to the author at: Code 6170, Naval Research Laboratory, Washington, D.C. 20375, if your laboratory is interested.

THE DEVELOPMENT OF $Ag^{O}Z$ FOR BULK ^{129}I REMOVAL FROM NUCLEAR FUEL REPROCESSING PLANTS AND PbX FOR ^{129}I STORAGE*

T. R. Thomas, B. A. Staples, and L. P. Murphy
Allied Chemical Corporation
Idaho Chemical Programs - Operations Office
Idaho National Engineering Laboratory
Idaho Falls, Idaho

ABSTRACT

Tests were conducted to develop silver-exchanged mordenite (AgZ) for removal of gaseous ^{129}I from nuclear fuel reprocessing plants. The effects of bed depth and hydrogen pretreatment on the elemental (I_2) iodine loading of AgZ were examined. The tests indicated that reduced AgZ ($Ag^{O}Z$) had about twice the capacity for iodine as AgZ, and at least 15-cm bed depths should be used for loading tests.

The effects of $H_2O(g)$, NO, NO_2, and bed temperature on the iodine loading of $Ag^{O}Z$ were determined. The highest loadings were obtained with NO in the gas stream. Using simulated dissolver off-gas streams, loadings of about 170 mg I_2/g $Ag^{O}Z$ and decontamination factors of 10^3 to 10^4 were obtained. This represents about 72% conversion of the silver to silver iodide. The data indicate that NO keeps the silver in the metallic state until silver iodide is formed. In the absence of NO, NO_2 may partially oxidize the silver to silver oxide and/or nitrate to cause lower iodine loadings. Water vapor and bed temperature appeared to have no effect on the iodine loadings.

Tests were conducted to develop a dry method for *in situ* regeneration of iodine-loaded $Ag^{O}Z$. A test bed of $Ag^{O}Z$ was recycled 13 times by loading it with I_2 and stripping the I_2 (as HI) with H_2. A 20% loss in iodine capacity was observed by the fourteenth loading. More tests are needed to determine if iodine loadings continue to decrease or become constant beyond the thirteenth cycle.

The iodine loadings of lead-exchanged zeolites, which were used to chemisorb HI during the recycle tests, were measured. Loadings up to 408 mg HI/g substrate were obtained. This represents about 90% use of the lead to form chemisorbed iodine. The iodine vapor pressures at 20°C over the substrates were predicted to be 10^{-6}, 10^{-8}, and less than 10^{-16} atm for lead-exchanged mordenite, lead-exchanged faujasite and reduced lead-exchanged faujasite, respectively.

A process-flow diagram was formulated for iodine recovery. Two parallel beds of $Ag^{O}Z$ are used to permit continuous iodine recovery. While one is being regenerated the other recovers iodine. The iodine is chemisorbed as silver iodide, stripped as hydrogen iodide, and chemisorbed on the lead bed as a form of lead iodide. The silver beds were sized for a 30-day operation in a fuel reprocessing plant before regeneration. About 5 days would be needed for regeneration. About 2 m^3 of iodine-loaded lead-exchanged faujasite would be

*Work performed under USDOE Contract EY-76-C-07-1540.

generated each year. The lead bed would be contained in canisters to permit transfer in and out of the bed holder and storage in 0.2 m^3 (55 gal) drums.

INTRODUCTION

The objectives of the ^{129}I Adsorbent and Storage Program conducted at the Idaho Chemical Processing Plant (ICPP) were to develop:

(a) Silver-exchanged zeolites for bulk ^{129}I removal from the dissolver off-gas (DOG) of Light Water Reactor (LWR) fuel reprocessing plants.

(b) A dry method for in situ regeneration of spent silver-exchanged zeolites.

(c) Lead-exchanged zeolites for the collection of iodine during regeneration of the silver-exchanged zeolites and as a final storage medium for immobilization of ^{129}I.

In the previous Air Cleaning Conference,[1] we reported a dry method for in situ regeneration of spent silver-exchanged faujasite (AgX). The data indicated a 50% loss in iodine loading occurred after five regenerations. Later investigations with silver-exchanged mordenite (AgZ) indicated no loss in iodine loadings after five regenerations. The efforts of the program were shifted to developing AgZ for bulk ^{129}I recovery. The objectives were:

(a) Determine the effect of hydrogen-pretreatment on the elemental-iodine (I_2) loading of AgZ.

(b) Determine the effects of water vapor, NO, and NO_2 on the iodine loadings of hydrogen-pretreated silver-exchanged mordenite (Ag^OZ).

(c) Conduct recycle tests using a bed of Ag^OZ in which the iodine was repeatedly loaded as I_2 and stripped as hydrogen iodide (HI).

(d) Perform iodine-loading tests on lead-exchanged zeolites with HI.

(e) Measure the iodine vapor pressures of chemisorbed iodine in lead-exchanged zeolites.

EXPERIMENTAL PROCEDURE

The lead-exchanged faujasite (PbX) was prepared by ion exchange with 1.6 mm spheres of Linde Molecular Sieve, Type 13X. The lead-exchanged and silver-exchanged mordenites (PbZ and AgZ) were prepared by ion-exchange with the sodium form of 10-20 mesh Norton Zeolon 900. A plug-flow procedure was developed for ion exchange. The method and apparatus are described elsewhere.[2] Fresh Ag^OZ (i.e., not regenerated) and Pb^OX were prepared by exposing 500 g batches of the AgZ or PbX to pure H_2 (5 L/min) at 500°C for 24 hours.

The test apparatus and general test procedure used for iodine-loading studies were described in the previous Air Cleaning Conference.[1] The apparatus used for regenerating the iodine-loaded $Ag^{O}Z$ (AgIZ) and transferring the iodine to PbX is described elsewhere.[2]

Recycle Tests on $Ag^{O}Z$

Iodine-loading and stripping tests were run repeatedly on a test bed of $Ag^{O}Z$. The $Ag^{O}Z$ was loaded with iodine in a simulated DOG stream, the bed dismantled, the iodine content determined, and the bed transferred to the regeneration-test apparatus. The recycle test conditions are given in Table I. Lead-exchanged zeolites were used downstream of the AgIZ during regeneration to recover desorbed iodine. The lead-exchanged zeolites tested were PbX, PbZ and PbX reduced to the metal ($Pb^{O}X$). Experimental conditions for these adsorbents were the same as those indicated for iodine stripping of AgIZ except for a 150°C bed temperature and 8 m/min superficial face velocity.

TABLE I

CONDITIONS FOR RECYCLE TESTS ON $Ag^{O}Z$

Experimental Variable	Iodine Loading	Iodine Stripping
Bed diameter (cm)	5	5
Bed depth (cm)	15	15
Particle size (mesh)	10-20	10-20
Superficial face velocity (m/min)	15	15
Bed temperature (°C)	150	500
Inlet pressure (mm Hg^{O})	700	760
Carrier gas	air	hydrogen
Iodine conc. at 21°C and 1 atm (mg/m^3)	1500	7400
NO_2 concentration (%)	2	0
NO concentration (%)	2	0
Dew point (°C)	35	nil
Iodine flux to and from bed ($mg/min \cdot cm^2$)	1.5	4.5

Iodine Vapor Pressure over Zeolites

The method for measuring the HI vapor pressure over silver-exchanged zeolites was reported in the previous Air Cleaning Conference.[1] Tests were also conducted to determine the vapor pressure of iodine loaded on PbX, $Pb^{O}X$, and PbZ (PbIX, $Pb^{O}IX$ and PbIZ, respectively). Samples were taken from beds of these materials used to

chemisorb HI during the regeneration of AgIZ. The sodium form of the substrate (NaX) was loaded with airborne-elemental iodine (NaIX) to serve as a reference case for the vapor pressure studies. The NaIX samples contained smaller amounts of iodine (4 wt%) than did $Pb^{o}IX$ (38 wt%), PbIX (40 wt%), and PbIZ (38 wt%). Static-gas blankets of air, hydrogen and nitrogen were used in the iodine-vapor pressure studies. Adsorbent samples were placed in the heated cell, and the absorbance by $I_2(g)$ in the cell was measured as a function of temperature. The experimental procedure and apparatus are described elsewhere.[3]

EXPERIMENTAL RESULTS

The Effect of H_2-Pretreatment on I_2 Loading

The effects of contact time and hydrogen pretreatment on the I_2 loading of AgZ were examined using an airstream face velocity of 15 m/min, a bed temperature of 100°C, and a dew point of 23°C. The test beds were pretest purged for 16 hr. The results along with the distribution of iodine from the top to the bottom of the bed are shown in Table II.

TABLE II

EFFECT OF CONTACT TIME AND H_2-PRETREATMENT ON THE I_2 LOADING OF AgZ

Total Bed Depth (cm)	(mg I_2/g Ag in each 2.5 cm segment) 1	2	3	4	5	6	(mg I_2/g AgZ)[b] Average
5	57	10	-	-	-	-	33 ± 7
5[a]	60	12	-	-	-	-	36 ± 7
15	71	70	68	67	47	9	56 ± 7
15[a]	138	136	123	94	34	5	88 ± 7

a H_2-pretreated

b Duplicate tests were run in all cases; the 95% confidence interval is based on a pooled variance.

The data indicate that the mass transfer zone (MTZ) is 7.5 to 10-cm deep under these conditions. In the 15-cm-deep beds, an effect due to hydrogen pretreatment is observed. In the saturation zone (i.e., the top 5 to 7.5 cm of the bed) the iodine loading of the hydrogen pretreated AgZ ($Ag^{o}Z$) is about twice that of the untreated AgZ.

Iodine Loading on $Ag^{o}Z$

The effects of water vapor, NO, and NO_2 on the iodine loading of $Ag^{o}Z$ were studied. All tests were run in airstreams using the following conditions: bed weight, 270 g; bed depth, 15 cm; bed diameter,

5 cm; superficial face velocity, 15 m/min; bed temperature, 150°C; airborne-elemental iodine concentration, about 1500 mg I_2/m^3; and decontamination factor at breakthrough, 10^3 to 10^4.

The iodine loadings and distribution throughout the bed are given in Table III. The data indicate that the first 5 to 7.5 cm of the test bed attains a saturation loading; the distribution of iodine is about constant. The remaining 7.5 cm is in the mass-transfer zone. In Table IV the average iodine loadings, along with the saturation- and mass-transfer zone loadings are given.

An analysis of the saturation-zone data based on a three-level factorial design and the 95% confidence interval for an effect indicate:

(a) NO effect = 40±12 mg I_2/g Ag^oZ; adding NO to the gas stream enhances the iodine loading.

(b) NO_2 effect = -12±12 mg I_2/g Ag^oZ; within the confidence limits of an effect, the negative influence of NO_2 is not clearly established.

(c) H_2O effect = -4±12 mg I_2/g Ag^oZ; the presence or absence of water vapor has no significant effect on the iodine loadings.

(d) NO x NO_2 interaction = 25±12 mg I_2/g Ag^oZ; the interaction between NO and NO_2 is large; at low levels of NO the effect of increasing NO_2 is a reduction in loading. At higher NO levels, the NO_2 effect becomes small.

(e) H_2O x NO_2 interaction = 11±12 mg I_2/g Ag^oZ; the interaction between water and NO_2 is insignificant.

(f) H_2O x NO = 7.5±12 mg I_2/g Ag^oZ; the interaction between water and NO is insignificant.

A similar analysis of the data in the mass-transfer zone and the overall average loading both indicate a large positive effect due to NO. However, no other main effects or interactions were significant.

Recycle Tests on Ag^oZ

The recycle of a bed of Ag^oZ was stopped after 13 cycles. The experimental conditions used are given in Table I. Table V shows the results of the loading tests and the distribution of the iodine throughout the bed.

During the regeneration tests, the desorbed HI from the AgIZ bed was chemisorbed on lead-exchanged zeolites downstream. Table VI gives the results of the loading tests. The data indicate that the best loadings are obtained on PbX and about 90% of the lead is being used to chemisorb HI. The loading on Pb^oX appears to be about half of that on PbX and PbZ under the same test conditions.

TABLE III

IODINE LOADING AND DISTRIBUTION vs. CONTAMINANT GASES

Test Conditions			mg I_2/g Ag^oZ in each 2.5 cm Segment[b]						
Water Vapor (%)[a]	NO_2 (%)	NO (%)	1	2	3	4	5	6	Avg. Loading (mg I_2/g Ag^oZ)
0	0	0	174	160	141	121	69	15	113
6	0	0	155	136	123	89	35	3	91
0	2	0	97	100	91	73	39	9	67
6	2	0	125	127	119	121	81	17	98
0	0	2	163	171	170	134	93	22	129
6	0	2	169	167	143	123	74	10	115
0	2	2	187	181	185	169	103	21	141
6	2	2	181	172	163	129	65	9	120

[a] Dew point = 35°C

[b] The average value of duplicate or triplicate tests

TABLE IV

IODINE LOADINGS IN SATURATION AND MASS-TRANSFER ZONES vs. CONTAMINANT GASES

Test Conditions			Loadings (mg I_2/g Ag^oZ)[a]		
Water Vapor (%)	NO_2 (%)	NO (%)	Saturation Zone[b]	Mass-Transfer Zone[c]	Overall Average
0	0	0	159 ± 17	69 ± 17	113 ± 12
6	0	0	138 ± 17	43 ± 17	91 ± 12
0	2	0	96 ± 17	41 ± 17	68 ± 12
6	2	0	124 ± 17	73 ± 17	98 ± 12
0	0	2	168 ± 14	90 ± 14	129 ± 10
6	0	2	159 ± 17	69 ± 17	115 ± 12
0	2	2	185 ± 14	98 ± 14	141 ± 10
6	2	2	171 ± 17	67 ± 17	119 ± 12

[a] The error limits represent the 95% confidence interval for duplicate or triplicate tests based on a pooled variance.

[b] The average loading on the first three segments in Table III.

[c] The average loading on the last three segments in Table III.

TABLE V

IODINE LOADING ON $Ag^{o}Z$ vs. NUMBER OF RECYCLES

Cycle	mg I_2/g $Ag^{o}Z$ in each 2.5 cm Segment						Avg. Loading (mg I_2/g $Ag^{o}Z$)
	1	2	3	4	5	6	
0	179	174	164	132	60	7	119
1	182	170	161	127	71	10	120
2	212	201	178	147	76	13	138
3	192	192	180	150	70	5	131
4	194	189	179	145	67	8	130
5	191	180	176	147	80	10	131
6	169	166	154	142	94	21	124
7	188	174	169	139	61	12	124
8	165	182	158	142	47	8	117
9	137	129	125	88	46	11	89
10	149	143	128	103	42	6	95
11	141	117	154	85	95	36	105
12	137	130	129	114	70	18	100
13	143	140	131	107	51	13	98

TABLE VI

HYDROGEN IODIDE LOADINGS ON LEAD-EXCHANGED ZEOLITES IN DRY HYDROGEN AT 150°C

Zeolite	No. of Tests	Iodide Loadings (mg HI/g Zeolite)	
		Average	Range
PbX[a]	5	408 ± 22[d]	378 - 436
$Pb^{o}X$[b]	1	192	-
PbZ[c]	2	380	361 - 398

[a] Lead-exchanged faujasite

[b] PbX exposed to H_2 at 500°C for 24 hr

[c] Lead-exchanged mordenite

[d] The 95% confidence interval of the average

HI Vapor Pressure over AgIZ

Prior to the $Ag^{o}Z$ recycle tests, the vapor pressures of HI (P_{HI}) over AgIZ vs. bed temperature and superficial face velocity were measured. The P_{HI} ranged from $1x10^{-4}$ to $2x10^{-3}$ atm, and the stripping rates of HI were calculated by:

$$\frac{(P_{HI})(cm^3\ H_2/min)\ (128\ mg\ HI/24.1\ cm^3)}{(\text{cross-sectional area of the test bed})} = mg\ HI/min \cdot cm^2$$

where the flow of H_2 and the P_{HI} were measured at one atm pressure and $21^{o}C$.

The response surface (see Figure 1) of the stripping rate vs. the two test variables was obtained by fitting the data to the second order model:

$$Y = 0.585 + 0.456\ X_1 + 0.477\ X_2 + 0.064\ X_1^2 + 0.0045\ X_2^2 + 0.352\ X_1X_2$$

where Y = mg HI/min·cm^2, X_1 = (temp-475)/75, and X_2 = (face velocity-369)/246 .

The coordinates at which duplicate data points were obtained are shown by the symbol "o" in Figure 1. At the 95% confidence level, all observed stripping rates for AgIZ agree within $\pm$ 11% of the predicted rate by the above equation. Possible changes in the response surface due to recycling $Ag^{o}Z$ were not studied.

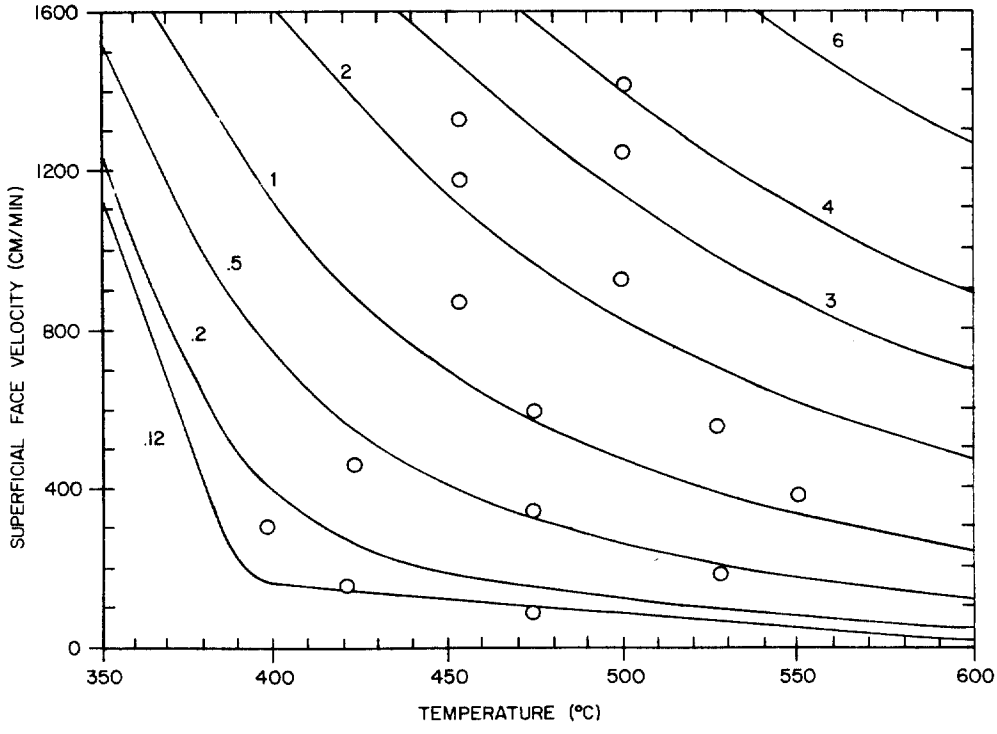

Figure 1. Stripping rate of HI from AgIZ (mg HI/min·cm^2)

I_2 Vapor Pressure over Lead-Exchanged Zeolites

Results of the iodine-vapor pressure studies were fitted by least squares to the equation:

$$\ln P_{I_2} = A - B/T$$

where P is the vapor pressure of elemental iodine in atmospheres and T is in K. The experimental data and curves are published elsewhere.[3] The values of A and B are given in Table VII. The values for P_{I_2} at 20°C were estimated by extrapolation.

TABLE VII

IODINE VAPOR PRESSURE DATA FOR CHEMISORBED IODINE ON LEAD-EXCHANGED ZEOLITES

Substrate	Gas Blanket	A	B	P_{I_2} at 20°C (atm)
PbIX	Air	15.3	9.47×10^3	4.0×10^{-8}
	Nitrogen	17.3	1.01×10^4	3.4×10^{-8}
Pb^OIX	Air	44.5	2.65×10^4	9.5×10^{-21}
	Nitrogen	51.6	3.02×10^4	2.3×10^{-16}
PbIZ	Air	6.6	5.53×10^3	4.4×10^{-6}
	Nitrogen	8.0	6.20×10^3	1.8×10^{-6}

I_2 Solubility Studies

In the solubility studies, about 70% of the iodine on the NaIX beds was eluted by hexane, indicating physisorption of elemental iodine. No iodine could be found in the hexane effluent from columns of Pb^OIX and PbIX. Previous tests have indicated that the water solubility of PbIX is less than that of PbI_2 (Ref. 1) which indicates that HI is not physisorbed. Thus, the results of the solubility studies suggest chemisorption of iodine by Pb^OIX and PbIX as some form of lead iodide.

DISCUSSION OF RESULTS

The Effect of H_2-Pretreatment on AgZ

As the data in Table II indicate, the effect of H_2-pretreatment only shows up in the 15-cm-deep beds. In the 5-cm-deep beds, the shape of the MTZ is probably cancelling out the effect of the increased iodine-loading capacity of Ag^OZ. As the reaction rate becomes slower, the MTZ increases and breakthrough occurs sooner, all other variables being equal. Consequently, tests should be conducted on deep beds to eliminate reaction rate as a variable.

In the saturation zone of test beds, Ag^oZ has about twice the iodine-loading capacity as AgZ (TABLE II). To conserve charge balance, half the iodine in AgZ must be bonded to Ag and the other half to the framework oxygens. There are eight cation sites per unit cell in mordenite.[4] Our substrate contains 20% silver by weight. Thus, if all the silver were converted to AgI and an equal amount were bonded to the framework, the mordenite could contain 448 mg I_2/g AgZ. A loading of 71 mg I_2/g AgZ represents about 16% of total capacity. This amounts to slightly more than one silver atom (12.5%) per unit cell forming AgI. Very little information is available on the location of the cation sites in mordenites. Four sodium sites have been located[4] in the 8-membered rings which interconnect the main channels (12-membered rings). Only the main channels are considered accessible for most molecules. Thus, at least 50% of the silver is not accessible. Perhaps two or three of the remaining four sites are within the interconnecting framework which could also account for the apparent 16% use of exchanged silver in AgZ.

Considerable work has been done to determine the state of the metal[5] when the metal-exchanged zeolite is exposed to hydrogen. Reduced metals become extremely mobile. The metals Cd, Hg, and Zn volatilize from the substrate. The metals Pt, Ni, and Ag migrate to the surface and form aggregates. In faujasites, reduction of the silver by H_2 at 250°C causes silver aggregates, which average 170 angstroms in diameter, to form.[6] The fraction of silver which remains within the zeolite framework was not determined. As the results in Table II indicate, about 60% of the silver is used in Ag^oZ. Since the charge imbalance on the framework oxygens has already been satisfied by protonation, the iodine must be bonded only to the silver.

At least five of the eight silver atoms per site may become available by migration from restrictive framework cavities to the surface of the substrate. In our recycle tests on Ag^oZ (Table V) about seven out of eight silver atoms per site were used after the third exposure to hydrogen.

Iodine Loading on Ag^oZ

A graphical presentation (Figure 2) of the data in Table IV illustrates the positive influence of NO on the iodine loadings. In the absence of NO, NO_2 has a negative influence. However, the large NO x NO_2 interaction (i.e., 25±12 mg I_2/g Ag^oZ) identified in the effect tests prevents a clear statistical interpretation of the positive and negative effects of NO and NO_2, respectively.

The desired reaction: $Ag^o(s) + 1/2\ I_2(g) \rightleftarrows AgI(s)$ (1)

has a driving force of about -14.6 kcal/mol at 150°C. In the presence of O_2 and NO_x, there are three more reactions to consider.

$$2\ Ag^o(s) + 1/2\ O_2(g) \rightleftarrows Ag_2O(s) \quad (2)$$

$$2\ Ag^o(s) + NO_2(g) \rightleftarrows Ag_2O(s) + NO(g) \quad (3)$$

$$Ag_2O(s) + NO_2(g) \rightleftarrows AgNO_3(s) + Ag^o(s) \quad (4)$$

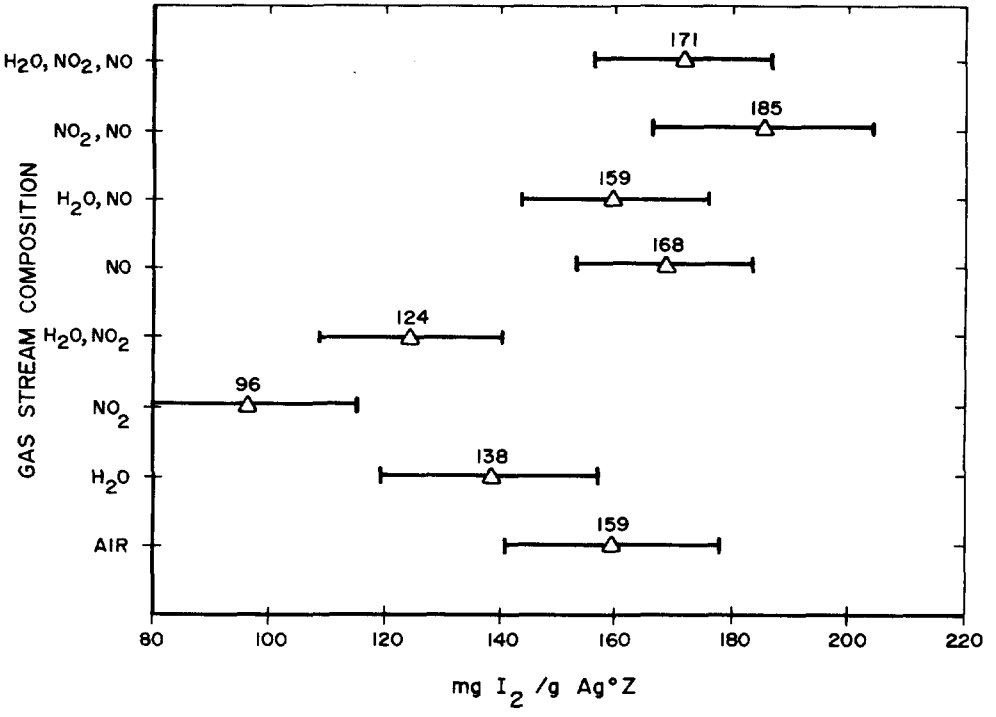

Figure 2. Iodine loadings in the saturation zone of Ag^oZ vs. gas stream composition at 150°C

The reaction free energies (ΔG) for reactions (2) through (4) are, respectively: -0.6, 5.6, and -12.3 kcal. Reaction (3) is probably the reason for the large NO x NO_2 interaction. As long as NO is present, any Ag_2O formed by reaction (2) should be reduced via reaction (3). The equilibrium pressure of NO(g) is given by:

$$\Delta G = -RT \ln P_{NO}/P_{NO_2}$$

Substituting ΔG = 5.6 kcal and P_{NO_2} = 0.02 atm, yields P_{NO} = 3×10^{-5} atm. For partial pressures of NO greater than 3×10^{-5} atm, Ag_2O should not form. In the absence of NO, the driving force to form $AgNO_3$ is about the same to form AgI from Ag^o(s).

Even though it is plausible that the oxide and nitrate may be involved, it is not clear why their formation would reduce the iodine loading in Ag^oZ. The reaction:

$$Ag_2O(s) + I_2(g) \rightleftarrows 2\ AgI(s) + 1/2\ O_2(g) \qquad (5)$$

has about the same driving force per mole of AgI formed as reaction (1). Up to 95% of the silver in $AgNO_3$-impregnated amorphous silicic acid will react with I_2(g) in the saturation zone.[7] Mechanistic studies indicate that iodine nitrate (INO_3) is formed via the reaction:[8]

$$AgNO_3(s) + I_2(g) \rightleftarrows AgI(s) + INO_3(g) \quad (6)$$

The INO_3 then reacts with more $AgNO_3$ to form the iodate, or decomposes to NO_2, O_2, and I_2. Also, mixtures of $AgNO_3$, AgI, and $AgIO_3$ are known to form eutectic mixtures with melting points[8] as low as 76°C. These facts present at least two possible explanations for the low iodine loading on Ag^oZ when only NO_2 is present. The INO_3 may find insufficient $AgNO_3$ to complete the reaction to the iodate. A eutectic melt may replace the silver aggregates and cover some of the available silver.

The effect of NO_2 on Ag^oZ will be a moot point for DOG applications. The primary NO_x species in the DOG of reprocessing plants will be NO. Consequently, the Ag^oZ should remain in the reduced state and the maximum loadings in Figure 2 should be obtained. A loading of 171 mg I_2/g Ag^oZ represents about 72% conversion of the Ag^o to AgI.

As indicated by the data in Table IV, water vapor did not affect the iodine loadings of Ag^oZ. There is no obvious reaction that should occur between Ag^o and $H_2O(g)$. Test results also indicate the absence of a temperature effect. The iodine loading of 132 mg I_2/g Ag^oZ at 100°C and 3% H_2O (the upper 7.5 cm in Table II) is the same as 138±17 mg I_2/g Ag^oZ at 150°C and 6% H_2O (in Figure 2). A comparative test was also made in dry airstreams containing 2% NO_2. At 250°C the iodine loading was 88 mg I_2/g Ag^oZ which is statistically the same as 96±17 mg I_2/g Ag^oZ at 150°C in Figure 2.

Recycle Tests on Ag^oZ

Figure 3 illustrates the iodine loadings in the saturation zones (the upper 7.5 cm loadings from Table V) vs. the number of recycles. The iodine loading on the thirteenth recycle is about 20% less than the initial loading. Linear extrapolation of the data indicates a 50% decrease in the initial loading would occur on the eighteenth recycle. However, further tests are needed to verify the extrapolation. The actual curve may be leveling out as indicated by the similar loadings obtained beyond Recycle 9. The increase in iodine loadings up to Recycle 2 is attributed to further reduction and/or migration of the silver to the surface of the substrate during regeneration. Beyond the second recycle, reduction in loading is attributed to pore collapse, which blocks access to Ag^o remaining in the pores, and/or formation of multi-layered silver aggregates which block access to the lower layers. Both of these processes should reach a point of no further effect; the amount of surface silver available for reaction should reach a steady state. However, the lower limit has not been established.

Iodine loadings and Vapor Pressure on Secondary Adsorbents

The iodine vapor pressures over PbIZ, Pb^oIX, and PbIX in H_2 increase rapidly with temperature. For example, the P_{I_2} over PbIX is $1x10^{-4}$ and $3x10^{-3}$ atm at 150 and 200°C, respectively (i.e., a

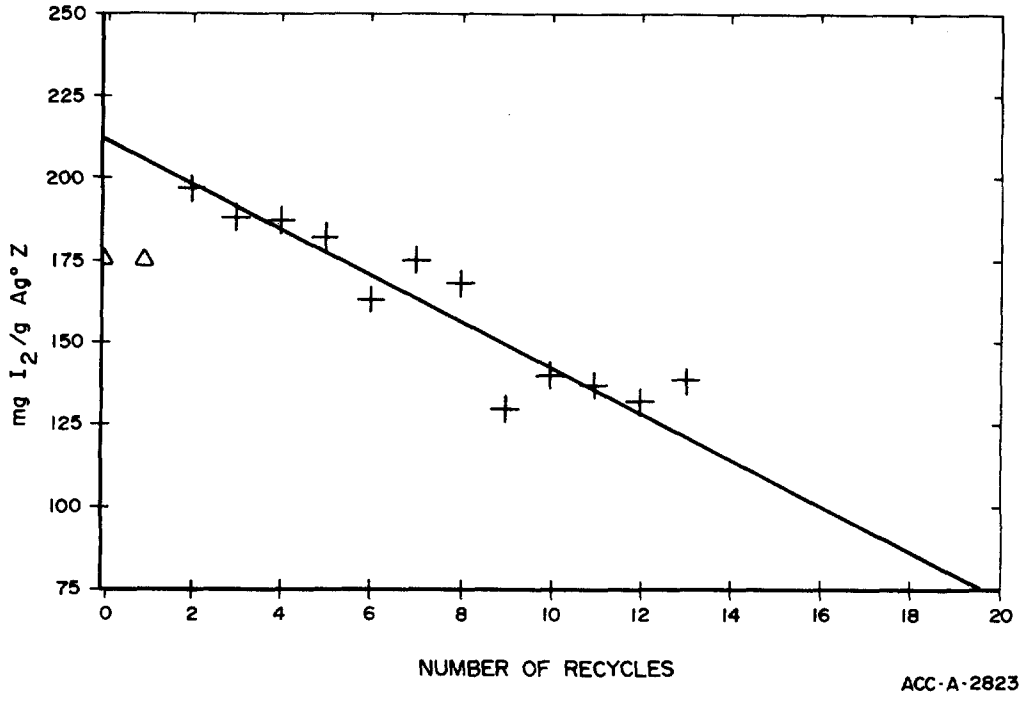

Figure 3. Iodine loadings of recycled Ag^oZ in the saturation zone

30-fold increase in P_{I_2}). While lower temperatures should result in higher decontamination factors, the bed temperature must be kept above 100°C to avoid condensation (in the PbX bed) of the water vapor desorbed from the AgIZ bed. The temperature effect on the HI loading of PbX was not studied. Our results indicate about 90% of the lead in PbX was used to chemisorbed HI at 150°C. Therefore, increasing the bed temperature could provide only a small increase (i.e., up to 10%) in the iodine loading. Since the low loading on Pb^oX is attributed to pore collapse, higher bed temperatures would probably have little effect on increasing the iodine loading. The iodine loadings on PbZ exceeded the stoichiometric ratio based on the lead content (i.e., a maximum of 247 mg HI/g PbZ for PbI_2 formation) which may be due to some physisorbed iodine or higher forms of lead iodide (i.e., H_2PbI_4). The best bed temperature for HI chemisorption on the lead-exchanged zeolites appears to lie somewhere between 100 and 150°C when both the instantaneous decontamination factor and the iodine loadings are considered. However, further testing is needed to confirm this, especially in the case of PbZ.

HI Vapor Pressure over AgIZ

The vapor pressure of HI over iodine-loaded AgX (AgIX) is close to that predicted for pure AgI.[1] The temperature-dependent vapor pressure curves for AgI and AgIZ are almost identical between 400 and 550°C. The data fitted to the equation $P_{HI} = e^A e^{-B/T}$, where T = K, is shown in Figure 4. We have found no basic difference between the

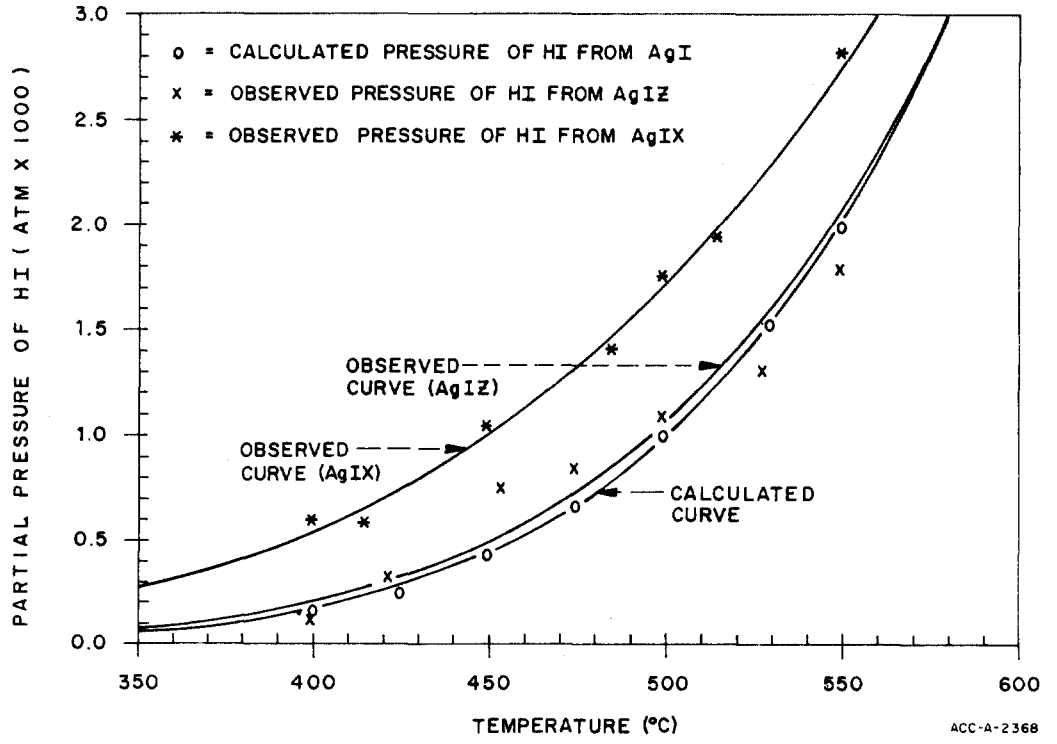

Figure 4. Vapor pressure of HI over AgI, AgIZ, and AgIX

HI vapor pressures over iodine loaded on AgX or $Ag^{o}X$ and on AgZ or $Ag^{o}Z$. This observation seems inconsistent with the concept that half the iodine in AgZ or AgX is bonded to the framework oxygens. However, it is inconsequential how the iodine is bonded in AgX and AgZ. Upon exposure to H_2 at 500°C, most of the silver ions are rapidly converted to the metal. Then the equilibrium:

$$AgI(s) + 1/2\ H_2(g) \rightleftarrows Ag^{o}(s) + HI(g) \qquad (7)$$

is established regardless of the source of HI(g). If HI could be easily formed from the iodine bonded to the framework oxygens, any amount in excess of the equilibrium pressure of HI(g) in equation (7) would be converted to AgI. Our data have indicated that this equilibrium is instantaneous because the partial pressure of HI is almost independent of the H_2 flow throughout the bed.

APPLICATION OF ADSORBENT TECHNOLOGY

The application of adsorbent technology to include regeneration and recycle of $Ag^{O}Z$ is illustrated by a block diagram in Figure 5 and a process-flow diagram in Figure 6. The assumed operational characteristics of a typical LWR fuel reprocessing plant are given in Table VIII. The fundamental data obtained from laboratory observations and used for calculations in the flow diagram are given in Table IX. The design criteria for the $Ag^{O}Z$ and PbX beds are given in Table X.

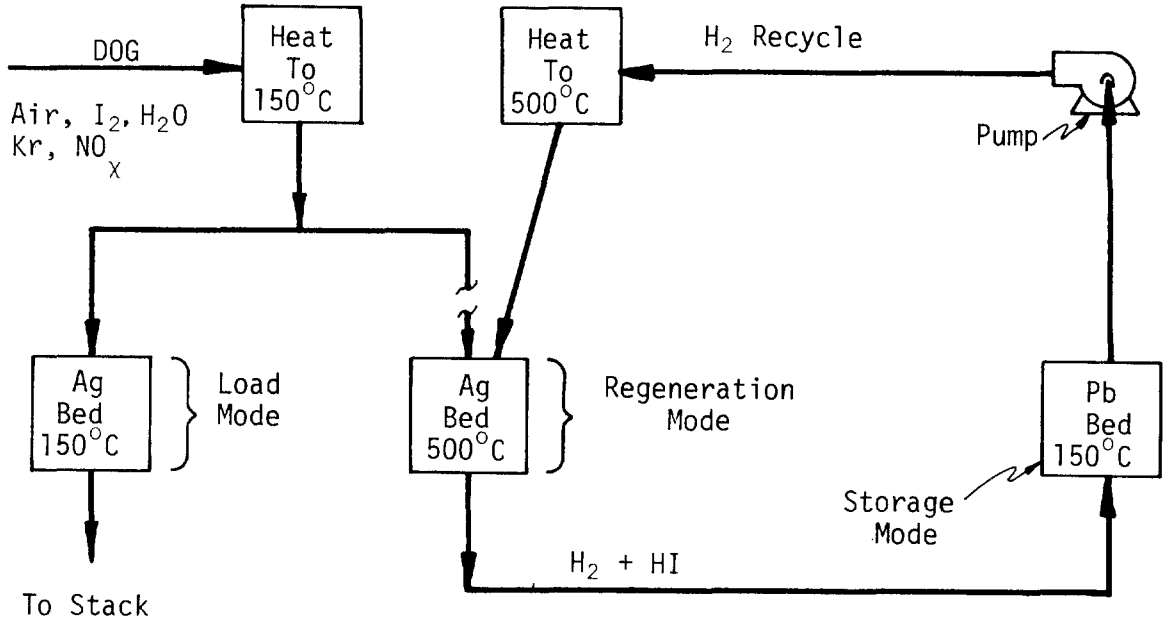

Load Mode Reaction: $2Ag^{O} + I_2 \rightarrow 2AgI$

Regeneration Mode Reaction: $2AgI + H_2 \rightarrow 2Ag^{O} + HI$

Storage Mode Reaction Approximated by: $Pb(OH)_2 + 2HI \rightarrow PbI_2 + 2H_2O$

Figure 5. Block diagram of iodine recovery process

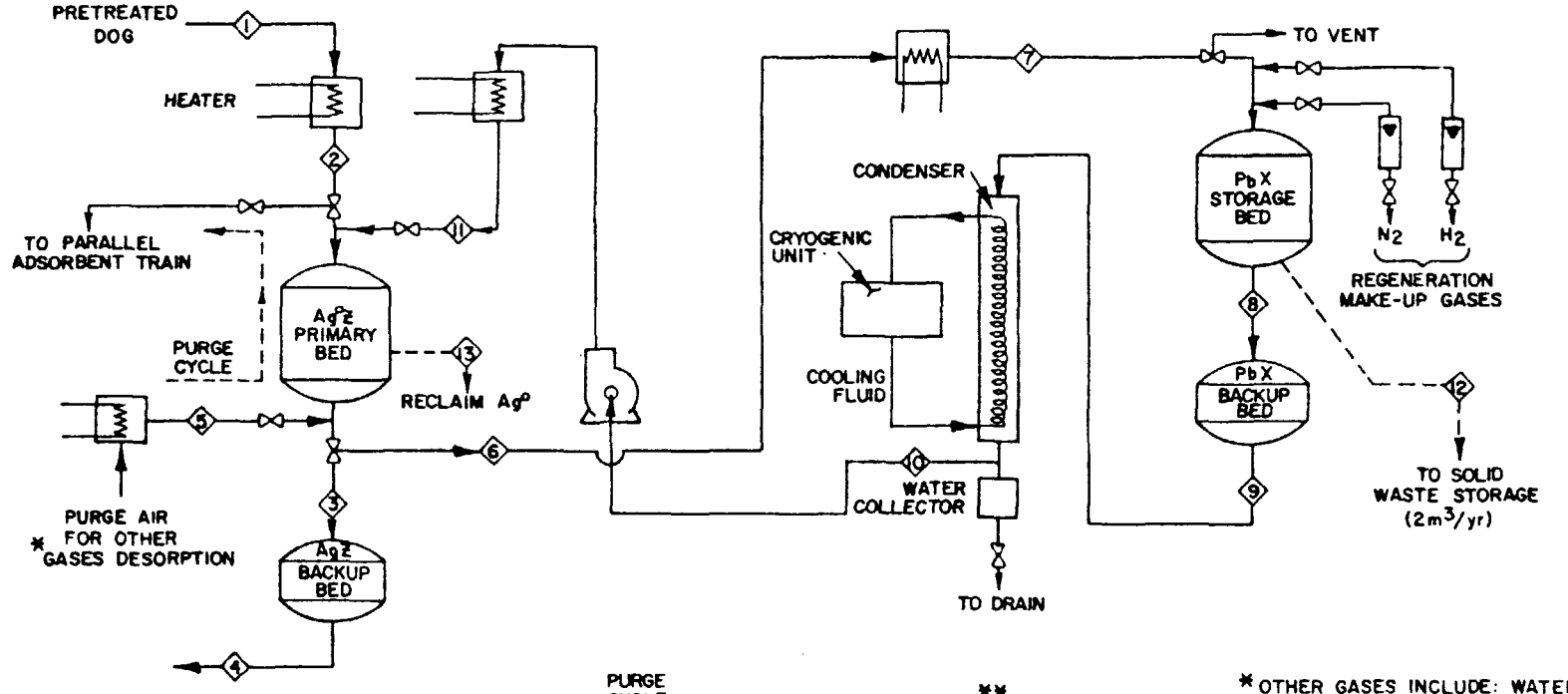

	LOADING CYCLE = 30 DAYS				PURGE CYCLE 2 DAYS	** REGENERATION CYCLE = 3 DAYS					
STREAM NO.	1	2	3	4	5	6	7	8	9	10	11
PRESSURE (atm)	1.0	1.0	0.8	0.75	1.1	0.94	0.94	0.87	0.85	0.85	1.0
TEMPERATURE (°C)	45	150	150	150	300	500	150	150	150	0	500
FLOW (m^3/h)	209	278	346	369	56	296	161	174	178	114	278
FLOW (kg/h)	233	233	233	233	38	9.6	9.6	9.6	9.6	9.6	9.6
NITROGEN	166	166	166	166	28	0	0	0	0	0	0
OXYGEN	51	51	51	51	9	0	0	0	0	0	0
OTHER GASES *	14.6	14.6	14.6	14.6	0.5	>0.6	>0.6	>0.6	>0.6	<0.6	<0.6
HYDROGEN	0	0	0	0	0	9	9	9	9	9	9
IODINE	7.1×10^{-2}	7.1×10^{-2}	7.1×10^{-4}	7.1×10^{-6}	0	0.26	0.26	2.6×10^{-3}	2.6×10^{-6}	2.6×10^{-6}	2.6×10^{-6}

* OTHER GASES INCLUDE: WATER VAPOR, NO_x, ARGON, AND KRYPTON AT 4.3, 7.4, 2.8 AND 0.09 kg/hr RESPECTIVELY.

** FLOWS FOR CLOSED LOOP. ABOUT 4 kg/yr H_2 NEEDED TO TRANSFER IODINE AS HI FROM Ag°Z TO PbX.

(12) SPENT PbX TO WASTE STORAGE

(13) LIFETIME OF Ag°Z UNKNOWN.

ACC-A-2622

Figure 6. Process flow diagram for iodine recovery from dissolver off-gas

TABLE VIII

ASSUMED OPERATIONAL CHARACTERISTICS OF AN LWR FUEL REPROCESSING PLANT

1.	Plant capacity	2000 tonne/yr
2.	Fuel burnup	28,700 MWd/tonne
3.	Cooling period	1.5 yr
4.	Plant on-stream time	300 d/yr
5.	Airflow through dissolver at 0°C and 1 atm press	2.83 m^3/min
6.	DOG pretreatment systems before iodine removal	H_2O/NO_x scrubber, deentrainer silica gel, and HEPA
7.	NO_x conc. after pretreatment	$\leq$ 2%
8.	H_2O dew point after pretreatment	35°C
9.	Volatility of I_2 from dissolver	> 99%
10.	Halide inventory from burnup:	
	$^{129}I + ^{127}I$	470 kg/yr
	^{81}Br	27 kg/yr
	^{81}Br normalized to ^{129}I	43 kg/yr
	Total halides as ^{129}I	513 kg/yr

TABLE IX

FUNDAMENTAL DATA FROM LABORATORY OBSERVATIONS

1.	Iodine loading on Ag^oZ	$\geq$ 100 mg I_2/g Ag^oZ
2.	Iodine loading on PbX	$\geq$ 300 mg I_2/g PbX
3.	Dry density of Ag^oZ	0.79 g/cm^3
4.	Dry density of PbX	0.85 g/cm^3
5.	Desorption rate of HI from Ag^oZ at 500°C, 1 atm and 15 m/min face velocity	4.5 mg HI/min·cm^2 in pure H_2
6.	Pressure drop across Ag^oZ at 150°C and 15 m/min face velocity	0.097 atm/m in air
7.	Pressure drop across Ag^oZ at 500°C and 15 m/min face velocity	0.03 atm/m in hydrogen
8.	Pressure drop across PbX at 150°C and 11 m/min face velocity	0.02 atm/m in hydrogen

TABLE X

DESIGN CRITERIA FOR $Ag^{O}Z$ and PbX BEDS

	face velocity (m/min)	diam (m)	length (m)	volume (m^3)	weight (Mg)	iodine loading (kg)
1. $Ag^{O}Z$ primary	15	0.63	2.1	0.65	0.51	51
2. AgZ backup	19	0.63	0.5	0.15	0.12	12[b]
3. PbX storage[a]	11	0.55	3.2	0.76	0.64	192
4. PbX backup	12	0.55	0.8	0.19	0.16	48[b]

[a] PbX storage bed consists of 4 self-contained cartridges designed to fit in 55 gal drums. Number of cartridges needed per/yr ∿11.

[b] During normal operation, the backup beds would not be loaded with iodine.

The $Ag^{O}Z$ primary bed was sized for a 30-day loading operation. During the adsorption of iodine, the bed would attain some saturation loading of H_2O, NO_x, HNO_3, and ^{85}Kr. Based on the work done by Sundaresan and coworkers,[9] we have assumed an upper limit of 51 kg of H_2O and 36 kg of NO_2 for 0.65 m^3 of $Ag^{O}Z$. During the 48-hr purge cycle, an average of 1.8 kg/hr NO_x/H_2O would be added to the 11.7 kg/hr NO_x/H_2O already present in the DOG. The combined load would increase the NO_x/H_2O flow to the parallel $Ag^{O}Z$ primary bed (not shown in flow diagram) by about 13% over normal operation. The two parallel $Ag^{O}Z$ adsorbent trains permit continuous iodine recovery while one of the beds is being regenerated.

After the purge cycle, the $Ag^{O}Z$ bed is isolated from the DOG and opened to streams 6-11. The air in the bed is purged off with nitrogen and vented just before the nitrogen inlet. Hydrogen is added to the nitrogen until the regeneration gas consists of 100% H_2. The $Ag^{O}Z$ primary bed is brought up to temperature, and the iodine stripped as hydrogen iodide. Any chemisorbed bromine would also be removed as HBr, but at a rate 100 times faster than iodine. The desorbed iodine and bromine are chemisorbed as some form of lead halide on the PbX. Residual water on the AgZ and the PbX beds would be partially removed by the condenser. The regeneration process is a closed loop in which the H_2 is recirculated. Although 9 kg H_2/hr would be recycled, only 4 kg H_2/hr would be required to transport the halides as HI and HBr to the PbX.

The transfer of iodine to the PbX would be discontinued when iodine is detected in stream 8. The self-contained cartridges in the PbX storage bed would be removed and placed in 55-gal drums for

storage. The PbX backup-bed cartridge would be repositioned at the top of the PbX storage-bed holder and new cartridges placed below it and in the backup-bed holder. This would provide a fresh backup bed for every new set of cartridges placed in the PbX storage-bed holder.

After regeneration of the $Ag^{O}X$ bed, it would be placed on standby status to remove iodine from the DOG when the parallel $Ag^{O}Z$ bed is saturated with iodine. With this design, the two $Ag^{O}Z$ beds would be regenerated five times a year. The long-term life of the $Ag^{O}Z$ beds has not been determined.

CONCLUSIONS AND SUGGESTED FUTURE WORK

The conclusions based on the experimental results and interpretation of the data are as follows:

1. In simulated DOG streams, elemental iodine loadings of 171±17 mg I_2/g $Ag^{O}Z$ can be obtained; about 72% of the Ag^{O} is converted to AgI.

2. NO has a positive effect on the iodine loading of $Ag^{O}Z$; conversion to the oxide or nitrate by NO_2 is blocked.

3. The iodine loading of AgZ (silver in the oxide form) is about half the iodine loading of $Ag^{O}Z$.

4. Water vapor up to a 35°C dew point and bed temperatures between 100 and 250°C have little or no effect on the iodine loading of $Ag^{O}Z$.

5. Regeneration and recycle of $Ag^{O}Z$ is a practical concept; the $Ag^{O}Z$ loses about 20% of its initial iodine-loading capacity after 13 recycles. Extrapolation of the data indicates no greater than 50% and no less than 20% loss in the loading capacity would occur after 18 recycles.

6. Storage of ^{129}I on PbX is a practical concept; iodine loadings of 408 mg I_2/g PbX with iodine vapor pressures less than 4×10^{-8} atm are obtainable.

7. $Pb^{O}Z$ may give the best combination of a high iodine loading and low iodine vapor pressure.

It is recommended that additional studies be done:

1. Measure the loading capacity of $Ag^{O}Z$ for airborne-organic iodides.

2. Conduct design verification studies on the regeneration and recycle of $Ag^{O}Z$ in pilot-plant studies.

3. Search for other silver-loaded substrates that might be more suitable for regeneration and recycle than $Ag^{O}Z$.

4. Complete the evaluation of the recycle life of $Ag^{O}Z$, i.e., measure the complete life of the adsorbent.

5. Determine the hydrogen iodide loading and iodine vapor pressure of $Pb^{O}Z$.

REFERENCES

1. B. A. Staples, L. P. Murphy, and T. R. Thomas, "Airborne elemental iodine loading capacities of metal zeolites and a dry method for recycling silver zeolite," Proceedings of the 14th ERDA Air Cleaning Conference, CONF-760822, p. 363 (August 1976).

2. T. R. Thomas, et al., "Airborne elemental iodine loading capacities of metal zeolites and a dry method for recycling silver zeolite," ICP-1119, Idaho National Engineering Laboratory, Idaho Falls, Idaho (July 1977).

3. L. P. Murphy, et al., "The development of $Ag^{O}Z$ for bulk ^{129}I removal from nuclear fuel reprocessing plants and PbX for ^{129}I storage," ICP-1135, Idaho National Engineering Laboratory, Idaho Falls, Idaho (December 1977).

4. D. W. Breck, "Zeolite molecular sieves," John Wiley & Sons, New York, NY, pp. 120-124 (1974).

5. Kh. M. Minachev and Ya. I. Isakov, "Catalytic properties of metal-containing zeolites," Zeolite Chemistry and Catalyst, ACS Monograph 171, J. A. Rabo, Ed., pp. 552-611 (1976).

6. D. J. C. Yates, "The stability of metallic cations in zeolites," J. Phys. Chem., Vol. 69, p. 1676 (1965).

7. J. G. Wilhelm and J. Furrer, "Head-end iodine removal from a reprocessing plant with a solid sorbent," Proceedings of the 14th ERDA Air Cleaning Conference," CONF-760822, p. 447 (August 1976).

8. K. C. Patil, et al., "The silver nitrate-iodine reaction: iodine nitrate as the reaction intermediate," J. Inorg. Nucl. Chem., Vol. 29, p. 407 (1967).

9. B. B. Sundaresan, et al., "Adsorption of nitrogen oxides from waste gas," Environ. Sci. and Tech., Vol. 1, p. 151 (February 1976).

SYMBOLS

AgX	Silver-exchanged faujasite
AgZ	Silver-exchanged mordenite
$Ag^{o}Z$	Ag in AgZ reduced with H_2
AgIX	AgX loaded with iodine
AgIZ	AgZ loaded with iodine
NaX	Sodium form of Type 13X faujasite
NaIX	NaX loaded with iodine
PbX	Lead-exchanged faujasite
PbZ	Lead-exchanged mordenite
PbIX	PbX loaded with iodine
PbIZ	PbZ loaded with iodine
$Pb^{o}X$	Pb in PbX reduced with H_2
$Pb^{o}IX$	$Pb^{o}X$ loaded with iodine

DISCUSSION

MIDLIK: It is my understanding that there is a problem with in-place testing of silver zeolite filtration systems. Is there a test plan or test procedure that is satisfactory to NRC? Our problem is related to type of agent used for leak testing.

T. R. THOMAS: This question is not relevant to my paper.

PICOULT: Current leak testing on silver zeolite adsorbers is being accomplished through the use of Freon.

HALLIGAN: I would like to comment on in-place testing of silver zeolite (AgZ) adsorbers. We have had some experience in this area. Our efforts using Freons, R-11 and R-112, were unsuccessful due to rapid breakthrough. We did, however, resort to the use of $CH_3{}^{127}I$ as the challenge agent and obtained performance test data with no difficulty.

VAN BRUNT: One might expect that unmixed beds might have a different and lower recycle efficiency than the mixed adsorbant beds used in your tests. Can you comment on this?

T. R. THOMAS: I anticipate that a bed regenerated and recycled in situ will perform better. In the lab tests, it was necessary to reassemble the bed repeatedly to load and strip the iodine. This caused attrition and dusting from bed handling that would otherwise not occur.

HAAG: Please comment on the operation of a silver zeolite regeneration step and the possible hazards involved with high hydrogen concentrations at high temperatures (500°C) in a reprocessing plant.

T. R. THOMAS: I think we have the capability to handle pure hydrogen safely. It is done in private industry to produce pure hydrogen in pressurized cylinders and in reactor technology to recombine radiolytic hydrogen. The safety requirements that might be imposed on the nuclear industry might make the recycle technology economically unattractive.

BROWN: How much hydrogen would be required to handle the annual recycle requirement in a 2000 MT/year fuel reprocessing plant?

T. R. THOMAS: About nine standard, size A, pressurized cylinders of H_2 would be required to transfer the iodine from the silver zeolite to a PbX bed. This is based on the stoichiometry of the stripping reaction.

FURRER: Have you made loading and recycling tests of your silver zeolite in real DOG? Maybe you have a loading of organics in your silver zeolite from the recycled acid?

T. R. THOMAS: No, we have not tested silver zeolite in actual DOG streams. Organics would interfere only if they condense and form a tar-like layer. If degradation products from tributylphosphate are found to be a problem, an additional adsorbent, specific for organic compounds, would be positioned upstream of the iodine adsorbent.

WILHELM: Did you measure the removal efficiency of the silver zeolite with metallic silver for organic iodides? Experiments in Karlsruhe showed that this material would not remove organic iodides.

T. R. THOMAS: No, we didn't make the measurements, but they are going to be made at another laboratory; and until they are,we won't know whether these materials will efficiently recover organic iodides.

RADIATION-INDUCED IODINE MIGRATION IN SILVER ZEOLITE BEDS*

A. G. Evans
Savannah River Laboratory
E. I. du Pont de Nemours & Co.
Aiken, SC 29801

Abstract

The radiation stability of iodine-loaded, silver-exchanged zeolite (AgX) was evaluated under dynamic flow conditions in the radiolysis facility at the Savannah River Laboratory. A series of three tests was conducted in which 1-in.-deep beds of 10 × 16 mesh AgX beads were loaded to approximately 6 mg ^{131}I-tagged elemental iodine per mg AgX over a 1-hr period. Test conditions included an intense radiation field (absorbed dose rate of $\sim 1.5 \times 10^7$ rads/hr), a steam-air mixture (80°C and 95% relative humidity) and a face velocity of 55 ft per minute. Iodine passing through the beds was collected on backup beds located outside the radiation field to determine the penetration occurring during the irradiation period. In the first test, radiation exposure was terminated at the end of the 1-hr loading period. In the second test, irradiation and gas flow continued for an additional 4 hr (total exposure of 5 hr). In the third test, the total exposure period was increased to 105 hr. At the end of each test the test bed was counted, then sectioned into ∿1/8-in.-deep segments and recounted to determine the spatial distribution of ^{131}I activity in the irradiated assembly. Two additional tests were conducted at I_2 loadings of ∿0.6 mg/g and an exposure period of 5 hr. The test bed was loaded with AgX in one test and with GX-176 carbon in the other test to determine the spatial distribution of I_2 at a lighter loading.

The long-term test (105-hr exposure) showed that little iodine migration occurred after an accumulated exposure of $\sim 1.6 \times 10^9$ rads (the cumulative penetration of ^{131}I was 0.7% for the entire test). Analysis of the irradiated test bed showed that more than 30% of the iodine activity remaining on the bed was located in the downstream half of the bed. About 3.9% of the iodine migrated to the last 1/8-in. section of the bed. The other tests, using shorter irradiation periods and lighter loadings, showed that the gross migration of iodine into the downstream sections of the bed was the result of the high iodine concentration in the gas stream during the loading phase (∿400 mg I_2/m^3 air during loading). Comparison of activity distributions after short-term and long-term irradiation indicates that up to 10% of the iodine was redistributed within the bed after prolonged exposure to intense radiation and flowing air. However, downstream migration from radiolytic decomposition of silver-iodine complexes is less important to the iodine distribution than is the rapid heavy loading.

Introduction

Silver-exchanged zeolite is currently used to adsorb airborne radioiodine in locations where hostile environments prevent the use of carbon-based adsorbers (for example, where oxidizing gases or elevated temperatures could cause ignition of carbon). Use of AgX has also been proposed in reactor applications where high-intensity radiation fields could be encountered should a major accident occur.

* The information contained in this article was developed during the course of work under Contract AT(07-2)-1 with the U. S. Department of Energy.

In view of the fact that silver halide compounds are used as photosensitive agents in photographic and x-ray film emulsions, some reservations have been expressed about the effectiveness of AgX in these latter applications. The principal concern was the possible chromatographic migration of iodine through the adsorber beds under dynamic flow conditions in the high-intensity radiation environment. The radiation stability tests of AgX were conducted in the SRL Radiolysis Facility[1,2] at the request of the Department of Energy to determine whether such migration occurs.

Discussion

A single, long-term exposure test was initially planned and executed. In this test, elemental iodine was loaded onto commercial AgX* over a 1-hr period in a high-intensity radiation field. This was followed by an extended (104-hr) desorption period in the radiation field with continued air flow. Iodine desorbed from the irradiated test bed was collected on backup beds which were changed at regular intervals to evaluate time-dependent desorption rates during the irradiation. The iodine loading on the test bed was about 6 mg I/g AgX on the 1-in.-deep test bed. Air flow was maintained at 55 ft/min face velocity and the adsorbed dose rate in the test bed was $\sim 1.5 \times 10^7$ rads/hr. A steam-air mixture (80°C and ~95% RH) was employed during the loading phase and for the first 4-hr desorption period. Except for two 4-hr periods, the remainder of the test was run at 35°C and ambient humidity (ranging from 20% to 35% RH at 35°C). Air at 45°C and 75% RH was intentionally introduced for 4 hr after 45-hr and 69-hr exposure to evaluate the effects of increased humidity on the desorption rate.

The specific test bed loading was chosen to be within the dynamic loading range of 1 to 10 mg I/g AgX found in the literature.[3-6] The 1-in. bed depth was dictated by the design of the radiolysis test facility, and the dose rate dictated by the specific activity of the ^{60}Co in the facility.

At the end of the radiation exposure period, the test bed was counted to determine the residual radioactive content, then carefully sectioned into ~1/8-in.-thick layers. Each of the layers was weighed and counted to determine the iodine distribution within the test bed.

Results of the desorption phase of the test showed that little migration of iodine occurred as a result of prolonged radiation exposure. The total penetration measured during the 105-hr test period was 0.743%. Measured desorption rates during the test are shown in Figure 1. Examination of the data shows that the desorption rates decreased with increasing accumulated exposure except for periods when high-humidity air was intentionally introduced. The desorption rates during the last 25 to 30 hr of the test remained fairly constant at about 1% of the peak desorption rate observed during the initial loading phase.

Analysis of the distribution of activity in the test bed showed that about 37% of the iodine remained in the front 1/4 in. of the bed and that nearly 4% had migrated to the last 1/8-in. segment of the test bed. The shape of the activity distribution curve (Figure 2) strongly suggests a "normal distribution" similar to that seen in ion exchange columns when an ionic species is moving through the resin beds. Numerical data are presented in Table I.

* 10 × 20 mesh beads, >98% exchanged. Purchased from CTI Nuclear, Inc., Denver, Colorado.

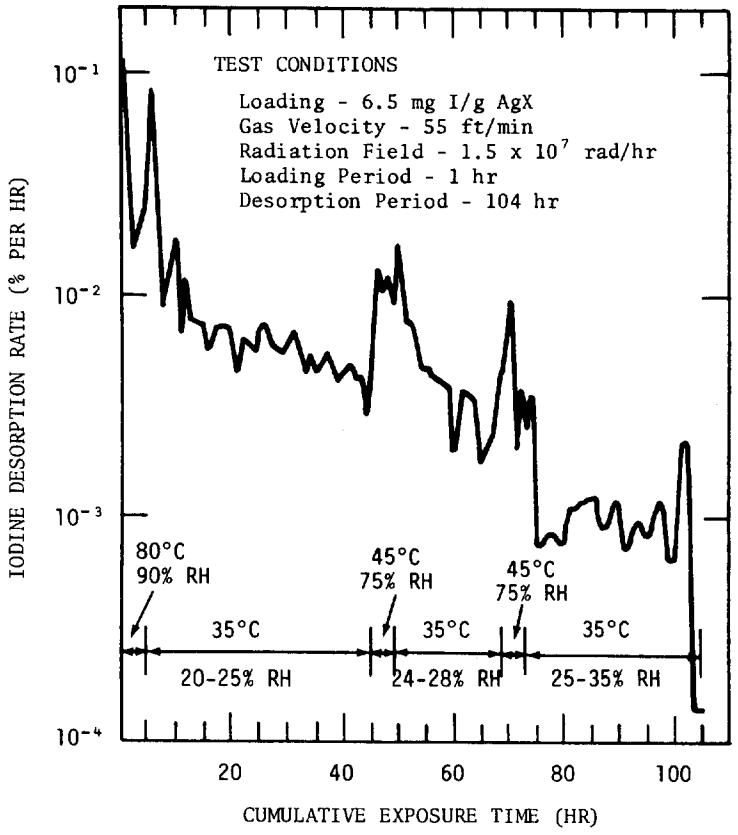

FIGURE 1
IODINE DESORPTION RATES FROM IRRADIATED AgX

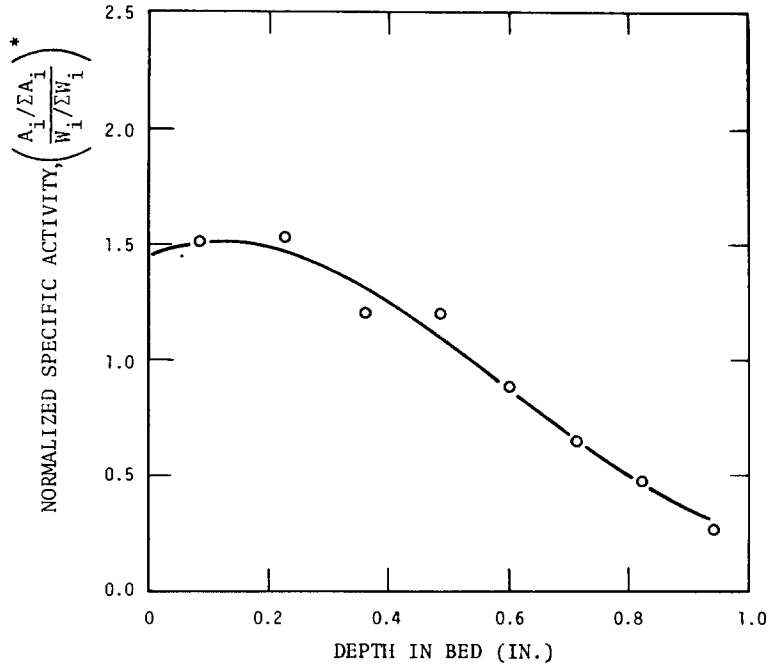

FIGURE 2
ACTIVITY DISTRIBUTION IN AgX BED AFTER 105-HR IRRADIATION

* see text

Table I. Radioactivity Distribution in AgX Bed After 105-hr Exposure.

Depth to Middle of Section, in.	Normalized[a] Specific Activity, $(A_i/\Sigma A_i)/(W_i/\Sigma W_i)$
0.083	1.504
0.227	1.520
0.351	1.203
0.486	1.192
0.602	0.881
0.716	0.647
0.827	0.482
0.944	0.262

a. Iodine loading - 6.5 mg I/g AgX, see text for discussion of normalization function.

This evidence of movement of activity in the test bed suggested additional tests in which shorter irradiation periods were employed to determine rate constants. A bed-sectioning experiment was also performed for GX-176* carbon for comparison (at a loading of 0.6 mg I/g C to stay within design loading limits).

The activity distributions in adsorber beds after 5-hr exposure (1-hr loading, 4-hr desorption) are shown in Table II and Figure 3 for GX-176 carbon (0.6 mg/g loading), AgX at 0.6 mg/g loading and AgX at ∿6 mg/g loading. Since adsorber weights and activity levels were not constant, it was necessary to normalize the data to allow direct comparisons. The normalization was made using the function

$$\frac{A_i/\Sigma A_i}{W_i/\Sigma W_i}$$

where: A_i = activity in an individual segment, c/s

W_i = weight of adsorber in that segment, g

ΣA_i = total activity in the test bed, c/s

ΣW_i = total weight of adsorber in the test bed, g

The data in Figure 3 show that the activity level in carbon decreases exponentially with increasing bed depth at 0.6 mg/g loading. At 0.6 mg/g loading some penetration into the AgX bed is evident. These data suggest a somewhat slower reaction rate for airborne iodine removal in the AgX than is the case for carbon. At a loading of 6 mg/g, AgX exhibits considerable migration. This migration into AgX is consistent with recently published data which indicates a reaction zone of up to 5 cm depth when inlet concentrations of ∿500 mg I/m^3 air are encountered.[7]

Thus, at least a portion of the activity found in the deeper layers of adsorber in the 105-hr irradiation test can be attributed to the high inlet iodine concentration and heavy loading.

* North American Carbon Company, Columbus, Ohio.

Table II. Radioactivity Distribution in Test Beds After 5-hr Exposure.

GX-176 Carbon[a] (0.65 mg I/g C)		AgX[b] (0.68 mg I/g AgX)		AgX[b] (6.2 mg I/g AgX)	
Depth, in.[c]	Normalized Activity[d]	Depth, in.[c]	Normalized Activity[d]	Depth, in.[c]	Normalized Activity[d]
0.072	5.604	0.069	3.661	0.080	1.827
0.192	1.590	0.188	2.828	0.228	1.478
0.289	0.340	0.293	1.464	0.347	1.294
0.405	0.0571	0.422	0.314	0.457	1.076
0.543	0.0085	0.561	0.0364	0.589	0.711
0.671	0.0020	0.686	0.0044	0.719	0.573
0.778	0.0005	0.807	0.0007	0.826	0.467
0.914	0.0000	0.933	0.0002	0.938	0.257

a. Product of North American Carbon Company, Columbus, Ohio.

b. Type III, 10 × 20 mesh beads, >98% exchanged, Product of CTI Nuclear, Inc., Denver, Colorado.

c. Depth to middle of bed section.

d. $(A_i/\Sigma A_i)/(W_i/\Sigma W_i)$, see text for discussion.

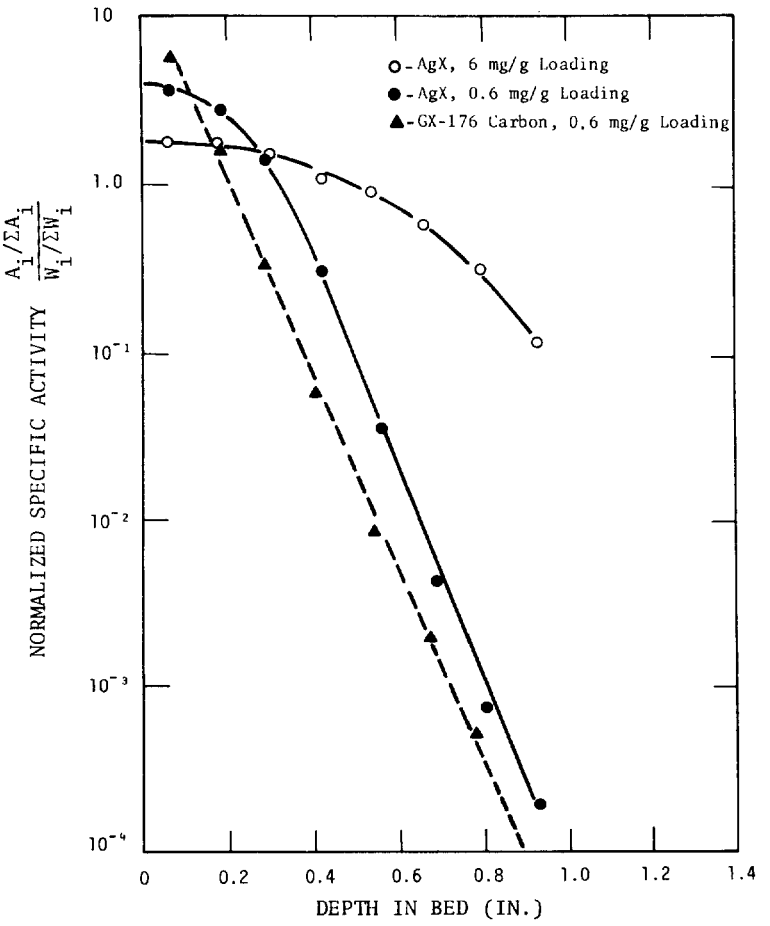

FIGURE 3
IODINE DISTRIBUTION IN TEST BEDS AFTER 5 HOURS EXPOSURE

To separate the heavy loading effects from the possible radiation effects, a third heavy loading experiment was performed in which the exposure time was reduced to 1 hr (the loading period only, with no subsequent desorption). Data for the three heavy loading (~6 mg/g) experiments are shown in Table III and Figure 4. The curves fitted to each set of data points were obtained by least squares methods assuming a normal distribution function (see Appendix).

Table III. Activity Distribution in Heavy Loaded AgX Beds After Irradiation.

1-hr Exposure (6.6 mg I/g AgX)		5-hr Exposure (6.2 mg I/g AgX)		105-hr Exposure (6.5 mg I/g AgX)	
Depth, in.[a]	Normalized Activity[b]	Depth, in.[a]	Normalized Activity[b]	Depth, in.[a]	Normalized Activity[b]
0.061	1.831	0.080	1.827	0.083	1.504
0.179	1.797	0.228	1.478	0.227	1.520
0.303	1.524	0.347	1.294	0.361	1.203
0.426	1.103	0.457	1.076	0.486	1.192
0.540	0.911	0.589	0.711	0.602	0.881
0.665	0.592	0.719	0.573	0.716	0.647
0.797	0.326	0.826	0.467	0.827	0.482
0.932	0.119	0.938	0.257	0.944	0.262

a. Depth to mid-section.

b. $(A_i/\Sigma A_i)/(W_i/\Sigma W_i)$, see text for discussion.

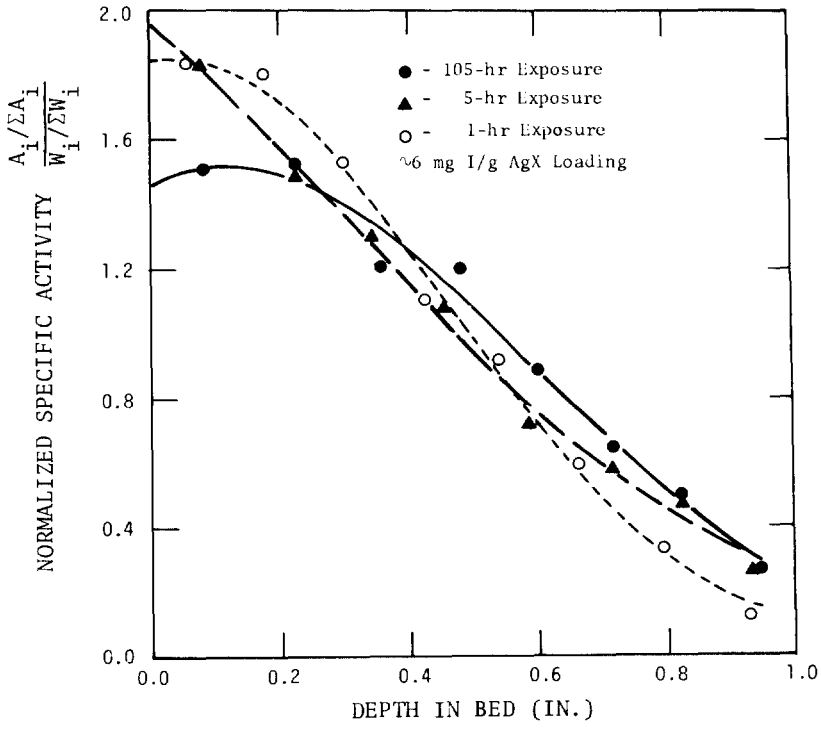

FIGURE 4
ACTIVITY DISTRIBUTION IN IRRADIATED AgX BEDS

Examination of the curves in Figure 4 shows that some discernible movement of activity from the front toward the rear of the test beds has occurred between each of the exposure periods. The magnitude of the movement cannot be obtained directly from the data as presented because of differences in segment depths, uncertainties in the effect of slightly different loadings and the magnitude of the experimental error, and because data cannot be expressed as specific activity of a bed segment.

Approximate numerical comparison of activity migrations can be made, however, if one assumes that the equations obtained in the curve fitting process (see Appendix) are reasonable approximations of the true iodine distributions. The equation for each curve can be integrated between the limits of X = 0 and X = 1 in. using the method shown in the Appendix. Corrections for activity desorbed from the the bed can now be made as shown below.

$$\frac{\int_0^1 f(x)\,dx}{1 - P} = T$$

where $\int_0^1 f(x)\,dx$ = total activity fraction on test bed

P = total activity fraction passing through test bed (penetration)

T = normalized total activity in test

Each equation can then be reintegrated between discrete limits and divided by T to obtain estimates of the normalized activity contained in equal depth segments of the bed. Calculated estimates of the activity contained in equal, 1/8-in.-deep segments (corrected for penetration) are given in Table IV.

Numerical estimates of the movements of iodine within the test bed can be made by determining the intersection points for each pair of curves (1-hr vs. 5-hr, 1-hr vs. 105-hr, and 5-hr vs. 105-hr exposures), then integrating the area under each curve from the bed front to the intersection point. The difference in integrated area plus the difference in desorbed iodine for each pair of curves is then the estimate of the total iodine migration between each exposure time. Calculated data are shown in Table V. The data indicate that between 1-hr and 105-hr exposures approximately 9.3% of iodine initially located in the first 0.41. in. of the bed moved to the rear of the bed. Another 0.6% of the iodine initially located in the rear of the bed moved out of the bed so that a total of about 9.9% of the total iodine migrated within or out of the 1-in.-deep bed as a result of radiation exposure. Similar comparisons in the time interval from 1-hr to 5-hr exposures indicate a migration of about 5.4% of the iodine, and that approximately 6.2% of the iodine was redistributed between 5-hr and 105-hr exposures.

In the proposed reactor applications, AgX adsorber beds of at least two inches depth would be used. Thus, an internal redistribution of $\sim$10% of the iodine in the first inch of bed depth would not compromise the integrity of the adsorber system.

Table IV. Estimated Iodine Content of Equal Test Bed Segments.

Segment Depth, in.	Estimated Iodine Content of Each Segment, % 1-hr Exposure	5-hr Exposure	105-hr Exposure
0.000-0.125	22.97	22.87	18.44
0.125-0.250	21.70	19.89	18.46
0.250-0.375	18.57	16.61	17.13
0.375-0.500	14.40	13.32	14.76
0.500-0.625	10.12	10.25	11.81
0.625-0.750	6.45	7.58	8.76
0.750-0.875	3.73	5.38	6.04
0.875-1.000	1.95	3.66	3.86
Thru Bed	0.11	0.44	0.74

Table V. Estimated Iodine Migration in Irradiated AgX Test Beds[a]

	Fraction of Total Iodine, % Curve 1	Curve 2	C(1)-C(2)
1-hr vs. 105-hr			
Test Bed Iodine[b]	67.60	58.31	+9.29
Desorbed Iodine	0.11	0.74	-0.63
Total Migration	-	-	9.92
5-hr vs. 105-hr			
Test Bed Iodine[c]	45.39	39.51	+5.88
Desorbed Iodine	0.44	0.74	-0.30
Total Migration	-	-	6.18
1-hr vs. 5-hr			
Test Bed Iodine[d]	82.01	76.96	+5.05
Desorbed Iodine	0.11	0.44	-0.33
Total Migration	-	-	5.38

a. One-in.-deep beds loaded to ∿6 mg I/g AgX, superficial face velocity of 55 ft/min and an absorbed dose rate of $\sim 1.5 \times 10^7$ rads/hr.

b. Fraction of iodine contained in the first 0.409 in. of the test bed.

c. Fraction of iodine contained in the first 0.268 in. of the test bed.

d. Fraction of iodine contained in the first 0.548 in. of the test bed.

References

1. A. G. Evans and L. R. Jones, *Confinement of Airborne Radioactivity - Progress Report: January 1971 - June 1971.* USAEC Report DP-1280, E. I. du Pont de Nemours and Co., Savannah River Laboratory, Aiken, SC (1971).

2. A. G. Evans and L. R. Jones, *Confinement of Airborne Radioactivity - Progress Report: July 1971 - December 1971.* USAEC Report DP-1298, E. I. du Pont de Nemours and Co., Savannah River Laboratory, Aiken, SC (1972).

3. D. T. Pence, F. A. Duce, and W. J. Maeck, "A Study of the Adsorption Properties of Metal Zeolites for Airborne Iodine Species," *Proceedings of the Eleventh AEC Air Cleaning Conference,* Richland, Washington, August 31-September 3, 1970, p 581, USAEC Report CONF 700816, NTIS, Springfield, VA (1970).

4. D. T. Pence, F. A. Duce, and W. J. Maeck, "Developments in the Removal of Airborne Iodine Species with Metal-Substituted Zeolites," *Proceedings of the Twelfth AEC Air Cleaning Conference,* Oak Ridge, Tennessee, August 28-31, 1972, p 417, USAEC Report CONF 720823, NTIS, Springfield, VA (1973).

5. J. G. Wilhelm and H. Schuttelkopf, "Inorganic Absorber Materials for Trapping of Fission Product Iodine," *Proceedings of the Eleventh AEC Air Cleaning Conference,* Richland, Washington, August 31-September 3, 1970, p 568, USAEC Report CONF 700816, NTIS, Springfield, VA (1970).

6. J. G. Wilhelm and H. Schuttelkopf, "An Inorganic Absorber Material for Off-Gas Cleaning in Fuel Reprocessing Plants," *Proceedings of the Twelfth AEC Air Cleaning Conference,* Oak Ridge, Tennessee, August 28-31, 1972, p 540, USAEC Report CONF 720823, NTIS, Springfield, VA (1973).

7. T. R. Thomas, B. A. Staples, L. P. Murphy, and J. T. Nichols, *Airborne Elemental Iodine Loading Capacities of Metal Zeolites and a Method for Recycling Silver Zeolite.* USERDA Report ICP-1119, Allied Chemical Corporation, Idaho Chemical Programs Operations Office, Idaho Falls, ID (July 1977).

Appendix

Curve Fitting Method

Depth distribution curves for the AgX test series were obtained by assuming that the general equations for the normal distribution curve best fit the experimental data

$$y = Ae^{-\frac{1}{2}\left(\frac{x-B}{C}\right)^2}$$

where: y = normalized specific activity functions

x = depth in test bed, in.

A = constant representing maximum value of y

B = constant related to depth displacement in bed

C = constant related to spread in data

A computer code was written in which the observed values of x (XOBS) and y (YOBS) were used for each test. In the program, a value for A, B, and C was assumed and a new value for Y (YCALC) was calculated for each XOBS value. The function

$$\Delta^2 = \sum_{i=1}^{8} (YCALC_i - YOBS_i)^2$$

was then evaluated. New values for B and C were then assumed and new y values calculated to obtain a new Δ^2 value. The process was repeated until the minimum value for Δ^2 was obtained for a constant value of A. The calculations were then repeated assuming a new value for A and an array of values for B and C. The equations obtained for each test represent the best fit found when values of A were incremented at intervals of 0.001 units and values of B and C were incremented at intervals of 0.0005 units. The "best-fit" constants found in this manner are given in Table AI.

Table AI. "Best-Fit" Constants for Depth Distribution Curves.

Test Duration, hr	Best Value Found For Constant		
	A	B	C
1	1.850	0.0520	0.3970
5	2.200	-0.3030	0.6185
105	1.510	0.1260	0.4560

Integration of Curves

To obtain the area under each curve, it is necessary to evaluate the integral

$$dy = A\int_0^1 e^{-\frac{1}{2}\left(\frac{x-B}{C}\right)^2} dx = \int_0^1 f(x)\, dx$$

Let $a = \frac{1}{2C^2}$ and $w = x - B$

then $dw = dx$

and $$\int_0^1 f(x)\, dx = A\int_{-B}^{1-B} e^{-aw^2}\, dw$$

but $$\int_0^Z e^{-aw^2}\, dw = \frac{\sqrt{\pi}}{2\sqrt{a}}\left[\mathrm{erf}(Z\sqrt{a})\right]$$

where $\mathrm{erf}(Z\sqrt{a})$ = the error function of a number whose value is $(Z\sqrt{a})$

$$\text{therefore: } A\int_{-B}^{1-B} e^{-aw^2}\,dw = \frac{A\sqrt{\pi}}{2\sqrt{a}}\left\{\text{erf}\left[(1-B)\sqrt{a}\right] + \text{erf}\left[B\sqrt{a}\right]\right\}$$

$$\text{substituting: } \int_0^1 f(x)\,dx = \frac{A\sqrt{\pi}}{2\sqrt{\frac{1}{2C^2}}}\left\{\text{erf}\left[(1-B)\sqrt{\frac{1}{2C^2}}\right] + \text{erf}\left[B\sqrt{\frac{1}{2C^2}}\right]\right\}$$

$$\int_0^1 f(x)\,dx = AC\sqrt{\frac{\pi}{2}}\left[\text{erf}\left(\frac{1-B}{C\sqrt{2}}\right) + \text{erf}\left(\frac{B}{C\sqrt{2}}\right)\right] \tag{1}$$

Equation 1 is the form used to integrate the curves for the 1-hr and 105-hr tests since both equations have positive values for B (the apex of the curve occurs within the limits of x = 0 to x = 1). For the 5-hr test, as well as evaluation of sections of test beds between the limits of x and x + Δx, the equation

$$\int_x^{x+\Delta x} f(x) = AC\sqrt{\frac{\pi}{2}}\ \text{erf}\left[\left(\frac{x+\Delta x-B}{C\sqrt{2}}\right) - \text{erf}\left(\frac{x-B}{C\sqrt{2}}\right)\right] \tag{2}$$

was used.

For the 5-hr test, x = 0 and Δx = 1.0.

For the bed sectioning data, x = front boundary of section (0.250 in.) and Δx = depth of section (0.125 in.).

The calculated fraction of iodine in any bed segment (corrected for penetration) can be determined from the equation

$$\frac{\int_x^{x+\Delta x} f(x)\,dx}{\int_0^1 f(x)\,dx \Big/ (1 - \text{Penetration})} \tag{3}$$

Thus, to find the fraction of iodine in the last 1/8-in.-deep segment of the test bed from the 1-hr test, from Equation 2 and Table A-I

$$\int_{0.875}^{1.000} f(x)\,dx = (1.850)\ (0.3970)\sqrt{\frac{\pi}{2}}\left[\text{erf}\left(\frac{1-0.0520}{0.3970\sqrt{2}}\right) - \text{erf}\left(\frac{0.875-0.052}{0.3970\sqrt{2}}\right)\right]$$

$$= 0.9205\left[\text{erf}(1.6885) - \text{erf}(1.4659)\right]$$

$$= 0.01954$$

From Equation 1,

$$\int_0^1 f(x)\,dx = (1.850)(0.3970)\sqrt{\frac{\pi}{2}}\left[\operatorname{erf}\left(\frac{1-0.0520}{0.3970\sqrt{2}}\right) + \operatorname{erf}\left(\frac{0.0520}{0.3970\sqrt{2}}\right)\right]$$

$$= 0.9205\left[\operatorname{erf}(1.6885) + \operatorname{erf}(0.0926)\right]$$

$$= 1.0008$$

1-hr penetration = 0.10631%

or $\dfrac{(0.01954)(1-0.00106)}{(1.0008)} = 0.01950 = 1.95\%$

The complete list of calculated distribution values for all three tests is shown in Table IV.

DISCUSSION

WILHELM: Do you think that the low desorption rate will be valid on doses 10 to 100 times higher than you reached in your experiments?

EVANS: I have no reason to believe there would be higher desorption rates at higher dose rates.

DEITZ: A few observations have been made on the thermal stability of a sample of silver zeolite after exposure to methyl iodide-127 in the RDT M-16 configuration at 30°C. The sample which had retained all of the methyl iodide was subjected to programmed heating (2.7°C/min.) with continuation of the air flow. Emission of iodine started suddenly at 130°C and became catastrophic at about 350°C. These observations indicate that the retention of iodine in the zeolite cage may not be as tight as some would wish.

OPERATIONAL MAINTENANCE PROBLEMS WITH IODINE ADSORBERS IN NUCLEAR POWER PLANT SERVICE

C. E. Graves, J. R. Hunt, J. W. Jacox and J. L. Kovach
Nuclear Consulting Services, Inc.
Columbus Ohio

Abstract

The start-up and inservice testing of adsorber systems and components and their maintenance show several problems which can be prevented by change in design, installation and operation procedures.

Major problems relate to:

a) Testability of systems and components to existing standards.
b) The accidental initiation of fire control water sprays and their consequences.
c) Severe corrosion developing in systems subjected to wetting or high moisture condition resulting in total mechanical failure of components.
d) Adsorbent settling and degradation occurring in storage and use of the components.

Each of the problems and their occurrence and partial or total prevention techniques are discussed.

I. Introduction

This paper is based on actual field maintenance and testing in addition to data and observations gathered during routine design, manufacture and servicing of iodine adsorber systems and components used in nuclear power plant applications.

Discussed are the most commonly encountered problems in start-up (acceptance) testing, inservice (surveillance) testing and maintenance of iodine adsorbers as well as a number of surprising yet predictable and avoidable difficulties.

It is hoped that this paper will aid the manufacturer, service and test personnel and, most importantly, the final user in avoiding pitfalls where possible and initiating the most effective corrective action when necessary.

II. Testability of Systems and Components to Existing Standards

In recent years manufacturers have become increasingly aware of the necessity of designing not only functionally acceptable adsorber systems but systems which can be safely and easily tested without requiring massive redesign and backfitting after field installation.

Hopefully the era of systems with adsorber trays welded to the mounting frame with safe access requiring complete system disassembly is only a dim memory of a maturing industry's infancy.

As systems are designed and built to current standards (ANSI N509-76) and, therefor, testable to current standards (ANSI N510-75) many problem areas will be eliminated. But what about yesterday's systems and components which are to a

large extent todays problems?

Consider the following descriptions of equipment recently encountered in the field. A number of the problems discussed apply to system components or sections other than specifically the adsorber section itself.

1. "It leaks --- It doesn't leak". A system blower was found literally hanging from the ceiling, suspended by steel cables. It was a small (approx. 1000 cfm) HEPA - Adsorber - HEPA design.

The first problem encountered was accurate measurement of flow. The problem was not lack of a straight duct run as is often the case,but rather a puzzling oscillation of flow. This oscillation, coupled with another problem to be discussed later, created an interesting morning of testing.

The flow oscillations were quickly traced to the flexible blower - plenum connection. Since the blower was freely suspended it was free to swing. The period of blower swing matched and caused the flow oscillation.

When the system was halide leak tested a significant "leakage" was detected. A retest (without system modification) showed insignificant (i.e., within specification limits) leakage. Detailed investigation of the system and its relationship to its environment determined that the system was "breathing". The area in which it was installed was randomly changing from a positive to negative pressure relative to the system due to the opening and closing of a personnel access door in a near-by room. At some point during the halide injection of the first test the system "exhaled" (became positive with respect to the surrounding area) and halide was expelled into the general system area to be picked up downstream of the adsorber through inleakage through the sheet metal and showed up as bypass leakage.

Often systems are tested prior to full flow balancing of the entire plant ventilation systems.

Even if an initial complete flow balance is performed to ensure a system operates within its design specifications, changes in other systems during plant operation may effect the subject system so design specifications cannot be met without a plant wide rebalance.

2. Deep Bed Adsorbers. The use of deep bed (gasketless) adsorbers is becoming more common. They offer many advantages such as:

A) Higher fission product removal efficiencies, particularly for organic forms.

B) Ease of maintenance with less frequent adsorbent changeout and absence of gaskets as potential leak paths.

C) Use of guard beds to prevent (or minimize) poisoning of the expensive impregnated main bed adsorbent.

D) On-site refilling.

E) Longer effective adsorbent life.

With these benefits there are also potential problems. Manufacturers must exercise extreme care in shop testing of these systems. If a leak is detected after field installation it is virtually impossible to pinpoint and repair. This is because the inlet and outlet flow paths are usually only a few inches wide and may be many feet deep. Such flow paths cause turbulence that makes scanning for leaks practically impossible and repair of a leak deep in the slot actually

impossible (without major structural disassembly usually requiring cutting). Guard beds are usually separated from the main bed by a single sheet of perforated metal which limits the ability to test or repair them individually and causes abrasion problems to be discussed later in this paper.

One recently tested system was found to have the perforated stainless steel screen installed with the rough side facing the adsorbent. Another was supplied by the manufacturer with a grain thief only 24" long. This did not reach past the blanked off top section which provides a carbon "head" so the carbon sampled was not exposed to system flow.

Many deep bed systems with guard beds have only 2" guard beds. Experience in testing the adsorbents from these systems shows that this is often insufficient to protect the main bed. One guard bed had such a high solvent loading that it was caked almost solid. An interesting point to be pondered and investigated is whether the presence of a guard bed creates a false sense of security in the minds of some users. Guard beds are designed to protect the main bed but will not mitigate the effects of painting or other sources of gross contamination in the area ventilated.

3. Zeolites.

Occasionally manufacturers will utilize conventionally designed adsorber units for zeolites. If the unit is sufficiently over designed to handle the increased weight of the zeolite the result can be satisfactory. Often the heavier zeolite causes problems of distortion, cell-frame interfacing and handling. Further the poor retention of halides by zeolites makes field leak testing very difficult. Currently R-112 (or R-112A) is the halide of choice since,of the halides approved for leak testing,it is retained the longest by zeolites. Unfortunately unless the zeolite is very dry and the air stream is low RH the retention is so short that a fully valid test is marginal. Designers and users of zeolite systems are cautioned about this problem. Additional study is required to determine the specific parameters of dryness of zeloite and RH of the airstream vs R-112 delay (retention) time on zeolites and investigation of other possible challenge agents.

4. Halide Background Interference During Halide Leak Testing.

High halide background concentrations due to use of degreasers, dye penetrents propellents, refrigerants, etc., are a constant source at concern during testing.

Occasionally one can literally be sitting on the problem. One system tested was plagued by uncommonly high halide interference. Inspection and testing of the area ventilated by the system did not reveal any substantial source of halide. The source of the problem in this case was an air conditioner unit located in the same room as the system - a common practice with control room emergency systems. This particular system had a make-up air grill in the same room as the air conditioner. The test team used its halide sensor to locate the compressor leak (which plant personnel had been unable to locate for several years) and then successfully tested the system.

III. Accidental Initiations Of Water Sprays And Their Consequences

Accidential initiation of water spray systems designed to mitigate the consequences of adsorbent fire may be caused by (but not limited to) the following:

A) Routine testing of electrical systems.

B) Inadvertent application of a heat source to system heat sensors during maintenance, repair or inspection.

C) Improper setting of thermo switches.

D) Flow failure with humidity control heaters energized.

E) High light levels in a unique system with photosensors for flame detection.

All these sources of accidential water spray initiation can be eliminated by proper initial design, attention to control sequence and interlocks and operating (maintenance) procedures.

Given the nightmare of an accidentally flooded deep bed (or any adsorbent) system,additional study and attention should be paid to non-water spray approaches, such as simply sealing the adsorber section off from air flow to extinguish by O_2 depletion and CO_2 creation or use of commercial halogenated hydrocarbon fire suppression systems. Both have shown excellent results in various industrial applications and appear to have significantly fewer drawbacks compared to water sprays.

IV. Corrosion Due To Wetting Of Adsorbers

Since almost all current adsorbents used for I131 control are impregnated with iodine any wetting causes immediate and severe corrosion problems. Everyone is aware of chloride corrosion and considerable effort is made to eliminate chloride contamination. All too few recognize that iodide corrosion is chemically similar and almost as bad as chloride. (Figure 1) Of course if there is no water there is no problem. In addition to the water spray problems just discussed the following are observed mechanisms whereby the adsorbent can (and has) been wetted.

A) Hydro testing of the system with adsorbers (and HEPAs) installed.

B) Unprotected fresh air intakes.

C) Area flooding.

D) Uninsulated duct runs resulting in condensation.

E) Poorly drained (or blocked) moisture separators.

F) Water leaks in cooling coils.

G) Improper adsorber storage.

H) Condensation from high RH in conjunction with cycling systems during testing.

The consequences of wetting of the impregnated adsorbent by any of these, or other, mechanisms is costly. (Figure 2) Examples are:

A) Impregnant leachout and spread of radioiostopes.

B) Loss of efficiency to control organic forms of I131.

C) Formation and spread of contaminated corrosion products.

D) Mechanical failure from corrosion. (Figure 3)

Since the majority of accidental adsorber wettings occur in systems not contaminated with significant radioactivity they can be spared irreparable damage and component and system failure can be avoided.

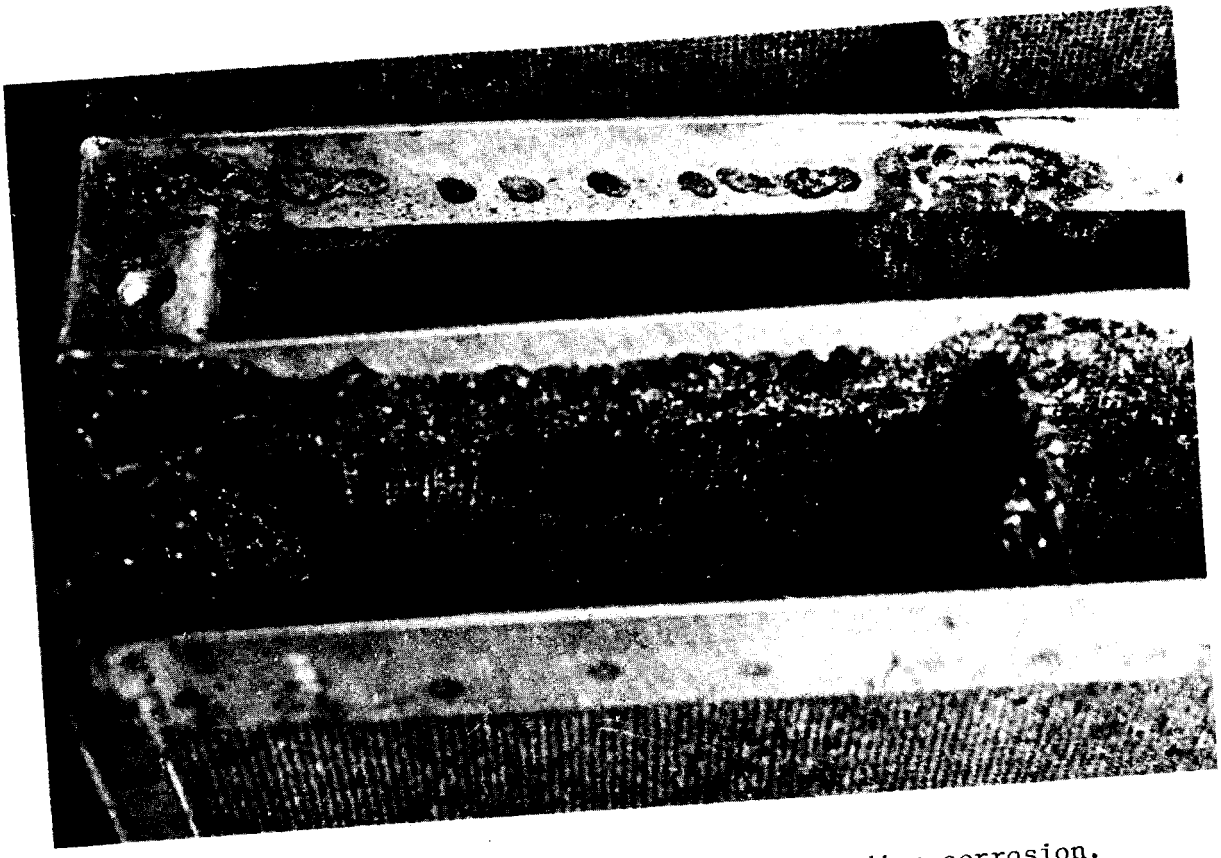

Figure 1 Tray type adsorber damaged by iodine corrosion.

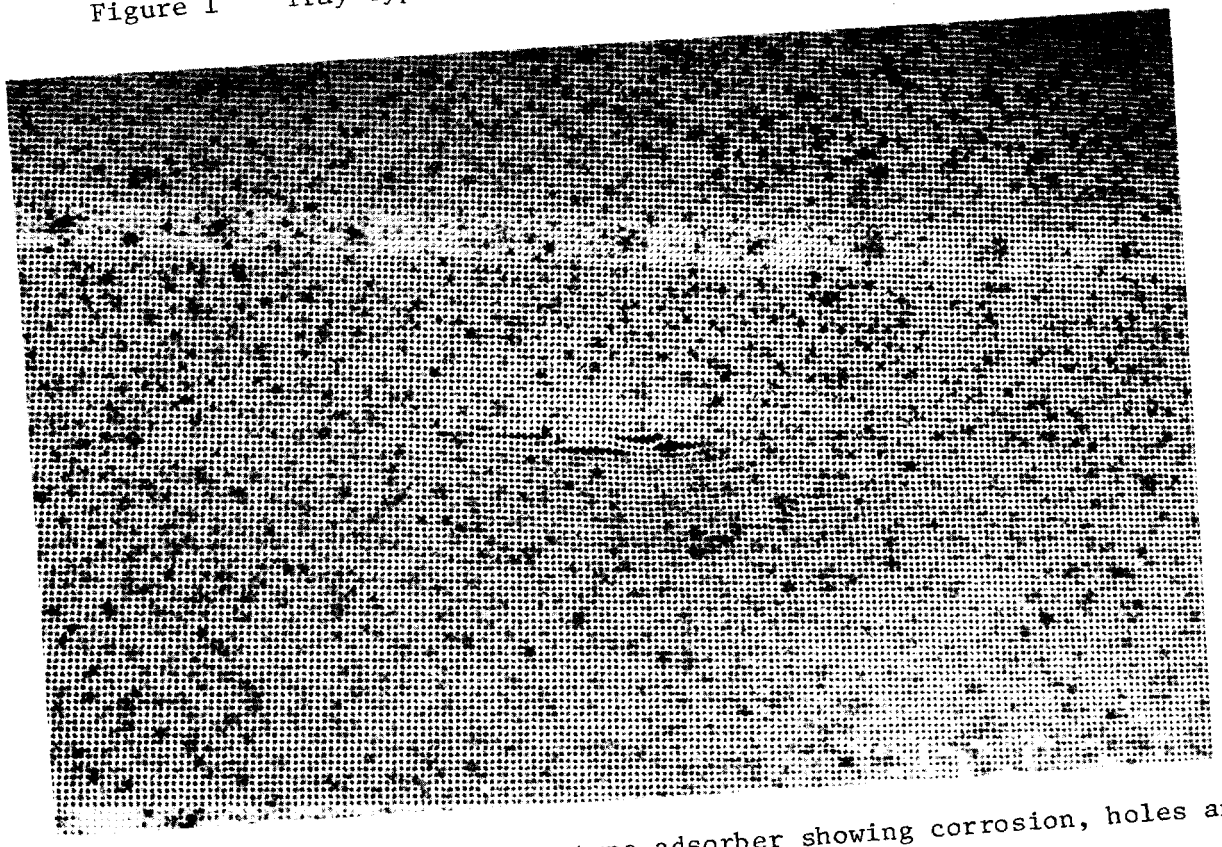

Figure 2 Perforated area of tray type adsorber showing corrosion, holes and a tear.

First the fact that the component or system has been wetted must be known. This requires a thorough understanding of each system in all modes. Detailed administrative procedures are required to ensure prompt reporting and action when wetting is suspected or confirmed.

The first step is of course to remove the wet cell or carbon. This removes the source of iodine from the system. The system must be carefully cleaned to remove any iodide contaminated material or water. This can be an extensive project in a deep bed or badly flooded tray type system. After gross clean-up of sludge and rinse with utility water, the wetted surfaces must be rinsed with deionized water treated with 0.1% sodium nitrite solution.

Badly corroded cells should be set aside for repair. Other cells should be rinsed in deionized water treated with sodium nitrite (0.1% solution). They should then be dryed and passivated per ASTM A380 Table A2 Part II Code G. They may then be refilled for reuse.

V. Adsorbent Settling And Degradation

Experience has shown the principle causes of adsorbent settling and degradation to be:

A) Improper filling (Figure 4 and Figure 5).

B) Improper adsorber design.

C) Improper adsorbent particle size.

D) Improper pretreatment of air.

E) Ventilation of poisoned atmosphere.

During on-site testing of an adsorber - HEPA system substantial bypass of the adsorber bank was detected (72%). Previous visual inspection had not revealed system deficiencies which would suggest leakage of such magnitude. Several adsorber units were removed at random and manually shaken. The adsorbent level was checked with a flashlight and found to be settled between 2 to 8 inches. Further investigation revealed that the cells had been refilled on-site.

They had not been vibrated during or after filling and had not been leak tested as individual cells. Current standards such as AACC CS-8T and ANSI N509-76 require cells be filled to maximum packing density and leak and pressure drop tested. While it is usually permissible to refill a single cell from which a sample has been taken if all proper procedures are followed by properly trained personnel, entire bank refilling by plant personnel will almost certainly result in unacceptable results, if inadequate filling equipment is used.

Many cell designs do not provide for adequate filling access. Ideally the entire filling surface should be open for proper filling. The smaller the fill opening the more difficult to obtain an acceptable fill.

While it should be an obvious requirement, some cells are still seen with mild steel components. Through bolts are the most common offender. It is not know if this is a design or material control problem.

As mentioned in the deep bed section of this paper there is a rough and smooth side on perforated metal. This is an inherent attribute of the material and its method of production. The smooth side should always be facing the carbon. The rough side will abrade the carbon to fines due to system vibration. This is

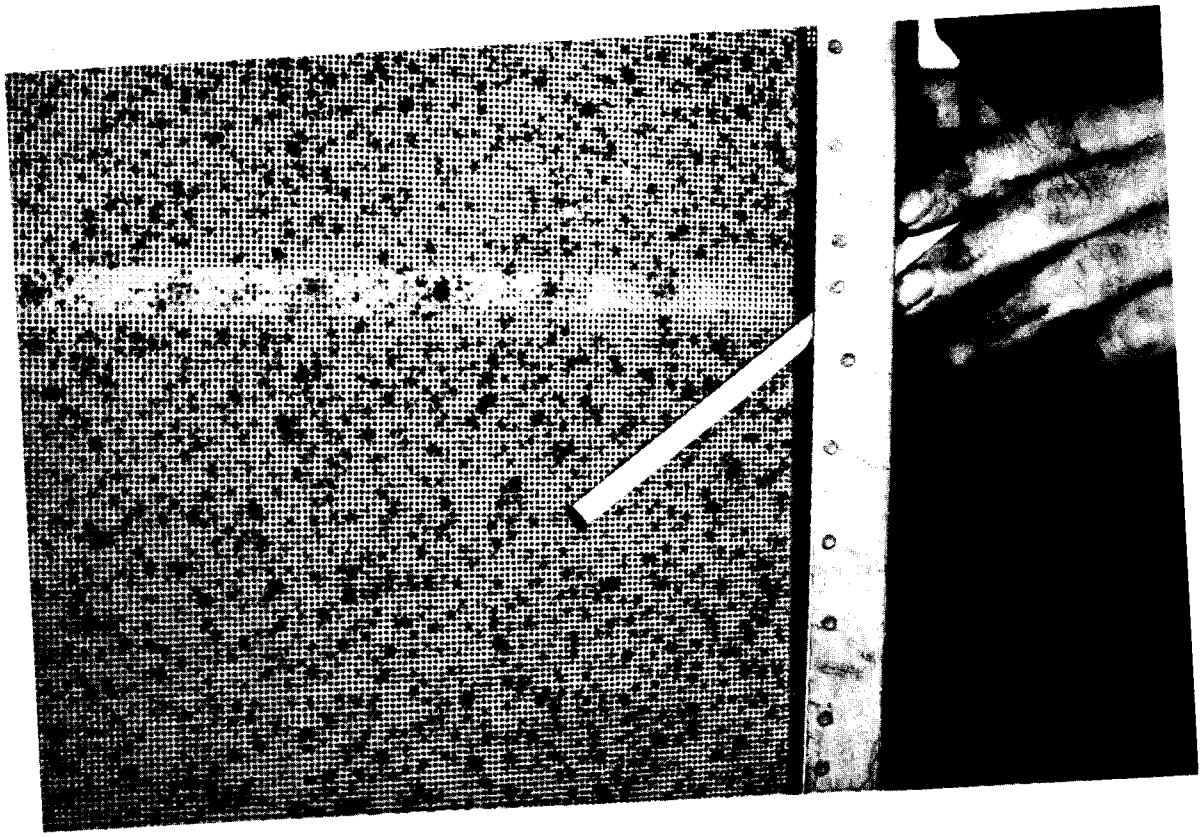

Figure 3 Mechanical failure of a tray type adsorber resulting from corrosion.

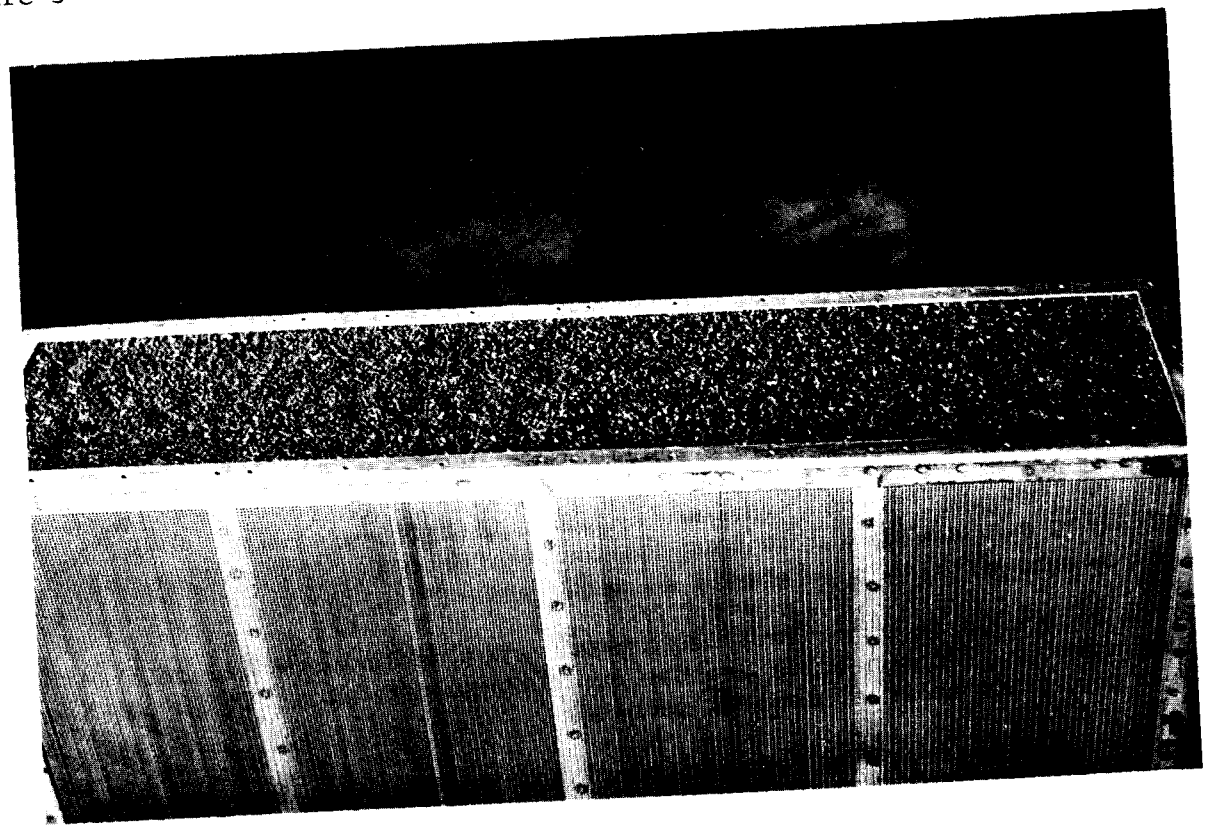

Figure 4 Stationary fill - tray type adsorber.

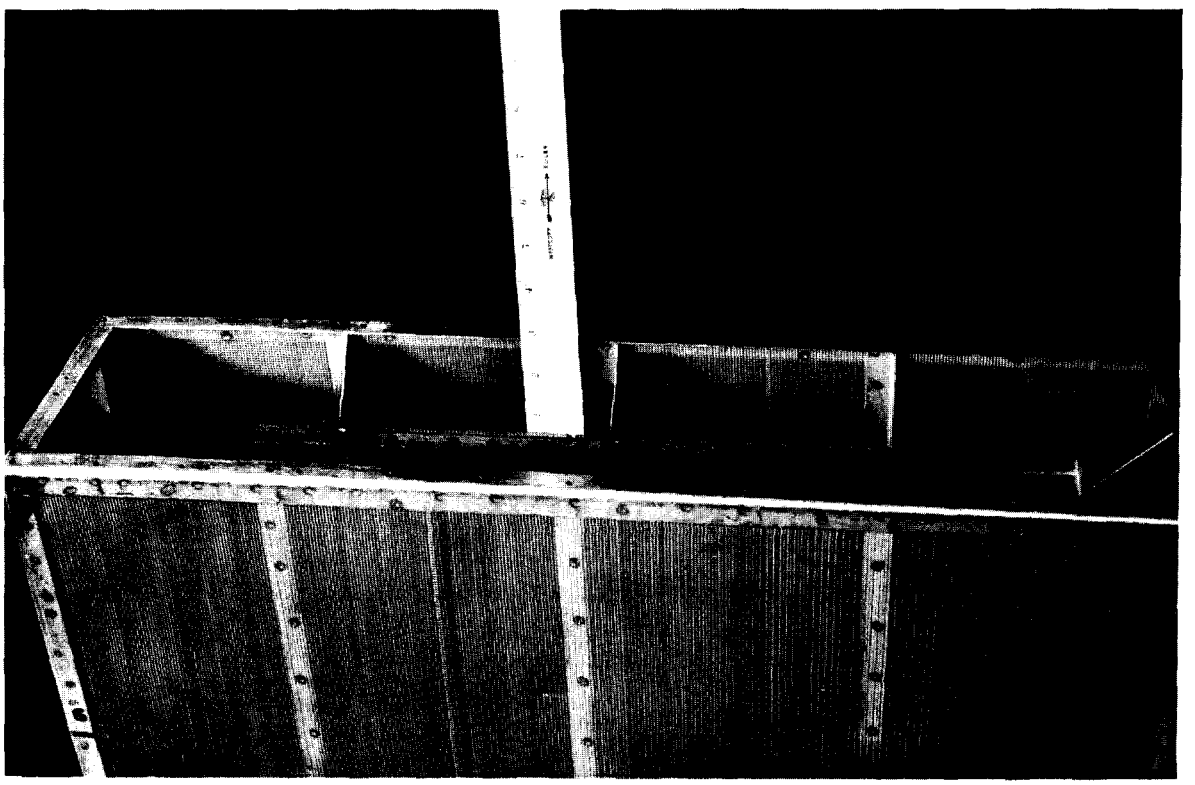

Figure 5 The same adsorber pictured in Figure 4 but after vibration to achieve maximum packing density.

particularly true if the packing is less than perfect. Experience has shown almost a random aspect perforated placement by some manufactures. In deep beds with guard beds there is an obvious problem if only a single sheet of material separates the two (2) beds.

Particular care must be taken in filling deep bed systems. With beds on the order of 6" deep and 10 ft high filling is extremely difficult. Filling must be performed with proper equipment and at the proper rate by trained personnel. Very large variations in packing density can and will occur if the carbon is simply dumped in from drums.

Although the point has been made many times by many people including papers at past Air Cleaning Conferences, there are still instances of large scale painting in areas ventilated by adsorbent systems with the system in operation.

Storage of adsorbent in bulk or in filled cells varies widely. There is general insufficient understanding of the requirements of clean heated (in cold climates) storage areas where there is minimum chemical contamination.

Two final points for consideration should be made. Some new plants still have either more than one size or simply nonstandard size adsorber cells which increase both cost and lead time on replacements. There is no technically valid reason for this design approach.

Another point is offered for consideration and possible study. Most plant Technical Specifications require filter system and adsorbent testing before refueling which certainly makes sense. The system may not be required to be retested until the next refueling cycle. Since refueling is usually the time for considerable maintenance it is also the time when there is a high probability of adsorbent contamination. We suggest that system testing after refueling is completed should be considered in addition to or instead of testing before refueling if the type of maintenance performed is conducive to organic contamination.

AECL IODINE SCRUBBING PROJECT

D.F. Torgerson and I.M. Smith
Atomic Energy of Canada Limited
Whiteshell Nuclear Research Establishment
Pinawa, Manitoba, R0E 1L0

Abstract

We describe a gas phase chemistry approach to organic iodide scrubbing which achieves large removal efficiencies for iodomethane and iodobenzene from air. Low energy electrons, ions, and reactive neutral species are generated using a corona discharge through which the gas flow is directed. Organic iodides are rapidly decomposed to form an inorganic, iodine-containing compound which precipitates from the flow. Electrons and negative ions appear to be the most effective scavengers for organic iodides since negative voltage discharges have the highest scrubbing efficiency. The iodine-containing precipitate is an amorphous iodine/oxygen compound which decomposes to form crystalline I_2O_5 on heating.

I. Introduction

In this paper, we discuss an approach to iodine scrubbing which uses gas phase chemistry to achieve large decontamination factors for iodomethane and iodobenzene. Airborne iodine can occur in a variety of chemical forms and the chemical distribution can be shifted by changes in conditions. Accordingly, we are interested in developing a procedure to scrub all possible species of iodine from air, including the highly penetrating organic forms. This paper summarizes some of the results to date.

II. Background

The basis for this work is the reaction of organic iodides with negative ions, electrons, and active neutral species. Iodomethane, for example, is an effective electron scavenger[1] and decomposes in the gas phase to form CH_3 and I^-. The cross-section for scavenging maximizes at an electron energy of 0.15 eV,[2] and the reaction therefore requires low energy electrons.

The study of negative ion-molecule reactions is important in the fields of radiation chemistry, combustion, gas discharges, and atmospheric chemistry. Much valuable information has been obtained on negative ion-molecule reactions using the flowing afterglow technique[3] and mass spectrometric methods.[4] These studies have shown that ion-molecule reactions are orders of magnitude faster than gas phase reactions not involving ions. Reactions between iodomethane and negatively charged oxygen species are exothermic, as illustrated below for just two of several possible reactions:

$$CH_3I + O_2^- \longrightarrow CH_3 + I^- + O_2 \qquad \Delta H = -0.25$$

$$CH_3I + O^- \longrightarrow CH_3O + I^- \qquad \Delta H = -2.94$$

Therefore, these reactions, along with direct electron capture, appeared to be reasonable bases for developing a CH_3I scrubbing procedure. Furthermore, since the organic moiety affects penetration of organic iodides through filter systems, decomposition to an inorganic iodine form seemed to have merit.

Although there are several conceivable ways to inject free electrons and negative ions into a gas stream, the simplest procedure is to use a low energy discharge. Corona discharges can be readily developed in air using a thin wire coaxially aligned with a hollow grounded cylinder. When negative high voltage is applied to the wire, the resulting discharge generates electrons having a broad energy spectrum as well as ionic species such as O^- and O_2^-.[5] Therefore, by passing organic iodide-contaminated air streams through a corona discharge, it was hoped that sufficient reactive species would be present to effect efficient decomposition.

In addition to ions, discharges in air produce neutral reactive species such as O and O_3. These can also contribute to organic iodide scavenging, but as noted earlier, neutral reactions are expected to be orders of magnitude slower than ionic reactions.

Finally, negative ions from nitrogen are unlikely to be formed in a corona discharge,[6] and N_2 may simply act as an inert carrier gas.

III. Experimental Method

Testing of this concept was carried out using a corona discharge tube of 2.54 cm diameter and 63 cm long. The central electrode was a tungsten wire of 0.2 mm diameter operated at 6-10 kV depending on the discharge current desired between the electrode and the grounded cylinder wall. A 13 MΩ resister was placed between the power supply and central electrode to act as a current limiter. Gas flow through the unit was controlled using rotameters and valves. Impurities were introduced into the air stream by diverting part of the flow through a vessel designed to saturate the gas with the appropriate species. The saturated gas was re-mixed with the main flow, and impurity levels could be changed by adjusting flow through the vessel. The reference flow for much of this work was 1000 cm^3/min containing 100 µg/g iodomethane.

Chemical analyses of the gas stream were performed on-line using an Extranuclear quadrupole mass spectrometer. The mass spectrometer was controlled using a Tennecomp TP 5/11 analyser which was programmed to run the experiments automatically and to analyse data between runs. Since non-radioactive iodides were used, the decontamination factor was defined as (initial concentration)/(final concentration).

IV. Iodomethane Scrubbing

Effect of Discharge Current and Polarity

Figure 1 shows how the CH_3I decontamination factor changes with discharge current using both negative and positive electrode voltages.

Decontamination factors greater than 10^3-10^4 could not be measured owing to detection sensitivity limitations.

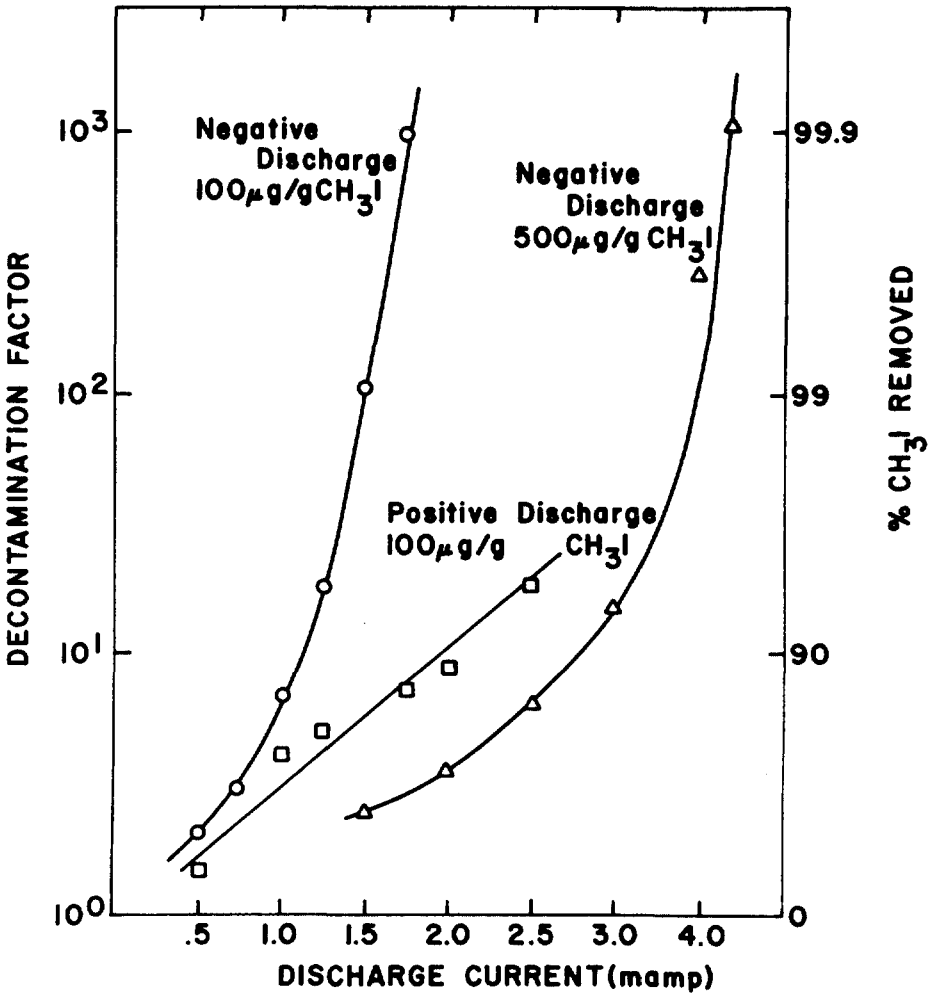

FIGURE 1
EFFECT OF DISCHARGE CURRENT ON CH_3I DF

The most striking feature of these curves is the rapid increase of DF with current when negative voltage is used. It is of interest, therefore, to consider the difference between positive and negative discharges.

Both negative and positive corona discharges produce a ∿ 2 mm radius discharge region centered on the wire electrode. However, species produced outside this region are quite different for the two discharges. A positive discharge is developed when free electrons in the discharge region (always present owing to cosmic rays and background radiation) are accelerated towards the positively charged electrode, and produce more free electrons by ionization of neutral air molecules. Positive ions are repelled by the wire and migrate towards the cylinder wall. In contrast, negative discharges result from bombardment of the central electrode by positive ions, and free electrons are repelled towards the cylinder wall along with negatively-charged dissociated products. Since the mean electron energy

outside the discharge region is 1-2 eV for the experimental conditions used in this work, only electron capture processes are possible. It appears, therefore, that negative species (e^-, O_2^-, O^-) are somewhat superior to positive ions for CH_3I scavenging.

It is noted from Figure 1 that to attain the same DF for higher CH_3I loadings, a larger discharge current is required. This is an expected result and indicates that the current can be suitably adjusted for the DF desired over a range of CH_3I concentrations. Since the curves in Figure 1 for negative discharges are sharply rising at the detection limits, it is possible that very large decontamination factors can be achieved.

Effect of Oxygen Concentration

The role of oxygen in CH_3I decomposition can be further examined by varying the O_2 concentration. Table I compares decontamination factors for different gas compositions using a discharge current of 2.0 mA.

Table I. CH_3I removal as a function of oxygen concentration.

Gas Composition	DF	% CH_3I Removal
0 % O_2/100 % N_2	2.5	60.5
2.6% O_2/ 97.4% N_2	682	99.85
5 % O_2/ 95 % N_2	5×10^3	99.98

In the absence of oxygen, free electrons account for virtually all negative current in the discharge tube. Thus, reaction with electrons is likely the dominant scrubbing mechanism. However, the presence of O_2 greatly enhances scrubbing efficiency. One possible explanation is that O^- and O_2^- are less mobile than electrons in the gas stream, thus increasing the probability of reactions with CH_3I. In addition, neutral reactive species are produced from O_2 which can contribute to CH_3I scrubbing for both positive and negative discharges.

Effect of Impurities

Impurities in the gas stream can have an effect on decontamination factors if the impurities compete for the active species. Some preliminary results indicate that water vapor does not affect the scrubbing process. At a flow of 500 cm^3/min, 100 µg/g CH_3I loading, and 0.5 mA discharge current, the removal efficiencies are 97.9% in dry air and 97.6% in air containing 2.5% water vapor. This is an expected result since the reactions between H_2O and O^- or O_2^- are endothermic, and reactions with electrons have a threshold of $\sim$ 3.8 eV. However, reactions of the type

$$NO_2 + O_2^- \longrightarrow NO_2^- + O_2 \qquad \Delta H = -3.4 \text{ eV}$$

$$CO_2 + O^- \longrightarrow CO_3^- \qquad \Delta H \sim -1.7 \text{ eV}$$

suggest that nitrogen oxides and CO_2 may be poisoning agents in the discharge. Figure 2 shows the effect of these compounds on CH_3I removal efficiency.

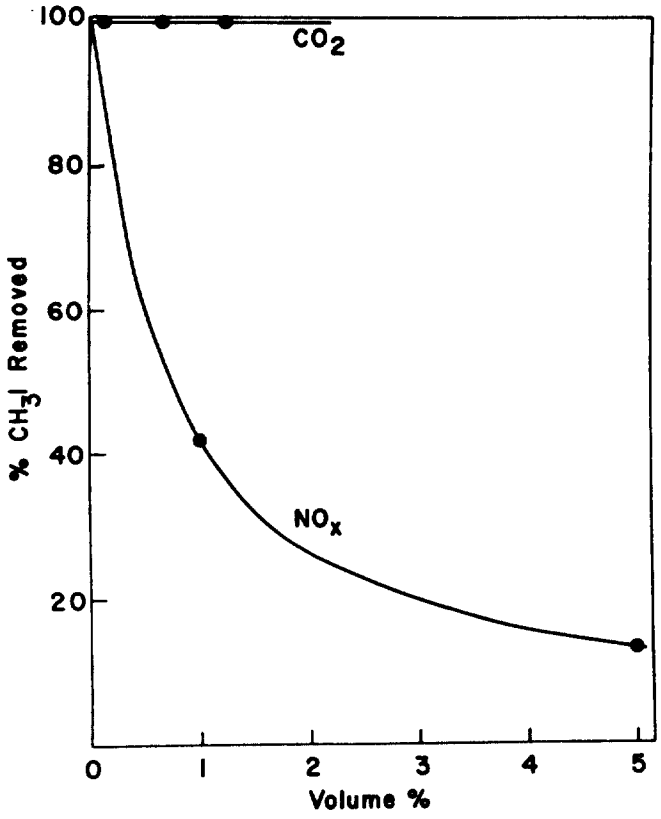

FIGURE 2
CH_3I REMOVAL EFFICIENCY AS A FUNCTION OF CO_2 AND NO_x CONCENTRATION

As expected, nitrogen oxides significantly reduce the scrubbing efficiency, but CO_2 has no effect. The reason for this difference can be understood by considering the following reactions:

$$CH_3I + CO_3^- \longrightarrow CO_2 + CH_3O + I^- \qquad \Delta H = -1.2 \text{ eV}$$

$$CH_3I + NO_2^- \longrightarrow NO_2 + CH_3 + I^- \qquad \Delta H = +1.4 \text{ eV}$$

The fact that CO_3^- is not stable in the presence of CH_3I explains why CO_2 has no effect on the efficiency. On the other hand, reactions with NO_2^- are endothermic. Therefore, NO_2 effectively scavenges the negative charge and seriously interferes with the scrubbing process.

The NO_2^- ultimately transfers its electron to the walls of the discharge tube without initiating any further reactions.

Nature of the Iodine Precipitate

The iodine precipitate is a white hygroscopic solid which initially liberates I_2 when stored at room temperature. Samples of the fresh precipitate have been analysed by direct probe mass spectroscopy, X-ray diffraction, thermal gravimetric analysis, and differential thermal analysis. These studies show that the precipitate is an amorphous solid containing iodine and oxygen, with perhaps traces of organic contaminants. Typical DTA and TGA curves are shown in Figure 3.

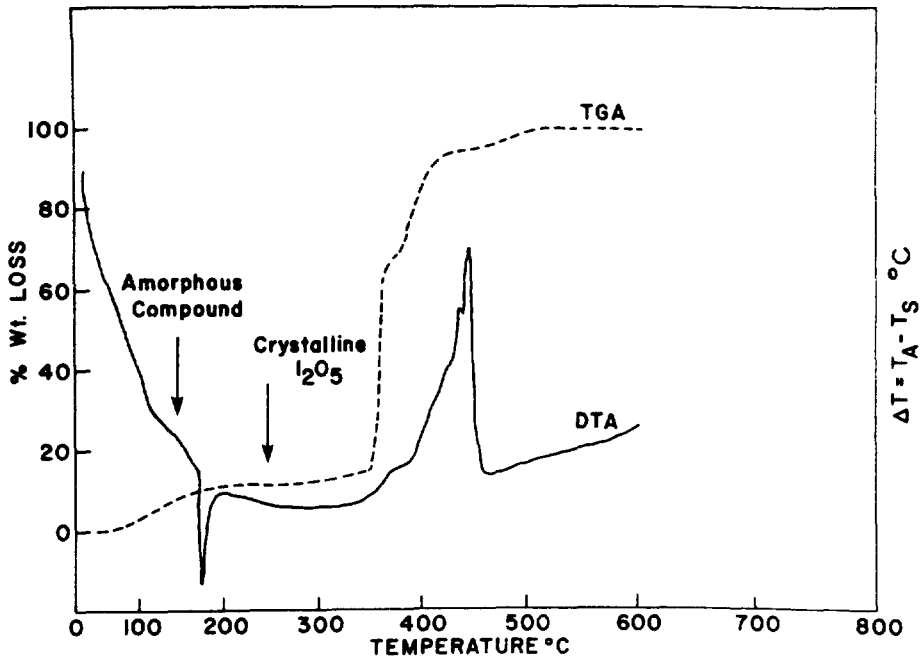

FIGURE 3
DTA (LEFT SCALE) AND TGA (RIGHT SCALE) CURVES
OBTAINED FOR THE IODINE PRECIPITATE

As shown by the TGA curve, the amorphous solid begins to decompose at ∿ 120°C and loses ∿ 15% of its weight. The DTA curve shows that this is an exothermic transition, leading to a crystalline product which has been identified as I_2O_5 by X-ray diffraction. At ∿ 350°C, the I_2O_5 begins to decompose to I_2 and O_2 in an endothermic reaction. This is the expected behaviour for I_2O_5.[7] Efforts to understand the chemical and physical properties of the amorphous solid are continuing.

V. Iodobenzene Scrubbing

Aromatic iodides have proven to be among the most difficult iodine species to remove from air using conventional filtering technology. However, enthalpies for the following reactions indicated that a gas phase chemistry approach might also be applicable to iodobenzene:

$$C_6H_5I + e^- \longrightarrow C_6H_5^{\cdot} + I^- \qquad \Delta H = -0.3 \text{ eV}$$

$$C_6H_5I + O_2^- \longrightarrow C_6H_5O^{\cdot} + IO^- \qquad \Delta H = -0.8 \text{ eV}$$

$$C_6H_5I + O^- \longrightarrow C_6H_5O^{\cdot} + I^- \qquad \Delta H = -4.0 \text{ eV}$$

Again, this is by no means a complete list of possible reactions, and it is felt that iodobenzene could be removed at least as effectively as CH_3I.

Figure 4 shows a plot of DF versus discharge power for air containing 80 µg/g C_6H_5I. Although these results are preliminary, it is evident that C_6H_5I removal is also feasible using a corona discharge.

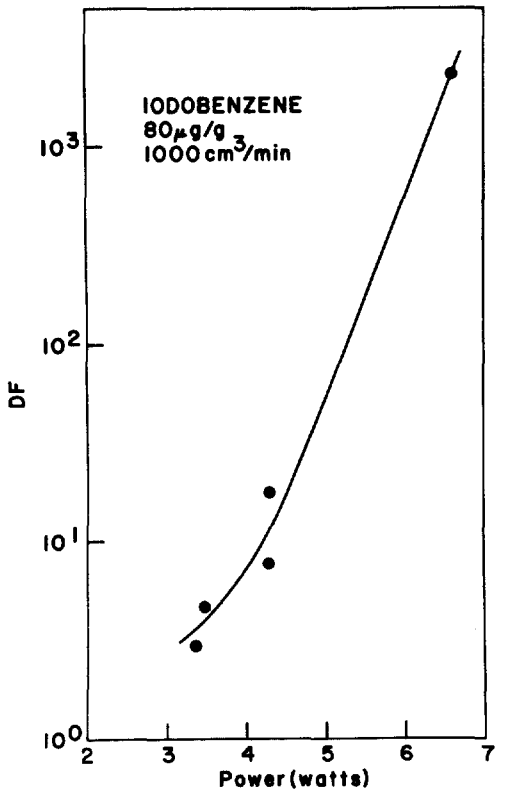

FIGURE 4
C_6H_5I DECONTAMINATION FACTOR AS A FUNCTION OF POWER FOR NEGATIVE DISCHARGE

VI. Conclusions

Gas phase chemistry is an appropriate mechanism for scrubbing organic iodides from air streams. Reaction enthalpies can be successfully used to predict the performance of the corona scrubber. Other iodine species (I_2, HI, HOI) should also be amenable to removal by reactions similar to those discussed here. While much work remains to be done, we believe that gas phase scrubbing is a viable approach to airborne iodine control.

VII. Acknowledgements

We should like to thank A. Wikjord, L. Hachkowski, and P. Taylor for their dedication to the iodine precipitate characterization studies.

VIII. References

1. R.F. Claridge and J.E. Willard, "Production of trapped radicals from alkyl halides in organic glasses by dissociative electron attachment and by photo dissociation", J. Amer. Chem. Soc., 87, 4992 (1965).

2. J.A. Stockdale, F.J. Davis, R.N. Compton, and C.E. Klots, "Production of negative ions from CH_3X molecules by electron impact and by collisions with atoms in excited Rydberg states", J. Chem. Phys. 60, 11, 4279 (1974).

3. E.E. Ferguson, "Thermal-energy negative ion-molecule reactions", Acc. Chem. Res. 3, 402 (1970).

4. J.L. Franklyn and P.W. Harland, "Gaseous negative ions", Ann. Rev. Phys. Chem. 25, 485 (1974).

5. L.M. Chanin, A.V. Phelps, and M.A. Biondi, "Measurements of the attachment of low-energy electrons to oxygen molecules", Phys. Rev. 128, 219 (1962).

6. E.W. McDaniel, Collision Phenomena in Ionized Gases, Wiley & Sons, New York, 1964, pp. 373, 381.

7. F.A. Cotton and G. Wilkinson, Advanced Inorganic Chemistry, Interscience, New York, 1962, p. 445.

DISCUSSION

VAN BRUNT: Have you done any sizing of a packed electrochemical reactor for this system?

TORGERSON: We have not yet done any sizing studies. At this point, the research is exploratory in nature, and we have concentrated on demonstrating that the basic ideas work.

VAN BRUNT: Have you investigated any other anode or cathode materials?

TORGERSON: We have investigated many anode and cathode materials. The critical component is the central wire, and we have found that tungsten is the best choice in terms of chemical reactivity and mechanical strength.

DEMPSEY: Where do the gases go when they interact and precipitate? How might you collect and remove them in an engineered system?

TORGERSON: The iodine compound precipitates on the walls of the apparatus, and can be mechanically collected. It appears that the precipitate can collect on the walls indefinitely without affecting efficiency. Moreover, you can precipitate the compounds onto any removal surface you wish. If the outer electrode is a mesh, most of the product passes through and plates out on whatever you have behind the mesh. There are, therefore, many possible engineered removal systems. For example, if you did not want a solid, you could even collect the product in a thin film of solvent flowing down the outer wall. An interesting approach would be to engineer the device to be both the scrubber and the storage container, leaving the iodine in solid form.

DETERMINATION OF THE PHYSICO-CHEMICAL ^{131}I SPECIES IN THE EXHAUSTS AND STACK EFFLUENT OF A PWR POWER PLANT

H. Deuber, J.G. Wilhelm

Laboratorium für Aerosolphysik und Filtertechnik,
Kernforschungszentrum Karlsruhe GmbH,
Postfach 3640, D-7500 Karlsruhe 1, W. Germany

Abstract

To quantify the credit that can be granted in the assessment of the ^{131}I ingestion doses and the improvement that can be achieved in the ventilation systems if differences of the physico-chemical ^{131}I species with respect to the environmental impact are taken into account, the fractions of the ^{131}I species were determined in the stack effluent and in various exhausts of a 1300 MW_e PWR power plant during a period of 3 months. Based on these measurements, calculations for different cases of filtration of the main exhausts for iodine were carried out.

The average fractions of elemental and organic ^{131}I were about 70 and 30 % respectively in the stack effluent during the time indicated. Elem. ^{131}I originated mainly from the hoods in which samples of the primary coolant are taken and processed. Org. ^{131}I was mainly contributed by the equipment compartments. If the hood exhaust had been filtered, as was the case with the equipment compartment exhaust, the fractions of elem. and org. ^{131}I would have been on the order of 50 % each and the calculated ^{131}I ingestion doses would have been a factor of 3 lower.

I. Introduction

Of the radionuclides released from nuclear power plants ^{131}I is the decisive one with respect to the radiation exposure of the population in the vicinity.(1) The radiation exposure by radioiodine is caused primarily by ingestion via the pasture-cow-milk-pathway. It is therefore dependent on the fractions of the physico-chemical ^{131}I species which feature different deposition velocities for pastures. In the Federal Republic of Germany a fallout velocity ratio of 100 : 10 : 1 is used for elemental (I_2), particulate, and organic (CH_3I) ^{131}I, the main airborne species, in calculations pertaining to the assessment of the ingestion doses caused by the release of ^{131}I or of the ^{131}I release limits. (2)

An efficient improvement of the ventilation systems of nuclear power stations in terms of reduction of elem. ^{131}I release rates can be anticipated, if iodine filters are installed in the exhausts which constitute the main sources of elem. ^{131}I. To evaluate the range of an eventual improvement of the ventilation systems and the credit for differences of the ^{131}I species in the stack effluents with respect to the environmental impact, the fractions of the ^{131}I species have to be measured in the various exhausts within the nuclear power plants and in the stack effluents.

In the United States of America ^{131}I species measurements have been carried out in BWR power plants. (3) In the Federal Republic of Germany ^{131}I species determinations over an extended period (12 and 6 months respectively) have been performed in the stack effluents of two modern PWR power plants of 1200 and 1300 MW_e respectively. (4,5)

(The ^{131}I activities discharged per year via the stacks were in the order of 10 mCi each in the last years.) In one of the PWRs (PWR 2) the fraction of elem. ^{131}I was about 30 %, in the other PWR (PWR 3) it was about 60 %, the balance consisting nearly entirely of org. ^{131}I in both cases. The differences are difficult to account for, since the ventilation systems of the plants are similar in principle.

Besides the ^{131}I species measurements in the stack effluent, the ^{131}I species fractionation is now being determined in the main exhaust streams of PWR 3. The results obtained during the first 3 months of the comprehensive program are the basis of this paper.

II. Method of Measurements

The ^{131}I species measurements in the Federal Republic of Germany mentioned are performed with the radioiodine species sampler developed at the Karlsruhe Nuclear Research Center (KfK). (6) This sampler is suitable for the determination of part., elem. (I_2), and org. (CH_3I) radioiodine. It consists in principle of a stainless steel tube (5 cm inside diameter) in which particulate filters and beds of sorbents for the specific retention of the mentioned radioiodine species (from the air conducted through) are mounted (Fig. 1). Each sampler component (particulate filters, beds of sorbents) is twofold so that conclusions concerning the discrimination of the species can be drawn. (The employment of the second particulate filter, however, is usually dispensed with in routine work.) The volume of the beds is 75 or 150 cm^3, the flow rate 3.6 or 7.2 m^3/h respectively, i.e. the residence time is kept at 0.075 s per bed. The sampling time is usually 1 week.

The retention of particles by the particulate filter GF/A is sufficiently high (a value of > 99.9 % has been measured under certain conditions), whereas the adsorption of I_2 and CH_3I is usually negligible.

The I_2 sorbent DSM 11 is obtained by impregnation (with a salt mixture) of a material consisting mainly of insoluble silicid acid with a certain pore structure. It exhibits a retention efficiency of > 99.9 % for I_2 and of < 0.5 % for CH_3I at a residence time of 0.1 s in the whole design parameter range (10 - 70°C, 20 - 80 % R.H.). (6) At the same residence time the removal efficiency of the KI impregnated carbon CG 0.8 for CH_3I is >> 99.9 % at 10 and 70°C in the case of 20 % R.H.; it is 89 and 96 % respectively at 10 and 70°C in the case of 80 % R.H. In the event of a high relative humidity a removal efficiency of > 99 % for CH_3I can be achieved by mounting additional beds of CG 0.8. Organic compounds of higher molecular weight, as for example C_6H_5I (iodine benzene), are collected by CG 0.8 better than CH_3I.

Counting of the ^{131}I activities of the sampler components is accomplished after demounting by Ge(Li) detectors. The detection limit as defined in this account (net counting rate equal to the standard deviation of the net counting rate) amounts to about 10^{-15} Ci $^{131}I/m^3$ at a sampling time of 1 week and a counting time of 1000 min. At a ^{131}I concentration of 10^{-13} Ci/m^3 for example, it is possible to measure ^{131}I species whose fractions total 1 %.

In Figs. 2 and 3 the results of ^{131}I species measurements in exhausts containing high and low percentages of elem. ^{131}I respectively are demonstrated. In both cases the differentiation of elem. and org. ^{131}I was excellent.

The samplers used in the measurements shown in Figs. 2 and 3 feature a pecularity: the employment of the sorbent IPH. This material is used in radioiodine species samplers for the specific retention of hypoiodous acid (HIO). (3, 8)

It has been employed in the KfK sampler on several occasions with results similar to those of Figs. 2 and 3, i.e. the percentages of ^{131}I on the IPH beds have been minimal. It is thus inferred that $H^{131}IO$ plays no significant part in the exhaust streams assayed here. No attempts are therefore made to detect $H^{131}IO$ in routine ^{131}I species measurements and the employment of IPH is dispensed with. If present, this species would be collected in the KfK sampler on CG 0.8, since the retention of $H^{131}IO$ by DSM 11 is negligible in a wide range of parameters. (7)

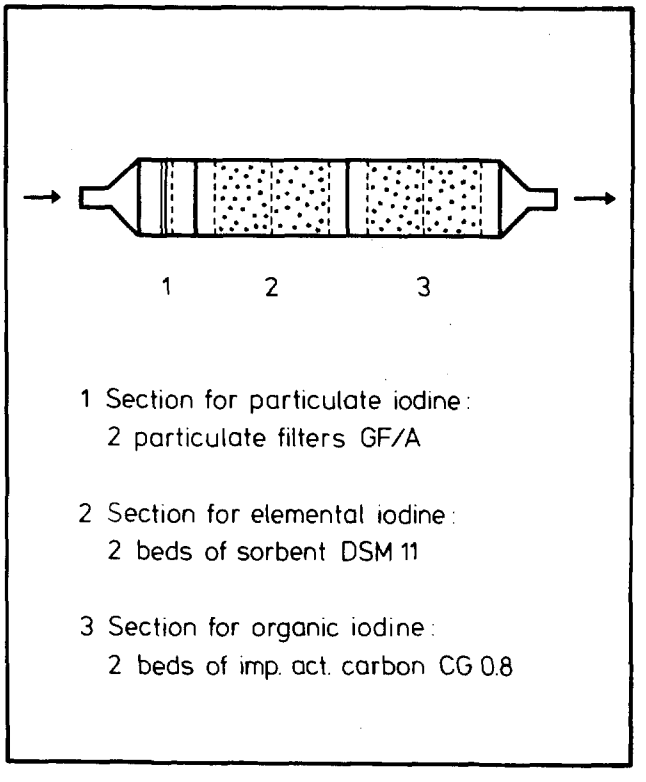

Radioiodine species sampler

Fig. 1

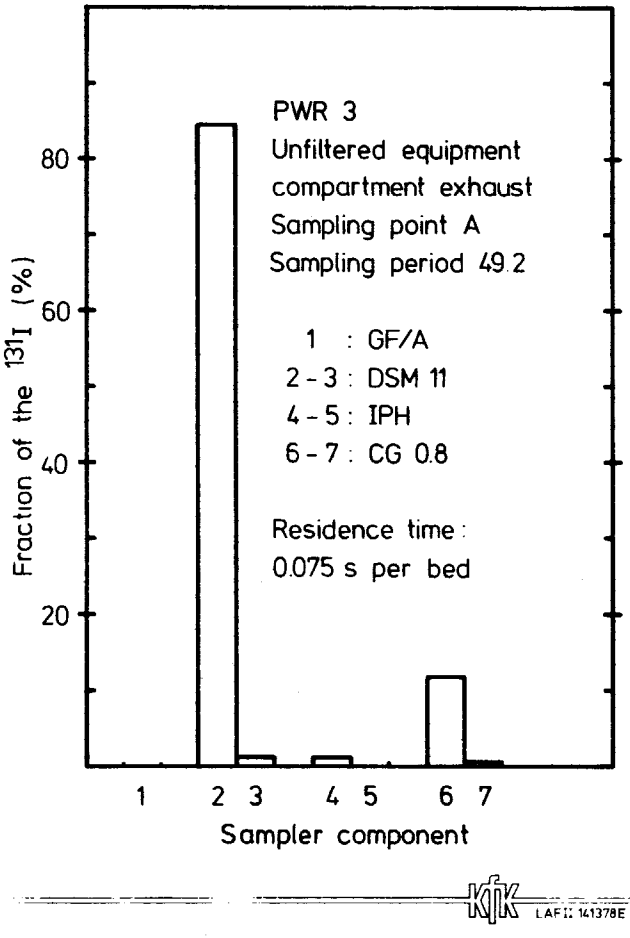

Distribution of the ^{131}I in the radioiodine species sampler

Fig. 2

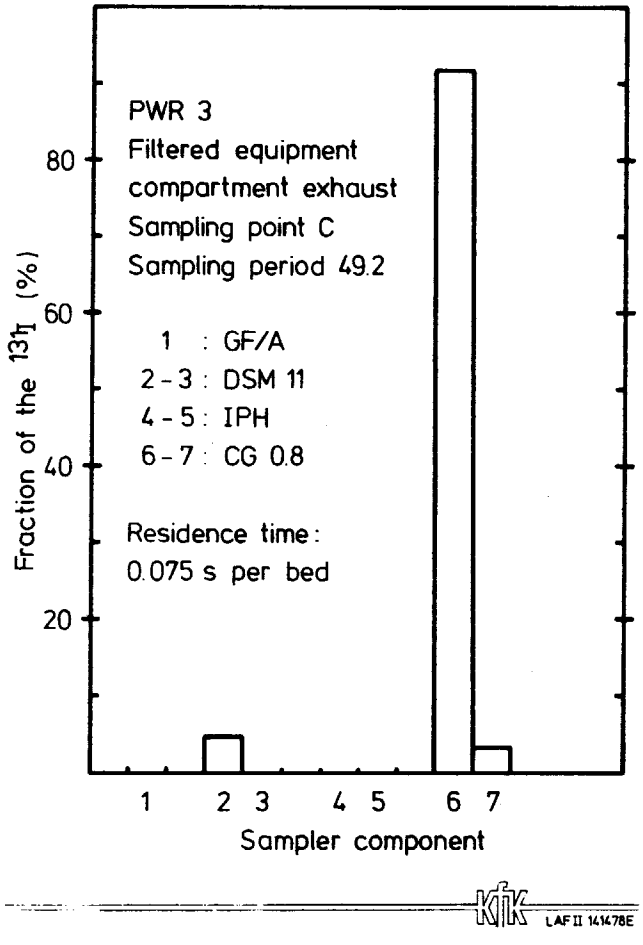

Distribution of the ^{131}I in the radioiodine species sampler

Fig. 3

III. Essential Data of the Plant Studied (PWR 3)

The flow diagram, flow rates, and sampling points of the exhausts are given in Fig. 4 and Table I. The activity sources contributing to the stack effluent are located in the reactor building and auxiliary building. The turbine building, whose ventilation air contains practically no activities, is exhausted by roof vents.

The exhausts of the equipment and operating compartments of the reactor building are usually filtered - depending on the pressure in the equipment compartments - by 1 or 2 iodine filters (between sampling points A and B and C respectively). In special cases, for instance during refueling outages, two other iodine filters located in the operating compartments (near sampling point D) can be put in operation for filtration of the air of the equipment and operating compartments (containment purging). These filters can be operated in recirculation and exhaust air mode. (In Fig. 4 only the exhaust air mode has been taken into consideration.)

The annular compartment exhaust is normally filtered by particulate filters (near sampling point H). For accidents filtration of the annular compartment exhaust by an iodine filter is provided for, as shown in the diagram.

The auxiliary building exhausts are filtered by particulate filters (near sampling point H). The upper and lower parts of the equipment compartments of the auxiliary building are exhausted separately (sampling points G and H respectively).

With the sampling locations B, C, E, F, G, H, all the main exhaust streams are covered. Sampling point A has been included so as to enable the determination of the decontamination factors of the equipment compartment exhaust filters. At sampling point D special ^{131}I species investigations were provided for (not dealt with in this report).

The sample extraction at the various sampling points was carried out isokinetically except for the stack effluent sampling point. Here the samples had to be extracted nonisokinetically from a by-pass (inside diameter: 25 mm; length to the stack: 13 m; material: polyethylene). Conclusions on the reliability of the results of the measurements at the stack effluent sampling point prior to and during the time covered in this report can be drawn from a correlation of these results with those obtained at the other sampling locations.

During the time covered in this account, i.e. during the sampling periods 36 to 48, the plant operated nearly constantly at between 50 and 60 % of the rated power, short of the sampling periods 47 and 48. At the beginning of sampling period 47 the reactor was shut down for refueling and maintenance. At the commencement of sampling period 48 containment purging was started. 1 day before the end off this sampling period the reactor pressure vessel was opened for removal of the fuel elements.

Table I Flow rates and sampling points of the exhausts.

Exhaust	Flow rate (m^3/h)	Sampling point
Equipment compartment exhaust [a]	1 200	A, B, C
Annular compartment exhaust [b]	61 500 [f]	E
Hood exhaust [c]	4 300	F
Auxiliary building exhaust [d]	41 000	G
Auxiliary building exhaust [e]	57 000	H
Stack effluent	165 000 [f]	I

[a] Exhaust from the equipment and operating compartments of the reactor building.

[b] Includes filtered air from the equipment and operating compartments of the reactor building, if the two iodine filters located in the operating compartments are operated in the exhaust air mode (containment purging).

[c] Exhaust from the laboratory hoods and the primary coolant sampling hoods.

[d] Exhaust from the upper parts of the equipment compartments of the auxiliary building, the staff rooms,and the laboratories.

[e] Exhaust from the lower parts of the equipment compartments of the auxiliary building.

[f] 74 500 and 178 000 m^3/h respectively during sampling period 48 because of containment purging (refueling outage).

IV. Results of the ^{131}I Species Measurements and Calculations

The total ^{131}I concentrations, total ^{131}I release rates, and ^{131}I species fractions observed at the various sampling points during the sampling periods 36 to 48 are listed in Tables II to V. Table V includes the corresponding values for the stack effluent calculated from the results of the measurements in the various exhausts. Figs. 5 to 7 show the measured and calculated total ^{131}I concentrations and the elem. and org. ^{131}I species fractions for the individual sampling periods. The ^{131}I species contributions of the different exhausts to the stack effluent are presented in Tables VI to VIII and in Figs. 8 to 12.

The results reveal that during sampling period 48 a fundamental change ocurred, attributable to the opening of the reactor pressure vessel and the containment purging. The total ^{131}I concentration of the annular compartment exhaust (which at sampling point E included filtered air from the equipment and operating compartments because of the containment purging) increased by more than 2 orders of magnitude. This resulted in a sharp increase of the ^{131}I species contribution of that exhaust and in a decrease of the ^{131}I contributions of the filtered equipment compartment and hood exhausts. The fraction of elem. ^{131}I in the stack effluent was smaller than 50 % in this sampling period, the first time during the sampling periods 36 to 48. This is in contrast with the findings for PWR 2, where the proportion of elem. ^{131}I increased to more than 90 % in the stack effluent when the reactor pressure vessel was opened. (4)

No increase of the total ^{131}I concentration in the equipment compartment exhaust occurred during sampling period 48, as would have been anticipated. Nor did a significant increase occur during the following sampling period. The proportion of elem. ^{131}I increased sharply, however, as can be seen in Fig. 2.

The average values of the results of the ^{131}I species measurements and calculations for the sampling periods 36 to 48 are given in Table IX and in Figs. 13 and 14. The averages of the measured fractions of elem. and org. ^{131}I in the stack effluent were about 68 and 31 % respectively. They agree to a high extent with those of the calculated fractions (69 and 29 % respectively). It is therefore inferred that the averages of the ^{131}I species fractions observed previously in the stack effluent of PWR 3 (60 and 39 % respectively) are reliable.

As for the averages of the measured and calculated total ^{131}I concentrations and release rates of the stack effluent, there is agreement within the standard deviations.

The main results concerning the contributions to the stack effluent are as follows:

(a) The contribution of the filtered equipment compartment exhaust was of all the exhausts the smallest for elem. ^{131}I (nearly 0 %) and the largest for org. ^{131}I (36 %). The total ^{131}I contribution was 11 %.

(b) In the case of the annular compartment exhaust all the individual contributions to the stack effluent were smaller than 10 %.

(c) The hood exhaust was the main contributor with respect to elem. ^{131}I (68 %) and total ^{131}I (55 %). It accounted for 21 % of the org. ^{131}I.

(d) All the individual contributions of the two auxiliary building exhausts were smaller than 25 %.

The dominant source of total ^{131}I was the equipment compartment exhaust. By filtration it was reduced by a factor of about 6 (Table IX). From Table X and Fig. 15 it can be seen that filter 1 (between sampling points A and B) was much less efficient for elem. and org. ^{131}I than filter 2 (between sampling points A and C). However the ratio of the average decontamination factors for elem. and org. ^{131}I was larger with filter 1 than with filter 2 (94 and 46 respectively). This means that the removal efficiency of filter 1 for elem. ^{131}I had decreased less than that for org. ^{131}I.

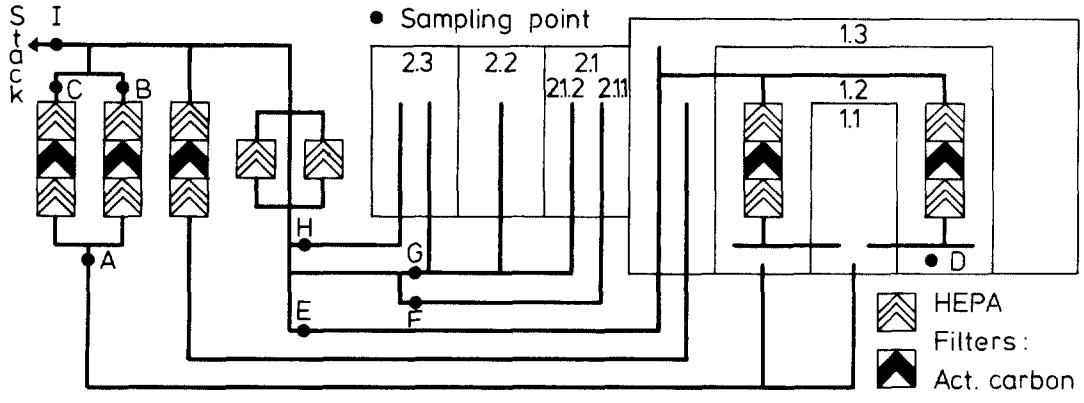

Reactor building :

1.1 Equipment compartments
1.2 Operating compartments
1.3 Annular compartment

Auxiliary building :

2.1 Laboratories (2.1.1 Hoods, 2.1.2 Rooms)
2.2 Staff rooms
2.3 Equipment compartments

Simplified exhaust flow diagram of PWR 3

Fig. 4

Table II Results of the ^{131}I species measurements in the equipment compartment exhaust.

Sampling period	Total ^{131}I concentration [a] (Ci/m^3)	Total ^{131}I release rate (Ci/s)	Fraction of the ^{131}I species [b] (%)			Detection limit [c] (%)
			Part. ^{131}I	Elem. ^{131}I	Org. ^{131}I	
Unfiltered equipment compartment exhaust (sampling point A)						
36	1.1 (-10)	3.7 (-11)	< 1	9	91	< 1
37	1.2 (-10)	4.0 (-11)	< 1	6	94	< 1
38	4.1 (-11)	1.4 (-11)	-	10	90	< 1
39	3.8 (-11)	1.3 (-11)	-	9	91	< 1
40	5.4 (-11)	1.8 (-11)	-	7	93	< 1
41	4.0 (-11)	1.4 (-11)	< 1	8	92	< 1
42	2.7 (-11)	8.9 (-11)	< 1	9	90	< 1
43	2.3 (-11)	7.8 (-11)	-	7	93	< 1
44	6.3 (-11)	2.1 (-11)	-	6	94	< 1
45	3.7 (-11)	1.2 (-11)	< 1	22	78	< 1
46	6.0 (-11)	2.0 (-11)	< 1	23	77	< 1
47	1.5 (-10)	5.1 (-11)	< 1	31	69	< 1
48	1.3 (-10)	4.4 (-11)	< 1	30	70	< 1
Filtered equipment compartment exhaust (s. periods 36-41: s.point B; s. periods 42-48: s.point C						
36	2.8 (-11)	9.3 (-12)	< 1	< 1	99	< 1
37	4.8 (-11)	1.6 (-11)	-	< 1	100	< 1
38	1.3 (-11)	4.2 (-12)	-	< 1	100	< 1
39	1.1 (-11)	3.6 (-12)	-	< 1	100	< 1
40	1.7 (-11)	5.6 (-12)	-	< 1	100	< 1
41	1.2 (-11)	3.9 (-12)	< 1	< 1	99	< 1
42	1.1 (-12)	3.5 (-13)	1	3	96	< 1
43	5.9 (-13)	2.0 (-13)	-	1	99	< 1
44	2.2 (-12)	7.5 (-13)	-	< 1	100	< 1
45	1.4 (-12)	4.8 (-13)	-	1	99	< 1
46	2.4 (-12)	7.8 (-13)	-	< 1	100	< 1
47	1.2 (-11)	4.0 (-12)	-	-	100	< 1
48	7.4 (-12)	2.5 (-12)	-	< 1	100	< 1

[a] Powers of 10 represented by the exponents in parentheses.

[b] Fractions smaller than the detection limits represented by dashes.

[c] Detection limit of the ^{131}I species, related to total ^{131}I.

Table III Results of the ^{131}I species measurements in the annular compartment and hood exhausts.

Sampling period	Total ^{131}I concentration (Ci/m^3)	Total ^{131}I release rate (Ci/s)	Fraction of the ^{131}I species (%)			Detection limit (%)
			Part. ^{131}I	Elem. ^{131}I	Org. ^{131}I	
Annular compartment exhaust (sampling point E)						
36	3.7 (-14)	6.3 (-13)	-	39	61	3
37	9.4 (-15)	1.6 (-13)	-	44	56	12
38	1.5 (-14)	2.6 (-13)	-	38	62	7
39	1.0 (-14)	1.7 (-13)	-	36	64	11
40	3.8 (-15)	6.6 (-14)	-	-	100	29
41	1.4 (-13)	2.4 (-12)	6	34	60	< 1
42 [a]	1.6 (-14)	2.7 (-13)	-	36	64	7
43 [a]						
44	1.4 (-14)	2.4 (-13)	-	11	89	8
45	9.0 (-15)	1.5 (-13)	-	25	75	12
46 [a]						
47	3.6 (-15)	6.1 (-14)	-	100	-	32
48	1.2 (-12)	2.5 (-11)	-	49	51	< 1
Hood exhaust (sampling point F)						
36	7.1 (-11)	8.5 (-11)	< 1	88	11	< 1
37	1.0 (-11)	1.3 (-11)	< 1	86	14	< 1
38	1.6 (-11)	2.0 (-11)	2	92	6	< 1
39	7.6 (-12)	9.1 (-12)	1	87	12	< 1
40	1.3 (-11)	1.5 (-11)	1	86	13	< 1
41	1.3 (-11)	1.6 (-11)	2	93	5	< 1
42	3.7 (-12)	4.5 (-12)	2	89	8	< 1
43	9.2 (-12)	1.1 (-11)	2	93	5	< 1
44	1.4 (-11)	1.7 (-11)	2	94	4	< 1
45	6.6 (-12)	7.9 (-12)	2	91	7	< 1
46	5.1 (-12)	6.1 (-12)	4	88	8	< 1
47	1.2 (-11)	1.5 (-11)	2	79	19	< 1
48	7.1 (-12)	8.4 (-12)	3	60	37	< 1

[a] No ^{131}I detected; total ^{131}I concentration corresponding to the detection limit and average of the ^{131}I species fractions of the preceding and subsequent sampling period used.

Table IV Results of the ^{131}I species measurements in the auxiliary building exhausts.

Sampling period	Total ^{131}I concentration (Ci/m^3)	Total ^{131}I release rate (Ci/s)	Fraction of the ^{131}I species (%)			Detection limit (%)
			Part. ^{131}I	Elem. ^{131}I	Org. ^{131}I	
Auxiliary building exhaust (sampling point G)						
36	2.8 (-12)	3.2 (-11)	-	71	29	< 1
37	1.4 (-12)	1.7 (-12)	-	63	37	< 1
38	3.6 (-13)	4.2 (-12)	-	94	6	< 1
39	3.5 (-13)	4.0 (-12)	2	73	25	< 1
40	7.5 (-13)	8.5 (-12)	2	68	30	< 1
41	6.9 (-13)	7.9 (-12)	4	65	31	< 1
42	2.8 (-13)	3.2 (-12)	5	77	18	< 1
43	4.1 (-13)	4.7 (-12)	4	84	12	< 1
44	1.2 (-13)	1.4 (-12)	-	65	35	2
45	1.0 (-13)	1.2 (-12)	-	65	35	2
46	1.3 (-13)	1.5 (-12)	-	58	42	2
47	9.4 (-13)	1.1 (-11)	2	93	4	< 1
48	9.2 (-13)	1.1 (-11)	-	32	68	< 1
Auxiliary building exhaust (sampling point H)						
36	1.0 (-13)	1.6 (-12)	-	9	91	2
37	1.3 (-13)	2.1 (-12)	2	15	83	2
38	1.1 (-13)	1.8 (-12)	-	-	100	2
39	2.8 (-14)	4.5 (-13)	-	57	43	8
40	3.7 (-14)	5.8 (-13)	13	16	71	6
41	1.5 (-13)	2.4 (-12)	9	28	63	1
42	6.1 (-14)	9.7 (-13)	-	45	55	4
43 [a]	3.7 (-14)	5.8 (-13)	32	31	37	6
44	1.5 (-14)	2.5 (-13)	-	-	100	14
45	7.1 (-14)	1.1 (-12)	-	22	78	3
46	6.6 (-14)	1.0 (-12)	-	25	75	3
47	1.2 (-13)	1.8 (-12)	-	18	82	2
48	3.2 (-13)	5.0 (-12)	-	55	45	< 1

[a] Values questionable because of short counting time for part. ^{131}I.

Table V Results of the ^{131}I species measurements and calculations for the stack effluent.

Sampling period	Total ^{131}I concentration (Ci/m^3)	Total ^{131}I release rate (Ci/s)	Fraction of the ^{131}I species (%)			Detection limit (%)
			Part. ^{131}I	Elem. ^{131}I	Org. ^{131}I	
Values measured (sampling point I)						
36	4.9 (-12)	2.3 (-10)	< 1	76	23	< 1
37	1.4 (-12)	6.6 (-11)	< 1	63	36	< 1
38	7.5 (-13)	3.4 (-11)	1	64	35	< 1
39	5.7 (-13)	2.6 (-11)	1	73	26	< 1
40	9.4 (-13)	4.3 (-11)	< 1	74	25	< 1
41	9.0 (-13)	4.1 (-11)	1	75	24	< 1
42	2.9 (-13)	1.3 (-11)	3	70	27	< 1
43	2.1 (-13)	9.5 (-12)	-	82	18	< 1
44	4.3 (-13)	2.0 (-11)	2	77	21	< 1
45	2.5 (-13)	1.1 (-11)	-	71	29	< 1
46	2.5 (-13)	1.2 (-11)	-	51	49	< 1
47	1.1 (-12)	4.8 (-11)	-	66	34	< 1
48	1.3 (-12)	6.3 (-11)	< 1	41	59	< 1
Values calculated from the results of the measurements at the sampling points B, C, E, F, G, H						
36	2.8 (-12)	1.3 (-10)	< 1	76	23	-
37	1.0 (-12)	4.7 (-11)	< 1	45	54	-
38	6.5 (-13)	3.0 (-11)	1	74	25	-
39	3.8 (-13)	1.7 (-11)	< 1	65	35	-
40	6.5 (-13)	3.0 (-11)	1	63	36	-
41	7.1 (-13)	3.3 (-11)	3	66	31	-
42	2.0 (-13)	9.3 (-12)	3	76	22	-
43	3.6 (-13)	1.7 (-11)	4	87	9	-
44	4.3 (-13)	2.0 (-11)	2	86	12	-
45	2.4 (-13)	1.1 (-11)	2	76	22	-
46	2.1 (-13)	9.5 (-12)	3	69	29	-
47	6.8 (-13)	3.1 (-11)	2	71	28	-
48	1.1 (-12)	5.2 (-11)	< 1	46	54	-

Table VI Contributions of the filtered equipment compartment exhaust to the stack effluent with respect to the ^{131}I species (s. periods 36-41: s. point B; s. periods 42-48: s. point C).

Sampling period	^{131}I species contribution (%)		
	Elem. ^{131}I	Org. ^{131}I	Total ^{131}I
36	< 1	31	7
37	< 1	62	34
38	< 1	56	14
39	< 1	60	21
40	< 1	52	19
41	< 1	38	12
42	< 1	17	4
43	< 1	13	1
44	< 1	32	4
45	< 1	20	4
46	< 1	29	8
47	< 1	46	13
48	< 1	9	5

Table VII Contributions of the annular compartment and hood exhausts to the stack effluent with respect to the ^{131}I species.

Sampling period	^{131}I species contribution (%)		
	Elem. ^{131}I	Org. ^{131}I	Total ^{131}I
Annular compartment exhaust (sampling point E)			
36	< 1	1	< 1
37	< 1	< 1	< 1
38	< 1	2	< 1
39	< 1	2	1
40	< 1	< 1	< 1
41	4	14	7
42	2	9	3
43	< 1	< 1	< 1
44	< 1	9	1
45	< 1	5	1
46	< 1	< 1	< 1
47	< 1	< 1	< 1
48	53	46	49
Hood exhaust (sampling point F)			
36	76	32	66
37	50	7	27
38	82	15	65
39	71	19	53
40	69	19	51
41	69	9	49
42	57	19	48
43	71	36	67
44	95	28	87
45	87	23	73
46	82	19	65
47	53	32	47
48	21	11	16

Table VIII Contributions of the auxiliary building exhausts to the stack effluent with respect to the ^{131}I species.

Sampling period	^{131}I species contribution (%)		
	Elem. ^{131}I	Org. ^{131}I	Total ^{131}I
Auxiliary building exhaust (sampling point G)			
36	23	31	25
37	48	24	35
38	18	3	14
39	26	17	23
40	31	24	29
41	24	24	24
42	35	29	35
43	28	37	29
44	5	20	7
45	10	17	11
46	13	24	16
47	46	5	34
48	14	26	20
Auxiliary building exhaust (sampling point H)			
36	< 1	5	1
37	2	7	4
38	< 1	23	6
39	2	3	3
40	< 1	4	2
41	3	15	7
42	6	27	11
43	1	14	4
44	< 1	11	1
45	3	36	10
46	4	29	11
47	2	17	6
48	12	8	10

Table IX Average values of the results of the ^{131}I species measurements and calculations for the various exhausts and the stack effluent.[a] Sampling periods 36-48.

Exhaust	Total ^{131}I concentration (Ci/m^3)	Total ^{131}I release rate (Ci/s)	Fraction of the ^{131}I species (%)[b]		^{131}I species contribution[b] to the stack effluent (%)		
			Elem. ^{131}I	Org. ^{131}I	Elem. ^{131}I	Org. ^{131}I	Total ^{131}I
Unfilt.eq.comp.(A)	6.9 ± 1.2(-11)	2.3 ± 0.4(-11)	13.6 ± 2.6	86.4 ± 2.6	-	-	-
Filt.eq.comp.(B,C)	1.2 ± 0.4(-11)	4.0 ± 1.2(-12)	0.5 ± 0.2	99.3 ± 0.3	0.0 ± 0.0	35.6±5.1	11.2±2.5
Annular comp. (E)	1.1 ± 0.9(-13)	2.3 ± 1.9(-12)	38.3 ± 6.8	61.4 ± 6.8	4.7 ± 4.0	7.0±3.5	5.0±8.7
Hood (F)	1.5 ± 0.5(-11)	1.7 ± 0.6(-11)	86.6 ± 2.5	11.6 ± 2.4	67.9 ± 5.3	20.5±2.6	54.8±5.2
Aux.building (G)	7.2 ± 2.0(-13)	8.2 ± 2.3(-12)	69.8 ± 4.5	28.7 ± 4.7	24.6 ± 3.6	21.6±2.6	23.2±2.6
Aux.building (H)	9.6 ± 2.2(-14)	1.5 ± 0.3(-12)	24.8 ± 5.2	70.9 ± 5.9	2.7 ± 0.9	15.2±2.9	5.8±1.0
Stack (I)	1.0 ± 0.3(-12)	4.7 ± 1.6(-11)	67.8 ± 3.1	31.3 ± 3.2	-	-	-
Stack[c]	7.2 ± 1.9(-13)	3.3 ± 0.9(-11)	69.2 ± 3.6	29.2 ± 3.7	-	-	-

[a] Uncertainties expressed as standard deviations.

[b] Calculated as averages of the values of the various sampling periods; slightly different average values result from the average ^{131}I species release rates.

[c] Calculated from the results of the measurements at the sampling points B, C, E, F, G, H.

Table X Decontamination factors of the equipment compartment exhaust filters [a]. Filter 1: s. points A and B; Filter 2: s. points A and C.

Filter	Sampling period	Decontamination factor		
		Elem. ^{131}I	Org. ^{131}I	Total ^{131}I
1	36	510	3.6	4.0
	37	130	2.3	2.5
	38	450	2.9	3.2
	39	360	3.2	3.5
	40	280	3.0	3.3
	41	50	3.2	3.4
	36 - 41 [b]	290	3.1	3.3
	36 - 41 [c]	± 70	± 0.2	± 0.2
2	42	90	24	25
	43	210	38	40
	44	1 900	26	28
	45	560	20	26
	46	1 500	20	25
	47	> 10 000	9	13
	48	1 400	12	18
	42 - 48 [b]	960 [d]	21	25
	42 - 48 [c]	± 310 [d]	± 4	± 3

[a] Sorbent: KI impregnated carbon, 8 - 12 mesh (filled into the filters 2 years prior to the measurements);
residence time: ∿ 0,5 s;
average relative humidity: 40 %;
average temperature: 30°C.

[b] Average value.

[c] Standard deviation of the average value.

[d] Calculated without consideration of sampling period 47.

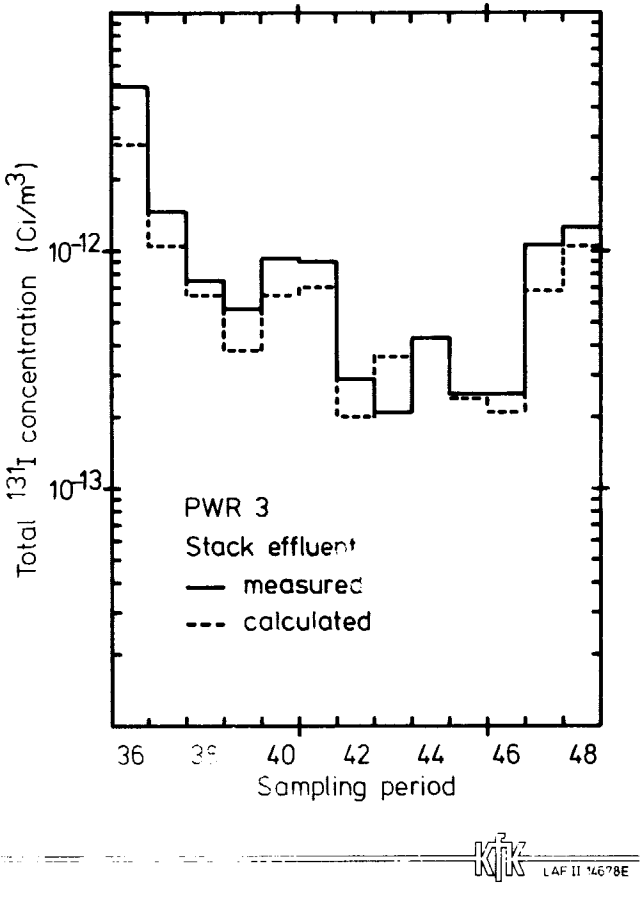

Total ^{131}I concentration as a function of time

Fig. 5

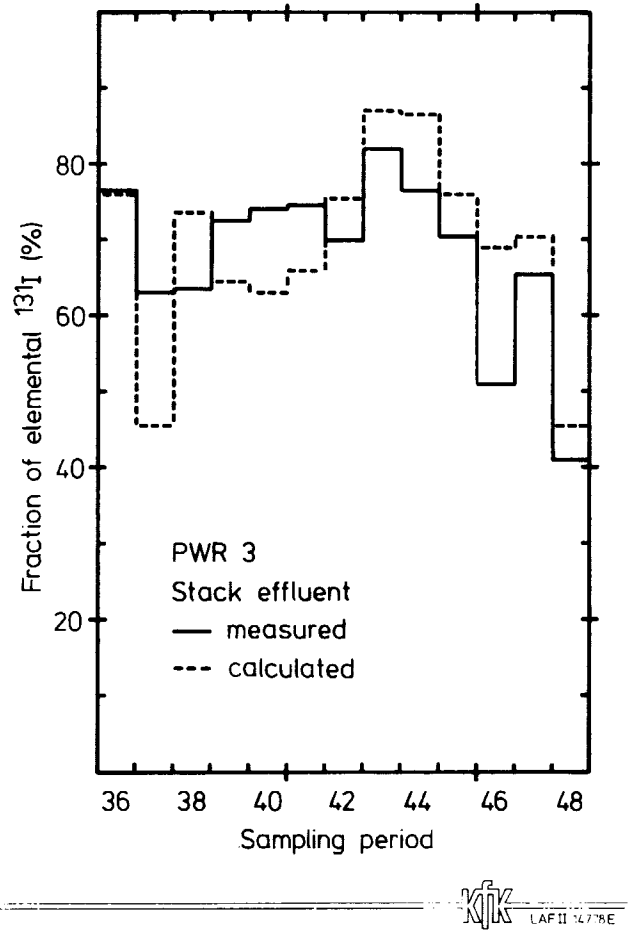

Fraction of elemental ^{131}I as a function of time

Fig. 6

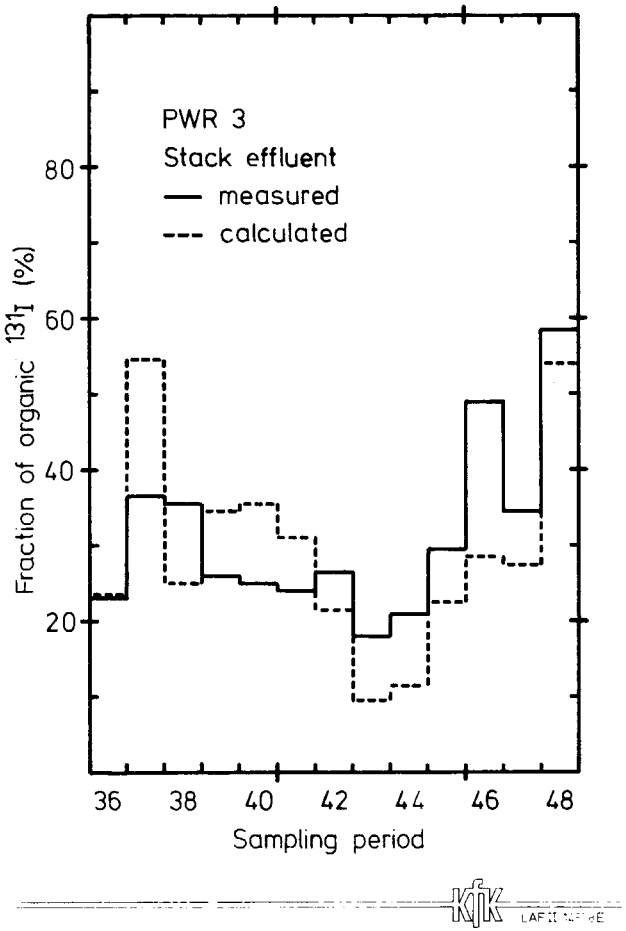

Fraction of organic ^{131}I
as a function of time

Fig. 7

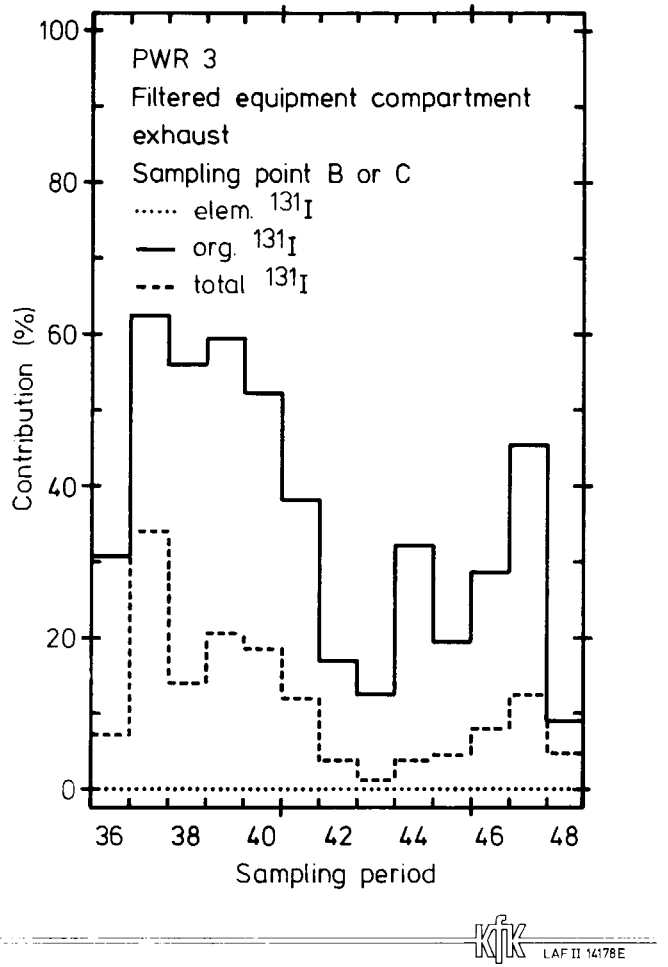

Contribution to the stack effluent with respect
to the ^{131}I species as a function of time

Fig. 8

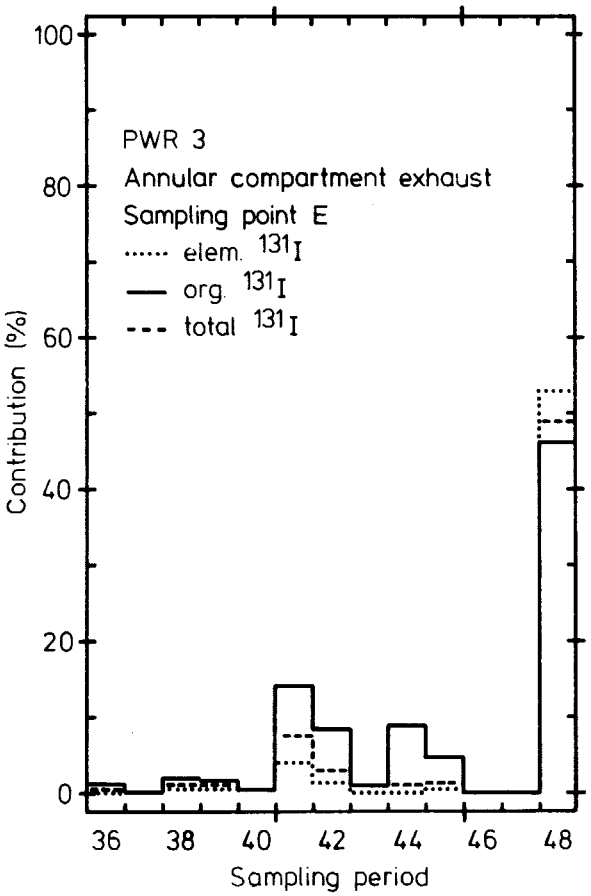

Contribution to the stack effluent with respect to the ^{131}I species as a function of time

Fig. 9

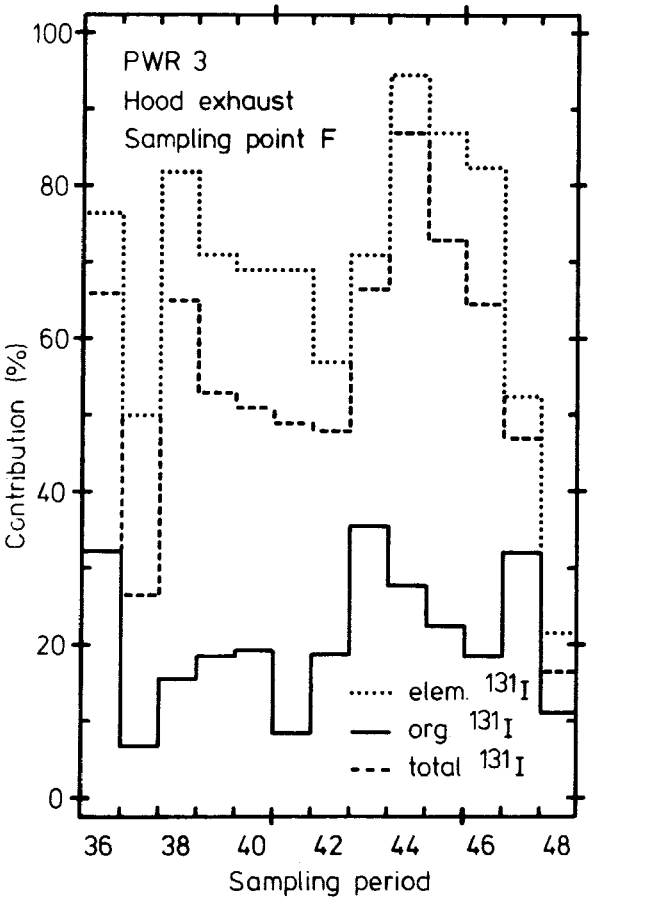

Contribution to the stack effluent with respect to the ^{131}I species as a function of time

Fig. 10

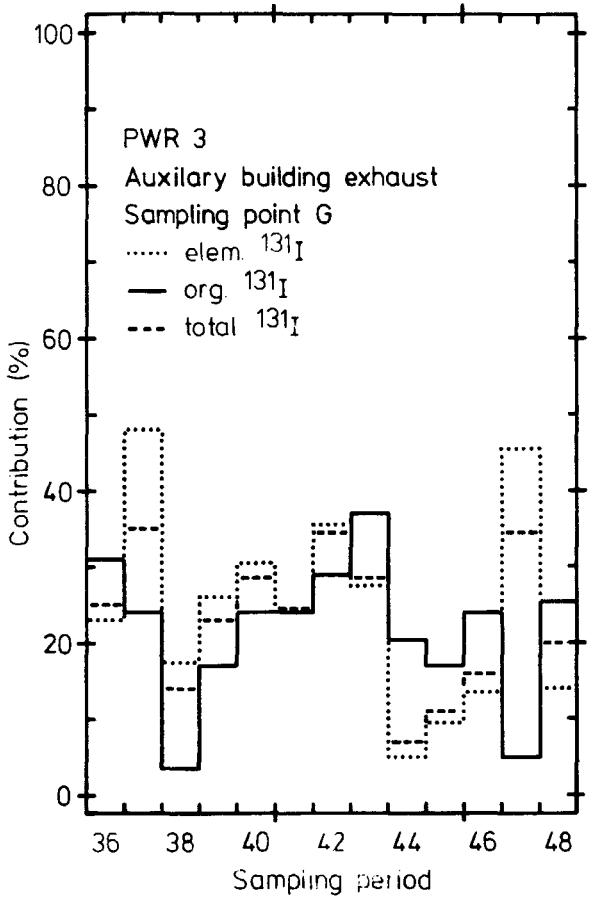

Contribution to the stack effluent with respect to the ^{131}I species as a function of time

Fig. 11

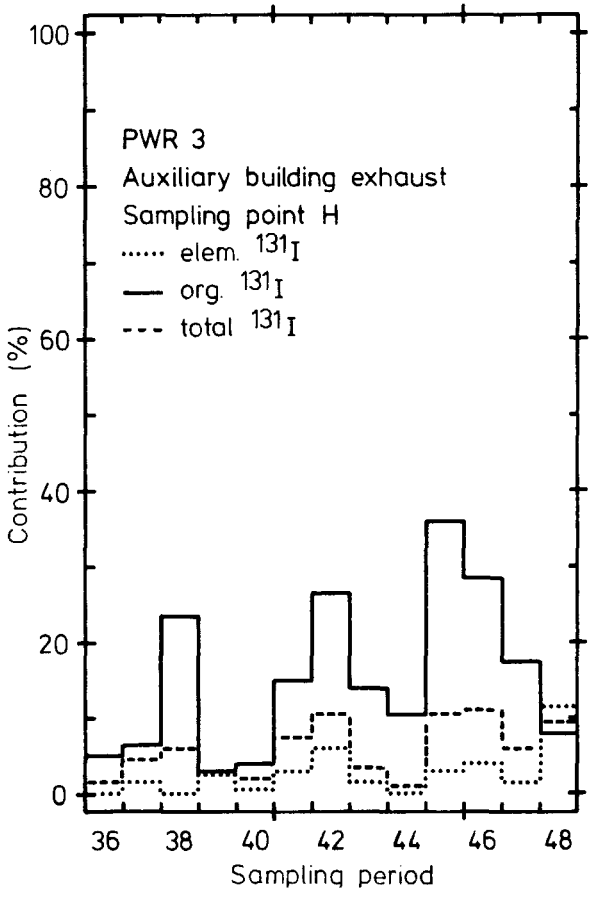

Contribution to the stack effluent with respect to the ^{131}I species as a function of time

Fig. 12

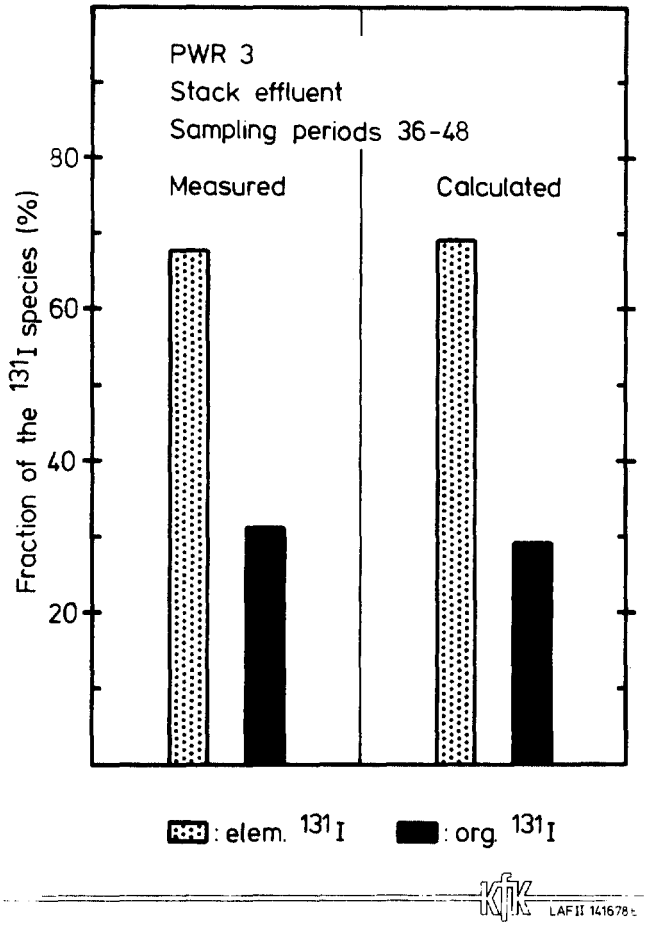

Average fractions of the ^{131}I species

Fig. 13

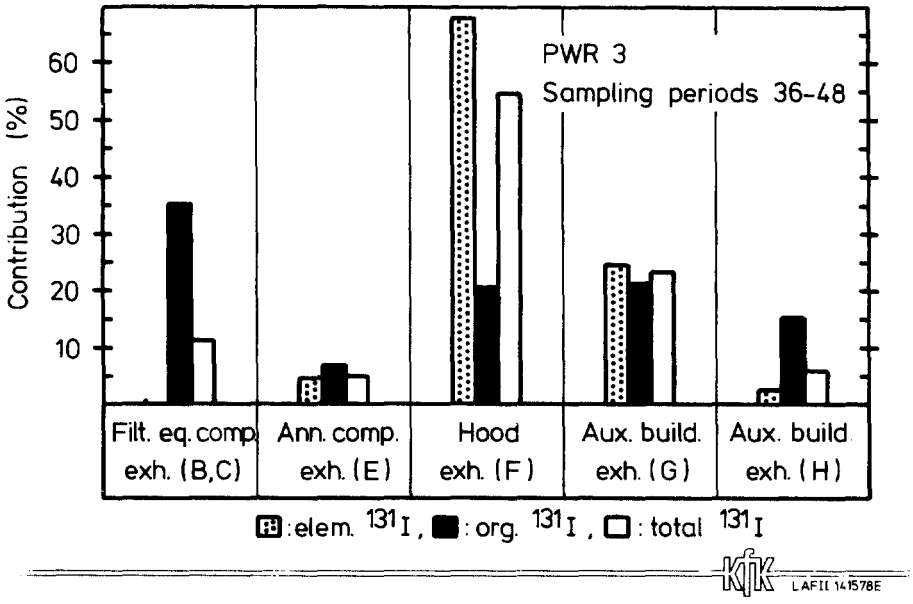

Average contributions of the various exhausts to the stack effluent with respect to the ^{131}I species

Fig. 14

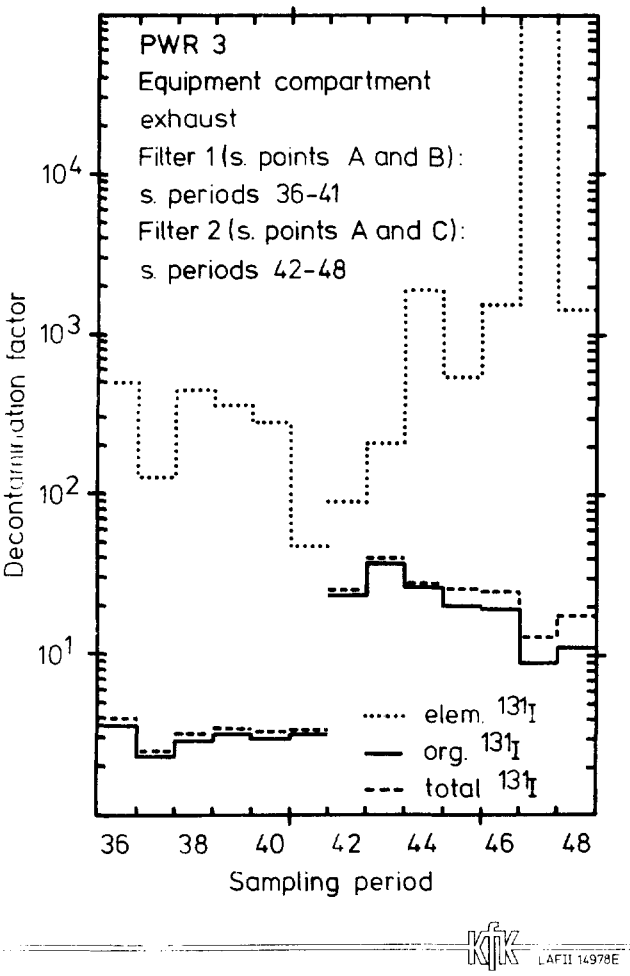

Decontamination factor as a function of time

Fig. 15

V. Calculation of Data Pertaining to the ^{131}I Stack Release for Various Cases of Filtration of the Equipment Compartment and Hood Exhausts

To generalize the experimental data of the sampling periods 36 to 48 to a certain extent various calculations were performed. In these calculations filtration of the major ^{131}I sources, i.e. the equipment compartment and hood exhausts, with different decontamination factors for the ^{131}I species, including decontamination factors of 1 for all species (no filtration), was assumed. The cases of filtration considered are shown in Table XI. For these cases the fractions of the ^{131}I species in the stack effluent, the ^{131}I species stack release rates, and the relative ingestion doses due to the total ^{131}I stack release were calculated.

The results are presented in Table XII and in Figs. 16 to 18. They may be summarized as follows:

(a) The fractions of elem. and org. ^{131}I are about 50 % each in case 1 (no filtration). The relative amount of elem. ^{131}I increases (with the total ^{131}I release rate lower than without filtration) if the equipment compartment exhaust is filtered (cases 2, 3), it decreases in the event of filtration of the hood exhaust (cases 4, 5). The ^{131}I species proportions are on the order of 50 % if both the exhausts are filtered with the same decontamination factors (cases 6, 7).

(b) The release rate of elem. ^{131}I diminishes to a small extent in the event of filtration of the equipment compartment exhaust (cases 2, 3), but to a high degree in the event of filtration of the hood exhaust (cases 4, 5). The highest diminution is obtained if both the exhausts are filtered.

(c) The relative ingestion doses due to the total ^{131}I release are approximated by the ratios of the elem. ^{131}I release rates in the various cases if a weighting ratio of 100 : 10 : 1 for elem., part., and org. ^{131}I is used. If both the equipment compartment and the hood exhausts are filtered, the relative ingestion dose is 28 % or 27 % (100 % in the case of no filtration at all). Case 2 with a relativ ingestion dose of 85 % approaches to the actual situation during the sampling periods 36 to 48. This means that by installation of an iodine filter in the hood exhaust with decontamination factors for part., elem. and org. ^{131}I of 100, 100, and 10 respectively, the actual ingestion dose would have been reduced by a factor of 3.

It is pointed out that the results obtained apply to specific conditions (of mainly power operation) only. Under other circumstances, especially in the case of an incident, different values may hold. In particular, the percentage of elem. ^{131}I may be high in unfiltered equipment compartment exhaust in the case of an incident so that the reduction of the elem. ^{131}I release rates and the ingestion doses achieved by filtration of this exhaust would be much higher than found above.

Table XI Different cases of filtration of the equipment compartment and hood exhausts used in the calculation of data pertaining to the stack release.

Case	Decontamination factor					
	Equipment compartment exhaust			Hood exhaust		
	Part. ^{131}I	Elem. ^{131}I	Org. ^{131}I	Part. ^{131}I	Elem. ^{131}I	Org. ^{131}I
1	1	1	1	1	1	1
2 [a]	100	100	10	1	1	1
3	100	1000	100	1	1	1
4	1	1	1	100	100	10
5	1	1	1	100	1000	100
6	100	100	10	100	100	10
7	100	1000	100	100	1000	100

[a] Approximates the actual situation(average decontamination factor of the equipment compartment exhaust filters about 13 for org. ^{131}I (Table X); no hood exhaust filter installed).

Table XII Calculated data pertaining to the stack release for various cases of filtration of the equipment compartment and hood exhausts.
Cases as indicated in Table XI; sampling periods 36-48.

Case	Fraction of the ^{131}I species (%)[a]		^{131}I species release rate (Ci/s)			Relative ingestion dose due to total ^{131}I release (%)[b]
	Elem. ^{131}I	Org. ^{131}I	Elem. ^{131}I	Org. ^{131}I	Total ^{131}I	
1	48.6 ± 2.6	50.4 ± 2.7	2.62 ± 0.67(-11)	2.58 ± 0.48(-11)	5.24 ± 1.07(-11)	100
2	71.8 ± 2.9	26.5 ± 3.0	2.24 ± 0.65(-11)	8.54 ± 2.36(-12)	3.14 ± 0.83(-11)	85.2 ± 24.5
3	77.0 ± 2.9	21.2 ± 3.1	2.24 ± 0.65(-11)	6.81 ± 2.16(-12)	2.96 ± 0.81(-11)	85.0 ± 24.5
4	28.7 ± 2.3	70.6 ± 2.4	1.11 ± 0.29(-11)	2.41 ± 0.43(-11)	3.53 ± 0.70(-11)	42.7 ± 10.9
5	28.5 ± 2.3	70.8 ± 2.4	1.09 ± 0.28(-11)	2.39 ± 0.43(-11)	3.50 ± 0.69(-11)	42.2 ± 10.9
6	49.3 ± 3.7	49.3 ± 4.0	7.32 ± 1.95(-12)	6.81 ± 1.94(-12)	1.43 ± 0.37(-11)	28.0 ± 7.4
7	59.0 ± 3.6	39.3 ± 4.0	7.15 ± 1.91(-12)	4.90 ± 1.72(-12)	1.22 ± 0.35(-11)	27.2 ± 7.3

[a] Calculated as averages of the fractions of the various sampling periods; slightly different fractions result from the ^{131}I species release rates, as shown in Fig. 16.

[b] Weighting ratio of the ^{131}I species release rates:
elem. ^{131}I : part. ^{131}I : org. ^{131}I = 100 : 10 : 1.

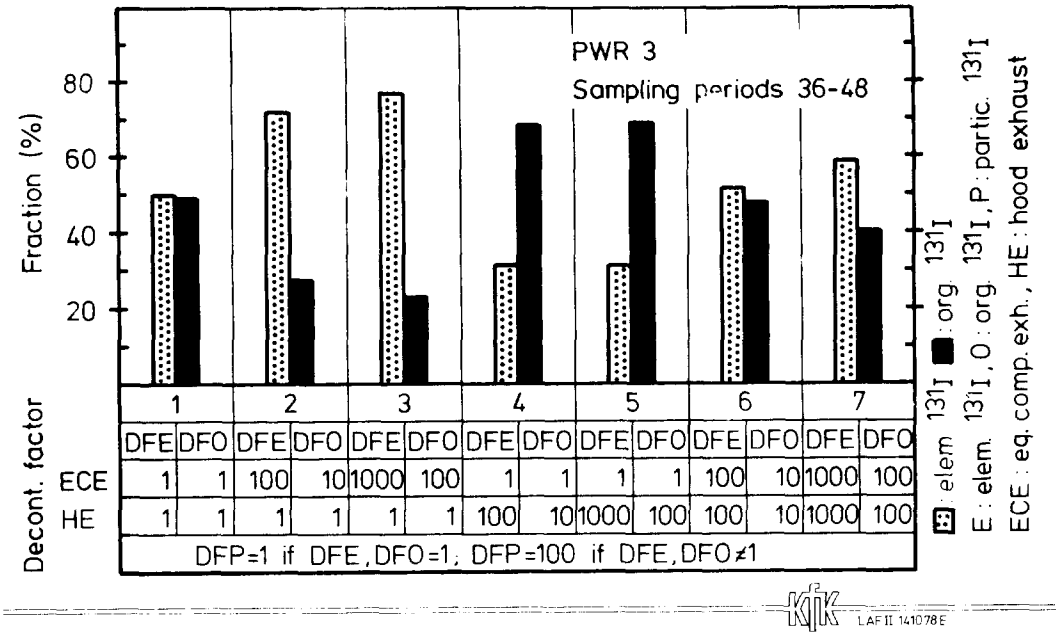

Calculated fractions of the ^{131}I species in the stack effluent for various cases of filtration of the equipment compartment and hood exhaust

Fig. 16

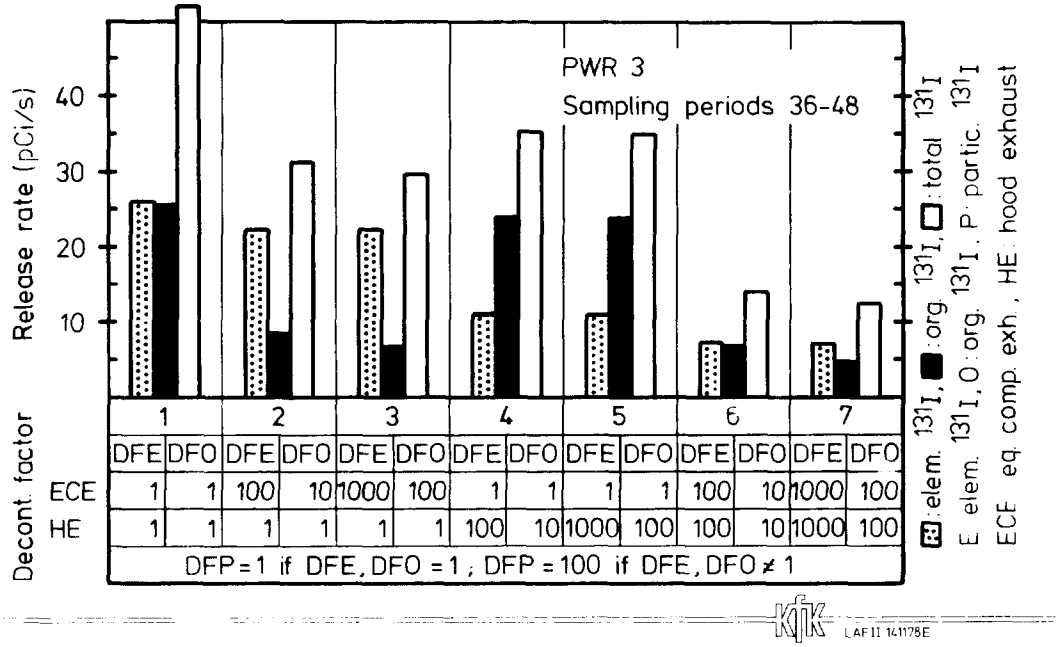

Calculated stack release rates of the ^{131}I species for various cases of filtration of the equipment compartment and hood exhaust

Fig. 17

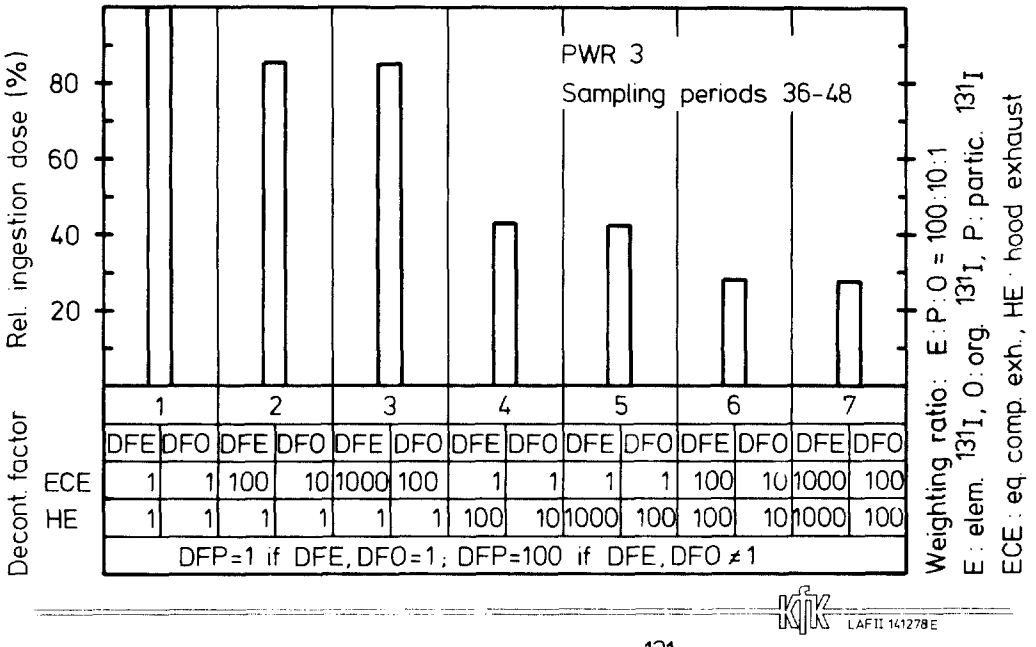

Calculated relative ingestion doses due to the total ^{131}I stack release for various cases of filtration of the equipment compartment and hood exhaust (1st case:100%)

Fig. 18

VI. Conclusions

The credit for differences of the ^{131}I species in the stack effluents of PWRs with respect to the environmental impact may be based under favorable conditions on release rates of elemental and organic ^{131}I in the ratio of 1 : 1 or in even lower ratios. But as the fractions of the ^{131}I species may differ substantially from plant to plant and be strongly influenced by the mode of exhaust filtration, i.e. by the location of the iodine filters, the decision to grant the credit mentioned for a specific plant should be based on ^{131}I species measurements in the stack effluent of the plant in question.

A considerable improvement of the ventilation systems of PWRs in terms of reduction of elem. ^{131}I release rates under normal operating conditions may be possible.

Acknowledgements

We wish to express our appreciation to Messrs. K. Bleier, R. Butz, and K.H. Simice who performed or evaluated the laboratory and in-plant measurements.

The special sponsorship of the Federal Minister of Research and Technology of the Federal Republic of Germany is gratefully acknowledged.

References

1. Wilhelm, J.G., "Iodine filters in nuclear power stations," KFK 2449 (1977).

2. Bundesminister des Inneren, "Allgemeine Berechnungsgrundlagen für die Bestimmung der Strahlenexposition durch Emission radioaktiver Stoffe mit der Abluft," Empfehlung der Strahlenschutzkommission, p. 65 (1977).

3. Pelletier, C.A., et al., "Sources of radioiodine at boiling water reactors," EPRI NP-495 (1978).

4. Deuber, H., Wilhelm, J.G., "Bestimmung der physikalisch-chemischen Komponenten des Radiojods in der Kaminabluft von Kernkraftwerken," KFK-Ext. 30/78-1 (1978).

5. Deuber, H., "Bestimmung von Iodkomponenten in der Abluft kerntechnischer Anlagen," KFK 2700 (to be published).

6. Deuber, H., "Bestimmung von Jodkomponenten in der Abluft kerntechnischer Anlagen," KFK 2435, p. 127-139 (1977); KFK 2500, p. 132-145 (1977); KFK 2600 (to be published).

7. Birke, G., "Abscheidung von ^{131}I in Form von HIO an verschiedenen Iod-Sorptionsmaterialien," KFK 2700 (to be published).

8. Emel, W.A., et al., "An airborne radioiodine species sampler and its application for measuring removal efficiencies of large charcoal adsorbers for ventilation exhaust air," CONF 760822, p. 389-431 (1976).

DISCUSSION

CARTER: A point of clarification, please; how long were the iodine filters in operation?

DEUBER: The first iodine filter had been in operation for about 2 years, the second one only occasionally prior to the measurements of the DFs.

CHAIRMAN BURCHSTED'S SUMMARY:

During the first half of this session a number of papers were presented which dealt with factors relating to the degradation of adsorbents. All of these factors had been discussed in earlier Air Cleaning Conferences at one time or another, but it is interesting to see that the empirical observations of earlier years are now yielding to mathematical treatment that gives us a better understanding of the mechanisms involved and lead to predictive possibilities and improved design in the future. Several factors also suggest the effects of different base carbons, activation methods, and impregnations that indicate the possibility of "designing" activated carbons for specific applications, e.g., stand-by treatment system service vs. continuously on-line system service, etc. The discussions of inherent characteristics that affect carbon degradation, as opposed to external (i.e., atmospheric) conditions that poison the carbon, led the Session Chairman to propose a distinctive nomenclature for use in the future: Aging as the generic term for degradation resulting from inherent factors (e.g., surface oxidation with time, inherent acid introduced during manufacture) and Weathering for degradation caused by external factors (i.e., atmospheric and environmental).

One of the papers by Dr. Dietz described a proposed test which defines the very important characteristic of attrition (often referred to as dusting). The results of that study were particularly interesting because they suggest a possibility of classifying adsorbents with respect to this characteristic. Finally, the paper by Romans suggests the possibility of testing activated carbons with a nonradioactive CH_3I challenge, a possibility that could simplify qualification, production, and surveillance testing in the future. However, Kovach pointed out that the test cannot reflect the isotopic exchange of ^{131}I for ^{127}I that is the primary mechanism for trapping the radioactive iodine fraction with KI and I_2 impregnated carbon. As the chairman noted, we don't really care if nonradioactive CH_3I comes off a carbon bed so long as we trap and hold the radioactive fraction. Wood points out, on the other hand, that the total CH_3I does have importance in the overall performance of the adsorption system. The papers not only suggest areas of further research in this field, but suggest many potential areas of interest to the engineer and designer.